Queen Mary
University of London

Roles of microRNAs in diseases of the human gastrointestinal tract

Anke Nijhuis

PhD Thesis

2015

Constance Travis PhD Studentship
Colorectal Cancer Genetics
Centre for Genomics & Child Health

Supervisor: Professor Andrew Silver
Second Supervisors: Dr Cleo Bishop & Professor Ian Mackenzie

Abstract

Crohn's disease (CD) and colorectal cancer (CRC) are major disorders of the intestine. Inflammation in CD often precedes fibrosis and stricture formation, and is linked to increased cancer risk. Hypoxia is a common feature of inflammation and CRC that can severely compromise the effectiveness of current therapy regimes including chemo-radiotherapy and maintenance of remission in CD patients. MicroRNAs (miRNAs) are key regulatory molecules involved in cellular proliferation, apoptosis and fibrosis, which are all modulated by hypoxia. This thesis aims to understand the role of miRNAs in these two intestinal diseases.

Microarray profiling identified differentially expressed miRNA in the intestinal mucosa overlying strictured and non-strictured CD tissue samples and in six CRC cell lines cultured in hypoxic conditions compared to normoxia. Validation experiments using qRT-PCR confirmed the differential expression of miR-29a, -29b, -29c, -34a, -493* and -708 in CD mucosa and miR-21, -210, -30d, -320a, -320b and -320c in CRC cell lines. Functionally, over-expression of miR-29b in CD intestinal fibroblasts modulated the down-regulation of collagen I and III transcripts and collagen III protein in a TGF-β-dependent manner. Furthermore, miR-29b induced indirectly the expression of the anti-apoptotic protein Mcl-1 via the cytokines IL-6 and IL-8. A positive correlation between miR-210 and the hypoxia marker CAIX was found in CRC tissue *in vivo*. Furthermore, HCT116 cells cultured under hypoxia were more resistant to the chemotherapy drug 5-FU than cells grown under normoxia. Knockdown of miR-21 or miR-30d under hypoxia may sensitise CRC cells to 5-FU. CRC cell lines grown under hypoxic conditions present an altered cellular metabolic profile compared to their normoxic counterparts.

This thesis has showed that critical miRNAs have a functional role in the progression of two important diseases of the intestine. The work presented highlights the potential of miRNAs as biomarkers and therapeutic targets to improve the clinical management of patients with digestive diseases.

Statement of originality

I hereby declare that this thesis is my own work and effort. Where alternative sources of information are used, this has been clearly noted. Any contribution made to the research in collaboration with others is explicitly acknowledged.

Signature:……

Date:……

Publications

Published

Nijhuis, A. Biancheri, P. Lewis, A. Bishop, CL. Giuffrida, P. Chan, C. Feakins, R. Poulsom, R. Di Sabatino, A. Corraza, GR. MacDonald, TT. Lindsay, JO and Silver, A. *In Crohn's disease fibrosis-reduced expression of the miR-29 family enhances collagen expression in intestinal fibroblasts.* Clin Sci (Lond), 2014. **127**(5): p. 341-50.

Manuscripts in preparation

Nijhuis, A. Bishop, CL. Curacello, R, Lindsay JO and Silver, A. *miR-29b up-regulates Mcl-1 via IL-6 and IL-8 in Crohn's disease intestinal fibroblasts.*

Nijhuis, A. Thompson, H. Bundy, J. Adams, J, Parker, A. Jalaly, A. Lewis, A. Poulsom, R. Jeffery, R. Thaha, M. Pollard, P, Soga, T. Bishop, CL and Silver, A. *Hypoxia responsive microRNAs in colorectal cancer influence drug response and metabolism.*

Published reviews

Lewis, A*. **Nijhuis, A***. Mehta, S*. Kumagai*, T. Feakins, R. Lindsay, JO and Silver, A. *Intestinal Fibrosis in Crohn's Disease: Role of microRNAs as Fibrogenic Modulators, Serum Biomarkers, and Therapeutic Targets.* Inflamm Bowel Dis, 2015. **21**(5): p. 1141-50. *These authors have contributed equally to the manuscript.

Mehta, S*. **Nijhuis, A***. Kumugai, T*. Lindsay, JO and Silver, A. *Defects in the adherens junction complex (E-cadherin/β-catenin) in inflammatory bowel disease.* Cell Tissue Res, 2014. *These authors have contributed equally to the manuscript.

Publications that I have contributed to

Lewis, A. Mehta, S. Hanna, LN. Rogalski, LA, Jeffery, R. **Nijhuis, A**. Kumagai, T. Biancheri, P. Bundy, JG. Biship, CL, Feakins, R. Di Sabatino, A. Lee, JC. Lindsay JO and Silver, A. *Low serum levels of microRNA-19 are associated with a stricturing Crohn's disease phenotype*.

Macfie, T. Poulsom, R. Parker, A. Warnes, G. Boitsova, T. **Nijhuis, A**. Suraweera, N. Poehlmann, S. Szary, J. Feakins, R. Jeffery, R. Harper, RW. Jubb, AM. Lindsay, JO and Silver, A. *DUOX2 and DUOXA2 form the predominant enzyme system capable of producing the reactive oxygen species H2O2 in active ulcerative colitis and are modulated by 5-aminosalicyclic acid*. Inflamm Bowel Dis, 2014. **20**(3): p. 514-24.

Acknowledgments

First and foremost, I am sincerely grateful to Professor Andrew Silver. He warmly welcomed me into his laboratory during my MSc degree in 2009 and gave me the opportunity to pursue a PhD at The Blizard Institute in 2011. During my PhD, he has given me undivided support, continuous advice and managed to put up with my endless banter. Secondly, I would like to say thank you to my second supervisors Professor Ian Mackenzie and Dr. Cleo Bishop. In particular, I am tremendously indebted to Cleo's help with experimental, write-up and non-work related matters. Despite her busy schedule, she always made time for a quick catch-up. I was very fortunate to have her as a supervisor and could not have done this without her.

I owe a lot to my colleagues and all members of our laboratory group, past and present. In particular, I would like to thank Sarah Macdonald, Alexandra Parker and Tammie Macfie who have taught me most of the laboratory techniques when I first started. Also, thanks to all other members of our research group; Amy Lewis, James Lindsay, Sham Mehta, Hannah Thompson, Kathryn Virdi, Richard Poulsom, Rosemary Jeffery, Nirosha Suraweera, Carla Felice, Cecilia Lai and Anil Ghosh. A massive thank you to my friends and colleagues of the Blizard Institute. There are too many to mention but special thanks to: Maddi, Kasia, Ngoc and the laboratory management. Also, big thanks to Luke Gammon who has patiently helped me with the hypoxia chamber and the IN Cell microscope. Furthermore, I would like to thank my funders. I am very grateful to the Constance Travis Charitable Trust and to Tony and Peta Travis for supporting me financially to do the research on colorectal cancer. Also, I would like to thank the Crohn's & Colitis UK for funding the work on Crohn's disease.

Finally, I am very grateful to my friends and family who have been positive and encouraging during the entire process. Being away from home was not always easy, but their help and support has inspired me to keep going. In particular, a big thanks to Yvonne, Menno and Kim for keeping me grounded when the task of writing became a bit too daunting!

Contents

List of figures

List of tables

Abbreviations

Abbreviation	Definition
5-FU	5-fluorouracil
AARs	Aminoacyl tRNA synthesases
AP	Alkaline phospohatase
APR	Abdominoperineal resection
BCIP	5-bromo-4-chloro-3'-indolylphosphate
BSA	Bovine serum albumin
cDNA	Complementary DNA
C14MC	Chromosome 14 miRNA cluster
C19MC	Chromosome 19 miRNA cluster
CDS	Coding sequence
CE-TOF/MS	Capillary electrophoresis time of flight mass spectrometry
CHiP	Chromatin immunoprecipitation
CIN	Chromosomal instability
CRC	Colorectal cancer
CRT	Chemoradiotherapy
Ct	Cycle threshold
DF	Dharmafect
DIG	Digoxygenin
DMEM	Dulbecco's modified eagles medium
DMSO	Dimethyl sulfoxide
DNA	Deoxyribonucleic acid
ECM	Extracellular matrix
ELISA	Enzyme-linked immunosorbant assay
EMT	Epithelial-to-mesenchymal transition
FAP	Familial adenomatous polyposis
FBS	Fetal bovine serum
FDR	First degree relative
FFPE	Formalin-fixed parafin embedded
FOBt	Faecal occult blood test
GFP	Green fluorescent protein
GWAS	Genome-wide association studies
HBSS	Hanks balanced salt solution
HNPCC	Hereditary non-polyposis colorectal cancer
HRE	Hypoxia-response element
IBD	Inflammatory bowel disease

IF	Immunofluorescence
IPA	Ingenuity pathway analysis
LNA	Locked nucleic acid
LOH	Loss of heterozygosity
LS	Lynch syndrome
MACS	Microsatellite and chromosome stable
miRNA	microRNA
MMR	Mismatch repair
MSI	Microsatellite instability
NBT	4-nitro-blue tetazolium
NGS	Next-generation sequencing
NSCD	Non-strictured CD
NTC	Non-targeting control
ODD	Oxygen-dependent degradation domain
OS	Overal survival
PCA	Principle component analysis
PCR	Polymerase chain reaction
PFA	Paraformaldehyde
PLS-DA	Partial least squares discriminant analysis
pre-miRNA	Precursor miRNA
qRT-PCR	Quantitative real-time PCR
RISC	RNA interference silencing complex
RNA	Ribonucleic acid
RT	Reverse transcription
SCD	Strictured CD
SSC	Saline-sodium citrate
TCA	Tricarboxylic acid cycle
TME	Total mesorectal excision
TNM	Tumour node metastasis
TRFs	Transfer RNA-derived RNA fragments
TSG	Tumour suppressor gene
UC	Ulcerative Colitis
UTR	Untranslated region

Gene list

Genes that are used more than once are listed.

Gene	Full name
AGO	Argonaute
ANGPT	Angiopoietin
APC	Adenomatous polyposis coli
ATG16L1	Autophagy-related 16-like 1
AXIN2	Axis inhibition protein 2
BCL	B-cell CLL/lymphoma
BIRC5	Survivin
CAIX	Carbonic anhydrase IX
CBP	CREB-binding protein
CDC25	Cell division cycle 25A
CTGF	Connective tissue growth factor
DCC	Deleted in colorectal carcinoma
DKK	Dickkopf
DNMT3A	DNA methyltransferase 3A
E2F3	E2F transcription factor 3
EGF	Epidermal growth factor
ERK	Extracellular-signal-regulated kinase
FASLG	FAS ligand
FGFRL1	Fibroblast growth factor receptor like-1
FN1	Fibronectin
GAPDH	Glyceraldehyde 3-phosphate dehydrogenase
GLUT	Glucose transporters
HIF	Hypoxia-inducable factor
IL	Interleukin
IRGM	Immunity-related GTPase family M
IRS1	Insulin receptor substrate
ISCU	Iron-sulfur cluster scaffold homolog
KRAS	Kirsten rat sarcoma viral oncogene homolog
LDHA	Lactate-dehydrogenase
MCL	Myeloid cell leukemia
MDP	Muramyl dipeptide
MEX3C	Mex-3 homolog C
MLH	MutL homolog

MMP	Metalloproteinases
MSH	MutS homolog
MYC	V-myc avian myelocytomatosis viral oncogene homolog
NOD2	Nucleotide-binding oligomerisation domain
PDCD4	Programmed cell death 4
PDGFB	Platelet-derived growth factor
PDK	Pyruvate dehydrogenase kinase
PGF	Placental growth factor
PHD	Proline hydroxylase
PIGN	Phosphatidylinositol glycan anchor biosynthesis class N
PLK-1	Polo-like kinase 1
PMS	Post-meiotic segregation
PPIB	Cyclophilin B
SIRT1	Sirtuin 1
SMAD	Mothers against DPP
SNAIL	Zinc finger protein SNAI1
TCF	Transcription factor
TGF-β	Transforming growth factor beta
TIMP	Tissue inhibitors of matrix metalloproteinase
TNF	Tumour necrosis factor
TP53	Tumour protein 53
TWIST	Twist related protein
VEGF	Vascular endothelial growth factor
VHL	von Hippel-Lindau
YB-1	Y-box binding protein 1
ZEB	Zinc finger e-box-binding homeobox
ZNF516	Zinc finger protein 516

Chapter 1: Introduction

My thesis is based on two diseases of the gastrointestinal tract: Crohn's disease (CD) which is one of the two inflammatory bowel diseases (IBD) and Colorectal cancer (CRC). Inflammation is a one of the risk factors for developing IBD-associated CRC and microRNAs (miRNAs) are able to regulate a large number of cellular processes that are important in health and disease. Therefore, my project is split up in two individual, but overlapping, project areas based around the functionality of miRNAs and the presence of hypoxia as a modulator of miRNA expression in both cancer and inflammation.

1.1 Colorectal Cancer

1.1.1 Background

CRC is the third most common cancer worldwide with approximately 1.4 million new cases and around 694,000 deaths in 2014 [1]. CRC is the collective term for all cancers that arise in the colonic segments (caecum, ascending, transverse, descending and sigmoid colon) and the rectum. CRC can occur anywhere along the colon but left sided CRC is more commonly seen [2] (Fig. 1.1). Biological ageing is a major risk factor for a large number of cancers including CRC. Incidence rates increase greatly from the age of 50, with the highest incidence in individuals over 85 year old [3]. Besides ageing, lifestyle habits can substantially contribute to the risk of developing CRC. High meat consumption [4], smoking [5] and heavy alcohol intake [5, 6] have all been linked to the development of CRC. Furthermore, an active lifestyle can reduce the risk of developing various cancers, including CRC. Physical activity is inversely correlated with risk in a dose-dependent manner [7, 8]. By contrast, the metabolic syndrome which includes a group of clinical measures, such as obesity, impaired glucose regulation (diabetes) and elevated blood triglyceride levels, is now closely linked to the increased incidence of CRC [9]. Indeed, studies have demonstrated that an active lifestyle in combination with a healthy diet could prevent a large proportion of CRC [10].

Members of families with a history of CRC are at increased risk of developing CRC. For instance, individuals with a first-degree relative (FDR) with CRC have a relative risk of 2.25 and this increases to 4.25 if there are multiple FDRs with CRC [11]. Also, a personal history of IBD, such as CD or Ulcerative Colitis (UC), increases the risk of developing CRC. In 1925, Crohn and Rosenberg first documented IBD-associated CRC [12] and to date approximately 10-15% of all deaths in IBD patients are due to CRC [13]. Therefore, close endoscopic surveillance to detect early neoplastic changes within the bowel is the recommended treatment management regime for IBD patients.

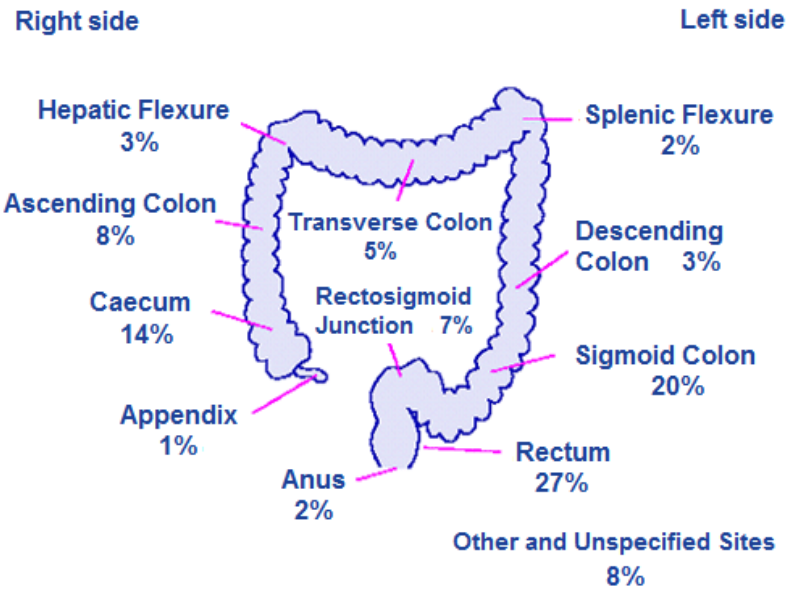

Figure 1.1. Distribution of CRC along the various colon segments. Approximately 60% of CRCs were diagnosed on the left hand side of the large bowel between 2007 and 2009 [2]. Figure adapted from [2].

1.1.2 Molecular genetics of CRC

Around 75% of all CRCs occur sporadically with no notable family history or identifiable inherited gene mutation. The remaining cases are either familial CRC (around 20%), where at least one blood relative has CRC but without a specific germline mutation, or hereditary CRC syndromes (5%) [14]. The next sections will introduce the various sub-types of hereditary CRC syndromes and elaborate on the key genetic events during tumourigenesis.

1.1.2.1 Tumourigenesis

The epithelium of the colon consists of tens of millions of crypts. Intestinal stem cells located at the bottom of each crypt multiply and daughter cells migrate upwards along the crypt. This process takes around three to six days during which the cells at the top die and are replaced by the continuous supply of new cells from below. CRC results from the progressive accumulation of genetic and epigenetic alterations that eventually lead to the transformation of normal colonic epithelium to adenocarcinoma as initially proposed in 1990 by Fearon and Vogelstein (Fig. 1.2) [15]. Despite recent advances in the field, this model remains one of the best paradigms of the molecular genetics of CRC. Genetic alterations often drive the neoplastic process by increasing cell population via activation of pathways involved in proliferation and growth, whilst inhibiting cell-cycle arrest and cell death. These genes can broadly be classed into oncogenes and tumour suppressor genes (TSGs). Generally, TSGs follow the "two-hit-hypothesis" proposed by Knudson [16], in which both alleles of the gene must be mutated for the gene to contribute to tumourigenesis. One frequently mutated TSG is tumour protein p53 *(TP53)* and homozygous loss of this gene is seen in around 50% of all cancers including 29% of all CRCs [17]. By contrast, a single mutation in one of the two alleles of certain oncogenes, such as kirsten rat sarcoma viral oncogene homolog (*KRAS)*, is sufficient to promote cancer development. Recent efforts have focused on large scale sequencing of CRC tissue, which has demonstrated the presence of tens of thousands of somatic mutations, although only a handful of these are considered crucial to "drive" tumourigenesis [18-21].

These driver genes are thought to give a selective growth advantage to the cell and to be fundamental in the development of CRC, unlike "passenger" mutations that seem to be insignificant with regard to tumour growth. CRC driver genes include adenomatous polyposis coli *(APC)*, *TP53* and *KRAS* and will be discussed in more detail below.

Genetically, the majority of CRCs (~80%) can be divided into two groups: chromosomal instable (CIN, ~60%) and microsatellite instable (MSI, ~20%) tumours, each displaying a distinct pattern of genetic alterations. More recently, an additional subgroup of cancers with microsatellite and chromosomal stable (MACS) tumours has been identified. Each group will be discussed in more detail below.

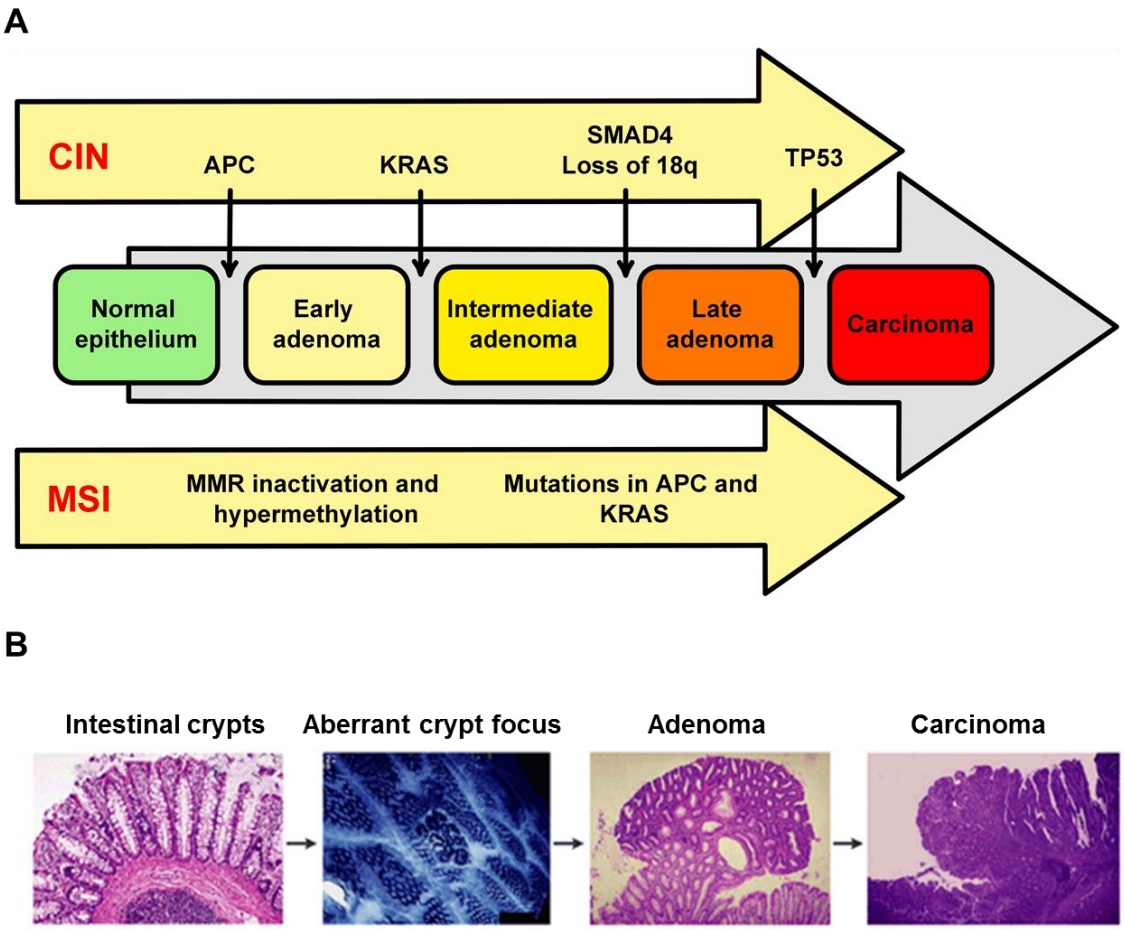

Figure 1.2. The adenoma-carcinoma sequence. (A) This overview of the adenoma-carcinoma model separates the genomic instability pathways between CIN and MSI. CIN is characterised by gross chromosomal losses and gains through genetic alterations. Mutations, in particular in *APC* and *KRAS*, are observed in the early stages of CRC, whilst mutations in *SMAD4*, loss of 18q chromosome and mutations in *TP53* are considered to be events contributing to transformation of late adenoma and carcinoma. The MSI pathway occurs through defects in the DNA mismatch repair mechanism. Mutations in *APC* and *KRAS* are often seen. (B) A schematic overview of the adenoma-carcinoma sequence in CRC. Early manifestations of colorectal neoplasia are aberrant crypt foci which could progress into adenomatous polyps. These polyps can acquire additional mutations and may progress into adenoma and eventually carcinoma. (Panel A and B are adapted from [22] and [23], respectively).

1.1.2.1.1 Chromosomal instability

CIN is characterised by an accelerated rate of allelic gains or losses and gross chromosomal abnormalities, and is present in the large majority of CRC cases. This may result in an imbalance in chromosome number (aneuploidy) and a high frequency of loss of heterozygosity (LOH). Tumours that develop through CIN often acquire mutations in *APC*, *TP53*, and the *KRAS* oncogene [24].

APC. In CRC, the *APC* gene was one of the first genes discovered in patients with familial adenomatous polyposis (FAP) [25, 26]. These individuals harbour a germline mutation in one copy of the *APC* gene and are predisposed to the development of large number of polyps that, if left untreated, will result in CRC. In addition, *APC* is frequently mutated in the majority of sporadic CRC [27]. APC is a key inhibitory molecule in the Wnt pathway promoting the degradation of β-catenin (Fig. 1.3). In the absence of APC, β-catenin is stabilised and is translocated to the nucleus. Here, it forms a complex with transcription factors resulting in transcription of Wnt target genes which are involved in proliferation and differentiation pathways [28]. Within the crypt of the colon, the constitutive activation of Wnt signalling leads to extensive proliferation of the stem/progenitor cells and development of cancerous tissue. Interestingly, genetic alterations in *APC* never lead to a complete loss of protein function suggesting that an optimal level of Wnt signalling is favourable in tumour progression, the so called the "just-right" theory [29]. Furthermore, in cases where *APC* is not directly mutated, the Wnt pathways is indirectly activated by mutations in other key players, such as axis inhibition protein 2 (*AXIN2)* [30] and β-catenin (*CTNNB1)* [31].

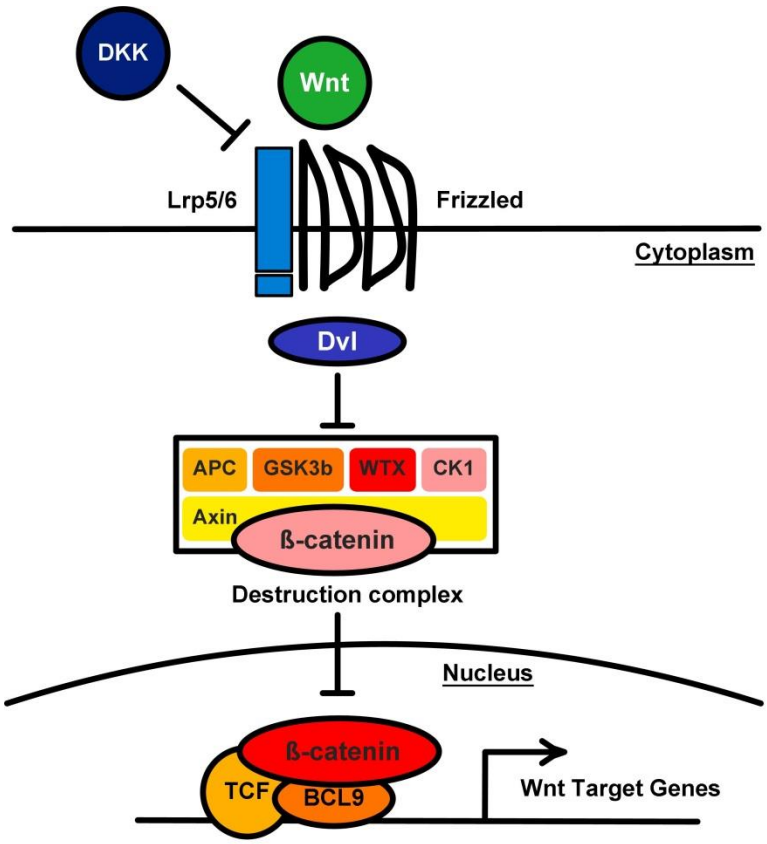

Figure 1.3. The canonical Wnt signalling. Activation of the canonical Wnt signalling pathway requires the binding of Wnt ligands to both Frizzled receptor and its co-receptor Lrp5/6. Activation induces stabilisation of β-catenin through Dishevelled (Dvl)-mediated inhibition of the destruction complex. Stabilised β-catenin accumulates in the nucleus where it recruits TCF and activates the transcription of Wnt target genes with the help of co-factors including BCL9. Secreted inhibitors such as DKK-1, DKK-2, and DKK-3 prevent canonical signalling through negative actions on Lrp5/6. Lrp5/6, LDL receptor-related proteins 5/6; DKK, Dickkopf; BCL9, B cell lymphoma 9; GSK3b, Glycogen synthetase kinase 3 beta; WTX, Wilm's tumour suppressor gene; CK1, casein kinase 1. Figure adapted from [32].

KRAS. The *KRAS* oncogene is mutated in 30-50% of CRC tumours [33] and is seen as a secondary event following loss of *APC* (Fig. 1.2). The Ras protein is part of the epidermal growth factor (EGF) pathway where it plays a role as an on/off switch. Mutations often result in a permanent "on" state of the pathway, leading to proliferation and malignant transformation. Interestingly, the status of *KRAS* is known to stratify patients with respect to therapeutic response: tumours with activating mutations in this gene do not respond to anti-EGFR targeted therapy with antibodies [34, 35].

TP53. P53 is known as the "The guardian of the genome" [36]. Induction of p53 through DNA damage and genotoxic stress results in growth arrest or apoptosis, and acts to reduce the risk of malignant transformation, which highlights the important function of this TSG [37]. Unsurprisingly, *TP53* is the most frequent mutated TSG in human cancers and approximately 29% of all CRC cases harbour mutations in this gene [38, 39]. Mutations in *TP53* are more often seen in more advanced stage CRC, suggesting that the mutation in *TP53* is a late event in the adenoma-carcinoma sequence (Fig. 1.2) [17, 40].

Other. Further additional alterations, such as loss of the 18q chromosome, are frequently observed in up to 70% of CRC [41]. A number of key genes are located on this chromosome segment, including deleted in colorectal carcinoma (*DCC*) [42], mothers against DPP homolog 2 *(SMAD2)* [43], and *SMAD4* [44]. Smad2 and 4 are both mediators of the transforming growth factor beta (TGF-β) pathway regulating cell growth and differentiation. Moreover, recent studies have identified three new CIN-suppressor genes: phosphatidylinositol glycan anchor biosynthesis class N (*PIGN)*; mex-3 homolog C (*MEX3C*); and zinc finger protein 516 (*ZNF516).* These genes are encoded on chromosome 18q are lost in 79% of tumours with an abnormal number of chromosomes [24].

Over the past decades, extensive research has pin-pointed the mutations involved in the adenoma-carcinoma sequence, which is visualised as a step-wise progression.

Nevertheless, it is the accumulation of the majority of these mutations, rather than the order, that appears pivotal for the development of CRC [15].

1.1.2.1.2 Microsatellite instability

MSI is characterised by hypermutation caused by functional loss of DNA mismatch repair (MMR) genes and occurs in around 15% of all sporadic CRC cases [45, 46]. Microsatellites are repetitive DNA sequences such as $(A)_n$ or $(CA)_n$ repeats that occur randomly throughout the genome. These sequences are particularly prone to changes through damage and replication, and mutations are mainly due to base-base mismatches that have escaped the cellular proofreading mechanism of DNA polymerases [47]. Duplication or loss of these repeats often results in frame shift mutations in the open reading frame that alter the amino acid sequence, thereby modifying the protein that is expressed. These frame shifts inevitably lead to mutations in important TSG or oncogenes which eventually contribute to the accumulation of mutations seen in CRC. The MMR system consists of six genes: MutL homolog 1 (*MLH1)*; MutS homolog 2 (*MSH2)*; *MSH3*; *MSH6*; post-meiotic segregation-1 (*PMS1)* and *PMS2* [48, 49]. They function as a back-up mechanism that recognises mutations and degrades the newly-synthesised strand in order to give the DNA polymerase a second chance to repair the DNA. When this MMR system is impaired, genome-wide mutations accumulate during DNA replication, usually within microsatellites, giving rise to MSI and eventually cancer.

The majority of sporadic microsatellite unstable cancers are CpG island methylator phenotype positive (CIMP+), resulting from promoter hypermethylation of the MMR gene *MLH1* [50]. This is in contrast to the mutations in the MMR genes which gives rise to the hereditary Lynch syndrome (LS) (Section 1.1.2.2), suggesting the existence of distinct underlying molecular pathways [51, 52]. For example, CIMP+ tumours are associated with mutations in the *BRAF* gene in both sporadic microsatellite stable and unstable tumours [53-55], which are rare in LS. Also, CIMP+ cancers are more frequently observed in the proximal colon compared to distal colon and rectal cancers [55-58],

indicating that CIMP+ tumours form a clear subgroup within MSI cancers. Screening for MSI in sporadic CRC tumours is important as this may have potential prognostic and therapeutic value. For instance, cancers with high MSI (H-MSI) are reported to have better clinical outcome than low or non-MSI tumours [59-61]. Also, H-MSI tumours are shown to be more resistant to first line drug treatments such as 5-fluorouracil (5-FU) [62-64].

1.1.2.1.3 Microsatellite and chromosome stable tumours

A third subgroup of tumours that are neither CIN nor MSI was first described in 1999 [65]. Georgiades and colleagues observed tumours that were microsatellite and chromosome stable or MACS. Although, subsequent studies have documented this subgroup of tumours in more detail, controversy about the true classification of this group remains. Several studies have demonstrated significant differences in clinicopathologic features of MACS tumours compared to the other two subtypes. For example, MACS tumours are more likely to develop in younger patients [66] and are localised more distal within the colon [67]. They have also shown to be more poorly differentiated [68] and more invasive at the time of diagnosis [56]. By contrast, two studies have demonstrated no significant differences in any clinicopathologic features [69, 70], however it should be acknowledged, that the sample size in the studies mentioned above are relatively small which may be a possible explanation for the opposing conclusions.

Despite the giant leap forward in defining the genetic changes and altered pathways in CRC since the first proposed mechanism by Vogelstein and Fearon, the exact underlying mechanism by which CRC evolves has yet to be defined. Our understanding of the true impact of the many genes identified as involved in the development of CRC remains incomplete. It is likely that only some of these genes are crucial for the survival and migratory phenotype of metastatic cancer cells. It is also quite possible that further oncogenes and TSG genes, that play a key role in the progression in CRC remain to be discovered.

1.1.2.2 Hereditary CRC syndromes

Hereditary CRC syndromes account for around 5% of all CRC cases; these cases are highly penetrant and passed on to the offspring in a Mendelian manner. Hereditary non-polyposis colorectal cancer (HNPCC), or Lynch syndrome (LS) and FAP make up the bulk of these syndromes. More rare CRC syndromes constitute the remainder of cases. The two main forms, LS and FAP will be discussed in more detail below, and all hereditary CRC syndromes are summarised in Table 1.1.

Table 1.1 Hereditary CRC syndromes. LS and FAP are the two main forms of hereditary CRC syndromes, both with high penetrance. Other rare forms of CRC syndromes make up the remaining hereditary CRC cases.

Syndrome	Features	Genetic mutation(s)
Lynch syndrome	Early onset, multiple colorectal polyps, ~80% penetrance	DNA mismatch repair genes, *MSH2*, *MSH6, MLH1*, *PMS2* [71-73]
Familial adenomatous polyposis	100-5000 adenomatous colorectal polyps, 100% penetrance	*APC* [25, 26]
MUTYH-associated polyposis	Multiple adenomatous colonic polyps (10-100)	*MUTYH* [74]
Peutz-Jeghers	Hamartomatous GI polyps (5-100), ~40% penetrance	*LKB1* [75, 76]
Juvenile polyposis	Early onset, Hamartomatous GI polyps (50-200), 10-40% penetrance	*SMAD4*, *BMPR1A* [77, 78]
POLE/POLD1	Early onset, multiple adenomas, dominant inheritence	*POLε/POLD1* [79, 80]

LS is the most common form of hereditary CRC and is an autosomal dominant condition in which individuals development a small number of polyps in the colon. Affected individuals have a cumulative risk of developing CRC of 60-70% in men and 30-40% in women [46, 81]. Patients harbour mutations in DNA MMR genes, most commonly in *MSH2*, *MLH1*, *MSH6* [72, 73] and *PMS2* [71], resulting in MSI. Besides CRC, patients with LS have an increased risk of developing other cancers such as endometrium and stomach cancers [82, 83].

FAP is the best characterised hereditary CRC syndrome where patients carry a mutation in one of the *APC* alleles [25, 26]. The syndrome is characterised by the development of many precancerous colonic polyps at a young age. Over time, the size and number of these polyps can increase significantly, ultimately reaching up to 5,000 in number. A large number of these polyps harbour a second mutation in the *APC* gene, of which the majority (>90%) are nonsense or frameshift mutations leading to a truncated APC protein. Due to the high number of precancerous polyps, nearly all FAP patients go on to develop CRC by the time they reach 40 years of age [84]. Therefore, the recommended management for germ-line mutation-positive members of families with FAP is early surveillance with endoscopy and genetic tests to identify carriers. Total resection of the colon is advised for patients that test positive for FAP (reviewed in [85]).

1.1.3 Diagnosis and treatment of Colorectal Cancer

1.1.3.1 Diagnosis

Over the past decade, the diagnosis of CRC has massively improved mainly due to national bowel cancer screening programmes. Since 2003, men and women between the ages of 60-74 that are asymptomatic are invited to participate in these programmes every two years. They consist of a faecal occult blood test (FOBt), using a kit which can be easily performed at home. Individuals whose samples test positive for traces of blood are

invited for a colonoscopy procedure, which involves the visualisation of the distal part of the colon with a camera. Biopsies are collected for histopathological examination and/or suspicious lesions can be removed during the same procedure. Certain risks are associated with a colonoscopy procedure; major risks such as bleeding and perforation of the bowel wall occurs in approximately 1 in every 1000 procedures [86, 87]. Despite these risks, colonoscopy in combination with FOBt remains the gold standard to evaluate colonic mucosa and detect early adenomas [88]. From March 2013, a new screening test is being piloted in six bowel cancer screening centres. Men and women from the age of 55 are invited for a flexible sigmoidoscopy to identify pre-cancerous polyps [89]. A sigmoidoscopy carries reduced risks compared to a full colonoscopy and this screening pilot will indicate whether similar diagnostic rates may be achieved with this less risky approach. Other techniques including CT and high-resolution MRI are valuable for precise localisation of the tumour and for accurately measuring the spread of the tumour into the surrounding tissue.

Once diagnosed, staging of the tumour is usually done according to the Tumour, Node, Metastasis (TNM) system. This is based on the local invasion, the degree of lymph node involvement, and whether there is any metastasis of the intestinal tumour to distant sites. The system is used to guide treatment management and prognosis and has been under continual refinement and its most recent revision (7^{th}) was published in 2010 [90]. The more advanced TNM staging system has been gradually replacing the Dukes' classification, which was the first clinical staging system [91-93]. In addition to TNM, a much broader staging system using numbers I to IV may be used, in which a higher number depicts a more aggressive cancer. Table 1.2 summarises the features of TNM staging in and shows the comparison to the other staging systems.

Table 1.2 Colorectal cancer staging systems. Overview of TNM staging definitions in CRC in relation to other staging systems.

	Definition
Primary Tumour (T)	
T1	Limited to mucosa and submucosa
T2	Extension intro but not through the muscularis propria
T3	Invasion of perirectal fat
T4	Invasion of adjacent structures
Nodes (N)	
N0	No involved lymph nodes
N1	Fewer than four regional nodes involved
N2	More than four regional nodes involved
N3	Distant nodes involved
Metastasis (M)	
M0	No metastasis
M1	Distant metastasis

Stages	T	N	M	Dukes' Classification
Stage 0	T(in situ)	N0	M0	
Stage I	T1	N0	M0	A
	T2	N0	M0	B1
Stage II	T3	N0	M0	B2
	T4	N0	M0	C2
Stage III	T1, T2	N1 or N2	M0	C1
	T3, T4	N1 or N2	M0	C2
Stage IV	Any T	Any M	M1	D

1.3.1.2 Treatment of Colorectal Cancer

Treatment of CRC is generally a combination of surgery, radiotherapy and chemotherapy; however, the tumour stage and the degree of tumour differentiation usually determine the treatment regime. Also, localisation matters as treatment management for colon and rectal cancers differ dramatically.

1.3.1.2.1 Colon cancer

The treatment of colon cancer is guided by tumour staging and the individual health of the patient. Survival rates for localised CRC (Stage 0 and I) have steadily increased (around 90%), and for these patients surgery alone has a high curative rate [94]. However, despite increasing efforts in the diagnosis of CRC, between 2004 and 2010 only 40% of all CRC cases were diagnosed at stage 0 to I [94]. For the majority of patients with stage II and III (node-positive) disease, post-operative adjuvant chemotherapy is recommended to decrease the risk of recurrence and increase survival rates. The chemotherapeutic agent 5-FU has been the standard first-line treatment for the past 40 years [95]. In recent years, the availability of other compounds in combination with 5-FU have broadened treatment options. Adjuvant treatment with 5-FU/Leucovorin has been shown to increase overall survival in a number of studies [96-98]. This combined treatment now forms the basis of treatment for patients with CRC stage III; the use in stage II CRC tumours is more controversial [99]. In advanced CRC (stage IV) the tumour has spread to neighbouring tissue and distant organs and surgery alone is unlike to cure these cancers. In addition to 5-FU/Leucovorin, compounds such as oxaliplatin (FOLFOX) and irinotecan (FOLFIRI) are often given. Despite the relatively high toxicity and unpleasant side effects, the use of FOLFOX [100-102] and FOLFIRI [103-106] has improved the survival in advanced CRC.

In recent years, research has shed light on the importance of particular molecules/pathways that may serve as potential therapeutic targets. Targeted therapies, such those using monoclonal antibodies, often have less severe side effects and can be

used in combination with other chemotherapy drugs. The use of panitumumab and cetuximab, which target the EGFR pathway, have shown promising potential in improving survival of patients with metastatic CRC when used in combination with conventional therapy such as FOLFOX and FOLFIRI [34, 35, 107-111]. However, some of these studies have demonstrated the efficacy only in *KRAS* wild-type tumours, indicating that *KRAS* mutation status can be used as a negative predictor of response to anti-EGFR treatments [34, 35].

1.3.1.2.2 Rectal cancer

Rectal cancer arises in the most distal part of the large bowel which extends from the end of the sigmoid colon to the anus. Due to its location, the management of rectal cancer is different to that of cancer of the colon. For individuals diagnosed with rectal cancer, assessment of the precise localisation is essential for optimal treatment. Accurate measurement of the tumour spread is generally done with high-resolution MRI in order to establish the depth of invasion in the bowel wall [112]. This pre-surgery work-up of tumour characteristics can significantly improve surgery outcome. Surgery techniques for rectal cancer have dramatically improved over the past century. Abdominoperineal resection (APR), removal of the rectum and the insertion of a colostomy (stoma), was the standard of care for nearly 80 years. Improvements were necessary to address the high mortality rates and morbidity, such as impotence and bladder dysfunction, and to decrease local recurrences. In 1982, the introduction of total mesorectal excision (TME) dramatically changed the management of rectal cancer. This surgery considers the plane of the tissues within the rectum allowing complete removal of the mesorectum, including its surrounding vessels and lymphatic system, which in turn reduces local tumour recurrence [113]. Due to these improvements, TME is now considered the gold standard surgical treatment for rectal cancer.

Neoadjuvant treatment in the form of pre-operative chemoradiation therapy (CRT) is the standard care for all patients with stage II and III rectal cancers. Decreased recurrence

rates are seen with pre-operative CRT compared to post-operative CRT, although trials demonstrated no effect of pre-operative CRT on overall-survival (OS) rates [114, 115]. Despite the controversial debate on the use of neoadjuvant therapy, there is a clear advantage to treating with radiation before TME in order to improve local control [116-118] and survival [119] in locally advanced rectal cancer. The main purpose is to down-size/down-stage the tumour in order to increase the resectability and decrease the chances of recurrence. Also, tumours close to the sphincter (muscle that controls incontinence) require traditional surgery removing the anal opening, necessitating a stoma. Down-sizing of the tumour can potentially allow for a sphincter-sparing TME which can improve quality of life post-surgery [120]. Despite the major improvements in the management of CRC, tumour resistance to current treatment regimens remains a key challenge. There is little understanding of the mechanisms that underlie this resistance. Stratification of patients most likely to benefit from certain treatment will improve outcome and reduce healthcare burden and costs, yet to date, no such prognostic marker has been identified.

1.1.4 Tumour hypoxia

Over the past decades, it has become apparent that the metabolic control of tumour cells and the tumour microenvironment are very important, and need to be considered alongside genetic and epigenetic stress changes to the cancer genome. Low oxygen tension (hypoxia) within solid cancers is one of the major contributions to therapy resistance (reviewed in [121-123]). Also, solid tumours with hypoxic regions have a poor prognosis and higher recurrence rates compared to their non-hypoxic tumours [124, 125]. In the absence of oxygen, tumour cells adapt by activating pathways that promote tumour cell survival and metastatic behaviour, making therapies targeting hypoxia-induced pathways a promising intervention.

1.1.4.1 Hypoxia-induced factors

Many of the cellular responses to hypoxia occur as a result of changes in hypoxia-induced-genes and these genes are under the strict control of hypoxia-inducible-factors (HIFs) [126]. HIF is a heterodimeric transcription factor that is composed of a constitutively expressed HIF-β subunit and one of the three oxygen-regulated alpha subunits (HIF-1α, HIF-2α or HIF-3α). Under normal oxygen concentrations, usually between 3.1-8.7% [127], the HIF-α subunits are rapidly degraded by hydroxylation of key proline residues in the highly conserved oxygen-dependent degradation domain (ODD; Fig. 1.4). Hydroxylation is carried out by specific proline hydroxylase enzymes (PHD1-3) [128, 129], and is necessary for the recognition of HIF-α by the von Hippel-Lindau (VHL) protein. VHL is the recognition component of the E3-ubiquitin-protein ligase complex which directs HIF-α for degradation by the 26S proteasome [130, 131]. As the oxygen tension drops, HIF-α units are increasingly stabilised, however, the oxygen sensing mechanism of HIF hydroxylases is not completely understood. Once stabilised, the HIF-α units will form heterodimers with the HIF-β subunit and translocate to the nucleus. Here, it activates transcription through interaction with cofactors CREB-binding protein (CBP) and p300. Evidence has emerged that these heterodimers bind directly to genes that contain hypoxia-responsive-elements (HRE) through the use of prediction tools and expression microarray analysis [132] and chromatin immunoprecipitation (ChIP) in combination with DNA microarray [133, 134] or gene expression arrays [135]. Furthermore, ChIP in combination with sequencing techniques enabled identification of additional HIF targets in alternative promoters and even in putative non-coding, intergenic regions [136]. In contrast to the main subunit HIF-1α, which is ubiquitously expressed, HIF-2α expression is restricted to particular cell types, including vascular endothelial cells, lung type II pneumocytes, cardiomyocytes and interstitial cells in the kidney [137]. Finally, HIF-3α has less amino-acid sequence homology with HIF-1α and HIF-2α and its regulatory mechanism is not fully understood [138].

Interestingly, a DNA microarray study revealed that over 2% of all human genes are directly or indirectly targeted by HIF-1α in endothelial cells [139]. Many of these targets have been shown to be involved in pathways such as cell survival, angiogenesis, tumour metastasis, and energy metabolism and will be discussed in more detail below.

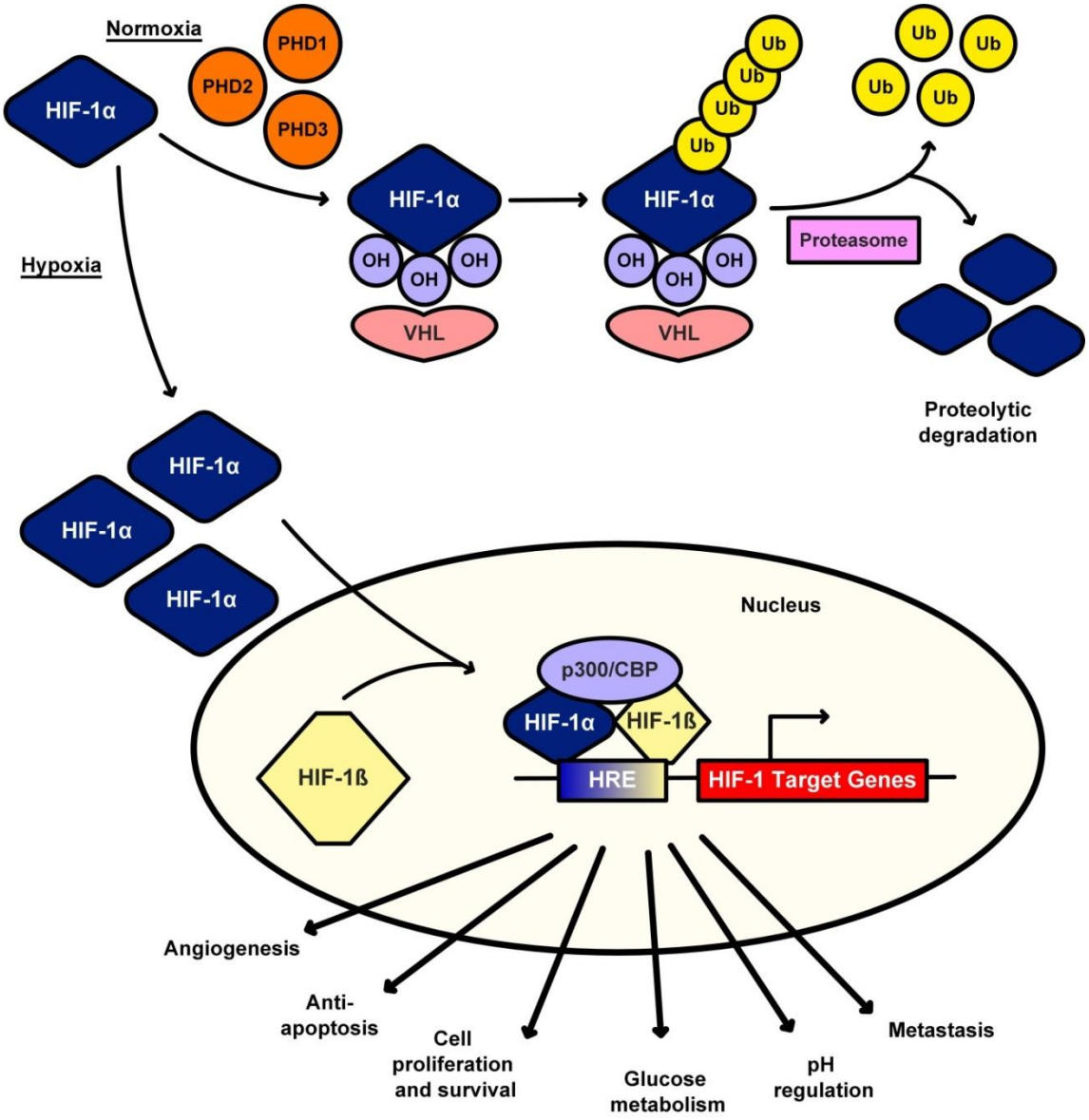

Figure 1.4. Stabilisation of hypoxia-inducible factor-1α by proline hydroxylation. In the presence of oxygen, hypoxia-inducable-factor 1 α (HIF-1α) is hydroxylated by prolyhydroxylases (PHD1-3) and targeted for ubiquitination, resulting in degradation by proteasomes. Under hypoxia, HIF-1α is stabilised and translocates to the nucleus. Here, it dimerises with HIF-1β and forms a complex with transcription factors p300/CBP, which allows transcription of target genes. HIF-1α regulates target genes involved in a wide spectrum of cellular pathways necessary for cells to adapt in hypoxic conditions. VHL, Von Hippel-Lindau; OH, Hydroxyl radical; Ub, ubiquitin; HRE, hypoxia response element. Figure adapted from [140].

1.1.4.2 Angiogenesis

Tumour expansion rapidly distances the tumour cells from local blood supply, thereby limiting access to oxygen and nutrients. In these situations, small molecules will fail to reach tumour cells and promote the production of signals that initiate the formation of new blood vessels from nearby pre-existing capillaries, a process called angiogenesis [141]. Key genes involved in angiogenesis are vascular endothelial growth factor (*VEGF*), angiopoietin 1 and 2 (*ANGPT1* and *ANGPT2),* placental growth factor (*PGF*), and platelet-derived growth factor B (*PDGFB*). In particular, VEGF stimulates the proliferation of endothelial cells to control the formation of new blood vessels and seems to be the key step to initiate angiogenesis [142, 143]. Early studies demonstrated that VEGF is up-regulated in a range of tumours, including CRC, and increased expression of VEGF in CRC is correlated with poor prognosis and survival [144]. For this reason, in the early 1990s, researchers focussed on angiogenesis blockers as a potential treatment for various tumours. The anti-VEGF monoclonal antibody (bevacizumab) was reported to potentially inhibit growth of tumour cell lines in mice [145], and clinical trials of chemotherapy combined with bevacizumab in metastatic CRC showed an increase in survival [146-148]. Therefore, the inhibition of angiogenesis with monoclonal antibodies may prove to be an important addition to the spectrum of treatment for CRC.

1.1.4.3 Tumour metastasis

Hypoxia is a crucial environmental factor that promotes cancer cells to dislodge from the intestinal tumour and induce cell migration to distant tissue and organs, called metastasis. The metastatic process is complicated and multifaceted and involves the coordination of various steps such as angiogenesis, epithelial-mesenchymal transition (EMT), extracellular matrix (ECM) modulation, extravasation out of the intestinal tissue, circulation, and intravasation and growth in secondary organs. Besides angiogenesis, HIF-1α target genes have been shown to be involved in each of the steps crucial for tumour metastasis (reviewed in [149]). For example, important EMT regulators, such as twist related protein 1 (TWIST1) [150], zinc finger protein SNAI1 (SNAIL) [151],

transcription factor 1 (TCF1), zinc finger e-box-binding homeobox 1 (ZEB1) and ZEB2 [152], have been shown to be regulated by HIF-1α and induce EMT and tumour cell dissemination. Furthermore, HIF-1α also increases the production of metalloproteinases (MMPs), such as MMP-1 and MMP-2, promoting intravasation [153]. Evidence of the involvement of hypoxia in many aspects of the metastatic process has enhanced our understanding of the key players in this process. This has provided novel potential therapeutic targets for anti-metastatic drugs in cancer therapy.

1.1.4.4 Energy metabolism

Tumour cells adapt to low oxygen conditions by down-regulating metabolic processes, such as mitochondrial oxidative phosphorylation, to reduce ATP utilisation. Under hypoxic conditions, tumour cells metabolise primarily glucose into lactate to meet most of their energy needs. This suppression of respiratory rate is predominantly orchestrated by HIF-1 (reviewed in [154]). Under normal oxygen conditions, pyruvate derived from the glycolytic pathway is converted into ATP through the tricarboxylic acid cycle (TCA) cycle. Hypoxia-induced expression of HIF-1 diminishes the rate of the TCA cycle by down-regulating the expression of pyruvate dehydrogenase kinase 1 (PDK1) [155, 156], a key enzyme for the initial step of the TCA cycle. As a consequence, pyruvate is converted into lactate by lactate-dehydrogenase A (LDH-A), which is induced by HIF-1 [157]. Furthermore, HIF-1 induces the expression of glucose transporters 1 and 3 (GLUT1, GLUT3) [158-161] further promoting the cellular glycolytic phenotype under hypoxic conditions.

Altered metabolism in tumour cells was observed as early as 1920s by Otto Warburg, who noticed that tumour cells were able to sustain high glycolytic rates even in the presence of abundant oxygen, commonly called the “Warburg effect” [162]. Notably, a wide spectrum of human cancers have since been shown to have high glycolytic rates [163]. This feature is now exploited in clinical oncology to detect a variety of cancers

including lung, CRC and breast cancer [164]. PET scans use the glucose analogue FDG to detect regions of high glucose uptake. To date, it is largely unknown why cancer cells maintain a high glycolytic rate under aerobic conditions, as this is far less efficient in producing ATP from glucose than the TCA cycle (two ATPs by glycolysis vs 36 ATPs via the TCA cycle). One hypothesis is that these cells have been exposed to low oxygen conditions previously and are, therefore, selected on their ability to adapt to harsh environments and compete for energy [165, 166]. Evidently, high aerobic glycolytic rates confer a significant proliferative advantage during malignant transformation. More complete understanding of the molecular and physiological consequences of this glycolytic phenotype might reveal potential targeted therapies in cancer.

1.1.4.5 Anti-HIF therapeutic strategies

As a master regulator of downstream cellular pathways under hypoxic conditions, HIF-1 is the most promising therapeutic target because hypoxic conditions trigger the activation of cellular pathways that are not generally induced in normal tissue [167]. Silencing of HIF-1 expression by gene interference has previously demonstrated anti-tumour activity *in vitro* and *in vivo* [168, 169]. However, validation of HIF-1 inhibitors *in vivo* is hampered by a lack of biomarkers consistently associated with HIF-1 in tumour tissue. Also, the HIF-1 inhibitors developed so far lack specificity and so HIF-1 inhibition cannot be separated from the off-target effects of these small molecules. Overcoming this challenge is essential before any potential therapeutic agents can be moved into a clinical setting. Nevertheless, two anti-HIF-1 small molecules, PX-478 [170, 171] and EZN-2208 [172, 173], have entered phase I clinical trials in patients with metastatic cancer after promising anti-tumour activity was observed in pre-clinical models. Results from these trials will provide insights into the therapeutic effect of blocking HIF-1 signalling in cancer patients. However, better molecular understanding of hypoxic pathways, such as how metabolic pathways in cancer are altered, is needed to improve patient selection for targeted treatment regimes and treatment-response monitoring.

1.2 Crohn's disease

1.2.1 Background

CD is one of the two types of IBD which, together with UC, forms a group of inflammatory conditions of the small and large intestine. Clinically, CD is a systemic relapsing-remitting disease with episodes of acute inflammation that predominantly affects the terminal ileum and colon [174]. CD causes significant morbidity with symptoms including abdominal pain, diarrhoea, rectal bleeding and weight loss. Incidence rates are higher in the western world compared to developing countries, with the USA and northern Europe having the highest rates. The aetiology of CD is not fully understood despite large cohort studies having provided strong evidence for the contribution of various influences including genetic susceptibility, environmental triggers and altered immune responses.

1.2.2 Genetic factors and environmental factors

Family history is a major risk factor for IBD with approximately 5-10% of all patients having a positive family history [175, 176]. For CD specifically, reports have shown a relative risk of 14 for relatives with patients with CD [177-179]. However, twin studies report a modest concordance between identical twins ranging from 20 to 50% [180-182], indicative of strong non-genetic components such as environmental triggers.

Early linkage mapping studies in 1996 described the first locus associated with CD (inflammatory bowel disease 1, *IBD1*), which was shared amongst affected individuals [183]. This region was later identified as nucleotide-binding oligomerisation domain containing 2 (*NOD2* or *CARD15)* [184] and is associated with susceptibility to CD [185, 186]. The protein encoded by the *NOD2* gene is an intracellular pattern recognition receptor that senses part of the bacterial peptidoglycan muramyl dipeptide (MDP). Therefore, mutations detected in this gene may be responsible for altered

immunorecognition of bacterial flora leading to unnecessary inflammation and susceptibility to CD [186]. However, *NOD2* mutations are not considered to be the initiating factor for CD. Only 20% of CD cases carry mutations in *NOD2* and these mutations are not linked with CD onset in Japanese individuals [187]. Also, NOD-2 deficient mice do not develop any spontaneous inflammatory lesions [188, 189]. More recently, genome-wide association studies (GWAS) have advanced our understanding of the role of genetics in CD aetiology. In 2005, a report identified genomic regions such as tumour necrosis factor (TNF) superfamily member 15 (*TNFSF15*) which encodes for TNF ligand related molecule 1 (TL1A), to be associated with CD susceptibility [190]. Also, genes implicated in autophagy in CD, including variants in autophagy-related 16-like 1 gene (*ATG16L1*) and immunity-related GTPase family M (*IRGM*), are susceptibility factors for CD [191-194]. Nevertheless, the contributions of genetic factors are complex and despite successful identification of susceptible loci, the precise functional allele or causative gene(s) in CD have not yet been defined.

1.2.3 Fibrostenosing phenotype in Crohn's Disease

The disease progression of CD can be grouped into three categories: inflammatory; penetrating/fistulating and a fibrostenosing phenotype. Within 10 years of diagnosis, approximately 37% of CD patients move from an inflammatory phenotype onto a penetrating/fistulating phenotype and 30% progress to a fibrostenosing disease phenotype [195]. Fistulas are abnormal connections of two body cavities, such as the rectum and the vagina, and usually require surgical intervention. The fibrostenosing phenotype has significant implications for the patient's health. For example, the estimated lifetime risk of surgery for patients with CD is as high as 70% [196]. Current medical therapies are unable to reverse fibrosis once a stricture has developed, and the removal of the narrowed tract represents the main indication for surgery in CD [197]. The surgical burden of disease has diminished since the introduction of biological therapy, but the costs related to surgery still accounts for a fifth of the total direct costs associated with management of CD [198]. The key initiatory and regulatory steps in the development of intestinal fibrosis

remain largely unknown. Downstream events in the process of intestinal fibrosis in CD include excessive synthesis and deposition of ECM components by mesenchymal cells such as intestinal myofibroblasts. A complex interplay between mesenchymal cells, inflammatory cascades, intestinal microbiota, pro-fibrotic mediators and the ECM itself suggests that fibrogenesis, once initiated, is a self-potentiating process (Fig. 1.5).

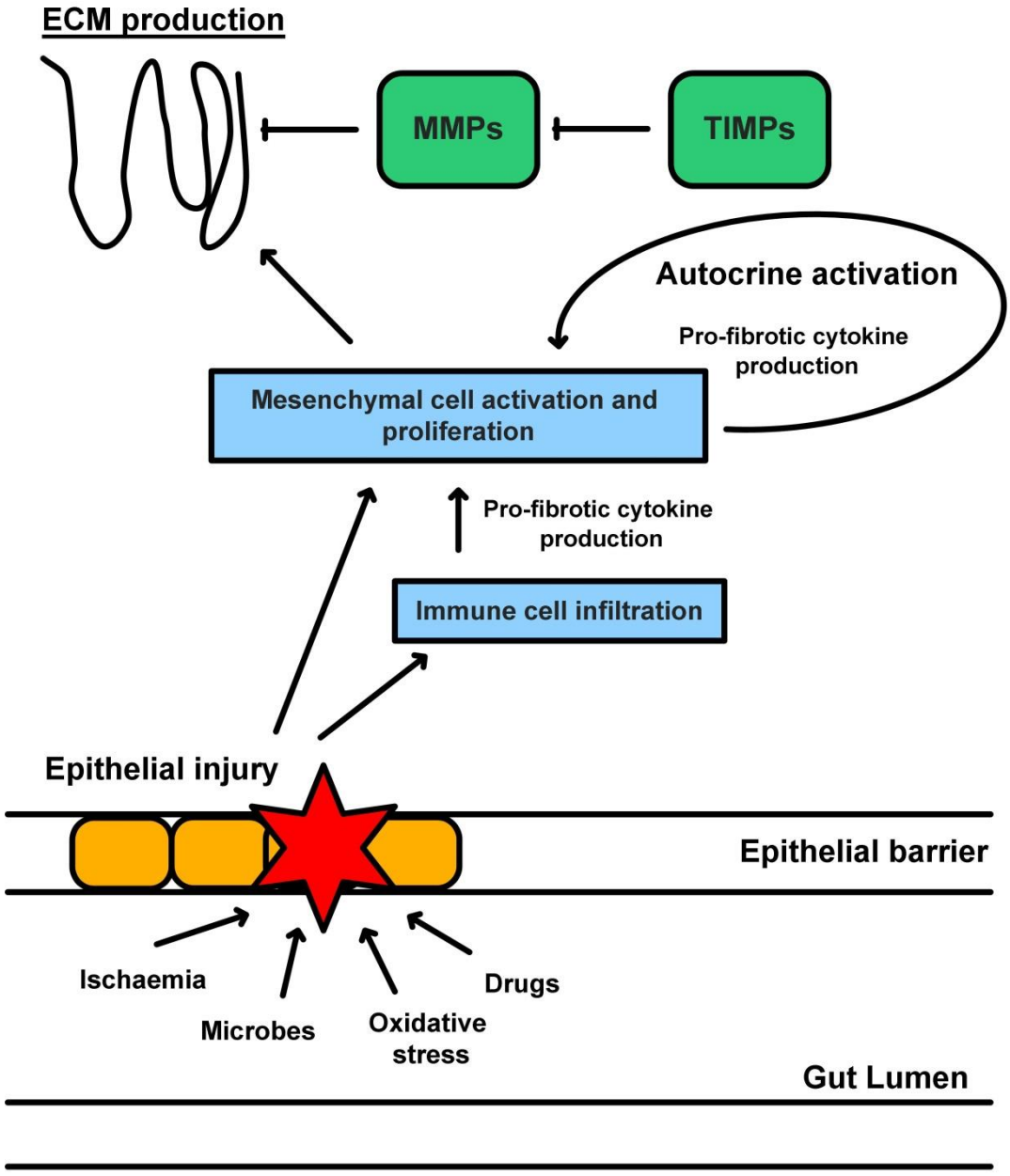

Figure 1.5. Schematic representation of the principle events responsible for the initiation and potentiation of fibrosis in the intestine. Epithelial injury and increased intestinal permeability result from gut ischaemia, oxidative stress and potentiation of injury by microbes and drugs. This leads to infiltration of immune cells into the intestinal wall which results in mesenchymal cell activation and proliferation via the secretion of pro-fibrotic cytokines and mediators. The mesenchymal autocrine mechanism allows the self-potentiation of fibrosis independently of inflammation. Finally, a balance exists between MMPs and TIMPs that ensures the regulation of ECM composition. ECM, extracellular matrix; MMPs, matric metalloproteinases; TIMPs, tissue inhibitors of matrix metalloproteinase. Figure adapted from [199].

There are still significant gaps in our knowledge of the complex network of fibrotic mediators in the development of fibrosis. Mounting evidence implicates the pro-fibrogenic cytokine TGF-β, in particular TGF-β1, as the main driver in fibrosis in various organs including the CD intestine [200-204]. TGF-β1 acts by binding to TGF-β receptor type II, subsequently activating and phosphorylating receptor type I [205] (Fig. 1.6). The resulting receptor complex phosphorylates Smad2 or Smad3, recruits Smad4, resulting in the translocation to the nucleus. Here, the complex binds to transcriptional co-activators, such as p300/CBP [206], to initiate gene transcription of various genes. In contrast to Smad2 and Smad3, Smad7 acts as an inhibitor of the TGF-β signalling pathway [207].

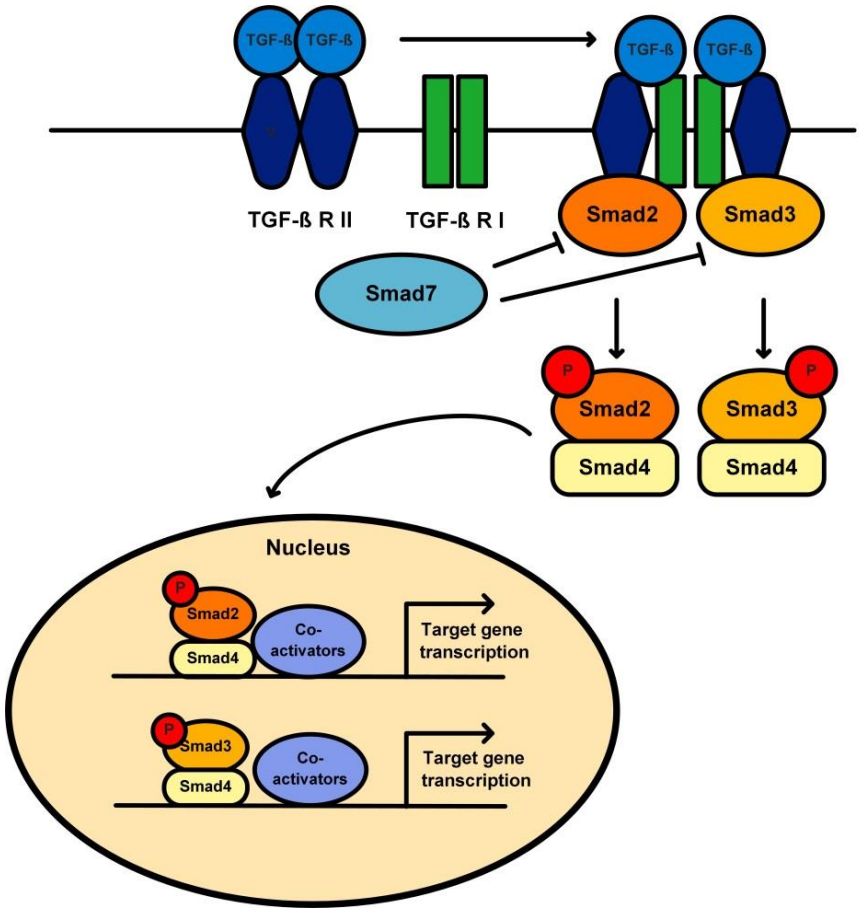

Figure 1.6. The TGF-β signalling pathway. Soluble TGF-β1 binds to the TGF-β receptor II (TGF-β R II) to initiate the formation of receptor complexes with TGF-β receptor I (TGF-β R I). Following phosphorylation of both Smad2 and Smad3, co-Smad4 aids accumulation in the nucleus. Within the nucleus, gene transcription is initiated with the help of other co-activators and transcription factors. Smad7 act as an antagonist, inhibiting the formation of Smad2/3 and Smad4 complexes. Figure adapted from [208].

TGF-β regulates the remodelling of the ECM by increasing the expression of a spectrum of molecules such as collagen I [209, 210], collagen II [209, 211, 212], collagen III [209, 210, 213], collagen IV [214-216], as well as the basement protein laminin [217-219] and interstitial matrix molecule fibronectin [217, 218, 220, 221]. In addition, TGF-β down-regulates collagenases (enzymes that break down collagen) MMP-1 [222-224], MMP-8 [222] and MMP-13 [222, 224-226] directly or indirectly via the up-regulation of their endogenous inhibitors TIMP-1 [223, 227-229], TIMP-2 [214, 223] and TIMP-3 [227, 230-232]. The overall net effect of these events shifts the equilibrium towards an increase in ECM protein deposition eventually leading to fibrosis.

Despite recent advances, our knowledge of the upstream factors that initiate and regulate stricture formation in CD remains very limited. Further functional studies are warranted to uncover potential therapeutic strategies to prevent or reverse fibrosis and relieve the surgical burden of CD patients. There is current unmet need for biomarkers that may indicate the presence of on-going fibrosis or predict which CD patients are at high-risk of developing a fibrostenosing phenotype (reviewed in [199]). miRNAs are a novel class of RNA regulators that have been implicated in many biological signalling pathways including cancer and fibrosis. To date, very little is known about the role of miRNAs in the control of fibrosis, in particular intestinal fibrosis.

1.3 MiRNAs

1.3.1 Background

MiRNAs were first discovered by Lee and colleagues in 1993, who reported that the gene lin-4 does not code for a protein but instead produces a pair of small RNAs [233]. These RNAs were shown to have complementarities to multiple sites in the 3' untranslated region (UTR) of the lin-14 gene [233] and this 3'UTR region was previously proposed to mediate repression of lin-14 product [234]. These initial observations demonstrated that components of the genome traditionally considered non-functional have regulatory capacity. High-throughput sequencing has led to the discovery of novel miRNAs [235-240], many of which still need to be functionally validated. miRNAs have the potential to regulate over hundreds of different mRNAs and, in turn, a single mRNA can be targeted by numerous miRNAs, resulting in the modulation of important biological pathways involved in proliferation, apoptosis and differentiation [241].

1.3.1.1 MiRNA biogenesis

MiRNAs are endogenous, small non-coding RNAs consisting of 20-23 nucleotides that are involved in post-transcriptional regulators of gene expression. Like messenger RNAs (mRNA), miRNAs are transcribed by RNA polymerase II (Fig. 1.7) [242, 243] and can be derived from independent genes or from introns of protein-coding genes. More than half of all miRNAs are clustered along the genome and are transcribed as a single polycistronic precursor RNA molecule that can mature into many individual primary miRNAs transcripts. Typically, there are two or three miRNA genes in a cluster, although, larger clusters have also been identified. For example, the miR-17/92 cluster consists of six miRNAs [244, 245], and the two largest clusters in the human genome are on chromosome 19 (Chromosome 19 miRNA cluster, C19MC [246, 247]) and chromosome 14 (C14MC [248]) which contain 46 and 52 miRNAs, respectively.

Clustered miRNAs tend to have similar sequences and are therefore thought to target similar genes or genes within the same cellular pathway. The double stranded primary miRNA (pri-miRNA) transcripts are cleaved by the Drosha/DiGeorge syndrome chromosomal region 8 (DGCR8) microprocessor complex following transcription to give rise to the precursor miRNAs (pre-miRNA). During this process, the RNase III enzyme Drosha cleaves at the 5' and 3' arms of the pri-miRNA hairpin while DGCR8 functions as a molecular ruler to determine the precise site of cleavage [249, 250]. The pre-miRNA is then exported from the nucleus into the cytoplasm by the GTP-mediated Exportin-5, where it is processed into a 20-23 nucleotide long miRNA/miRNA* duplex [251] by Dicer/Argonaute (Ago). The guide strand (miRNA) remains associated with Ago forming a RNA-Induced Silencing Complex (RISC) (Fig. 1.7). The passenger strand (miRNA*) is conventionally degraded shortly after the unwinding process although reports have demonstrated that these strands can also act as guide strands [252-254]. To avoid confusion, the nomenclature of miRNA has shifted towards the use of miR-3p (from the 3' arm) and -5p (from the 5' arm) for each miRNA strand. This alternative nomenclature (-3p and -5p) will be used for the remainder of this thesis.

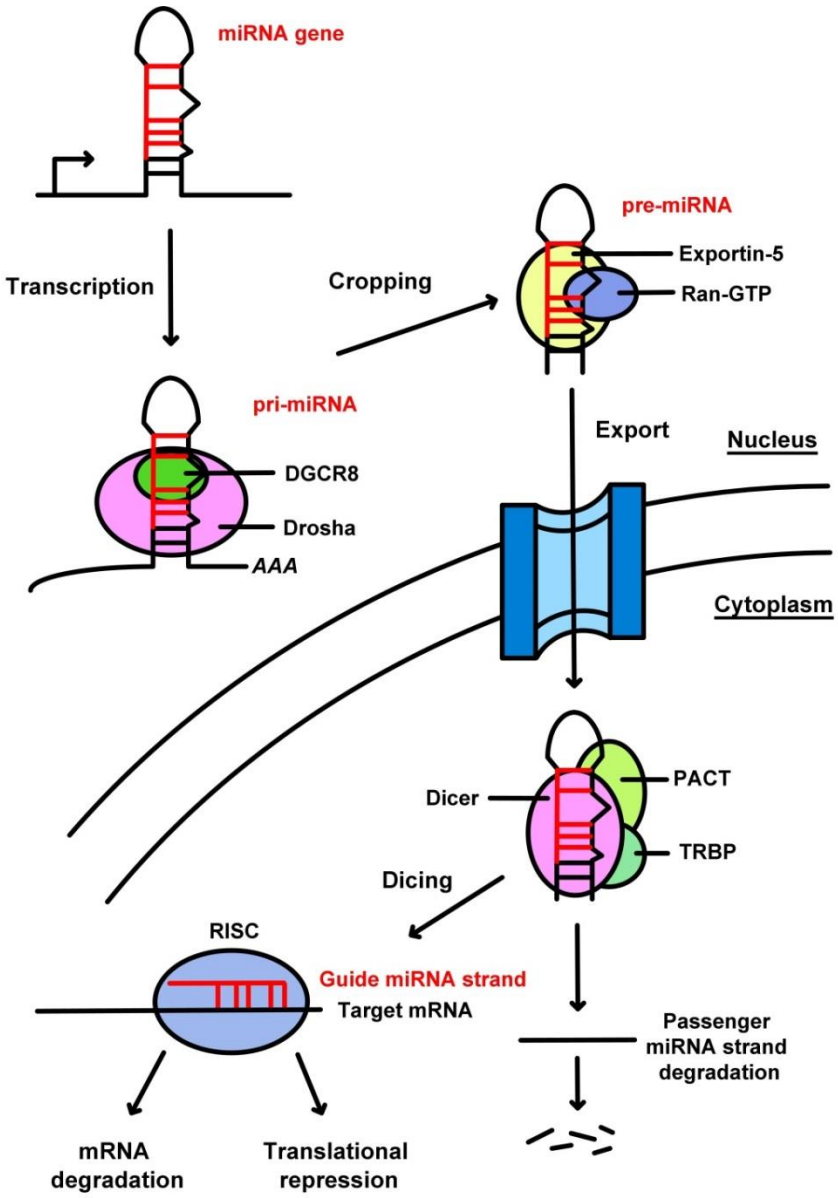

Figure 1.7. miRNA biogenesis and RNA interference. MiRNAs are non-coding RNAs that are transcribed from independent miRNA genes or intragenic regions. Pri-miRNAs are cropped by Drosha and DGCR8, and exported out of the nucleus by the Exportin-5/Ran-GTP transporter. In the cytoplasm, the pre-miRNA is spliced by Dicer, and gives rise to the mature miRNA, which in turn is associated with Ago proteins to form the RISC complex. Gene target repression is mediated through mRNA cleavage or translational inhibition. DGCR8, DiGeorge syndrome chromosomal region 8; TBRP, TAR RNA-binding protein; PACT, proteinactivator of the interferon induced protein kinase; RISC, RNA induced silencing complex. Figure adapted from [255].

1.3.1.2 MiRNA target repression

The binding of a miRNA to its mRNA targets occurs through complementary Watson-Crick base pairing within the 5'-UTR, 3'-UTR or the coding sequence (CDS) of the mRNA, although pairing at the 3'-UTR is most often seen [256]. Conserved base pairing is centered on nucleotides 2-7 at the 5' end of the miRNA, the so-called "seed region" [257, 258]. MiRNAs repress target gene expression in two main manners, namely mRNA degradation or translation inhibition. In plants, miRNAs display a high degree of sequence complementary to their target genes which allows mRNA degradation through cleavage of the mRNA transcripts [259-261]. For animal miRNAs, it remains controversial to what extent each mode of action contributes to the regulation of the target genes [262]. Initial high-throughput methods indicated that miRNAs predominantly function through mRNA degradation [263]. However, re-analysis of this data revealed a large amount of translation repression [264]. In support of this, other studies have also demonstrated miRNA-mediated translational repression without mRNA degradation [265-268]. The primary function of miRNAs is now thought to involve interference with the translational initiation process [265, 269-273]. In addition, miRNAs have been shown to mediate up-regulation of gene targets [274, 275], which are predominantly observed under specific conditions such as cellular quiescence [275]. The miRNA-mediated regulation of the transcriptome involves a complex network with many aspects, including biogenesis and regulatory mechanisms, still requiring full elucidation.

1.3.2 MiRNAs in colorectal cancer

MiRNAs play significant roles in regulating protein expression and thus have a role in regulating a variety of cellular signalling pathways. Not surprisingly, miRNAs are often dysregulated in various diseases, including cancers and have been extensively studied and reported (more than 15,000 hits on Pubmed for "microRNAs AND cancer", as of 07/05/2015). Calin and colleagues first demonstrated a role for miRNAs in cancer when they showed deletion and down-regulation of miR-15 and miR-16 in lymphocytic leukaemia [276]. Since then, aberrantly expressed miRNAs have been documented in

nearly every cancer (reviewed in [255]). Furthermore, deep sequencing and miRNA microarrays have consistently demonstrated altered miRNA expression patterns in CRC tumours compared to normal tissue (reviewed in [277]). Most human miRNAs are located in regions vulnerable to amplification or deletions and can, therefore, function as oncomiRNAs [278] or tumour suppressor miRNAs [279]. No less than 20 different studies have reported altered miRNA expression profiling between CRC tissue samples and normal tissue (reviewed in [277]). Important miRNAs that have been implicated in the tumourigenesis of CRC in more than one study are discussed below.

1.3.2.1 OncomiRNAs

miR-135b. Oncogenic miR-135b is up-regulated in CRC [280-284]. Functional 3'-UTR luciferase reporter assays demonstrated that miR-135 can directly repress the expression of *APC* [281] thereby associating miR-135 with the Wnt signalling pathway, which is frequently mutated or repressed in the early stages of CRC. *In vivo* studies show that silencing miR-135b significantly reduces tumour number and load in an animal CRC model [285], suggesting miR-135b may be a potential therapeutic target for CRC treatment.

miR-21. miR-21 is one of the most intensively studied oncogenic miRNAs. Its up-regulated expression has been demonstrated in CRC tumours [286], and correlated with lymph node positivity and the presence of distant metastases [287]. MiR-21 is involved in the majority of oncogenic cellular pathways including cell proliferation, invasion, apoptosis and metastasis; however, reports have shown that miR-21 exerts its function mainly through the inhibition of cellular apoptosis [288, 289]. Many targets involved in apoptosis have been shown to be directly targeted by miR-21 including TSG programmed cell death 4 (*PDCD4*) [290], B-cell CLL/lymphoma 2 (*BCL2*) [291, 292] and FAS ligand (*FASLG*) [293]. In addition, in colon cancer cells, miR-21 is induced by DNA damage and serum starvation, subsequently repressing the expression of cell division cycle 25A (*CDC25A*) resulting in modulation of cell cycle progression [294].

1.3.2.2 Tumour suppressor miRNAs

Let-7 family. One of the most abundantly dysregulated miRNAs in human cancers is the let-7 family. In humans, this family is composed of 13 members located on eight different chromosomes [295]. Members of the let-7 family are often down-regulated in various cancers including lung [296], gastric [297], ovary [298], and CRC [299]. Gene targets of this family include cell cycle regulators and promoters of growth, including *KRAS* and v-myc avian myelocytomatosis viral oncogene homolog (*MYC)*, and their expression represses cell proliferation and growth [296, 300]. Interestingly, recent studies demonstrate that let-7a expression is increased in metastatic CRC with activating *KRAS* mutations [301] and high levels of this miRNA might rescue anti-EGFR treatment in metastatic CRC [302].

miR-143/145. In 2003, Michael and colleagues were the first to demonstrate repressed levels of miR-143 and miR-145 in CRC compared to normal tissue [303]; this has been subsequently validated by others [304]. Both miRNAs are transcriptional targets of the p53 pathway [305, 306] and can regulate cell growth and proliferation *in vivo* and *in vitro* [304]. MiR-143 suppresses cell growth by directly repressing translation of *KRAS* [307], DNA methyltransferase 3A *(DNMT3A*) [308] and extracellular-signal-regulated kinase 5 (*ERK5*) [309], whilst miR-145 targets insulin receptor substrate 1 (*IRS-1*) [310] and *MYC* [306] to propagate its tumour suppressor activity.

miR-34a. Another direct target of the TSG p53 is miR-34a [311-316], which has been reported to be lost in CRC tissue compared to normal tissue [317-319]. Similar to the pro-apoptotic function of p53, miR-34a regulates several cellular events including cell cycle, migration and apoptosis [311, 320]. MiR-34a targets sirtuin 1 (*SIRT1*), a histone deacetylase, and its down-regulation activates p53 activity creating a positive feedback loop [321]. P53-independent activation of the IL-6R/STAT3/miR-34a feedback loop suppresses CRC tumour progression *in vivo* in mice [322], demonstrating the existence of alternative upstream regulators of miR-34a.

1.3.2.3 MiRNAs in hypoxia

As discussed previously, hypoxia is one of the environmental conditions linked to tumour growth as well as resistance to treatment (Section 1.1.4). Initial reports examined the changes in expression of miRNAs to alterations on oxygen tensions [323]. Here, a robust signature of 27 miRNAs was identified in a variety of cell types under 0.2% oxygen [323]. One of the miRNAs that has been robustly shown to be induced under hypoxic conditions is miR-210. This miRNA is up-regulated in various hypoxic cell lines [323-328] and its up-regulation is mediated through HIF-1 binding at the HRE binding site in the promotor of miR-210 [329-331]. The function of miR-210 has now been intensively studied and has been implicated in a number of cellular pathways including cell cycle regulation [326, 332, 333], angiogenesis [334-337] and cellular metabolism [338-342]. However, opposing results suggest that miR-210 could act as an oncogene as well as a TSG (reviewed in [343]). For example, miR-210 can promote cancer cell proliferation by inhibiting the pro-apoptotic protein E2F transcription factor 3 (*E2F3*) [344]. In contrast, other reports have suggested a pro-apoptotic role for miR-210 via targeting the fibroblast growth factor receptor like-1 (*FGFRL1*) [345]. These contradictory observations suggest that the role for miR-210 under hypoxia is cell type and context dependent. However, these findings are still in accordance with the heterogeneity of the hypoxic response which can influence both cell death and cell survival [346]. Furthermore, miR-210 affects cellular metabolism by directly targeting iron-sulfur cluster assembly proteins (ISCU1 and ISCU2) [339-342]. These proteins are predominantly responsible for mitochondrial respiration and energy production. MiR-210-mediated down-regulation of ISCU1/2 results in a decreased metabolic activity and corresponds with the HIF-dependent decrease in TCA cycle [155]. This, in turn leads to increased glycolysis, eventually controlling cellular survival during hypoxic stress.

The expression of miR-210 is up-regulated in a variety of cancers including breast [325, 347-349], head and neck [350, 351], pancreatic [352-354], lung [355-357], renal [342,

358, 359] and ovarian cancer [360]. Therefore, elucidating the role of miR-210 in CRC would provide further insights into this hypoxamir in solid tumours.

1.3.3 MiRNAs in Crohn's disease

Studies investigating altered miRNA expression in IBD including CD are very limited. To date, two studies have identified altered miRNA expression between CD and healthy control tissue [361, 362]. A number of miRNAs were significantly increased in CD tissue compared to healthy controls. Worryingly, there was only limited overlap between the two reports (reviewed in [199]). Also, no comprehensive analysis of the role of these miRNAs in intestinal fibrosis has been performed. By contrast, miRNAs expression profiles of fibrosis in other organs have been extensively documented (summarised in Table 1.3). Selected miRNAs important in the development of fibrosis are outlined below.

miR-200 family. The miR-200 family (miR-141, -200a, -200b, -200c and -429) regulate EMT, a major contributor to fibrosis of the kidney [363-365], heart [366], and liver [367, 368]; here, loss of E-cadherin is a classic hallmark. Furthermore, animal studies have identified a role for EMT in the development of intestinal fibrosis [369]. Down-regulation of the miR-200 family is considered a characteristic feature of EMT [370]. This family is thought to modulate EMT through targets such as *ZEB1* and *ZEB2*, which are transcription repressors of E-cadherin [370], resulting in a reduction of E-cadherin. Recent studies have demonstrated that overexpression of miR-200 family members increased E-cadherin expression and hindered EMT *in vitro* [371].

miR-29 family. Altered expression of the miR-29 family has been implicated in the pathogenesis of fibrosis in various organs. For example, the expression all three members is reduced in fibrosis of the kidney [372, 373] and liver [374]. Additionally, miR-29b is down-regulated following myocardial infarction [375], in the lungs of patients with

idiopathic pulmonary fibrosis [376, 377] and in skin fibroblasts of patients with systemic sclerosis (SSc) [378]. MiR-29 regulates directly the levels of ECM molecules by targeting the 3'-UTR of various collagen genes including *COL1*, *COL3* and *COL4* [375, 378, 379]. Importantly, for its role in intestinal fibrosis, miR-29 expression is inhibited by LPS stimulation and TNF-α treatment in a NFκβ-dependent manner [374], suggesting a link between inflammation and fibrosis. In addition, the expression of miR-29 is also modulated by histone-deacetylases (HDACs). Low levels of miR-29b are associated with high HDAC-2 expression in models of Duchenne's muscular dystrophy where fibrosis is a significant feature of the disease phenotype [380, 381]. Conversely, miR-29 expression is increased by application of class II HDAC inhibitors in hepatic stellate cell activation [382], suggesting that epigenetic DNA modifications may also have a role in the regulation of miR-29 and therefore have relevance in the treatment of fibrosis.

Table 1.3 miRNAs altered in fibrosis. Dysregulated miRNAs in fibrosis of various organs. MiRNAs that were dysregulated in two or more organs were included.

MiRNA	Organs	Anti-/pro-fibrotic	Role
miR-132	Heart, liver	Anti	Inhibits myofibroblast differentiation [383, 384]
miR-15/miR-16	Liver, lung	Anti	Increases apoptosis signalling [385, 386]
miR-155	Liver, lung	Pro	Inhibits mesenchymal-epithelial cross talk [387, 388]
miR-17/92	Liver, heart, lung	Anti	Down-regulates *CTGF* and *TSP-1* [389-391]
miR-199a/b	Heart, lung	Pro	Increases ECM production [392, 393]
miR-200a/b	Kidney, liver	Anti	Decreases TGF-β signalling and TGF-β-mediated EMT [387, 394, 395]
miR-21	Lung, heart, kidney	Pro	Activates TGF-β signalling via *SMAD7* repression [396-398]
miR-29	Skin, heart, lung, kidney, liver	Anti	Down-regulates various ECM molecules [372-378]
miR-30c	Heart, lung	Anti	Down-regulates CTGF signalling [384, 390]

1.3.4 MiRNAs in the clinic

Cancer remains a leading cause of death worldwide due to lack of early detection, the inability to predict recurrence after treatment and a shortage of targeted or tailored therapies directly appropriate to the patient and their cancer. Given that survival and prognosis are dependent on the tumour stage at the time of detection, diagnostics tools for early detection are extremely important. In particular, there is a significant need for biomarkers that can be used for screening in a non-invasive manner for diagnosis, disease progression, outcome and response to therapy. One of the key advantages of using miRNAs as biomarkers is their low degradation rate compared to mRNA or protein, and the ease with which they can be detected in frozen or fixed tissue as well as a range of biological fluids, such as blood [399, 400], urine [401] and faeces [402].

1.3.4.1 Diagnostic miRNAs in CRC

Early profiling data demonstrated that miRNAs could classify different tumour types including CRC [279, 403]. Interestingly, these studies indicate that miRNAs may be more reliable than mRNA profiles in the same samples, indicating the potential of miRNAs for profiling in cancer diagnosis. Current screening methods for CRC (FOBt) lack sensitivity which means a large number of cancers may be missed [404] (approximately 30-50%; [405]), and further highlighting the need for better biomarkers. Early reports demonstrated that Cox-2 mRNA levels in faeces successfully detected 20 out of 29 CRC cases [406] and this significantly increased when used in combination with MMP7 mRNA [407], suggesting that RNA molecules could potentially be used for early cancer diagnosis. More recently, a number of studies have since investigated the expression levels of miRNAs in stool samples for diagnostic purposes. miR-143 and miR-145 were decreased in the stool of CRC patients [402, 408], which is in accord with the down-regulation of both miRNAs observed in CRC tissue [303, 309]. Further studies have detected altered miRNA expression in CRC stool samples with reasonably high sensitivity and specificity: miR-144* (sensitivity 74%, specificity 87%; [409]); miR-92a (sensitivity 71.6%, specificity 73.3%; [410]); miR-34b/c (sensitivity 75%, specificity 87.2%; [411]); miR-21 (sensitivity 55.7%, specificity 73.3%; [410]); and miR-135b

(sensitivity 78%, specificity 68%; [412]). Strikingly, miR-92a was down-regulated after the tumour was removed [410] and miR-135b significantly correlated with tumour staging [412].

Many studies have aimed to investigate the use of circulating miRNAs in the blood for diagnostic purposes in CRC. Initial studies by Ng and colleagues reported altered circulating levels of miRNAs in the plasma of CRC patients compared to controls [413]. In this study, miR-92 was found to be up-regulated in the plasma of patients with CRC, an observation which was later confirmed by others [414]. In accordance with stool miRNA expression, circulating miR-92 was decreased following tumour removal suggesting that this particular miRNA may be used as a marker for tumour recurrence [413].

1.3.4.2 Predictive/prognostic miRNAs in CRC

Current predictive or prognostic biomarkers for tumour progression or treatment response in CRC are limited. To address this, the use of miRNAs as potential biomarkers has been explored intensively. One particular miRNA (miR-21) has great potential for both prognostic and predictive purposes. Several studies have correlated high miR-21 levels with clinicopathological features including lymph node positivity [287], metastasis [287], poor therapeutic response [286, 415] and shorter disease free survival [286, 416]. In addition, miR-21 has now been reported to be associated with a worse prognosis in at least nine other cancers, which correlates with the oncogenic activity of miR-21 in a range of malignancies. Therefore, miR-21 may be used as a prognostic classifier in a variety of cancers.

Tumour resistance to conventional therapy is a major concern in the treatment and management of CRC. Recent studies have identified altered miRNA profiles associated with resistance that could potentially stratify patients for certain treatment options. Interestingly, miR-21 is associated with tumour resistance to the chemotherapy drug 5-FU

[286]. In addition, the expression levels of let-7g and miR-181b were inversely correlated with 5-FU analogue S-1 treatment, but did not correlate to patient survival [417]. CRT exposure in rectal cancer was associated with increased levels of miR-125b and miR-137 and correlated with poor treatment outcome [418]. Further studies showed that a subset of 13 miRNAs could form a specific signature that was strongly associated with response to CRT [419, 420]. These reports highlight the potential use for miRNA expression profiles as diagnostic as well as prognostic or predictive biomarkers. However, further large scale clinical studies are needed to assess their true potential.

Finally, the lack of consistency between miRNA expression profiling studies with regards to experimental design and/or data analysis is a major concern [421]. Key factors for these discrepancies include the variation in miRNA extraction processes, the quality and quantity of the extracted miRNAs and, most importantly, the normalisation processes during analysis. With a lack of suitable housekeeping genes, normalisation for circulating miRNAs is notoriously difficult. Small nuclear/nucleolar RNAs such as RNU6B, RNU44 and RNU48 are often used [413, 422, 423]. However, their expression can vary greatly under different conditions [361, 423] and their use should be validated on a case-by-case basis. In addition, exogenous spiked-in RNAs, such as cel-miR-39, cel-miR-54 or cel-miR-238 may also be used as normalisation controls [399, 424, 425]. Experimental variation and the lack of consensus on normalisation strategies for circulating miRNAs make comparing various studies extremely difficult.

1.4 Hypothesis and aims

In the management of CD, fibrosis and subsequent stricture formation is a major complication and often requires surgical intervention. Currently, there is no gold standard measure for disease activity and progression. Imaging of the bowel by MRI or CT scan are readily used, however, they are costly and submit the patient to ionizing radiation. While these tools are necessary and useful for the evaluation of the disease activity, they offer no significant prognostic value. Therefore, there is an unmet clinical need for robust prognostic biomarkers.

Understanding the reasons for tumour resistance and developing a way to identify and predict individuals who would benefit the most and least from neo-adjuvant therapy, remain crucial aims for the management of CRC. The tumour microenvironment, such as low oxygen conditions, are crucial factors that influence the tumour response to conventional therapies of which the underlying mechanisms remain poorly understood.

MiRNAs are non-coding RNAs involved in important biological processes including proliferation, differentiation and apoptosis. Over the past two decades, the amount of studies on miRNAs has been exponentially rising and they are now considered key regulatory molecules in a variety of processes including inflammation and tumourigenesis. It is important to understand fully their involvement in intestinal cancer and inflammatory disease and to assess their potential as biomarkers and therapeutic targets. My hypotheses have been developed with these factors in mind.

Firstly, I hypothesise that miRNA expression profiles are altered between mucosa-overlying non-strictured (NSCD) and mucosa-overlying-strictured (SCD) areas of intestinal tissues in CD patients.

Aims to test this hypothesis:

1. Identify and validate differentially expressed miRNAs between paired NSCD vs SCD tissue samples (Chapter 3);
2. Isolate and optimise transfection protocols in intestinal fibroblasts from CD patients (Chapter 3);
3. Elucidate the functional role of candidate miRNAs in intestinal fibroblasts isolated from CD patients and their localisation in intestinal tissues of CD patients (Chapter 3);
4. Determine the expression of the miR-29 family in NSCD vs SCD tissues (Chapter 4); and
5. Elucidate the role of miR-29b in intestinal fibroblasts isolated from CD patients in respect to its regulation of ECM molecules (Chapter 4).

Secondly, I hypothesise that miRNAs are differentially expressed under hypoxic conditions in CRC *in vitro* and *in vivo*, and influence the response to chemotherapy drugs.

To address this hypothesis I aim to:

1. Identify and validate differentially expressed miRNAs under hypoxic conditions *in vitro* using six CRC cell lines as a model (Chapter 5);
2. Validate candidate miRNAs in CRC *in vivo* and correlating its expression to hypoxia marker (Chapter 5);
3. Elucidate the role for candidate miRNAs in drug resistance under hypoxic conditions *in vitro* (Chapter 5); and
4. Identify cellular metabolic changes under hypoxic conditions in six CRC cell lines (Chapter 5).

Chapter 2: Material and Methods

2.1 Crohn's disease patient recruitment

Surgical resection specimens from patients with stricturing CD were collected (Table 2.1). Diagnosis of CD was ascertained according to the usual clinical criteria [426]. To exclude inflammation as an experimental variable, mucosal specimens were taken from macroscopically non-inflamed SCD and NSCD ileum and colon. The site and extent of disease were established by endoscopy, histology and radiology and strictured areas identified during surgery. CD patients had not taken steroids for at least three months prior to resection, and none were taking methotrexate or anti-TNF-α agents at the time of surgery. The study received the appropriate local Ethics Committee approvals (East London REC2) and informed consent was obtained in all cases.

Table 2.1. Patients who underwent surgical resection for stricturing complications. Fresh surgical resection specimens and archived Formalin-fixed paraffin embedded blocks of 22 CD patients. Samples were used where indicated. NSCD: Non-stricture CD, SCD: stricture CD.

Sample ID	Location	Tissue sample	Array	Validation (RNA)	Functional studies (cell culture)	Archive blocks
CD1	Ileum	NSDC + SCD			√	
CD2	Ileum	NSCD + SCD			√	
CD3	Ileum	SCD			√	
CD216	Ileum	NSCD + SCD	√	√		
CD328	Colon	NSCD	√			
CD347	Colon	SCD	√			
CD353	Ileum	NSCD + SCD	√	√		√
CD360	Colon	SCD	√			√
CD362	Ileum	SCD	√			√
CD373	Ileum	NSCD + SCD	√	√		√
CD377	Colon	NSCD	√			
CD381	Ileum	SCD	√			
CD397	Ileum	NSCD + SCD		√		
CD398	Ileum	NSCD + SCD				√
CD417	Ileum	NSCD + SCD		√		
CD419	Ileum	NSCD + SCD				√
CD425	Ileum	NSCD + SCD		√	√	√
CD435	Ileum	NSCD + SCD		√		
CD484	Ileum	NSCD + SCD		√		
CD495	Ileum	SCD			√	
CD522	Colon	NSCD			√	
CD637	Ileum	SCD		√	√	

2.2 MiRNA arrays

Total RNA (2 µg) from 12 (Table 2.1) mucosa overlying strictured areas or mucosa overlying non-strictured CD areas were analysed by Illumina v.2.0 miRNA array platform which covers 95% of all miRNAs in miRBase v.12 [427]. A workflow of the array is depicted in Fig. 2.1. Array data processing and analysis were performed with Illumina GeneStudio software (www.illumina.com). Total RNA (2 µg) of six colorectal cell lines grown under three different oxygen conditions (20.9%, 1% and 0.2%) for 48 hr were analysed using the LNA 7th version miRNA array which covers 3,100 miRNAs in miRBase v.19 (Exiqon, Denmark). The hypoxic state was confirmed for each of the cell lines by western blot of HIF-1α (data not shown). Data was normalised to the plate intensity mean and then log transformed.

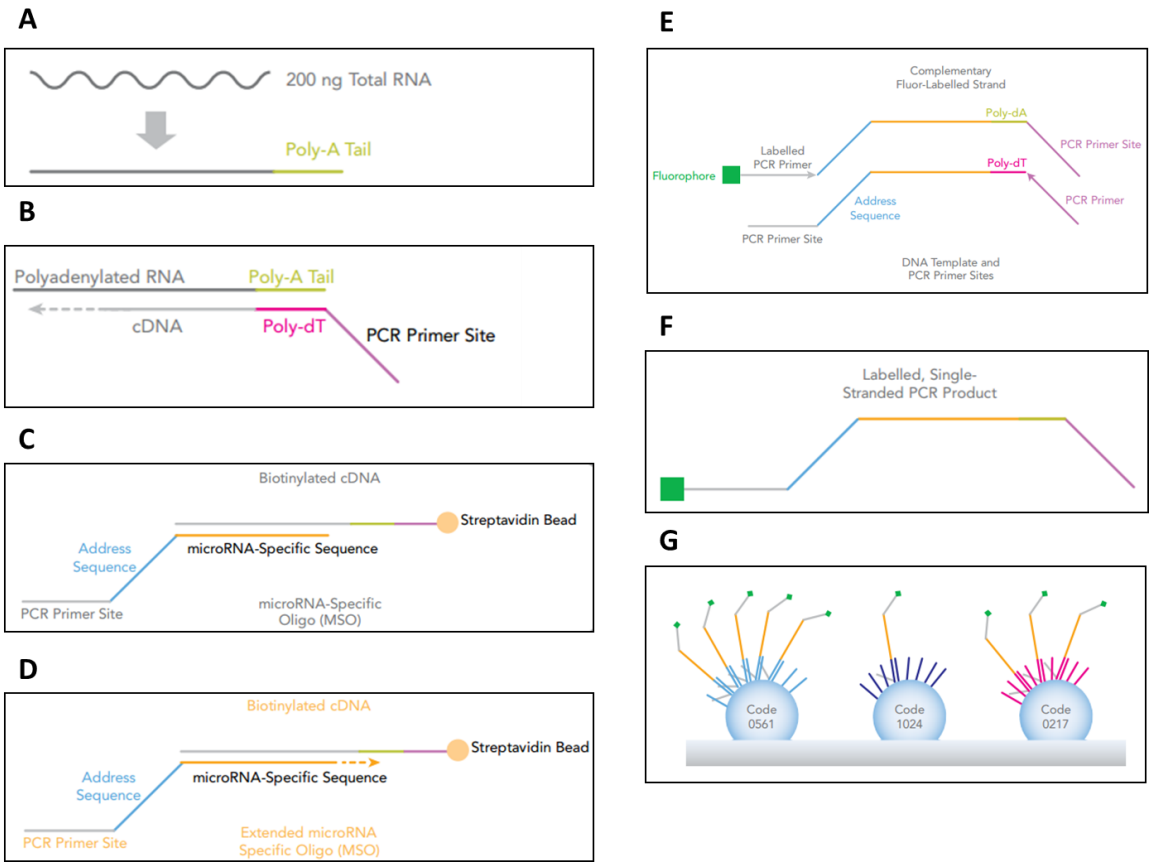

Figure 2.1. Illumina miRNA array workflow. (A-B) 200ng of RNA is polyadenylated and reverse transcribed into cDNA using biotinylated oligo-dT primers with a universal PCR sequence at its 5'-end. (C-D). The biotinylated cDNA is annealed to a set of miRNA-specific oligos (MSOs) that correspond to all the targeted miRNAs on the array. A MSO contains three parts; 1) 5'end with a universal PCR primer site 2) an address sequence that complements a corresponding capture sequence on the array 3) 3' end with a miRNA-specific sequence. After the oligos are annealed they will undergo extension only if their 3' bases are complementary to the sequence in the cDNA template. (E-F) A fluorescently labelled complementary strand is produced using the common PCR primers from the extended MSO. (G) The labelled strands are hybridised to the bead on the array containing the complementary address sequence. Fluorescent intensity is measured at each bead position corresponding to each individual miRNA.

2.3 Isolation of intestinal fibroblasts

Human fibroblasts were obtained from mucosal layers of surgical resections in complete Dulbecco`s Modified Eagles Medium (DMEM, PAA, UK). Full thickness resection of strictured areas and non-inflamed areas were examined macro- and microscopically, and mucosa was separated from the muscle layers before being washed twice with Hank's Balanced Salt Solution (HBSS, Invitrogen, UK) with 1 mM EDTA for 10 min at 37°C under gentle agitation to remove epithelial cells. Specimens were cut into smaller pieces and incubated in 20 ml DMEM with 1 mg/ml collagenase type 1α (R&D Systems, USA), and 10 U/ml DNase I (Roche, UK) for 60-90 min under gentle agitation. Cells were washed once with Phosphate Buffered Saline (PBS, Invitrogen, UK) and resuspended twice with DMEM and then cultured in T25 cm^2 flasks.

2.4 Cell culture maintenance of CRC cells and intestinal fibroblasts

Cell culture was performed in flow hoods using sterile handling techniques. Three colon cancer cell lines (DLD-1, HCT116 and HT29), three rectal cancer cell lines (HT55, SW837 and VACO4s) and cervical cancer cell line HeLa were grown in T75cm^2 vented flasks (VWR, UK) at 37°C in a 5% CO_2 atmosphere containing 15ml DMEM supplemented with 10% Fetal bovine serum (FBS, PAA, UK), and 100 U/ml penicillin and 100 µg/ml streptomycin (PenStrep, PAA, UK). All cancer cell lines were kind gifts from Professor Ian Tomlinson (Wellcome Institute for human genetics, University of Oxford). Mutation status for six CRC cell lines are summarised in Table 2.2. For the maintenance of the intestinal fibroblast cultures DMEM (ATCC, UK) supplemented with 10% heat-inactivated FBS (Gibco, UK) and PenStrep was used. For hypoxic experiments, cells were maintained under three different oxygen tensions (20.9 % oxygen, 1% oxygen and 0.2 % oxygen) and 5% CO_2. The oxygen concentration was controlled by Invivo2 1000 Hypoxia Workstation (Ruskinn Life Sciences Ltd, USA).

Table 2.2 Mutation status for CRC cell lines.

Cell line	Origin	MSI	APC	KRAS	P53
DLD-1	Colon	+	1417 del 1bp	GGT/TGT c12	Codon 241
HCT116	Colon	+	WT	GGC/GAC c13	WT
HT29	Colon	-	853 CAG -> TAG	WT	Codon 273
HT55	Rectum	-	1131 CAA -> TAA	WT	WT
SW837	Rectum	+	1450 CGA -> TGA	GGT/GTT c12	Codon 248
VACO4s	Rectum	-	1354 del 5bp	GGT/GTT c12	WT

2.5 Optimisation of transfection in intestinal fibroblasts

Three doses (0.3 µL, 0.4 µL and 0.5 µL) of four different transfection agents (DharmaFect (DF) 1 to 4, Dharmacon, UK) were used to optimise transfection conditions of intestinal fibroblasts. Cells were transfected with 60 nM negative control siRNA tagged with 488 fluophore (#Cat number, Qiagen, UK) for 48 hr. Cells were fixed with 3.7% paraformaldehyde (PFA, Sigma, UK) being stained with Hoechst 33342 (1:5,000, Invitrogen, UK) and CellMask Deep Red (1:20,000, Invitrogen, UK) for 15 min and imaged on the IN Cell Analyzer 1000 microscope (GE Healthcare, UK). Cells were imaged with a 10X objective with a triChroic mirror. Hoechst stained nuclei were imaged with $350_{ex}/455_{em}$ filters, 488-tagged siRNA was imaged with $490_{ex}/525_{em}$ filters and CellMask Deep Red was visualised using $645_{ex}/705_{em}$ Transfection efficiency was assessed using the IN Cell Developer v1.8. DF3 reagent at showed the most consistent transfection pattern and efficiency and was selected for further optimisation. Various concentrations of DF3 and 60 nM siGLO Red siRNA (DY-547, #D-001630-02, Dharmacon, UK) were used for optimisation. This siRNA targets housekeeping gene cyclophilin B (*PPIB*). Media was changed 24 hr post transfection and cells were stained 72 hr post transfection with Hoechst 33342 for 15 min before being fixed with 3.7% PFA. Cells were imaged with the IN Cell Analyzer 1000 microscope and viewed at 10X objective with a triChroic mirror (61003bs*): Hoechst stained nuclei were imaged with $350_{ex}/455_{em}$ filters and siGLO staining was imaged with $555_{ex}/605_{em}$ filters. Cells were then subjected to immuno-fluorescence with monoclonal rabbit antibody against Cyclophilin B (Section 2.8), and anti-rabbit Alexa-Fluor-488 labeled secondary antibody

(1:500, Abcam, UK). IN Cell Developer v.1.8 (GE Healthcare, UK) was used to analyse the transfection efficiency and reduction of Cyclophilin B protein expression by siGLO siRNA to determine optimal transfection conditions.

2.6 Optimisation of transfection in CRC cell lines

The HCT116 cell line was optimised for seeding density and concentration of transfection agent Lipofectamine 2000 (LF2000, Invitrogen, UK) in 96 well plates by transfecting 30 nM of Allstars non-targeting control (NTC, #SI03650318, Qiagen, UK), siGLO siRNA, and polo-like kinase-1 siRNA (PLK-1, #SI02223837, Qiagen, UK). PLK-1 kinase is required for cell division and inhibition has shown to be pro-apoptotic [428] and serves as a killing control. Media was changed 24 hr post transfection and siGLO siRNA localisation was visualised under a fluorescent microscope. 72 hr post transfection cell viability was measured using CellTitre Blue Reagent (Invitrogen, UK) according to manufacturer's protocol. Optimum transfection conditions were determined when viability with PLK-1 siRNA was lowest and viability with NTC was similar to non-treated cells.

2.7 Transfection of fibroblasts and TGF-β stimulation

Pre-miR and anti-miR transfection. Intestinal fibroblasts were seeded overnight (Nunc, UK) before being transiently transfected with 30 nM NTC, 30 nM pre-miRNA or 60 nM anti-miR (all Qiagen, UK) using DF3. Lipid containing media was replaced 24 hr post transfection and cells were fixed for immunofluorescence 48 hr post transfection. RNA was extracted for qRT-PCR and supernatants were collected for ELISA experiments.

TGF-β treatments. Intestinal fibroblasts were seeded overnight. The following day, cells were treated with 10 ng/ml TGF-β for 48 hr. RNA was extracted for qRT-PCR and supernatants were collected for ELISA experiments.

Pre-miR and anti-miR transfection + TGF-β treatments. Intestinal fibroblasts were transfected as above for 24 hr before being treated with 10ng/ml TGF-β for 48 hr. Cells were fixed with 3.7% PFA for immunofluorescence.

2.8 Immunofluorescence (IF)

Intestinal fibroblasts cell cultures and CRC cells transfected in 96 well plates were fixed with 3.7% PFA for 15 min at RT before being washed with PBS and permeabilised in 0.1% Triton-X100 (Sigma, UK) in PBS for 20 min. Cells were washed and blocked for 30 min with 0.25% Bovine Serum Albumin (BSA, Sigma, UK) in PBS before incubated for 2 hr with primary antibody (Table 2.4 for details). Cells were washed for 30 min with PBS/BSA (0.25%) and incubated for 2 hr with Alexa-Fluor-488 conjugated secondary antibody (1:500, Invitrogen, UK), Hoechst 33342 (1:10,000 Invitrogen, UK) and CellMask Deep Red (1:20,000, Invitrogen, UK) for 2 hr. Cells were washed twice with PBS before being imaged on the IN Cell Analyzer 1000 microscope. Pixel intensities were compared to NTC transfected cells. IN Cell Developer v1.8 was used to analyse the images.

2.9 Enzyme-linked immunosorbant assay (ELISA)

Supernatants were taken from intestinal fibroblast cultures transfected with pre-miR, anti-miR and controls. Cytokines IL-6 and IL-8 were measured using R&D DuoSet ELISA kits using manufacturer's protocol (R&D, USA).

2.10 MiRNA extraction & Quantitative Real-Time PCR (qRT-PCR)

Total RNA including small RNAs was extracted from samples using the miRNeasy kit (Qiagen, UK) according to manufacturer's protocol. RNA concentration was determined using the NanoDrop Spectometre (Nano-Drop Technologies, USA). miRNA Reverse Transcriptase (RT) kit (Applied Biosystems, UK) on 10 ng RNA was used for reverse transcription. RT products were incubated with Taqman miRNA probe and Universal PCR Mastermix (Applied Biosystems, UK) on a 7500 Fast System RealTime PCR cycler (Applied Biosystems, UK) according to manufacturer's protocol. Fold changes were calculated using the $2^{\wedge-\Delta\Delta Ct}$ method normalised to endogenous control miRNAs [429]. Housekeeping genes that were used to normalise qRT-PCR data is summarised in Table 2.3.

Table. 2.3. Normalisers used for qRT-PCR.

Sample	Normaliser mRNA	Normaliser miRNA
CRC cell lines	GAPDH	RNU19b
CRC tissue	-	Geomean of miR-16 and let-7a
Intestinal mucosa	GAPDH	miR-26b
Intestinal fibroblasts	GAPDH	RNU6B

2.11 Total RNA extraction & qRT-PCR of gene expression

Total RNA, excluding small RNAs, was extracted using the RNeasy kit (Qiagen, UK) according to manufacturer's protocol. RNA concentration was determined using the NanoDrop Spectrometer (Nano-Drop Technologies, USA). RT was performed using the High-Capacity-RNA to cDNA kit (Applied Biosystems, UK) in a 20 µL reaction. cDNA was incubated with Taqman assays (20x) and Universal Mastermix no UNG on a 7500 Fast System RealTime PCR cycler according to manufacturer's protocol. Fold changes were calculated using the $2^{\wedge-\Delta\Delta Ct}$ method.

2.12 5-Fluorouracil (5-FU) drug treatments of HCT116

HCT116 cells were seeded at 5,000 cells per well in 96 well plates overnight. The following day, cells were treated with various concentrations of 5-FU (1 µM, 5 µM, 10 µM, 100 µM or 1mM) together with vehicle control, and cultured under three oxygen conditions (20.9%, 1% and 0.2%) for 48 hr. Cells grown in 96 well plates were fixed with 3.7% PFA for 15 min and nuclei were stained with Hoechst 33342 (1:10,000) for 30 min. Cells were imaged with the IN Cell 1000 microscope using a 4X objective with a triChroic mirror (61003bs*). Hoechst stained nuclei were imaged with $350_{ex}/455_{em}$ filters. Nuclei were counted using the IN Cell Developer v1.8 and cell number was expressed relative to vehicle treated cells.

2.13 5-FU drug treatment and transfection of HCT116

HCT116 cells were reverse transfected with 30 nM pre-miR, NTC and 60 nM anti-miR in 96 well plates. The following day, media was replaced with 10 µM 5-FU or vehicle control containing media. Cells were cultured under three oxygen conditions (20.9%, 1% or 0.2%) for 48 hr. Cells were fixed with 3.7% PFA for 15 min and nuclei were stained with Hoechst for 30 min. Cells were imaged with the IN Cell Analyzer microscope using a 4X objective in combination with $350_{ex}/455_{em}$ filters. Nuclei were counted using the IN Cell Developer v1.8 and expressed relative to vehicle treated cells.

2.14 Zeocin kill curves

HeLa cells were plated in 6 well plates at 400,000 cells per well. The following day, cells were treated with a range of concentrations of Zeocin (250 µg/ml-1000 µg/ml, Invitrogen, UK). Cell death was monitored by eye for two weeks and media containing Zeocin was replaced every 2-3 days. Optimal Zeocin dose was determined at the lowest fatal concentration.

2.15 HeLa transfection optimisation

HeLa cells were plated in 6 well plates at 400,000 cells per well. The following day cells were transfected using 2ug of pcDNA-EGFP plasmid (pcDNA-EGFP plasmid was a kind gift from Dr. P. Kemp, Imperial College, UK) and a range of LF2000 doses. Media was changed 24 hr post transfection and cells were fixed with 3.7% PFA for 15 min. Cells were incubated with Hoechst 33342 (1:10,000) for 30 min before being imaged on the IN Cell 1000 microscope. Images were analysed on the IN Cell Developer v1.8 and GFP transfection efficiency was determined.

2.16 MISSION® Target ID Library transfection

HeLa cells were plated in 6 well plates at 400,000 cells per well. The following day, cells were transfected with 2 μg MISSION® Target ID library plasmids using optimised LF2000 dose (12 replicates). The media was changed 24 hr post transfection and cells were treated with the optimised dose of Zeocin 72 hr post transfection. Target ID Library plasmids contain a Zeocin-resistance element and thus transfected cells are able to survive the Zeocin treatment, whilst non-transfected cells die. Cells were cultured in Zeocin-containing media until all control cells were dead. Cells were pooled and expanded until cells were ready for cryo-preservation.

2.17 Tissue Immunohistochemistry

The HIF-1α responsive protein, carbonic anhydrase IX (CAIX), was used to stain rectal cancer tissue samples for areas of hypoxia. Six NSCD and 3 SCD blocks were stained for p53. 4 μm thick sections of the Formalin-fixed paraffin embedded (FFPE) samples were cut followed by de-waxing, hydration and blocking in goat serum. Sections were incubated with primary antibody mouse-anti-CAIX (1:50, SantaCruz, UK) or mouse-anti-p53 (1:250, Abcam, UK) for 2 hr. Mouse-HRP secondary (1:500, Dako, UK) was incubated for 2 hr followed by washing and DAB incubation. Control samples were used

to ensure complete staining (stomach tissue for CAIX, breast cancer for p53). Analysis for CIAX staining was undertaken using a light microscope and two blinded observers following a staining protocol adapted from [430]. p53 staining was analysed and reported by a consultant pathologist (Professor Roger Feakins, Department of histopathology, The Royal London Hospital).

2.18 Extraction of small RNAs from FFPE sections

FFPE slides from 13 rectal cancers were used for miRNA extractions. Haematoxylin & Eosin staining was performed to determine the tumour tissue area by a pathologist (Professor Roger Feakins). Ten adjacent sections (10 µm) were then used for miRNA extraction using the RecoverAll Total Nucleic Acid Isolation kit (Ambion, Applied Biosystems, USA) according to manufacturer's protocol. RNA concentration was determined using the NanoDrop Spectrometer (Nano-Drop Technologies, USA).

2.19 In situ hybridisation of miRNAs on FFPE sections

Sections (3 µm) were cut from FFPE tissue blocks in an RNAse free water to avoid RNA degradation. Slides were deparaffinised in xylene and ethanol solutions (100% - 95% - 70%) at RT and incubated in PBS for 5 min. A schematic overview of the miRNA detection steps is shown in Fig. 2.2. Sections were then incubated with Proteinase-K (10 µg/ml) for 15 min at 37 °C before being washed in PBS, dehydrated in ethanol solutions (70% - 95% - 100%) and air dried for 15 min or until the tissue was dry. Double-DIG-labelled miRNA probes (miR-210, miR-21, miR-34a and scrambled; Exiqon, Denmark) were diluted in hybridising buffer (Exiqon, Denmark). The following concentrations were used: miR-210 (40 nM), miR-21 (40 nM), miR-34 (60 nM) and scrambled (60 nM). Slides were incubated with 25 µL of probe mixture at 56 °C for 1 hr on a slide hybridiser (Omnislide Thermal Cycler, Thermo Scientific, UK) and washed with saline-sodium citrate (SSC) buffer at 56 °C (5xSSC 5 min, 1xSSC, 5 min, 1xSSC 5 min, 0.2xSSC 5 min,

0.2xSSC 5 min) and 0.2xSSC for 5 min at RT. Slides were incubated with blocking buffer for 15 min before subjected to anti-DIG-AP reagent (1:600, Exiqon, Denmark) at RT. Slides were washed with PBS-tween and incubated with anti-AP substrate (NCT-BCIP, Roche, UK) for 2 hr at RT to create a blue precipitate. Slides were then washed in water before counterstained with Nuclear Fast Red (Vector, UK) for 1 min at RT. Slides were rinsed in running tap water for 10 min and dehydrated in ethanol solutions (70% - 95% - 100%) and mounted with Eukkitt mounting medium (Sigma, UK). Slides were scanned using a slide scanner (Core Pathology, Pathology Department, Royal London Hospital) to produce high quality images.

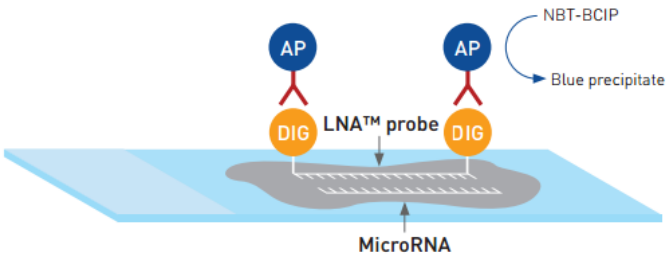

Figure 2.2. Schematic overview of the Exiqon in situ hybridisation protocol. MiRNAs were de-masked with Proteinase-K treatment to allow access of the double-DIG-labelled LNA probes to hybridise with the miRNA. The digoxigenins are recognised by a anti-DIG antibody conjugated with Alkaline Phospohatase (AP), which converts the substrates 4-nitro-blue tetazolium (NBT) and 5-bromo-4-chloro-3'-indolylphosphate (BCIP) into a blue precipitate.

2.20 Cell metabolite analysis

Three colon cancer (DLD-1, HCT116 and HT29) and three rectal cancer (HT55, SW837 and VACO4s) cell lines were cultured under three oxygen conditions (20.9%, 1% and 0.2%) for 48 hr as described previously (Section 2.4). Cells were washed twice in 5% Mannitol (Wako, Japan) and incubated with 1 ml of methanol containing 3 standards (Methionine sulfone, MES and CSA each at 25 µM). The cells were then counted, flash frozen on dry ice and shipped to the Institute for Advanced Biosciences in Japan for capillary electrophoresis time of flight mass spectrometry (CE-TOF/MS) analysis.

2.21 Statistics

General statistics. Graphpad Prism analysis software was used to perform Student's *t*-tests and one-way ANOVA tests as denoted. A p-value of less than 0.05 was considered statistically significant. Experiments are performed in duplicates in three independent experiments, unless otherwise stated.

Multivariate analysis. A partial least squares discriminant analysis (PLS-DA) is a supervised multivariate classification technique, and so care must be taken to avoid over-fitting. However, it is possible to fit with respect to one variable, and then examine the separation in another variable. Here, a supervised model to differentiate the six cell lines was fitted, and the miRNAs were examined for (unsupervised) separation with respect to oxygen tension. The loadings were then interrogated in order to identify potential miRNAs for further investigations.

Multiple linear regression. The relationship between miRNA expression (dependent variable) was modelled against the independent variables oxygen tension (numerical variable) + cell line (categorical variable). This enabled us to identify miRNAs were significantly ($p<0.05$) associated with oxygen tensions once the effect of cell line has been allowed for.

Table 2.4. Primary antibodies

Antigen	Company details	Dilution
Cyclophilin B	Abcam (#ab16045)	1:200
CAIX	Santa-Cruz (#N-19)	1:50
Collagen I	Novus Biologicals (#NB600-405)	1:200
Collagen III	Abcam (#ab7778)	1:500
Mcl-1	Abcam (#32087)	1:200
P53	Abcam (ab26)	1:250

Chapter 3: Differential expression of miRNAs in intestinal fibrosis

3.1 Introduction and aims

Progression to intestinal fibrosis and subsequent stricture formation is a frequent complication in CD and has significant health implications of the individual patient. The lifetime risk of surgery for patients with CD is as high as 70% [196], with the majority indicated for stricturing disease. Current medical therapies are unable to reverse fibrosis, and the factors that initiate and drive CD fibrosis are not well understood [197]. Aberrant expression of miRNAs is associated with multiple disease pathologies including cancer, immunity and inflammation [431-434]. MiRNA dysregulation is involved in the development of fibrosis in various organs, including the lung, kidney, liver and heart (reviewed in [435]), some of which are summarised in Table 1.3 (Section 1.3.3). To date, the dysregulation of miRNAs in intestinal fibrosis in CD has not yet been investigated.

Aims for this chapter:

1. Identify differentially expressed miRNAs between non-inflamed mucosa overlying non-stricturing CD (NSCD) and -stricturing CD (SCD) tissues of CD patients with the use of a miRNA array;
2. Validate selected candidate miRNAs in an independent set of paired NSCD and SCD tissue samples;
3. Isolate and maintain intestinal gut mucosal fibroblasts from patients with CD and optimise protocols for transient transfection of miRNAs;
4. Investigate down-stream targets of candidate miRNA(s) via transient transfection in intestinal fibroblasts. mRNA levels of key ECM molecules were assessed by qRT-PCR; and
5. Determine the localisation and expression of candidate miRNA(s) in NSCD and SCD tissue samples using i*n situ* hybridisation techniques.

3.2 MiRNA microarray between NSCD and SCD tissue

To identify the differentially expression of miRNA between six NSCD and six SCD tissue samples, a miRNA microarray (Illumina v2.0) was performed. The mucosa was used in this study as it has previously been shown that events here reflect those associated with the fibrotic changes occurring in the deeper tissue layers during fibrogenesis [201]. Patient and sample details can be found in Table 2.1 (Section 2.1). The bead-based array contains 1,146 miRNAs probes covering more than 97% of known miRNAs in miRBase v.12.0 [427]. A workflow with detailed description of the array is described in the methods section (Section 2.2). Fluorescent signal intensities of each miRNA for each of the 12 samples was analysed using GenomeStudio Software (www.illumina.com). Data was subjected to quantile normalisation which reduces variation by normalising the distribution of the probe intensities between the sample groups. This type of normalisation is recommended for high density oligonucleotide microarray technology [436]. Normalised expression values of the miRNAs were used for statistical analysis (corrected paired Student-Test) in GenomeStudio.

To visualise the miRNA expression patterns between the NSCD vs SCD samples, negative log10 values of the p-value were plotted against log2 fold change values to create a volcano plot (Fig. 3.1A). The scatter plot quickly identifies any significant changes in expression in miRNA expression between NSCD and SCD tissues, and this analysis identified 18 significantly increased and 11 significantly decreased miRNAs in SCD versus NSCD tissues ($p<0.05$). A heatmap containing the normalised expression values of all of the significant differentially expressed miRNAs is shown in Fig. 3.1B.

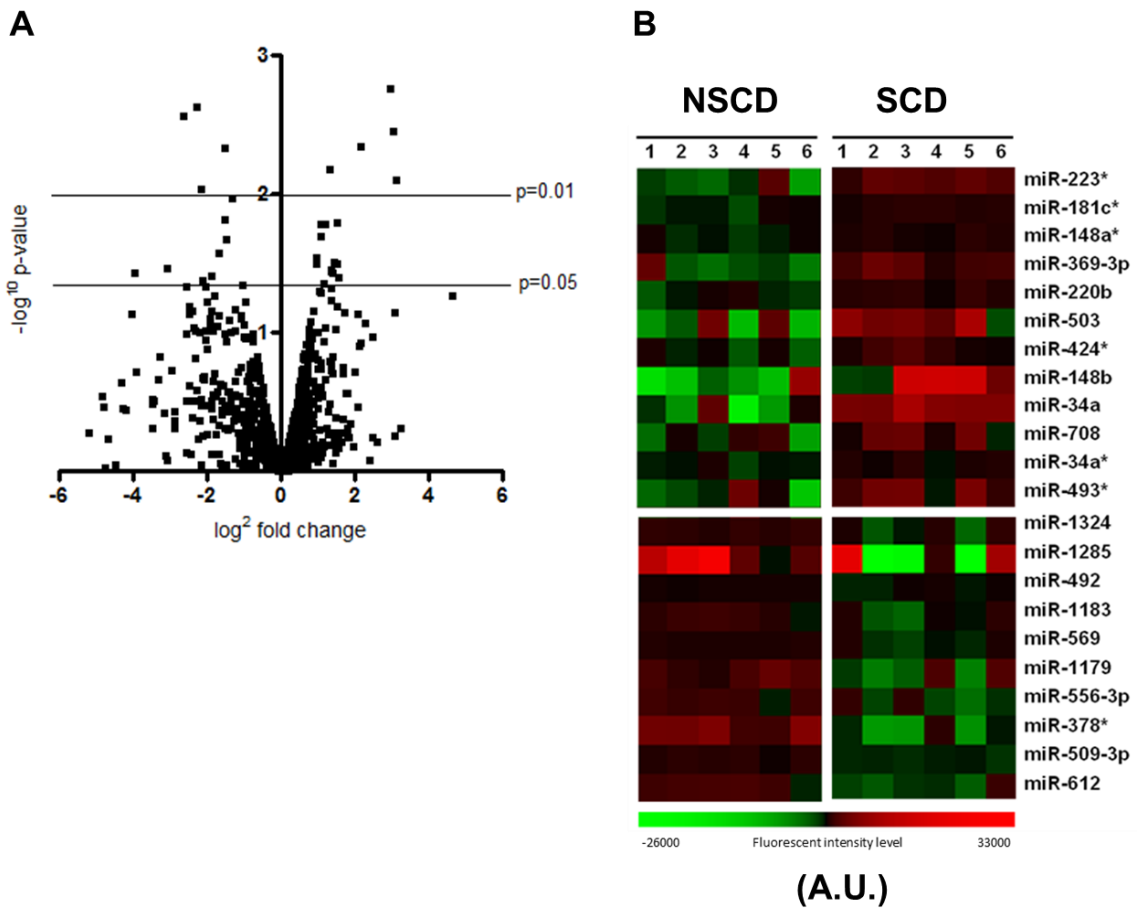

Figure 3.1. Differentially expressed miRNAs between six NSCD and six SCD tissues. (A) A volcano plot containing all miRNAs detected by the array. Negative log p-values are plotted against the log fold change values between NSCD and SCD samples. Lines represent p=0.05 and p=0.01. Any miRNAs present above these lines are considered significant. (B) Heatmap of normalised fluorescent intensity levels (A.U.) of 29 miRNAs with a $p<0.05$ between NSCD and SCD samples. The top panel demonstrates up-regulated and bottom panel down-regulated miRNAs in SCD tissue vs NSCD tissue. Increased expression is shown in red and decreased expression shown in green.

3.3 MiRNA validation by qRT-PCR

To validate the findings of the miRNA array using a different technique, qRT-PCR was performed. Six up-regulated miRNAs (miR-148b, -223*, -34a, -493*, -503 and -708) and one down-regulated miRNA (miR-1285) were selected for further validation on an independent set of eight paired NSCD and SCD tissue samples (Table 2.1, Section 2.1). These miRNAs were selected based on p-values and/or a link to fibrosis in the literature (Table 3.1).

Table 3.1. Candidate miRNAs selected for validation and their link to fibrosis. miRNAs are ranked in numerical order.

miRNA (p-value)	**Role**
miR-148b (p=0.020)	Targets LTBP1 which is involved in the pro-fibrotic TGF-β pathway [437]
miR-223* (p=0.002)	No link to fibrosis
miR-34a (p=0.029)	↑ Cardiac fibrosis [438], ↑ Liver fibrosis [387, 439, 440], ↑ Kidney fibrosis [441]
miR-493* (p=0.048)	↑ in lung fibrosis [442]
miR-503 (p=0.017)	Correlated to scleroderma (fibrosis of the skin) [443]
miR-708 (p=0.031)	Targets Aquaporin-1 which is down-regulated in liver fibrosis [444]
miR-1285 (p=0.045)	No link to fibrosis

A key challenge for the analysis of qRT-PCR data is the normalisation step. In contrast to an array, qRT-PCR relies on the stable expression of one or two references genes which will be different depending on tissue and cell type. Three reference miRNAs (let-7a, miR-16 and miR-26b) that showed consistent expression between the different samples were picked from the array, and were assayed in the validation sample set. Cycle threshold (Ct) values of all three reference miRNAs for both NSCD (n=8) and SCD (n=8) samples were measured and mean values are shown in Fig. 3.2A. None of the three miRNAs showed a significant change between the two groups (let-7a, p=0.0538; miR-16, p=0.0548; miR-26b, p=0.0591). All three miRNAs were close to significance, however, miR-26b exhibited the least variation within the two groups of samples (*Ct StDev*: let-7a,

NSCD=1.04, SCD=0.605; miR-16, NSCD=1.46, SCD=0.44; miR-26b, NSCD=0.73, SCD=0.42) and was selected as the reference gene for the validation of the target miRNAs. In support of this, miR-26b was recommended by Applied Biosystems as a suitable reference gene for human tissue samples [445]. The seven candidate miRNAs (miR-148b, -223*, -34a, -493*, -503, -708 and -1285) were measured in eight independent matched NSCD and SCD tissue samples and the data normalised to miR-26b (Fig. 3.2B). Statistical analysis (paired Student's t-test) confirmed the significant up-regulation of three miRNAs by qRT-PCR (miR-493*, p=0.0096; miR-708, p=0.0112; miR-34a, p=0.0165). Two miRNAs were not significant changed (miR-223*, p=0.090 and miR-148b, p=0.2000).

Two miRNAs (miR-1285 and miR-503) were only detectable in five of the eight paired samples tested. Relative expression of miR-1285 and miR-503 in the five pairs is shown in Fig 3.2C. The relative fold changes between NSCD and SCD in the five pairs were not significant (miR-1285, p=0.1331 and miR-503, p=0.3672), although, the mean fold change in the SCD versus NSCD samples correlated to the expression pattern observed in the array (miR-1285, down-regulated in SCD vs NSCD and miR-503, up-regulated in SCD vs NSCD). In conclusion, these data demonstrate that the up-regulation of miR493*, miR-708 and miR-34a was successfully validated between NSCD and SCD tissue samples.

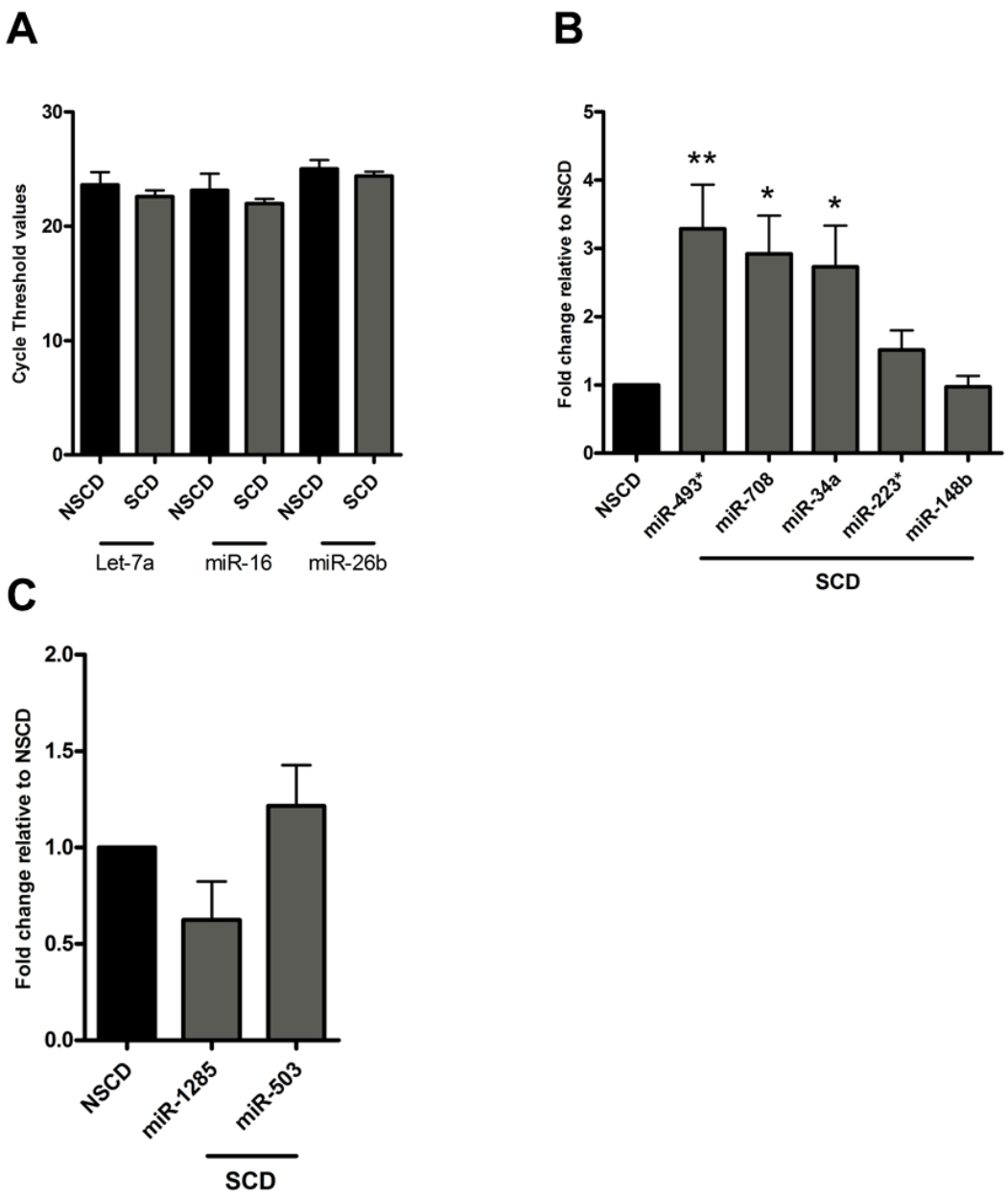

Figure 3.2. Validation of seven miRNAs by qRT-PCR. qRT-PCR in eight matched paired NSCD and SCD tissue samples. (A) Ct values for three endogenous control miRNAs (let-7a, miR-16 and miR-26b; n=8) (B) qRT-PCR of five selected miRNAs normalised to miR-26b. Fold change of normalised expression between NSCD and SCD tissues is shown. (C) Fold change of normalised expression of miR-1285 and miR-503 between in NSCD and SCD samples (n=5). Bars represent mean values with SEM. *$p<0.05$ and **$p<0.01$.

3.4 Transfection of intestinal fibroblasts from mucosa from CD patients

The downstream impact of a miRNA is determined by its target mRNAs and the pathways they are involved in. Exogenous over-expression of miRNAs via transient transfection is a commonly used method to identify molecular pathways that are controlled by the miRNAs. To study the pathways affected by the differentially expressed miRNAs, intestinal fibroblasts were isolated from six SCD and four NSCD tissue samples (Table 2.1, Section 2.1). This particular cell type was chosen because in fibrosis, fibroblasts are considered responsible for the over-production of ECM molecules. Fibroblasts were isolated from patients undergoing surgery for stricturing CD, using methods described previously by others [446] (Section 2.3). To test the transfection efficiency of the fibroblast cultures, CD495si cells (Table 2.1, Section 2.1) were transfected in duplicates with three doses (0.3 µL, 0.4 µL and 0.5 µL) of four transfection reagents from Dharmacon (Dharmafect (DF)1-4). CD495si cells were one of the first fibroblast cells cultures isolated and were used to optimise transfection conditions. Fibroblasts were transfected with 60 nM NTC-siRNA tagged with Alexa Fluor-488 for 48 hr. Hoechst stained nuclei and NTC-488 tagged siRNA were imaged on the IN Cell Analyzer microscope 1000. The percentage of transfected cells was calculated using the IN Cell Developer v1.8 (Section 2.5).

The majority of the cells were transfected regardless of which dose or transfection reagent used. A transfection efficiency of >98% was observed at even the lowest dose (0.3 µL) for all four DF reagents (Data not shown, images Fig. 3.3A-E). A slight drop in total cell number was noted using the lowest dose, 0.3 µL *(% reduction in cell number relative to untransfected cells*: DF1, 14.7%; DF2, 8.5%; DF3, 11.5%; DF4, 8.3%; Fig. 3.3F). Comparing intracellular siRNA distribution, DF3 showed a better, more homogenous distribution of the 488-tagged siRNA (Fig. 3.3G), whereas the other three DF reagents exhibited siRNA localisation in endosomal vesicles (DF1, Fig. 3.3H; DF2 and DF4, data not shown). These vesicles are targeted for destruction, which consequently decreases

siRNA concentration and functionality (reviewed in [447]). This localisation was also observed using the DF3 reagent at concentrations higher than 0.3 µL (DF3 0.5 µL; Fig. 3.3I). Therefore, DF3 was selected for further transfection optimisation experiments.

As mentioned previously, fibroblasts transfected with 0.3 µL of DF3 and NTC-488 tagged siRNA showed a reduction of 11.5% in cell number. This extent of toxicity following transfection is commonly seen and is generally accepted, however, follow-up experiments (Section 3.5) showed that fibroblasts transfected with other siRNAs did not display this amount of cell death (Fig. 3.4C) suggesting that it was the NTC-488 tagged siRNA that contributed to this toxicity in this particular experiment.

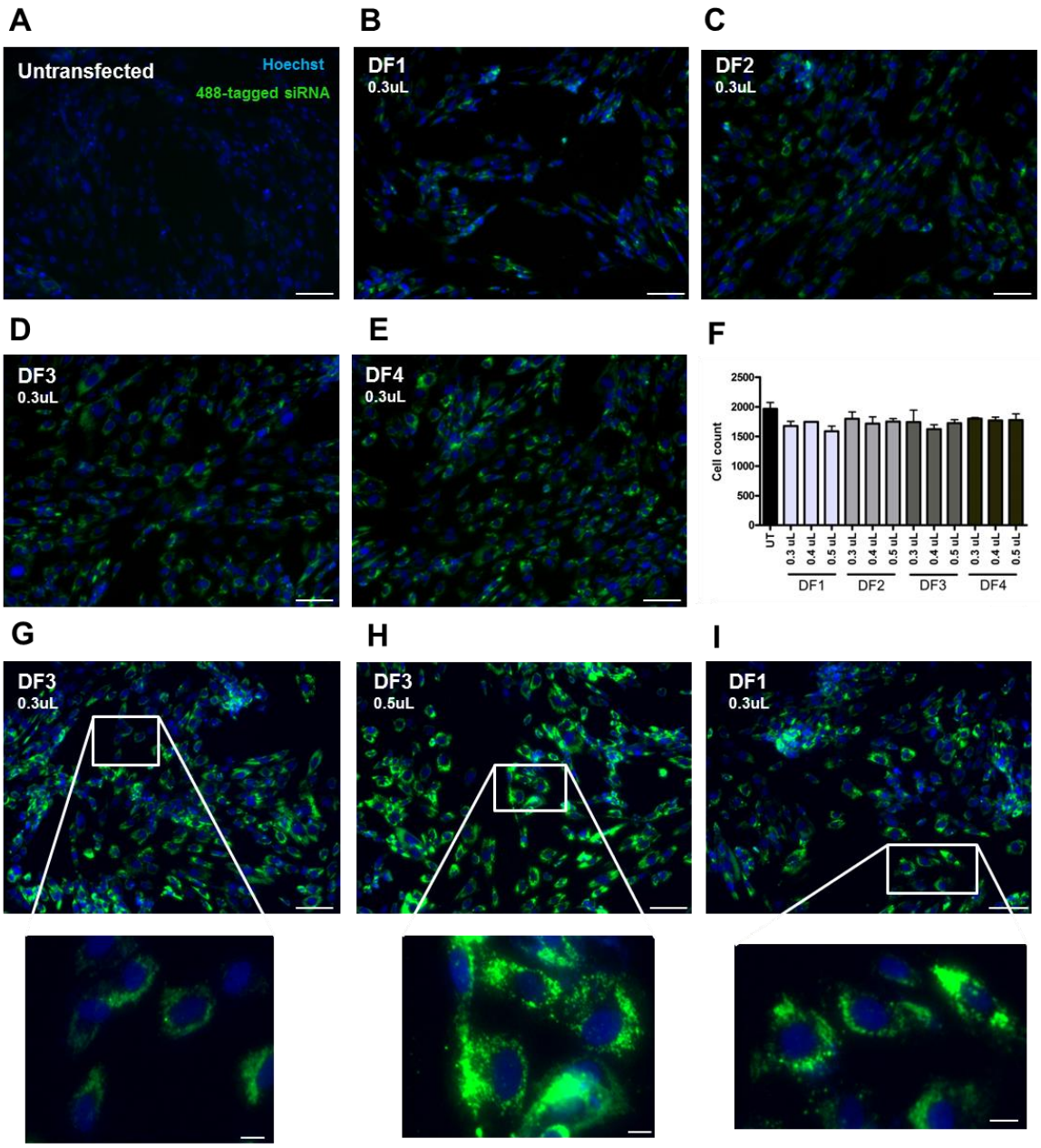

Figure 3.3. Transfection optimisation using fluorescent tagged siRNA. Three doses (0.3 µL, 0.4 µL and 0.5 µL) of four DharmaFect reagents (DF, 1-4) were optimised for transfection efficiency of intestinal fibroblasts (n=1). (A-E) Hoechst-positive nuclei and 488-tagged siRNA staining for all DF reagents at the lowest dose, 0.3 µL. (F) The cell count between the different concentrations and DF reagents. (G-I) Homogenous cellular distribution of 488-tagged siRNA using DF3 at 0.3 µL with digitally zoomed image. (H) Endosomal vesicle siRNA localisation using DF3 at the highest dose, 0.5 µL, with digitally zoomed image. (I) Endosomal vesicle siRNA localisation using DF1 at 0.3 µL, with digitally zoomed image. Bars represent mean values with SEM. Size bar 100 µm (A-E, G-I) and 20 µm (G-I, digitally zoomed images).

3.5 Optimisation of transfection of intestinal fibroblasts with DF3

To achieve optimal transfection conditions, fibroblasts were transfected using various doses (0.1 µL, 0.2 µL and 0.3 µL) of transfection reagent DF3 with or without (mock transfected) siGLO siRNA. SiGLO is a fluorescently tagged siRNA targeting the housekeeping gene cyclophilin B (*PPIB),* which may subsequently be assayed at either the mRNA or protein level to determine siRNA functionality. Cells were fixed 72 hr post-transfection, and stained with Hoechst 33342 and an antibody against PPIB (Section 2.8), then imaged on the IN Cell Analyzer microscope 1000. Using the IN Cell Developer v1.8, an overlaying mask was created using the Hoechst-positive nuclei (Fig 3.4A-B). This mask was then used to define nuclear pixel intensity in the cyclophilin B fluorescent channel. Hoechst stained nuclei were counted and cell number for each transfection condition was determined. There was no difference in cell number between the untransfected fibroblast and the various transfection conditions within this single optimisation experiment (Fig. 3.4C). However, there was a slight decrease in total nuclei count of untransfected cells (mean cell count=1715) compared to earlier experiments (Section 3.4, Fig. 3.3F, mean cell count=1966). The fibroblasts (CD495si) have undergone several passages between the two set of experiments and are therefore closer to their intrinsic replicative senescence stage. Cell division rates decrease when fibroblasts reach this stage, and this could account for the lower total nuclei count between the two set of experiments. Pixel intensity of cyclophilin B expression was determined for each dose (0.1 µL, 0.2 µL, 0.3 µL) and plotted as a frequency distribution (Fig. 3.4D-F). For all three doses, cyclophilin B expression was decreased by siGLO siRNA compared to mock transfected cells (transfection reagent only), indicated by the shift of the frequency distribution line towards the left. The strongest down-regulation in cyclophilin B pixel intensity was observed following transfection with 0.3 µL (representative images, Fig. 3.4G-J). Taking into account that DF3 doses higher than 0.3 µL resulted in endosomal vesicle localisation and elimination of the siRNA (Section 3.5), 0.3 µL was chosen for future siRNA transfection of the isolated fibroblasts.

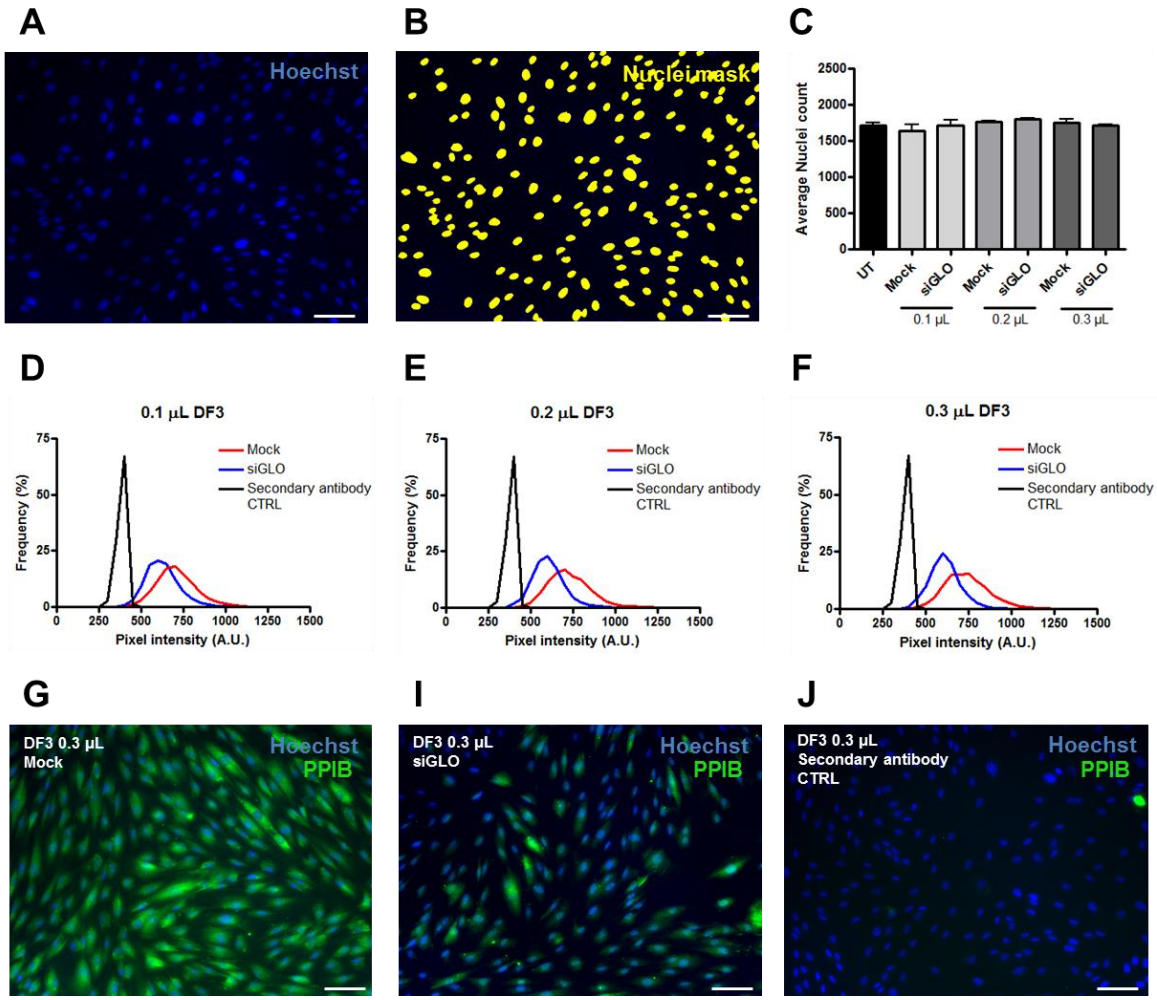

Figure 3.4. Transfection optimisation in fibroblasts using siGLO siRNA. CD495si fibroblasts were transfected in triplicates with three different Dharmafect (DF) 3 doses (0.1 µL, 0.2 µL or 0.3 µL) with or without 60 nM siGLO siRNA (n=1). (A-B) Hoechst-positive nuclei were imaged (A) and nuclei defined using the IN Cell Developer, and a mask generated (B) for subsequent quantification. This mask was then applied to the cyclophilin B staining. Nuclei were counted and cyclophilin B pixel intensity was measured. (C) The graph represents the nuclei count of the various doses of the three DF3 doses. (D-F) The graph represents frequency distributions of cyclophilin B pixel intensity of cells transfected with siGLO (blue line) or lipid only (mock, red line) for the three DF3 doses. Secondary antibody control pixel intensity represents the level of background pixel intensity (black line). (G-J) Representative images of mock and siGLO transfected cells in combination with 0.3 µL DF3. Bars represent mean values with SEM. Size bars 100 µm.

3.6 MiR-34a does not alter the mRNA expression of fibrosis-associated genes

Following successful transfection of the intestinal fibroblast cell cultures, functional studies were conducted to determine the role of the differentially expressed miRNAs between NSCD and SCD tissue samples that were identified by the miRNA microarray and subsequent qRT-PCR validation (Section 3.2 and Section 3.3). Out of the three validated miRNAs (miR-34, -493* and -708; Fig 3.2B), literature reports for miR-34a showed it had previously been involved in fibrosis of the lung, heart and kidney (Table 3.1), whereas the link between fibrosis and miR-493* or miR-708 was more ambiguous. Additionally, miR-34a has been previously shown to modulate the expression of key mediators in TGF-β pathway such as *SMAD4* [448] and *MMP* genes [439]. Therefore, miR-34a was selected for further downstream analysis in fibroblasts isolated from CD patients. In mammals, the miR-34 family consists of three processed mature miRNAs (miR-34a, -34b and -34c) encoded by two different genes on separate chromosomes. Its own transcript transcribes miR-34a while miR-34b and miR-34c have a common primary transcript (Fig 3.5A).

To investigate the downstream effects of miR-34a, intestinal fibroblasts were transfected with NTC and pre-miR-34a and incubated for 72 hr to enable overexpression of miR-34a in the cells. RNA was extracted, assayed for gene expression by qRT-PCR and normalised to the housekeeping gene glyceraldehyde 3-phosphate dehydrogenase *(GAPDH)*. A number of mRNA targets associated with fibrogenic pathways were investigated based on online prediction tools and/or validated by others. These were *COL1A2*, *COL3A1*, connective tissue growth factor (*CTGF)*, fibronectin (*FN1*), *MMP2* and *SMAD4*. Survivin (*BIRC5*) was selected as a positive control gene as it is targeted by miR-34a [449]. To confirm that the transfection with pre-miR-34a was successful, expression levels of miR-34a were measured. For the normalisation of miRNAs in cells, Applied Biosystems recommended miR-16 [445]. Also, RNU6B has been previously used for normalisation in fibroblasts from other organs [450, 451], therefore, both miR-16

and RNU6B expression was assayed in fibroblasts transfected with NTC or pre-miR-34a. RNU6B expression was not significantly altered between these conditions (data not shown), and was used to normalise miRNA expression in future experiments on isolated fibroblasts. An increase of miR-34a expression in cells transfected with pre-miR-34a confirmed that the transfected was successful (Fig. 3.5B).

mRNA expression of the seven genes is displayed as fold change in expression between fibroblasts transfected with NTC and pre-miR-34a (Fig. 3.5B). Statistical analysis revealed no significant differences between cells transfected with NTC and pre-miR-34a, however, the slight down-regulation in expression of *SMAD4* was close to significance. (*MMP2*, p=0.088 n=4; *SMAD4*, p=0.0540, n=4; *COL1A2*, p=0.9074, n=8; *COL3A1*, p=0.3361, n=8; *FN1*, p=0.2155, n=4; *CTGF*, p=0.0541, n=4; *BIRC5*, p=0.1805, n=4; Fig. 3.5D). The mean value of the positive control *BIRC5* was lower than NTC treated cells (fold change=0.746), but this was not significant. These data suggest that miR-34a does not alter the expression of fibrosis-associated mediators at the mRNA level in intestinal fibroblasts. This observation lead to the speculation that the role of miR-34a in intestinal fibrosis may not be fibroblast-related but that miR-34a may be involved in regulatory events other cell types such as epithelial cells. To test this hypothesis, *in situ* hybridisation of miR-34a was performed (Section 3.8) to determine which cells express miR-34a.

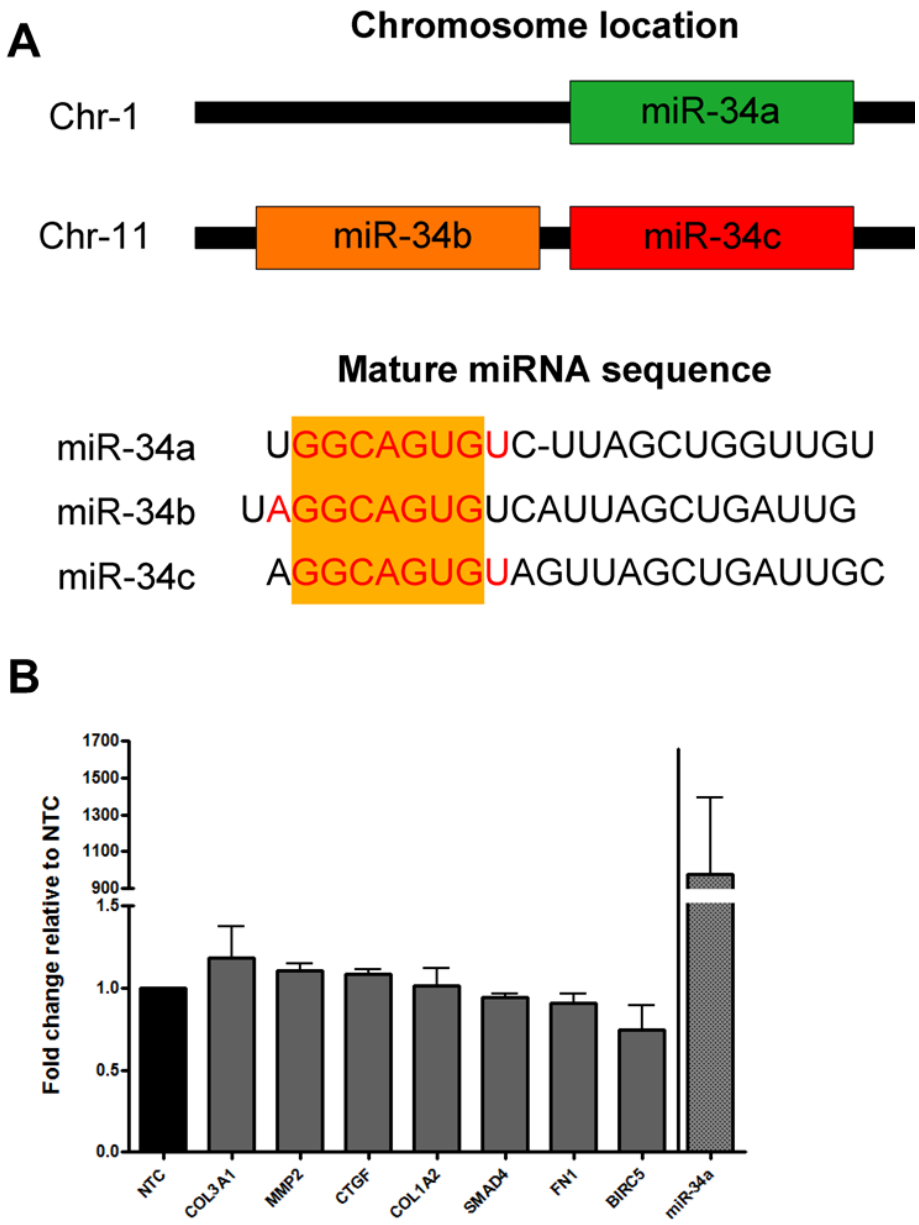

Figure 3.5. Overexpression of miR-34a does not alter mRNA expression of key fibrosis-associated genes. (A) Schematic overview of the chromosomal location of the three family members of the miR-34a family. Two genes located on chromosome 1 and 11 encode the miR-34 family. Its own transcript encodes miR-34a whereas miR-34b and miR-34c share a common primary transcript. Each seed sequence is shown in red and the majority of nucleotides are shared amongst the three members (shaded box in orange). (B) Isolated fibroblasts (n>4) transfected with NTC and pre-miR-34a. qRT-PCR of six fibrosis-associated genes and the positive control *BIRC5* normalised to *GAPDH*. The expression of miR-34a was normalised to RNU6B. Fold change in normalised expression is shown. Bars represent mean values with SEM.

3.7 Expression of p53 is not altered in intestinal fibrosis

Previous reports have indicated that members of the miR-34 family (miR-34a, miR-34b/c) are a direct target of TSG p53 [311, 312, 315, 316], a transcription factor activated in response to various stress signals leading to cell cycle arrest and apoptosis (reviewed in [452]). In addition, recent literature reports have suggested a link between p53 and liver fibrosis [389]. The next section was aimed to identify the role of p53 in intestinal fibrosis by determining its expression at both mRNA and protein level in NSCD and SCD tissues.

In 2007, a number of groups showed that the TSG p53 is a positive upstream regulator of miR-34a and miR-34b/c [311, 312, 315, 316]. The promoters for both miR-34a genes contain conserved p53-binding sites as well as CpG islands, and methylation of both promoters has been reported in various human cancers [319, 453-456]. p53 is a potent tumour suppressor which triggers the activation of anti-proliferative cellular responses resulting in apoptosis, cell cycle arrest or senescence (reviewed in [452]). In addition, the *TP53* gene is the most frequently mutated tumour suppressor gene in human cancer [457, 458]. It is, therefore, not surprising that the over-expression of miR-34a and miR-34b/c can cause cell cycle arrest [311, 315, 459] and inhibit proliferation and colony formation [313]. Thus, as a direct target of p53, miR-34a and miR-34b/c may act as key mediators of p53's tumour suppressor function.

The miR-34 family has been studied predominantly in the context of cancer but the p53/miR-34 axis in fibrosis much less defined. For example, reports show up-regulation of p53 in idiopathic pulmonary fibrosis [460, 461], and in liver fibrosis where p53 was correlated to CTGF expression [389], a well-known marker for fibrosis. Furthermore, p53 inhibition prevented CTGF-mediated fibrosis in the kidney of rodents [462, 463] and p53 expression was shown to be induced by the pro-fibrotic cytokine TGF-β [462]. By contrast, activation of p53-mediated senescence in hepatic stellate cells was found to limit liver fibrosis in mice [464]. Additionally, p53 deficient cardiac fibroblasts isolated from mice exhibited an increase of collagen I and III production, which are key ECM

molecules implicated in the development of fibrosis. The role for p53 in intestinal fibrosis however, remains unclear. Given that miR-34a was identified and validated as up-regulated in SCD compared to NSCD sample tissues, the aim here was to examine the role of p53 in intestinal fibrosis in CD by determining its expression at both mRNA and protein level.

Initially, *TP53* mRNA was measured via qRT-PCR in six matched paired NSCD and SCD tissues and expression was normalised to *GADPH*. *TP53* expression levels between the two groups was not significantly different (p=0.252; Fig. 3.6A). Protein level of p53 was also assessed in tissues of CD patients with (n=7) or without (n=6) fibrosis via immunohistochemistry. Staining was analysed and reported by a consultant pathologist (Professor Roger Feakins, Department of histopathology, The Royal London Hospital) who determined the percentage of p53-positive cells at two different staining intensity levels (1: weak and 2-3: moderate / strong). p53-positive staining in epithelial cells, immune cells (dendritic cells), and lamina proprial stromal cells was expressed as a percentage of total cell population analysed (Table 3.2). Immunohistochemistry showed a variable but generally low level of staining in epithelial, immune and lamina proprial stromal cells in both NSCD and SCD tissues. Often, a significant minority or in some cases a majority of normal crypt epithelial cells showed weak staining for p53. However, moderate / intense p53 staining was always focal and, even in the most strongly stained areas, was confined to <1% to 10% of epithelial cells (Table 3.2, arrows Fig. 3.6B). By contrast, the most strongly stained areas in the ulcerated fibrotic bowels showed moderate / intense staining in 25% to 50% of crypt epithelial cells (arrows, Fig. 3.6C). These areas of intense p53 staining were typically close to the fibrotic lesions. Fibroblasts and other connective tissue cells showed little or no p53 expression, regardless of the presence or absence of ulceration and/or inflammation (arrows, Fig. 3.6D). This data indicates that the increase of p53 expression in fibrotic CD tissue seems to be in the epithelium as a response to fibrotic ulceration and/or inflammation. The lack of p53 staining in lamina proprial stromal cells would suggest that p53 does not play a direct role in these stromal cells, and might not a have a direct effect on the production of ECM in these cells.

The up-regulated p53 expression in epithelial cells is in contrast to the lack of differential expression of *TP53* mRNA expression between the six matched NSCD and SCD tissues. This might be due to the fact that the RNA from epithelial cells represents only a fraction of the total RNA extracted from the mucosa. Therefore, the moderate / intense staining of p53 protein that was observed in epithelial cells in overlying fibrotic areas was perhaps not reflected at the RNA level.

Previous results indicated that miR-34a did not regulate the expression of any fibrosis related genes (Section 3.6) and its main upstream regulator, p53, was not expressed in fibroblasts in SCD tissue samples (Section 3.7). These observations suggest that the role for miR-34a in intestinal fibrosis might not be fibroblast-related and that it may be functional in other cell types such as epithelial cells. The next section aims to determine which cells express miR-34a in NSCD and SCD tissues by performing *in situ* hybridisation.

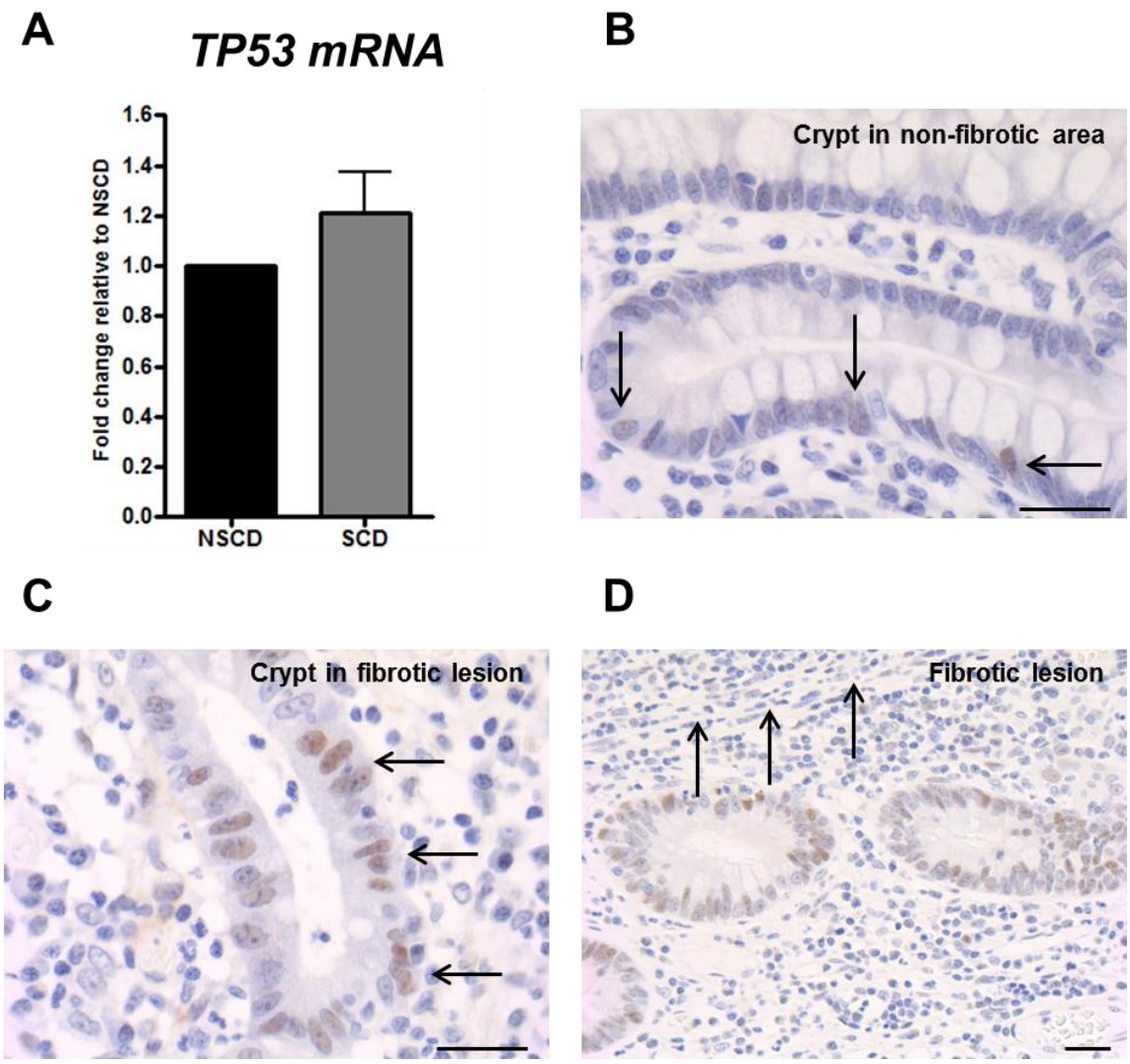

Figure 3.6. Increased expression of p53 in epithelial cells in crypts overlying fibrotic lesions. (A) qRT-PCR of *TP53* mRNA in six matched NSCD and SCD tissue samples. Expression normalised to *GADPH*. (B-D) IHC of p53 in FFPE tissue from CD patients analysed by Professor Roger Feakins. (B) Weakly p53-positive cells (black arrows) in normal crypts. (C) Moderate / strong p53-positive cells (black arrows) in crypts localised near fibrotic ulcers. (D) Negative lamina proprial stromal cells (black arrows) around fibrotic lesions. Bars represent mean values with SEM. Size bar is 100 μm.

Table 3.2. Immunohistochemistry staining of p53 in NSCD and SCD tissue. Classification of percentage of p53-positive cells in both normal (NSCD, n=6) and fibrotic (SCD, n=7) areas in CD patients. Percentage of staining in two staining intensities (1: weak, 2-3: moderate/strong) in three different cell types were noted. For the crypts, a minimum of 20 crypts in the most strongly staining area were measured per sample. NA, not applicable.

ID	Type	Crypts		Follicular dendritic cells		Lamina proprial stromal cells	
		% staining intensity 1	% staining at intensity 2-3	% staining intensity 1	% staining at intensity 2-3	% staining intensity 1	% staining at intensity 2-3
CD362	NSCD	10-20	<1	40	5	<1	0
CD417	NSCD	20	5	NA	NA	10	0
CD401	NSCD	50	10	NA	NA	1	0
CD398	NSCD	40	5	30	<1	<5	0
CD425	NSCD	50	<1	10	<1	10	<1
CD419	NSCD	40	10	NA	NA	<1	0
CD362	SCD	80	10-50	10	1	0	0
CD417	SCD	90	40	5	1	10	1
CD401	SCD	80	50	25	2	10	1
CD398	SCD	80	35	NA	NA	10	1
CD425	SCD	50	30	30	2	10 (by lesion)	<1
CD373	SCD	80	40	80	5	15-20	1
CD419	SCD	50	30	40	2	5	0

3.8 Expression of miR-34a expression in gut mucosa is localised to the epithelial cells

In situ hybridisation allows miRNA expression analysis to be performed directly in tissues. This facilitates the identification of miRNA expression in specific cell types or the expression pattern in tumours. Detection probes for miRNAs often contain locked nucleic acids (LNA) which increase hybridisation affinities over standard probes [465, 466]. Exiqon is one of the leading companies that produce commercially available LNA probes for the majority of miRNAs in miRBase (www.miRbase.com). Section 2.19 and Fig. 2.3 show a detailed overview of the *in situ* hybridisation methodology performed.

The aims for this part of my thesis were:

1. To determine the localisation of miR-34a in the mucosa of patients; and
2. Compare the expression pattern of miR-34a between NSCD and SCD.

One of the most important steps in the *in situ* protocol is the proteinase-K treatment which digests the tissue allowing the probe to access the cell and bind to the miRNA. Too little digestion and the probe will not be able to hybridise, whereas too much digestion can lead to over-digestion of the tissue and cause increased signal to noise ratios. The incubation time with proteinase-K was therefore optimised. Three time points (15 min, 30 min or 45 min) were performed in combination with 60 nM of miR-34a LNA probe on slides from FFPE blocks colon cancer tissue. Figure 3.7 shows images from the optimisation of miR-34a with three different proteinase K digestion times (A. 15 min, B. 30 min and C. 45 min; Fig 3.7). Expression of miR-34a illustrated a staining intensity which correlated positively to an increase in digestion time; ranging from minimal staining after 15 min to strong staining after 45 min of proteinase-K digestion. Background staining increased after proteinase-K treatment for 45 min (black arrows; Fig 3.7C) and therefore, a 30 min digestion time was selected for further *in situ* hybridisation experiments with miR-34a.

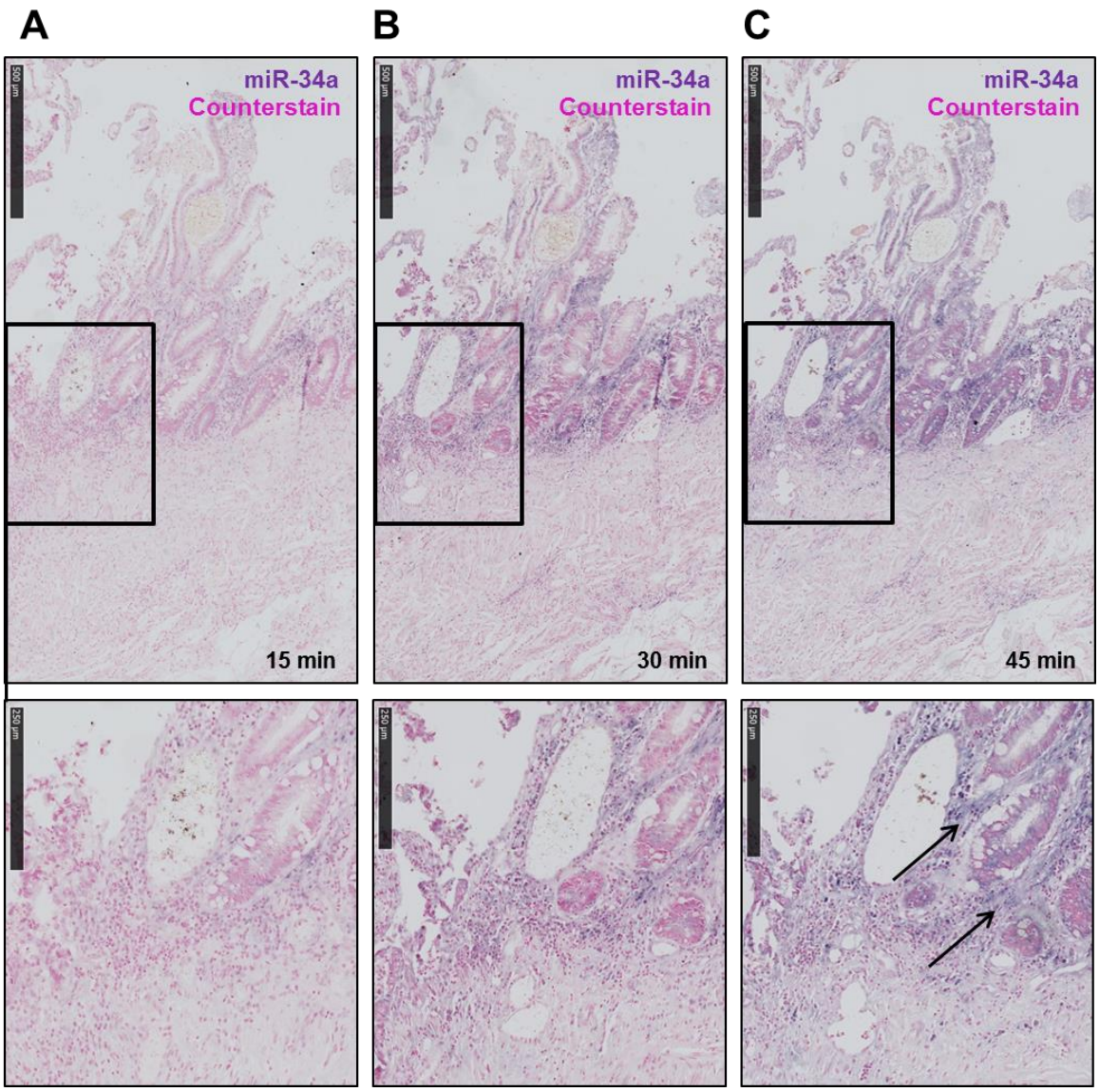

Figure 3.7. Optimisation of *in situ* hybridisation of miR-34a in colon cancer tissue. (A-C) Tissue was incubated with 10 µg/ml proteinase-K for three time points (15 min, 30 min and 45 min) followed by hybridisation with 60 nM miR-34a double-DIG-labelled LNA probe. miR-34a staining in blue and nuclear counterstain in red. Black rectangles outline the position of the zoomed images shown below.

To determine the expression of miR-34a in the gut mucosa, ten FFPE blocks (five SCD, five NSCD, matched tissues from the same patient) were subjected to *in situ* hybridisation with double-DIG-labelled LNA probes for miR-34a (60 nM) and a negative control (scrambled sequence, 60 nM). Sections were treated with 10 ug/ml proteinase-K for 30 mins as previously optimised. Images of one pair of matched tissue (SCD and NSCD) are shown in Fig. 3.8. In general, miR-34a staining was predominantly observed in the epithelial cells in the mucosal crypts as well as some of the immune cells (black arrows; Fig. 3.8A, C). Minimal to no expression of miR-34a was seen in the stromal-like cells (red arrows; Fig. 3.8A, C), although without a marker for mesenchymal cells, stromal cells were hard to distinguish from other cell types with the use of a nuclear counterstain alone. Serial sections were hybridised with a double-DIG-labelled LNA probe for a scrambled sequence (negative control) which demonstrated no positive staining (Fig. 3.8B, D), indicating that the miR-34a staining observed in adjacent sections is specific.

In only two of the five paired tissue blocks, miR-34a expression was even and homogenous across the slide. The other three showed patchy staining, which may be due to uneven tissue digestion and/or uneven incubation of the hybridising probe. Because of this it was difficult to draw any conclusions as to whether the expression of miR-34a was altered in mucosa-overlying strictured areas compared to mucosa-overlying non-strictured areas. Although, staining in the two paired tissue blocks did not show obvious differences in expression levels in the epithelial cells or immune cells (Fig. 3.8A, C).

In conclusion, miR-34a expression in the gut mucosa is predominantly localised to epithelial cells and not in stromal-like cell types. This observation is in accordance with the fact that p53, a major upstream regulator of miR-34, was also mainly found to be expressed predominantly in epithelial cells (Section 3.7). These results indicate that the functional role for miR-34a in gut fibrosis may not be directly in fibroblasts, but indirectly through the interaction between fibroblasts and other cell types with elevated miR-34a expression, such as epithelial cells.

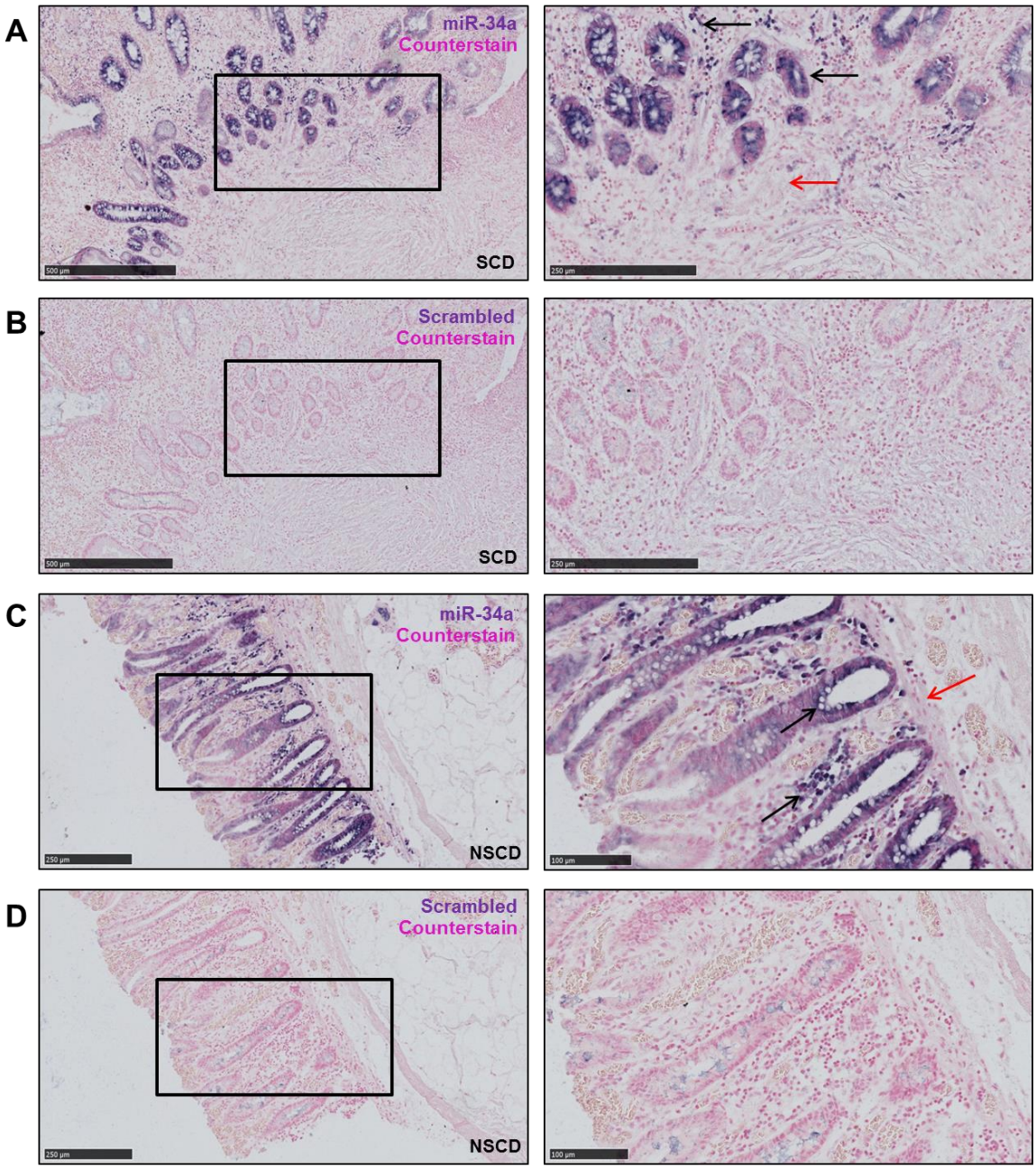

Figure 3.8. The expression of miR-34a is localised to epithelial cells in the gut mucosa. (A-D) Images of two blocks of gut tissue from the same patient (1 SCD, 1 NSCD) hybridised with 60 nM double-DIG-labelled LNA probe against miR-34a or a scrambled sequence (negative control). Black rectangles outline the position of the zoomed images shown on the right. Black arrows indicate positively stained epithelial cells and immune cells, red arrows indicate negative staining in the stromal-like cells. Size bars shown.

3.9 Discussion and future work

3.9.1. Differentially expressed miRNAs between NSCD and SCD mucosal tissue

Previous reports have indicated that molecular changes in the overlying mucosa layer can mimic events in underlying tissues [201]. MiRNAs regulate many cellular processes including proliferation, differentiation and apoptosis. I, hypothesised therefore, that the miRNA expression profile between NSCD and SCD areas is different. To test this, changes in miRNA expression were determined in mucosa samples from NSCD and SCD tissues and subsequent analysis identified 29 differentially expressed and significant differentiated miRNAs (Section 3.2). Although others have investigated the differential expression between CD and healthy controls [361, 362], my study was the first to profile altered miRNA expression in the mucosa of intestinal fibrosis in CD. Comparison between my data with data from the arrays mentioned above highlighted only a single commonly altered miRNA (miR-34c-5p,[362]), however, given the differences in sample groups, a true comparison is difficult.

The up-regulation of three miRNAs (miR-34a, -493* and -708) in SCD tissues compared to NSCD was validated by qRT-PCR. Two miRNAs (miR-223* and -148b) were not significantly changed and two (miR-1285, -503) could only be detected in five of the eight paired samples that were tested (Section 3.3). One of the advantages of the Illumina array is its high sensitivity to detect low abundance miRNAs. This could explain why miR-1285 and miR-503 were not detected in all of the samples by qRT-PCR. However, for the samples in which miR-1285 and miR-503 could be detected, the type of dysregulation was in accordance with that identified by the array (miR-1285 down-regulated in SCD vs NSCD, miR-503 up-regulated in SCD vs NSCD). In our laboratory, we continue to collect additional paired NSCD and SCD tissue samples. Future work could include further examination of both miR-503 and miR-1285 expression levels in these samples.

The expression of miR-708 was up-regulated in SCD vs NSCD and validated by qRT-PCR (Section 3.3). This contradicts the findings of Huebert and colleagues, who identified miR-708 as one of the down-regulated miRNAs in cirrhotic (end-stage resulted from fibrosis of the liver) endothelial cells [444]. The expression of miRNAs is context dependent and may vary greatly between various tissue and cell types providing an explanation for these contradicting observations. As the array presented here was performed on the mucosa, which comprises of a number of cell types, it will therefore be important to determine the localisation of miR-708 within CD tissue samples (as was done for miR-34a in this thesis). For example, miR-708 has been found to induce apoptosis in renal cancer cells [467] and it would be very interesting to investigate the localisation of miR-708 in the gut mucosa in CD. As I have observed the localisation of pro-apoptotic miR-34/p53 axis in epithelial cells, the expression of miR-708 could therefore lend support to this pro-apoptotic signalling within the epithelial cells during fibrogenesis. On the other hand, if miR-708 is expressed in mesenchymal-like cells, functional studies could be performed on intestinal fibroblasts to elucidate the downstream mechanisms of miR-708 in intestinal fibrosis in CD.

Validation by qRT-PCR showed that miR-493* displayed the largest fold increase in SCD vs NSCD tissues. Only one other report has suggested a potential role for miR-493* in fibrosis. Milosevic and colleagues demonstrated an increase of miR-493* expression in idiopathic pulmonary fibrosis [442]. Interestingly, miR-493* is a member of the second largest miRNA cluster (C14MC) in the human genome and is located at the imprinted DLK-1/DIO3 domain on the human chromosome 14q32 [248]. This domain is maternally imprinted and consists of numerous repeated, intron-embedded miRNAs that are processed from a single long non-coding RNA. A large number (n=24) of miRNAs from this cluster has been previously shown to be up-regulated in tissue samples from patients with pulmonary fibrosis [442]. Also, the expression of 13 C14MC miRNAs was induced by TGF-β, implicating these miRNAs in the pathogenesis of fibrosis [442]. On the array presented in this thesis (Section 3.2), three other members of this cluster were shown to be up-regulated in SCD vs NSCD (miR-323-3p, -369-3p, and -487b). Future work could

attempt to validate these miRNAs on our paired NSCD and SCD tissue samples. A synergistic up-regulation of more members of this cluster would strengthen the hypothesis that this cluster is involved in intestinal fibrosis in CD.

TGF-β has been shown to be involved in the activation of Wnt signalling by decreasing Wnt pathway antagonist DKK-1 resulting in increased fibrosis [468]. The online target prediction program miRBase (www.microrna.org) predicts that *DKK1* might be targeted by a number of members of the C14MC cluster (miR-136, -376a, -376b, -433, -493*, -496, -543, and -656). Strikingly, an additional four miRNAs that were up-regulated in the array (miR-148b, -223*, -34a, and -493*) are also predicted to target this Wnt-antagonist. The link between these miRNAs and DKK1/Wnt signalling has not yet been investigated.

Therefore, a novel line of investigation would aim to:

1. Validate additional members of the C14MC in paired NSCD vs SCD tissue samples via qRT-PCR;
2. Investigate the effect of the validated miRNAs on Wnt signalling activation. This could be done via transient transfection of candidate miRNAs in combination with a Wnt activity reporter construct (TCF-LEF-reporter) in intestinal fibroblasts. These experiments should be performed in the presence of TGF-β stimulation to elucidate the role of both TGF-β and the miRNAs on Wnt signalling activity; and
3. mRNA and protein expression of key Wnt signalling mediators, including DKK1, could be assayed following transfection of the validated miRNAs in intestinal fibroblasts.

3.9.2. miR-34a does not alter the mRNA expression of fibrosis-associated genes

Intestinal fibroblasts were isolated from mucosa from six CD patients undergoing surgery for stricture formation (Table 2.1) using methods described by others [446] (Section 2.3). The benefit of using intestinal fibroblasts isolated cells from the gut of patients with CD

is the ability to demonstrate the role of candidate miRNAs in a physiologically relevant context i.e. gut fibrosis. However, transfection of isolated cells from primary tissue is notoriously difficult and transfection of intestinal fibroblasts has only been reported by one other group [469]. However, I have now shown that intestinal fibroblasts can be transfected successfully with siRNA/miRNAs using a lipid based system (Section 3.4 and Section 3.5).

Overexpression of miR-34a via transient transfection of pre-miR-34a demonstrated no significant change in mRNA expression of fibrosis-associated genes between NTC and pre-miR-34a transfected fibroblasts (Section 3.6). Both *MMP2* and *SMAD4* were selected based on their 3'UTR containing predicted sites for miR-34a. However, my data showed that miR-34a does not influence these genes at the transcriptional level. mRNA expression levels of survivin (*BIRC5*), which previously validated to be target by miR-34a [449] and used a positive control, was not significantly altered following overexpression of miR-34a. A literature search later revealed that miR-34a down-regulates the expression of survivin solely at the protein level whilst its mRNA level remains unchanged [470], thereby providing an explanation for why miR-34a failed to reduce the mRNA levels of *BIRC5*. Although miR-34a expression levels were induced nearly 1000-fold following transfection with pre-miR-34a (Section 3.6), additional evidence is needed to confirm successful transfection. Future experiments to further investigate potential targets for miR-34a will have to include other positive controls such as *SIRT1* [471] or *BCL2* [472], which have been previously validated at the mRNA level. Ideally, phenotypic controls such as cell viability and/or cell number should be used. A decrease in these parameters could provide evidence that miR-34a is functional within the cell as miR-34a is known to be a potent inducer of apoptosis [471, 473].

Many studies focus on the effect of miRNAs on mRNA degradation whilst reports show that translational repression by miRNAs can account for the majority of their regulatory function [266, 474]. In fact, genome-wide studies suggest that some targets are solely repressed at the translational level [475, 476]. These studies highlight the need for protein

expression analysis and future work may aim to further investigate miR-34a targets at the protein level by techniques such as western blotting or immunohistochemistry. Given the fact that miR-34a was predominantly expressed in epithelial cells, functional studies, such as over-expression of miR-34a in this cell type may be a more appropriate way to determine the role for miR-34a during fibrogenesis.

3.9.3. p53 is expressed in epithelial cells overlying fibrotic areas in the mucosa of CD patients

The TSG p53 is an upstream activator of miR-34a and miR-34b/c [311, 312, 315, 316], suggesting a role for p53 in intestinal fibrosis. Therefore, in Section 3.7, the expression of p53 was investigated in intestinal fibrosis at mRNA and protein level via qRT-PCR and IHC, respectively. *TP53* transcript levels in six matched NSCD and SCD tissues showed no significant change between the two groups. Quantification of p53 protein expression of normal and fibrotic lesions of CD patients indicated an increase in p53 protein within the epithelial cells of the crypts surrounding fibrotic lesions. No p53-positive stromal cells were observed in either normal tissue or fibrotic lesions. The presence of p53-positive epithelial cells in fibrotic lesions confirmed the findings of others that report an up-regulation of p53 in the epithelial cells of patients with pulmonary fibrosis [460, 461]. This observation was linked to the induction of the p53-mediated apoptosis signalling pathway [460, 461]. Thus, p53 may not be involved directly in the fibroblasts-associated events during intestinal fibrosis in CD. It has been proposed that idiopathic pulmonary fibrosis results from epithelial cell injury and the subsequent activation of underlying mesenchymal cells (reviewed in [477]). More recently, this cross talk between epithelial and mesenchymal cells was shown in oesophageal fibrosis [478]. Together, these findings support a role for the pro-apoptotic signalling through p53 in epithelial cells in intestinal fibrosis.

3.9.4. miR-34a is present in the epithelial cells in the mucosa of CD patients

To investigate the location of miR-34a in the gut of CD patients, *in situ* hybridisation of miR-34a was performed on five matched pairs of NSCD and SCD tissues. Unfortunately, the staining of miR-34a was uneven in the majority of sections investigated. The majority of publications that include *in situ* hybridisation of miRNAs use a probe against small RNA U6 as a positive control for the staining technique. U6 is expressed ubiquitously and should, therefore, be present in all cell types. However, one of the down-sides of using U6 as a control is the fact that this small RNA is present only in the nucleus. For the hybridisation probe to reach the nucleus, longer digestion times are required compared to miRNAs in the cytoplasm. For example, when gut sections were stained with U6, both positive and negative stained patches within the same slide were observed (Appendix Fig. 1). The positively stained patches appeared more digested than the negative patches, suggesting that more tissue digestion is required for the U6 probe to be able to access the nucleus and hybridise with U6 small RNA. This makes the use for U6 as a positive control questionable in this context.

As the expression of miR-34a was uneven across the slide, and the lack of an appropriate positive control, I was unable to make any conclusion as to whether the expression of miR-34a was altered between mucosa-overlying strictured areas and non-strictured areas. However, I can report that the expression of miR-34a was predominantly found in epithelial cells with weak staining in stromal like cells. This observation is in accordance with previous *in situ* reports which demonstrate the expression of miR-34a in epithelial cells of bladder carcinoma [479] and breast cancer [480, 481]. Furthermore, I showed that one of its main upstream regulators, p53, is also expressed in the epithelial cells (Section 3.7), which may indicate the activation of the p53/miR-34 axis in these cells. Functionally, any role for miR-34a in intestinal fibrosis is likely to be localised to epithelial cells and not in fibroblasts. As mentioned in Section 3.9.3, the activation of sub-epithelial stromal cells has been proposed to be a secondary event following epithelial cell injury in pulmonary fibrosis, which might also potentially be the case for intestinal

fibrosis in CD. To further investigate this line of research, the following experiments could be performed:

1) A repeat of the *in situ* hybridisation of miR-34a in paired NSCD and SCD tissues alongside multiple miRNAs as controls (e.g. miR-210 and miR-21). We know from experiments performed later on in this thesis (Section 5.4) that miR-210 is expressed in epithelial cells and that miR-21 is predominantly observed in stromal cells in CRC tissue. The use of these miRNAs as controls would allow me to draw conclusions about the localisation and relative expression of miR-34a in NSCD and SCD tissues;
2) To investigate whether the expression of miR-34a is altered between NSCD and SCD tissues with the use of *in situ* LNA probes conjugated with fluorescent dyes. This would facilitate accurate quantification of the miRNA expression levels in tissue. The IN Cell Developer v1.8, which has been used in this thesis to quantify fluorescent images, could be used for this purpose;
3) To investigate co-localisation of miRNAs and potential gene targets, co-staining could be performed. In our laboratory, miRNA *in situ* has been successfully combined with regular immunohistochemistry. This technique would allow identification of co-localisation of miR-34a and other proteins such as p53; and
4) Finally, to investigate the cross-talk between epithelial cells and fibroblasts, organotypic cultures could be used. For example, epithelial cells (preferably primary/non cancer cells) should be stably transfected with miR-34a expression vectors and cultured on top of intestinal fibroblasts for various amounts of time (3-14 days). Cultures would be fixed and then stained for ECM markers such as collagens and α-SMA. This would test whether the up-regulation of miR-34a within the epithelial cells can potentially induce the activation of fibroblasts and promote production of ECM by these cells.

Chapter 4: Reduced expression of miR-29b in CD up-regulates collagen expression in intestinal fibroblasts

4.1 Introduction and aims

The preceding chapter identified differentially expressed miRNAs between NSCD and SCD tissues (Section 3.2 and Section 3.3). The microarray used to determine the expression is capable of detecting low abundance miRNAs due to the technology's high sensitivity. Hence, 40 miRNAs that were highly expressed in CD tissues were not detected as differentially expressed because of their fluorescence being outside the detectable range (Appendix Table 1). This was the case for miR-29b, one of the three members of the miR-29 family (miR-29a, -b and –c). The miR-29 family has been predominantly studied in cancer and is known for its tumour-suppressor function (reviewed in [482]). In addition, the miR-29 family is down-regulated in fibrosis of various organs [372-378], although not in the intestine where changes in miR-29 expression are yet to be investigated [372-378]. Aims for this chapter:

1. Determine the expression of the miR-29 family in intestinal fibrosis in CD;
2. Investigate down-stream targets of miR-29b in intestinal fibroblasts via transient transfection and assess the expression of ECM molecules, such as collagen I and III, at the mRNA and protein level in the presence and absence of TGF-β; and
3. Identify the effect of miR-29b on a down-stream target, myeloid cell leukemia-1 (Mcl-1), and the mRNA and protein level.

Part of this chapter formed the basis of a manuscript published in Clinical Science in 2014 [483].

4.2 MiR-29 family is down-regulated in CD fibrosis, regulates COL1A2 and COL3A1, and collagen III protein expression

The human miR-29 family consists of miR-29a, miR-29b-1, miR-29b-2, and miR-29c. The gene encoding the precursors of miR-29a and miR-29b-1 is located on chromosome 7, whilst miR-29b-2 and miR-29c are on chromosome 1 (Fig. 4.1A). Sequences of the mature miR-29 strands largely overlap, and are highly conserved in human, mouse and rat. In fact, the sequence of miR-29b-1 and -2 are identical and are collectively referred to as miR-29b. Additionally, the three mature miR-29 strands share corresponding sequences at nucleotide positions 2-7, which is known as the seed region (orange shaded areas; Fig 4.1A). This region is involved in facilitating the binding between the miRNA and its target mRNA and, as a result, the predicted target genes for the miR-29 family widely overlap. The miR-29 family has been previously implicated in the pathogenesis of fibrosis in various organs. For example, the expression of all three members is reduced in fibrosis of the kidney [372, 373] and liver [374]. Additionally, miR-29b is down-regulated following myocardial infarction [375] in the lungs of patients with idiopathic pulmonary fibrosis [376, 377] and in skin fibroblasts of patients with systemic sclerosis [378]. To date, the role for the miR-29 family in intestinal fibrosis in CD remains unexplored.

Because the signal for miR-29b was saturated on the array, the expression of the miR-29 family was validated in nine paired NSCD and SCD tissues by qRT-PCR. Expression values were normalised to miR-16 and fold change in SCD relative to NSCD is calculated. All three members of the miR-29 family were significantly down-regulated in SCD samples compared to NSCD (n=9, miR-29a, p=0.0002; miR-29b, p=0.0010; miR-29c, p=0.0114; Fig. 4.1B). The expression of miR-29b demonstrated the largest decrease in fold change in SCD relative to NSCD and miR-29b was, therefore, selected for further functional studies. In addition, reports have indicated that the dysregulation of key mediators in fibrosis of various organs is predominantly controlled by miR-29b [372, 484].

Online predication tools indicate that miR-29b targets both *COL1A2* and *COL3A1* (www.microRNA.org), both of which have been validated by other groups using 3'-UTR luciferase assays [375, 379]. In addition, both *COL1A1* and *COL3A1* are important in intestinal fibrosis [485, 486] and were up-regulated in SCD relative NSCD tissue samples (Appendix Fig. 2). To validate these findings in intestinal fibrosis, fibroblasts isolated from CD patients were transiently transfected with NTC, pre-miR-29b or anti-miR-29b. Expression of *COL1A2* and *COL3A1* mRNA were assessed by qRT-PCR and normalised to *GAPDH*. Fold change in expression compared to NTC demonstrated a significant down-regulation of both *COL1A2* and *COL3A1* by pre-miR-29b (*COL1A2* and *COL3A1*, $p<0.0001$; Fig.4.1C). Additionally, both genes were significantly up-regulated following transfection with anti-miR-29b relative to NTC (*COL1A2*, $p=0.037$; *COL3A1*, $p=0.0015$; Fig. 4.1C). This data shows that miR-29b modulates the expression of both collagens at the mRNA level.

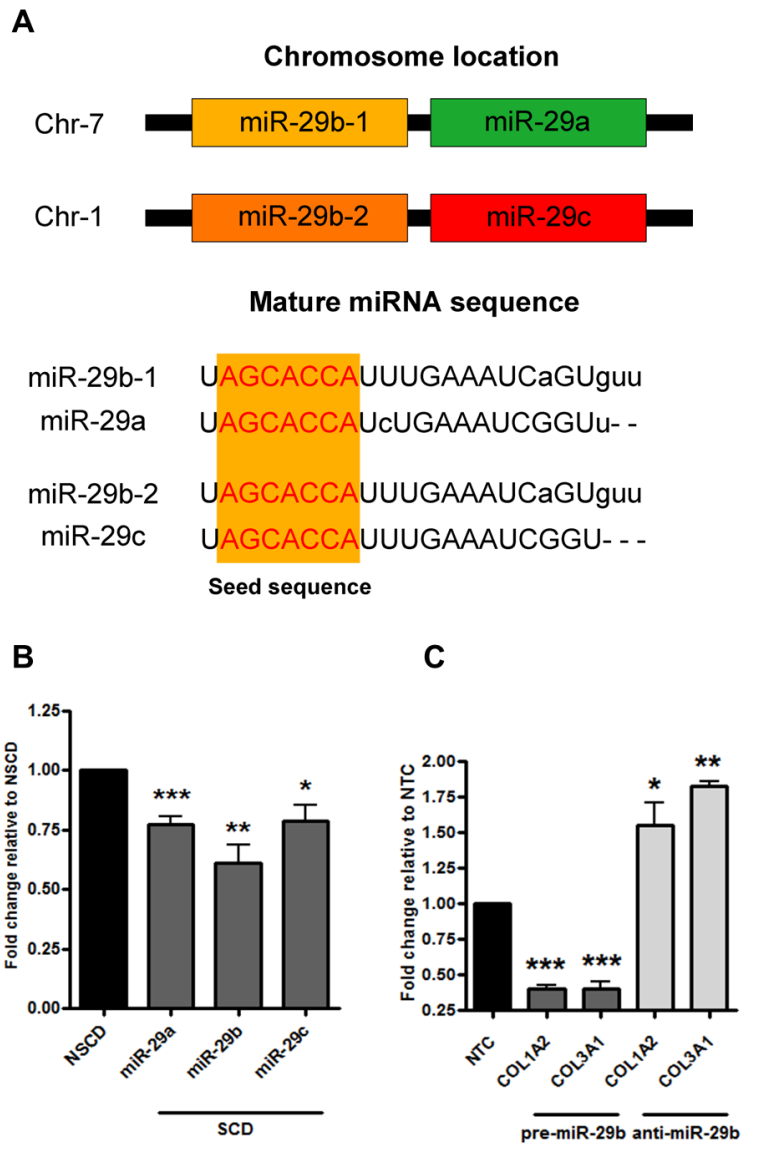

Figure 4.1. miR-29b is down-regulated in intestinal fibrosis and modulates *COL1A2* and *COL3A1* mRNA (A) Schematic overview of chromosomal location of the human family members of the miR-29 family. The miR-29 family is encoded by two genes located on chromosome 7 and 1. The mature sequence of miR-29b-1 and -2 are identical and referred to as miR-29b. All members share the same seed sequence highlighted in orange. (B) qRT-PCR of the three members in nine matched NSCD and SCD tissue samples. Expression normalised to miR-16. The graph represents the fold change in expression relative to NSCD. (C) Intestinal fibroblasts (n>3) transfected with NTC, pre-miR-29b or anti-miR-29b for 72 hr. qRT-PCR of *COL1A2* and *COL3A1* mRNA expression is normalised to *GAPDH*. The graph represents the fold change relative to NTC. Bars represent mean values with SEM. *p<0.05, **p<0.01 and ***p<0.001.

To investigate the effect of miR-29b on collagen I and III protein levels, immunofluorescence was performed. Intestinal fibroblasts were transfected with NTC, pre-miR-29b or anti-miR-29b for 72 hr. Cells were fixed and stained with Hoechst 33342, CellMask Deep Red, and antibodies against collagen I or III. The IN Cell Analyzer 1000 microscope was used to image the cells under identical exposure conditions. A mask overlying the CellMask Deep Red stained cells was created using the IN Cell Developer v1.8. Hoechst-positive nuclei were used to clump-break the overlaying mask (Fig 4.2A-C), which was subsequently used to define cellular pixel intensity of both collagen I and III in individual cells. Fold change in median pixel intensities between NTC and pre-miR-29b or anti-miR-29b transfected fibroblasts was calculated. Fibroblasts transfected with pre-miR-29b demonstrated a significant decrease in pixel intensity for collagen III compared to cells transfected with NTC ($p=0.0069$; Fig. 4.2D), whereas collagen I protein was not altered by pre-miR-29b ($p=0.163$; Fig. 4.2D). Finally, fibroblasts transfected with anti-miR-29b did not alter endogenous collagen I or III protein levels. This observation was in contrast to the up-regulation of *COL1A2* and *COL3A1* mRNA expression following transfection with anti-miR-29b (Fig. 4.1C). Representative images of fold change in Fig. 4.2D are shown in Fig.4.2E.

Together, this data demonstrates that the miR-29 family is down-regulated in intestinal fibrosis in CD. Furthermore, miR-29b is able to regulate both collagen I and III at the mRNA level, and collagen III at the protein level. Collagen I protein level was not altered by miR-29b in this particular experimental set-up, and this will be reviewed in the discussion chapter (Section 4.6.2).

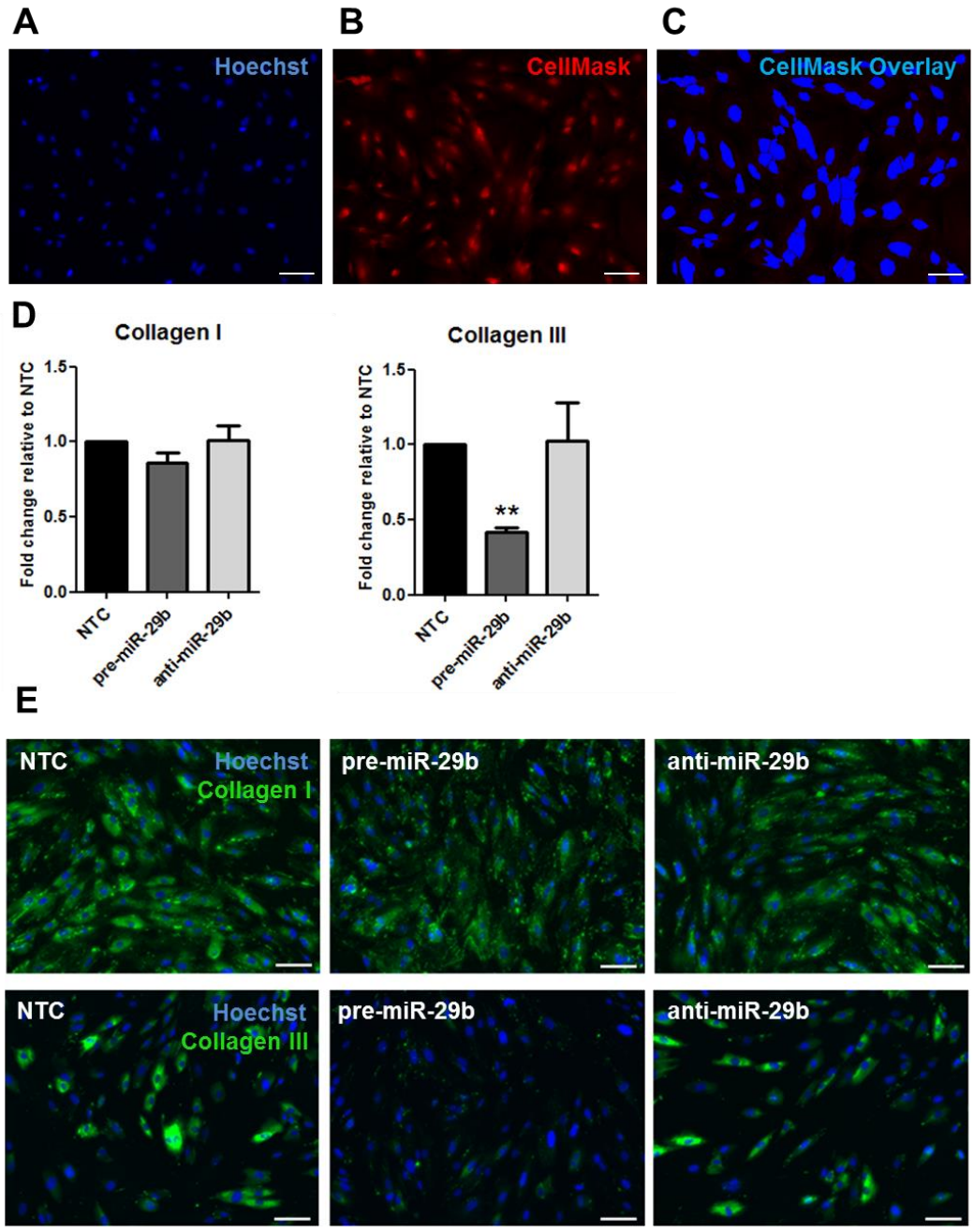

Figure 4.2. miR-29b down-regulates collagen III protein. Intestinal fibroblasts (n=3) were transfected with NTC, pre- or anti-miR-29b for 72 hr and stained with Hoechst 33342 and antibodies against collagen I and III. (A-C) Hoechst 33342 and CellMask Deep Red staining created an overlaying mask in the CellMask channel, which was then used to define pixel intensity of collagen I and III in individual cells. (D) The graphs represent the fold change in median pixel intensity following transfection. (E) Representative images of collagen I and III following transfection with NTC, pre-miR-29b or anti-miR-29b. Bars represent mean values with SEM. **p<0.01. Size bar is 100 μm.

4.3 TGF-β up-regulates collagen by down-regulating miR-29b expression

One of the key pro-fibrotic cytokines involved in the development of fibrosis in various organs is TGF-β (reviewed in [487]). TGF-β increases pro-fibrotic mediators through SMAD-mediated transcription (Section 1.2.4). MiRNAs have been shown to be regulated by TGF-β signalling and have the potential to work synergistically (reviewed in [488]). Indeed, reports have indicated that TGF- β increases the production of ECM proteins via the down-regulation of miR-29b in cardiac [375], kidney [372] and liver fibrosis [374]. In order to validate this role for TGF-β in intestinal fibrosis, fibroblasts were treated with TGF-β (10 ng/ml) for 48 hr and assayed for the expression of miR-29b and both *COL1A2* and *COL3A1* genes by qRT-PCR. Expression of *GAPDH* and miR-16 were used to normalise for the collagen mRNA and miRNA expression, respectively. Fold change relative to untreated fibroblasts (NT) showed a significant down-regulation of miR-29b ($p=0.0199$; Fig. 4.3A) and an up-regulation of *COL1A2* and *COL3A1* expression (*COL1A2*, $p=0.002$; *COL3A1*, $p=0.006$; Fig. 4.3A). In accordance with previous reports, this data suggests a link between the down-regulation of miR-29b and the up-regulation of *COL1A2* and *COL3A1* expression.

Next, the association between TGF-β, miR-29b and the downstream targets collagen I and III was explored further. As TGF-β down-regulates the expression of miR-29b and subsequently up-regulating *COL1A2* and *COL3A1*, I hypothesised that by restoring endogenous levels of miR-29b levels via transfection with pre-miR-29b, this up-regulation of *COL1A2* and *COL3A1* could be reversed. Likewise, reducing the endogenous levels of miR-29 by transfection with anti-miR-29b would further enhance the effect of the TGF-β treatments.

To test this, intestinal fibroblasts were transfected with NTC, pre-miR-29b and anti-miR-29b for 24 hr before treatment with TGF-β (10 ng/ml) for 48 hr. The expression of

COL1A2 and *COL3A1* was assayed via qRT-PCR, and the fold change between cells transfected with pre-miR-29b or anti-miR-29 relative to cells transfected with NTC was calculated. As predicted, cells transfected with pre-miR-29b prior to TGF-β treatment demonstrated a significant inhibition of both *COL1A2* and *COL3A1* mRNA transcripts (*COL1A2*, p=0.0012; *COL3A1*, p=0.0034; Fig. 4.3B). In addition, decreasing the levels of endogenous miR-29b by transfection with anti-miR-29b prior to TGF-β treatments resulted in a significant increase in expression of both collagen transcripts (*COL1A2*, p=0.0115; *COL3A1*, p=0.0282; Fig. 4.3B). Together, this data suggests that the up-regulation of both collagen gene transcripts is potentially mediated through the down-regulation of miR-29b by TGF-β.

In order to validate this observation at the protein level, immunofluorescence was performed using antibodies against collagen I and III. Intestinal fibroblasts were transfected with NTC, pre-miR-29b and anti-miR-29b for 24 hr before treatment with TGF-β (10 ng/ml) for 48 hr. Cells were fixed 72 hr following transfection and stained with Hoechst 33342, CellMask Deep Red and antibodies against collagen I and III. Median pixel intensities of both collagen I and III in individual cells was determined as described previously (Section 4.2; Fig. 4.2 A-C). Fold change in median pixel intensities for pre-miR-29b or anti-miR-29b relative to NTC transfected cells (all TGF-β treated) was calculated. Once more, it was hypothesised that by modulating endogenous levels of miR-29b via transfection with pre-miR-29b or anti-miR-29 prior to the TGF-β treatment could modulate the expression of collagen I and III proteins.

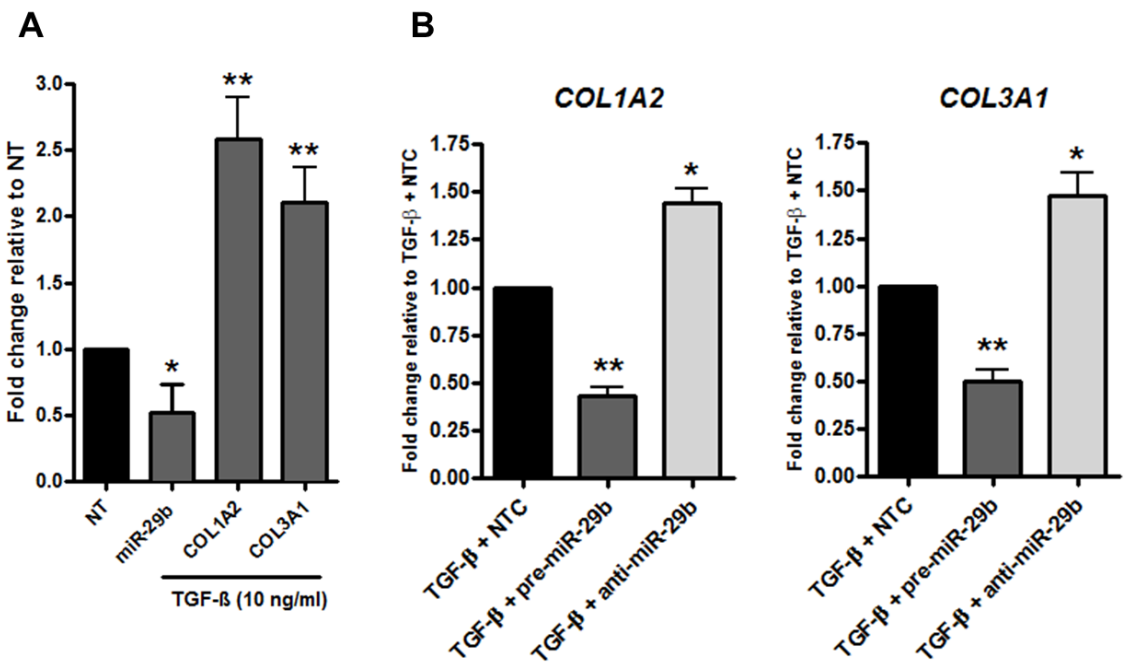

Figure 4.3. TGF-β up-regulates *COL1A2* and *COL3A1* mRNA through the down-regulation of miR-29b. (A) Intestinal fibroblasts (n>4) were treated with TGF-β (10 ng/ml) for 48 hr and expression levels of *miR-29b*, *COL1A2* and *COL3A1* were assayed by qRT-PCR. The graph represents the fold change in gene expression relative to untreated cells (NT). (B) Intestinal fibroblasts (n=4) were transfected with NTC, pre-miR-29b or anti-miR-29b for 24 hr prior to TGF-β (10 ng/ml) treatment. The graph represents the fold change of *COL1A2* and *COL3A1* expression following transfection with pre-miR-29b or anti-miR-29b relative to NTC (all TGF-β treated). Bars represent mean values with SEM. *p<0.05 and **p<0.01.

The transfection of pre-miR-29b prior to TGF-β treatment significantly down-regulated the expression of collagen III ($p=0.0069$; Fig. 4.4A), which supports previous data showing down-regulation of *COL3A1* mRNA expression (Fig 4.3B). By contrast, collagen I protein expression was not altered following transfection with pre-miR-29b and TGF-β treatments (collagen I, $p=0.7816$; Fig. 4.4A), despite the down-regulation of *COL1A2* mRNA (Fig. 4.3B). This lack of modulation of collagen I protein by pre-miR-29b prior to TGF-β treatment was consistent with data shown in Section 4.2, which showed that intestinal fibroblasts transfected with pre-miR-29b alone also failed to alter collagen I expression (Fig. 4.2D). Similarly, transfection of anti-miR-29b prior to TGF-β treatment also failed to up-regulate either one of the collagen protein levels (Fig 4.4A), indicating that that there are other, more dominant, factors that drive the expression of collagen I and III when miR-29b is absent. In summary, this data suggests that TGF-β can modulate collagen III protein via the down-regulation of miR-29b.

In humans, it has been suggested that miRNAs may potentially target up to 30% of all genes [489] and online prediction tools such as miRWalk propose a large number of predicted targets for miR-29b, many of which have been subsequently validated (http://www.umm.uni-heidelberg.de/apps/zmf/mirwalk/). Therefore, the next section aims to explore additional targets for miR-29b that may be involved in the pathogenesis of intestinal fibrosis independently from its regulatory effect on ECM molecules such as collagen.

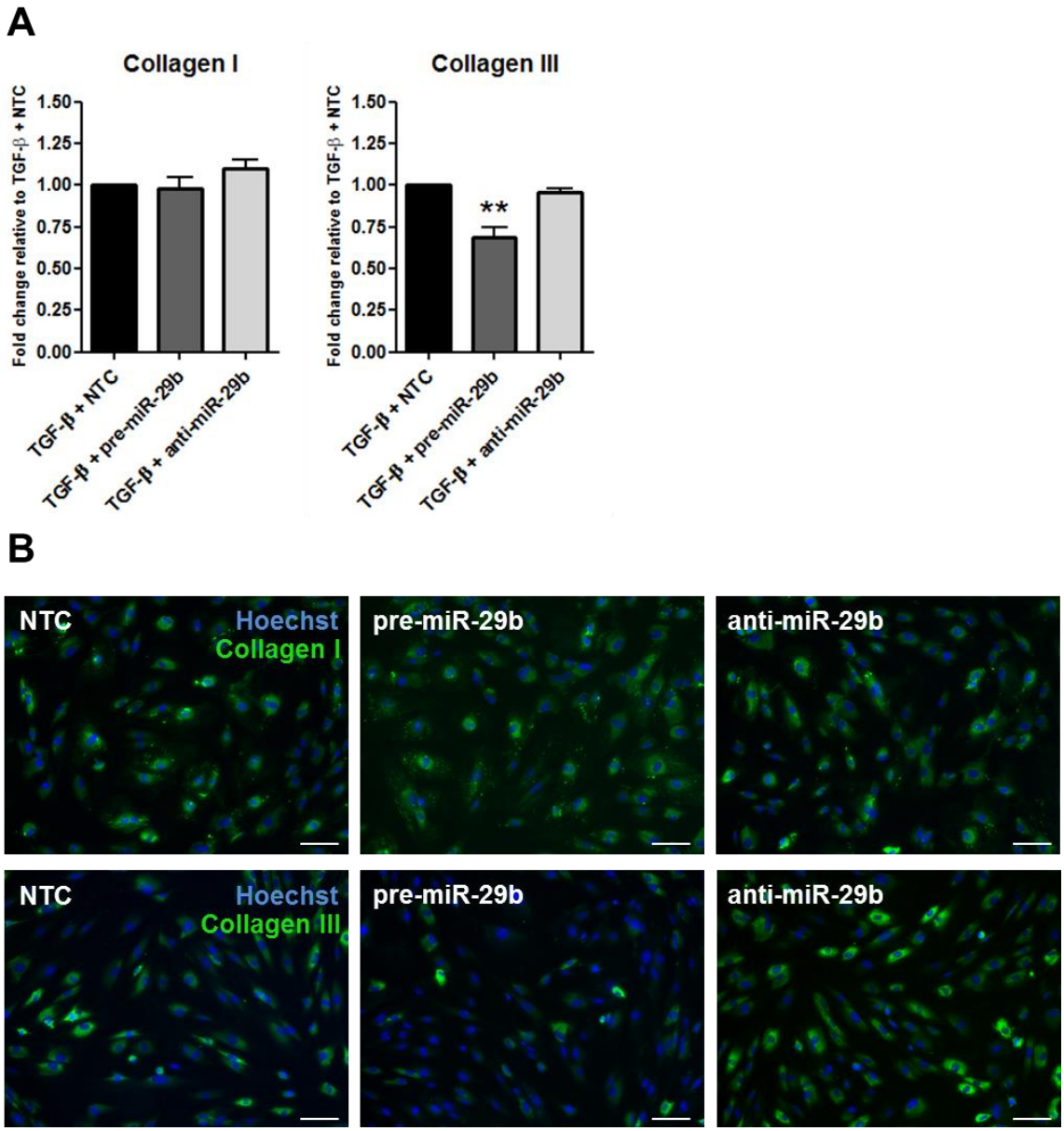

Figure 4.4. TGF-β up-regulates collagen III protein expression through the down-regulation of miR-29b. Intestinal fibroblasts (n=5) were transfected with NTC, pre-miR-29b or anti-miR-29b prior to TGF-β (10 ng/ml) treatment. Cells were stained with Hoechst 33342, CellMask Deep Red and antibodies against collagen I and III. (A) The graphs represent the fold change in median pixel intensity following transfection with pre-miR-29b or anti-miR-29b relative to NTC (all TGF-β treated). (B) Representative images of collagen I and III following transfection with NTC, pre-miR-29b or anti-miR-29b. Bars represent mean values with SEM. **p<0.01. Size bar is 100 μm.

4.4 MiR-29b up-regulates Mcl-1 mRNA and protein levels

Intestinal wound healing following the damage by inflammation is a complex sequence of events where inflammatory cells induce the activation of sub-epithelial fibroblasts. The production of ECM molecules by these fibroblasts and their ability to contract the wound area, play important roles in intestinal wound healing. Chronic inflammation disturbs this physiological response which can eventually leads to an increase in the production of ECM molecules by fibroblasts. The over-production of ECM molecules is normally avoided by the activation of apoptosis pathways from cues in the intercellular space, resulting in the removal of ECM-producing cells. One hypothesis for the over-production of ECM molecules by activated fibroblasts is decrease of apoptosis signalling in these cells. Indeed, reports have recently indicated that fibroblasts that are resistant to apoptosis might play a role in pulmonary fibrosis [490]. However, this phenomenon remains unexplored in intestinal fibrosis in CD.

The aim of this section was to explore additional targets for miR-29b that may influence the susceptibility to apoptosis in isolated intestinal fibroblasts. Online prediction tools identified Mcl-1, a member of the Bcl-2 family, as a miR-29b target in four of the five target prediction sites (TargetScan, MiRWalk, miRanda and DIANA Tools). The predicted binding site of miR-29b is within the 3'UTR of *MCL1* and is shown in Fig. 4.5A. More importantly, several groups have now validated this prediction demonstrating that miR-29b binds to the 3'-UTR of *MCL1* [491-496]. The human *MCL1* gene consists of three exons which undergo alternative splicing to form three mRNA transcripts: the long *MCL-1L*, the short *MCL-1S* and the extra short *MCL-1ES* (Fig. 4.5B) [497-501]. The Mcl-1L protein is anti-apoptotic and shows 35% homology with the C-terminus of the anti-apoptotic Bcl-2 proteins, containing Bcl-2 homology domains (BH)-1, BH2 and BH3 [497]. Due to a frameshift, Mcl-S and Mcl-1ES only contain a single BH3 domain and are similar to BH3-only pro-apoptotic proteins [498]. Three studies, limited to the liver, have shown that Mcl-1 attenuates liver fibrosis in mice [502-504] and that the deletion of Mcl-1 in hepatocytes results in liver cell damage caused by spontaneous induction of apoptosis

[502, 504]. To date, the potential role of Mcl-1 in intestinal fibrosis remains unexplored, thus, the effect of miR-29b on Mcl-1 in isolated intestinal fibroblasts was investigated. Intestinal fibroblasts were transfected with NTC or pre-miR-29b and expression of Mcl-1 mRNA was assessed via qRT-PCR. Fold change in expression compared to NTC-transfected fibroblasts demonstrated a significant increase in the expression of Mcl-1 isoforms (*MCL-1L/MCL-1ES*, p=0.004; *MCL-1S*, p=0.0008; Fig. 4.5C). The TaqMan assay used for *MCL-1L* also detects *MCL-1ES* and, therefore, the two could not be distinguished using this probe. However, this data suggests that miR-29b up-regulates the mRNA expression of *MCL-1L/ES* and *MCL-1S* in intestinal fibroblasts. This finding was unexpected considering that previous reports have confirmed the direct binding between miR-29b and the 3'-UTR of *MCL1* with luciferase reporter assays [491-493]. However, these reports demonstrate that miR-29b down-regulates Mcl-1 at the protein level and does not change the mRNA expression [492]. Therefore, the protein levels of Mcl-1 were assessed following transfection with pre- and anti-miR-29b.

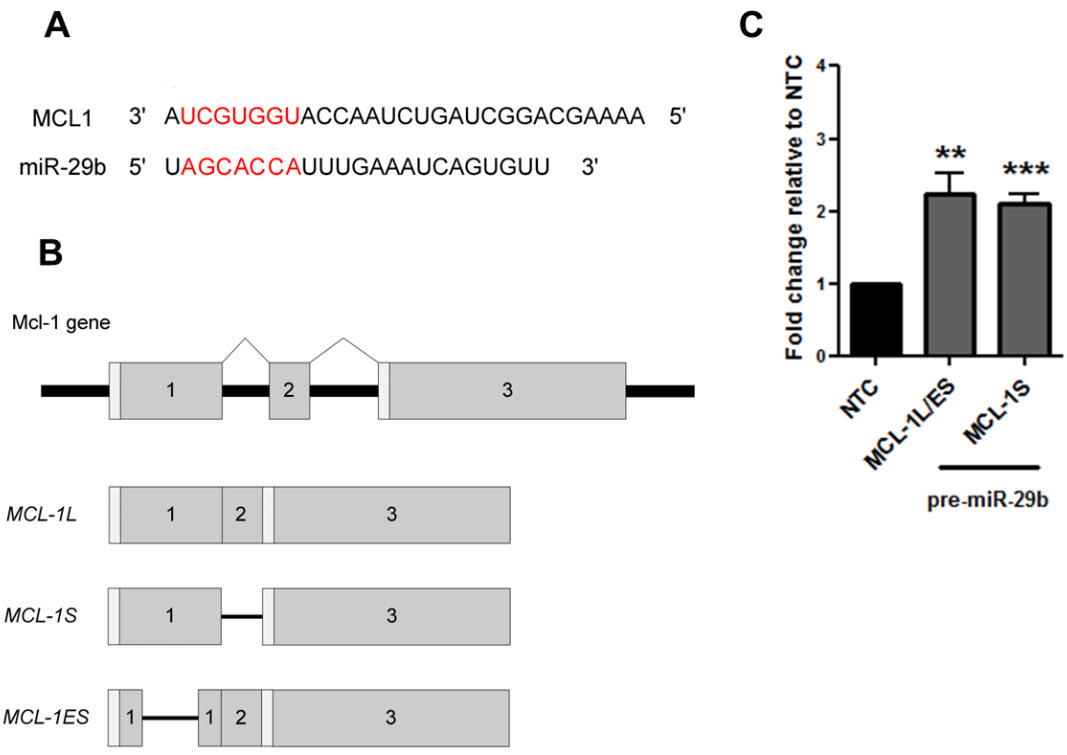

Figure 4.5. miR-29b upregulates Mcl-1. (A) Predicted binding site between miR-29b and *MCL1*. Nucleotides in red indicate complementary binding between the seed sequence of miR-29b and the 3'UTR of *MCL1*. (B) Schematic overview of Mcl-1 gene consisting of three exons. Alternative splicing potentially produces three isoforms: *MCL-1L*, containing the full length of all three exons; *MCL-1S*, exon 2 is lost due to alternative splicing; and *MCL-1ES*, in which the first exon undergoes alternative splicing. (C) Intestinal fibroblasts (n>5) transfected with NTC and pre-miR-29b. The graph represents the fold change in expression of *MCL-1L/ES* and *MCL-1S* m0easured by qRT-PCR. Bars represent mean values with SEM. **p<0.01 and ***p<0.001.

To explore further the effects of miR-29b on Mcl-1, protein expression of Mcl-1 was determined by immunofluorescence on intestinal fibroblasts. Fibroblasts were transfected with NTC, pre-miR-29b or anti-miR-29b and cells were fixed 72 hr following transfection and stained with Hoechst 33342 and an antibody against Mcl-1. Cells were imaged using the IN Cell Analyzer 1000 microscope under identical exposure conditions. Mcl-1 protein localised in discrete nuclear foci (Fig. 4.6A). The IN Cell Developer v1.8 was used to create a mask overlying the foci (Fig. 4.6B). This mask, in combination with Hoechst-positive nuclei, was used to determine the median Mcl-1 foci mass within each nuclei (foci mass/nuclei = (total foci pixel intensity x total foci area)/total nuclei count). Fibroblasts transfected with pre-miR-29b demonstrated a significant increase in foci mass compared to NTC, and transfection with anti-miR-29b resulted in a significant decrease in Mcl-1-positive foci mass (pre-miR-29b, $p=0.0029$; anti-miR-29b, $p=0.0003$; Fig. 4.6C). Representative images with digital zoom are shown in Fig. 4.6D-F. In conclusion, this data combined demonstrated that miR-29b induces an increase of Mcl-1 at both mRNA and protein levels in intestinal fibroblasts.

In contrast to plant miRNAs, human miRNAs display only limited complementarity to their target mRNA and can mediate inhibition through translational repression, rather than mRNA degradation [233, 505-507]. Although some miRNAs have been shown to up-regulate their mRNA targets (reviewed in [508]), this appears to be an exception to the rule. As miR-29b has been previously validated to target the 3'-UTR of Mcl-1 by others, the up-regulation of Mcl-1 by miR-29b observed here may be indirect through the modulation of up-stream regulators of Mcl-1. The following section aims to investigate the potential regulation of miR-29b on two established up-stream regulators of Mcl-1, interleukin (IL)-6 and 8.

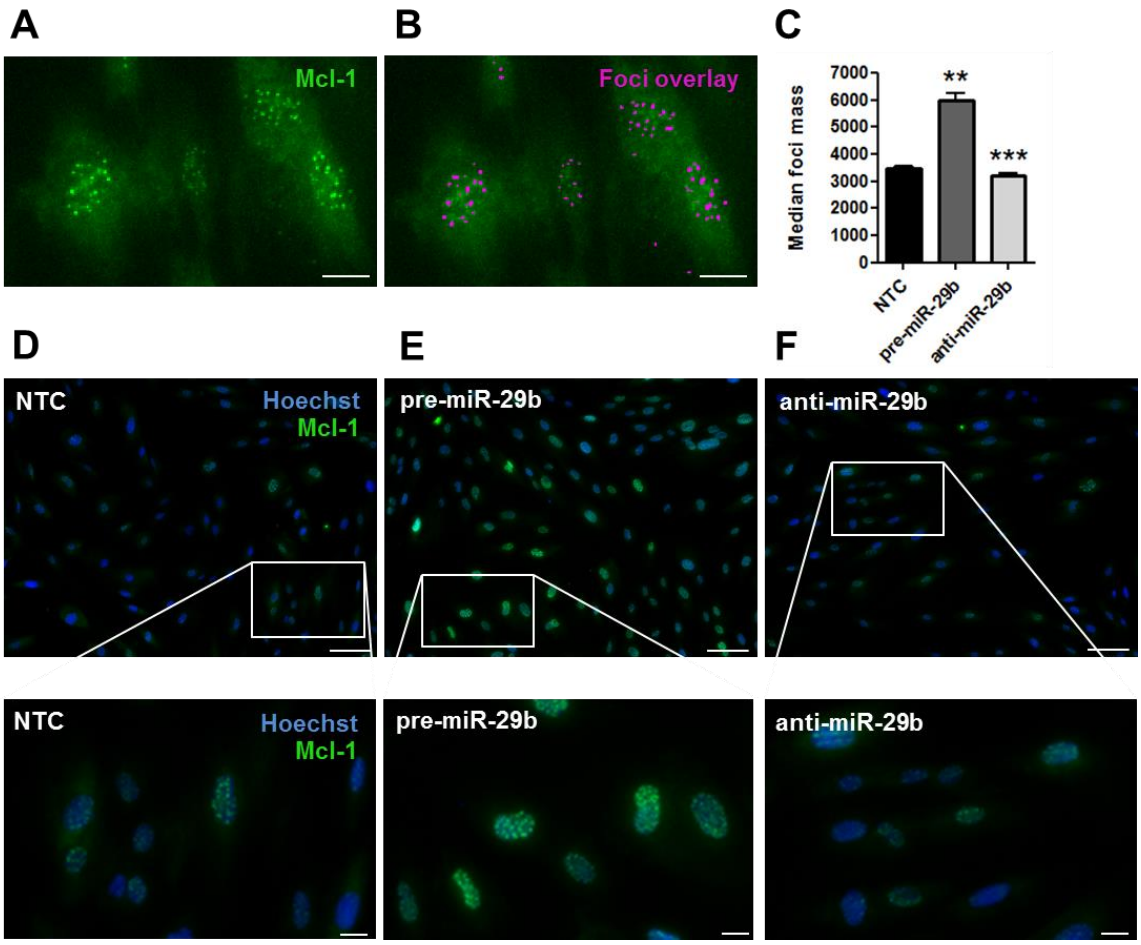

Figure 4.6. miR-29b up-regulates Mcl-1 mRNA and protein. Intestinal fibroblasts (n=3) were transfected with NTC, pre-miR-29b and anti-miR-29b for 72 hr. Cells were fixed and stained with Hoechst 33342 and an antibody against Mcl-1. (A-C) Mcl-1 positive foci were used to create an overlaying mask. This mask was then used to define foci mass in individual cells. The graph represents the fold change in median foci mass/nuclei following transfection with pre-miR-29b or anti-miR-29b relative to NTC. (D-F) Representative images Mcl-1 following transfection with NTC, pre-miR-29 or anti-miR-29b. Bar represents mean values with SEM. **p<0.01 and ***p<0.001. Size bar 20 µm ((A-B), digitally zoomed images of (D-F)) and 100 µm (original images D-F).

4.5 MiR-29b up-regulates Mcl-1 potentially IL-6 and IL-8

One of the most potent inducer of Mcl-1 is through IL-6 [509, 510]. IL-6 is a classic pro-inflammatory cytokine crucial in mounting an effective immune response. Recent studies have shown that IL-6 can induce collagen I expression [511] and its expression was found to be up-regulated in renal fibrosis in mice [512]. Furthermore, IL-6 has been implicated in a variety of fibrotic conditions via alternative trans-signalling pathways (cells that do not normally express the IL-6 receptor, but become responsive to IL-6 due to high levels of soluble IL-6 receptor present in extracellular matrix) [513]. A second cytokine, IL-8, has also been shown to increase the expression of Mcl-1 [514], and elevated serum levels of IL-8 are reported to be associated with fibrosis in chronic liver disease [515].

To investigate the regulatory effect of IL-6 and IL-8 on Mcl-1, intestinal fibroblasts were treated with IL-6 or IL-8 (both 10 ng/ml) for 4, 8 or 24 hr. Cells were fixed and stained with Hoechst 33342 and an antibody against Mcl-1. Cells were imaged on the IN Cell Analyzer 1000 microscope under identical exposure conditions and the IN Cell Developer v1.8 was used to calculate the median foci mass of Mcl-1 in the nuclei as described previously (Section 4.4, Fig. 4.6A-B). Fibroblasts treated with either IL-6 or IL-8 for 4 hr up-regulated the mass of Mcl-1-positive foci, of which IL-6 approached significance. (IL-6, p=0.064; IL-8, p=0.033; Fig. 4.7A). Stimulation for longer than 4hr (8 hr or 24 hr) diminished this up-regulation (8 hr, IL-6, p-0.589; IL-8, p=0.378; 24 hr, IL-6, p=0.960; IL-8, p=0.152; Fig. 4.7A). Additionally, mRNA expression of *MCL-1L/MCL-1ES* and *MCL-1S* was measured by qRT-PCR following stimulation of IL-6 or IL-8 (10 ng/ml) for 4 hr. Fold change in expression relative to NT fibroblasts demonstrated no change in *MCL-1L/MCL-1ES* (IL-6, p=0.2143; IL-8, p=0.3201; Fig. 4.7B) nor *MCL-1S* mRNA (IL-6, p=0.1306; IL-8, p=0.9216; Fig. 4.7C). These results confirmed that both IL-6 and IL-8 can induce the up-regulation of Mcl-1 protein following 4hr of treatment. However, they failed to alter the expression of *MCL-1* at the mRNA level. In conclusion, this data shows that both IL-6 and IL-8 have the ability to increase the protein level of Mcl-1 (IL-6 approached significance).

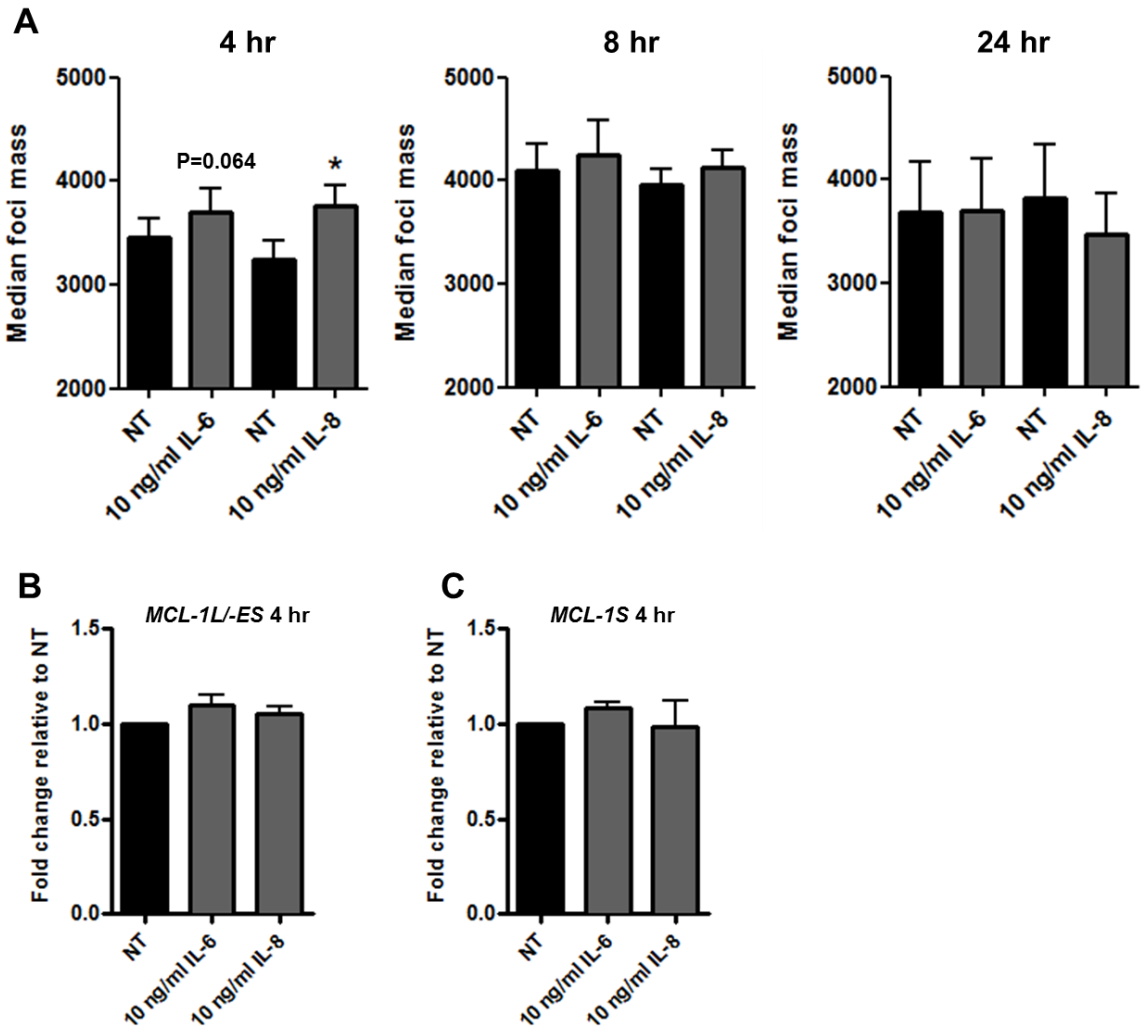

Figure 4.7. Mcl-1 protein expression is induced by IL-6 and IL-8 (A) Intestinal fibroblasts (n=5) were treated with 10 ng/ml of IL-6 or IL-8 for 4, 8 or 24 hr**.** Cells were fixed and stained with Hoechst 33342 and an antibody against Mcl-1. The graphs represent the median Mcl-1 foci mass/nuclei following treatment with 10 ng/ml IL-6 or IL-8 relative to NT. (B-C) Intestinal fibroblasts (n=3) were treated with 10 ng/ml of IL-6 or IL-8 for 4 hr. qRT-PCR was performed on extracted RNA and expression of *MCL-1L/ES* and *MCL-1S* mRNA was determined. The graphs represent the fold change relative to NT. Bars represent mean with SEM. *p<0.05.

To test the hypothesis that miR-29b might up-regulate Mcl-1 indirectly via IL-6 or IL-8, intestinal fibroblasts were transfected with NTC and pre-miR-29b. Messenger RNA expression for *IL6* and *IL8* was assessed via qRT-PCR and normalised to the housekeeping gene *GAPDH*. Fibroblasts transfected with pre-miR-29b showed a significant increased fold change of *IL6* compared to NTC transfected cells (p=0.0077; Fig. 4.8A). *IL8* mRNA levels were also up-regulated by pre-miR-29b and approached significance (p=0.06, Fig. 4.8A). Furthermore, ELISA measured the production of IL-6 and IL-8 by fibroblasts in the supernatant following transfection with NTC or pre-miR-29b. The production of IL-6 and IL-8 were both significantly increased by fibroblasts transfected with pre-miR-29b compared to NTC (IL-6, p=0.0027; IL-8, p=0.0268; Fig. 4.8B). These results suggest that miR-29b up-regulates the mRNA expression of *IL6* and *IL8* and their production into the extracellular space.

I have demonstrated previously that miR-29b has the ability to down-regulate *COL1A2* and *COL3A1* in intestinal fibroblasts (Section 4.2). This has been demonstrated by others to be directly through the 3'-UTR of both genes [375, 379]. To identify whether the miR-29b/IL-6/IL-8 axis may also affect collagen genes, mRNA expression of both *COL1A2* and *COL3A1* was measured following stimulation with IL-6 or IL-8 (10 ng/ml). Fold change in expression relative to NT fibroblasts demonstrated no change in the expression of either *COL1A2* or *COL3A1* following stimulation with 10 ng/ml IL-6 (*COL1A2*, p=0.1988, *COL3A1*, p=0.1997; Fig. 4.8C) or 10 ng/ml IL-8 (*COL1A2*, p=0.2274; *COL3A1*, p=0.1222; Fig. 4.8C).

In conclusion, this data suggests that miR-29b indirectly up-regulates Mcl-1 protein expression via IL-6 and IL-8.

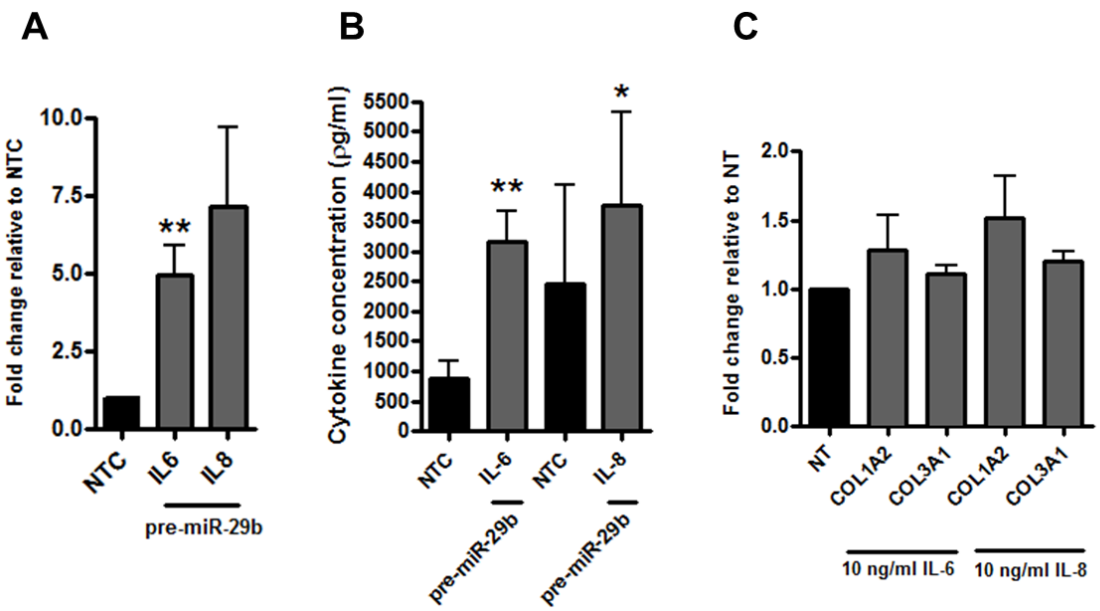

Figure 4.8. miR-29b up-regulates IL-6 and IL-8. (A) Intestinal fibroblast (n=6) were transfected with NTC and pre-miR-29b for 48 hr. The graph represents the fold change in expression of *IL6* and *IL8* mRNA measured by qRT-PCR. (B) Supernatant was collected from fibroblasts transfected with NTC and pre-miR-29b after 48 hr. The graphs represent the production of IL-6 and IL-8 measured by ELISA. (C) Intestinal fibroblasts (n=3) were treated with 10 ng/ml of IL-6 or IL-8 for 4 hr. qRT-PCR was performed on extracted RNA and expression of *COL1A2* and *COL3A1* mRNA were measured. The graph represents the fold change relative to NT. Bars represent mean values with SEM. *$p<0.05$ and ** $p<0.01$.

4.6 Discussion and future work

4.6.1 The expression of miR-29 family is reduced in SCD vs NSCD tissues

One of the major advantages of the Illumina v.2.0 array is its sensitivity and the ability to detect low abundance miRNAs with limited amounts of starting RNA. However, this sensitivity becomes a crucial limitation when evaluating highly expressed miRNAs are present in the sample, as this leads to saturation of the fluorescent signal for the relevant probes. This meant that differences in abundantly expressed miRNAs could not be revealed using this platform leading potentially to omission from subsequent downstream data analysis. One of the miR-29 family (miR-29b) was saturated on the array, and was therefore investigated further, along with the other members, miR-29a and miR-29c. Validation by qRT-PCR demonstrated that all three family members were down-regulated in SCD vs NSCD tissues (Section 4.2). This observation is in accordance with previous reports of fibrosis in other organs [372-378], indicating that the miR-29 family plays a key role in the pathogenesis of fibrosis in various organs.

4.6.2 miR-29b down-regulates *COL1A2* and *COL3A1* mRNA and collagen III protein

MiR-29b was selected for further functional studies, as reports have confirmed that this family member is most frequently implicated in the down-stream events leading to fibrosis. mRNA levels of *COL1A2* and *COL3A1* were down-regulated and up-regulated following transfection with pre-miR-29b or anti-miR-29b in isolated fibroblasts, respectively. This echoes previous reports in cardiac fibroblasts [375], skin fibroblasts [378], and human trabecular meshwork cells [379]. This also demonstrates that the effect of miR-29b on ECM molecules, such as collagens, is consistent in fibroblasts originating from various organs. Protein expression analysis of collagen I and III by immunofluorescence demonstrated a reduction of collagen III following transfection with pre-miR-29b. However, collagen I protein levels remained unchanged despite the down-regulation of *COL1A2* mRNA by pre-miR-29b. Protein expression is dependent on many factors, including protein turn over, and a literature report demonstrated that the turn-over

rate of collagen I protein is much slower than that of collagen III [516]. The effects of transient transfection are temporary and last around 72-96 hr, depending on cell doubling time and cell type. This may explain why transfection with pre-miR-29b resulted in down-regulated expression of *COL1A2* but did not modulate collagen I protein level within this time-frame. Future experiments to tackle this problem could include the use of expression vectors to create a cell line that stably expresses miR-29b over a period of time. Analysis of collagen I protein in these cells could determine if sustained expression of miR-29b suppresses the expression of collagen I protein over a longer time course.

4.6.3 TGF-β up-regulates collagen via the down-regulation of miR-29b

TGF-β is a potent mediator in major fibrotic events, including CD fibrosis [201]. Intestinal fibroblasts stimulated with TGF-β displayed elevated expression of *COL1A2* and *COL3A1* and suppressed miR-29b expression (Section 4.3). This is in accordance with previous studies in fibroblasts from the heart [375], lung [377] and liver [374], which demonstrated repression of miR-29b by TGF-β. Additionally, in intestinal fibroblasts, TGF-β stimulation following the over-expression of miR-29b demonstrated a repression of the TGF-β-mediated-up-regulation of *COL1A2* and *COL3A1* (Section 4.3). This suggests that TGF-β potentially exerts its pro-fibrotic effects by suppressing miR-29b expression in CD, and that this might be universal in fibrogenesis of various tissues.

Further experiments should aim to investigate the role of miR-29 in the pathogenesis of fibrosis *in vivo* mouse models of intestinal fibrosis. Unfortunately, models for IBD are generally focused on the inflammation side and these animals do not live long enough to develop fibrosis in the way that humans do. Hence, most of the current research is directed towards mechanistic *in vitro* functional experiments. However, a recent IL-10 KO mouse has demonstrated features of intestinal fibrosis [517]. The authors showed an increase in ECM molecules in the mucosa, submucosa and muscularis of these mice at week 16, together with an increase in gene expression of TGF-β, collagen I and α-SMA [517].

To further this line of research I would aim to:

1. Establish a working collaboration with Yuan and colleagues in order to investigate the mRNA/miRNA expression in IL-10 KO mice. For instance, intestinal tissue could be sampled at various time points of IL-10 KO mice. These could then be profiled for miRNA and/or mRNA analysis, preferably using a high-throughput platform such as microarray or RNA sequencing. This would provide useful insights into the altered mRNA/miRNA expression during the course of fibrosis in these mice, and could potentially highlight targets that may be involved in the early steps of intestinal fibrosis;
2. Identify genome-wide targets for miR-29b using the Target ID Library system. Given the fact that the expression of miR-29 family is dysregulated during fibrosis in various organs, large scale identification of their targets would provide important insight into the functional role of this family. Genome-wide transcriptome analysis following over-expression of miR-29b in mouse models has been previously conducted [518, 519]. However, both analyses were performed in the context of a diseased mouse model (liver fibrosis [518]; muscle dystrophy [519]). I would therefore, propose to use the Target ID Library system to identify genome-wide targets that are directly targeted by miR-29b; and
3. To date, only one miR-29 KO mouse has been generated. Kogure and colleagues produced a tissue-specific knockout of the miR-29ab locus, ablating miR-29a and miR-29b expression in the hepatic stellate cells in the liver [518]. This resulted in an increased susceptibility to fibrosis and impaired cell survival following fibrogenic stimuli in the liver of these mice, compared to WT mice. Future experiments to investigating the role of miR-29b in intestinal fibrosis could include the production of a conditional miR-29 KO mouse specific to gut fibroblasts. Intestinal tissue would be sampled at various time points and investigated for fibrosis markers to elucidate whether the loss of miR-29b in intestinal fibroblasts is sufficient to initiate intestinal fibrosis.

4.6.4 Mcl-1 expression is induced by miR-29b

Transfection with pre-miR-29b in intestinal fibroblasts showed an increase of Mcl-1 at both the mRNA and protein level. Furthermore, Mcl-1 protein was up-regulated following transfection with pre-miR-29b (Section 4.4). This result was unexpected as many groups have previously identified a direct down-regulation of Mcl-1 by miR-29b using 3'UTR-luciferase reporter assays, as well the down-regulation at RNA and protein level [491-494].

The Mcl-1 gene undergoes alternative splicing to produce three potential isoforms: *MCL-1L*, *MCL-1S* and *MCL-1ES*. The Taqman assays used to determine the mRNA levels of the Mcl-1 isoforms were not able to distinguish between *MCL-1L* and *MCL-1ES*. Nevertheless, qRT-PCR demonstrated that up-regulation of both *MCL-1L/MCL-1ES* and *MCL-1S* (Section 4.4), suggesting that Mcl-1 is induced by miR-29b. Future experiments could aim to pinpoint exactly which isoform is modulated by pre-miR-29b. For instance, Kim and colleagues, identified the three isoforms using distinct primer sequences [500]. Experiments with these primers on RNA from cells transfected with miR-29b would allow discrimination between the three different isoforms and demonstrate whether all of them are regulated by miR-29b.

Due to the lack of protein isolated from intestinal fibroblasts, Mcl-1 antibody validation was performed on six CRC cell lines (HCT116, DLD-1, HT55, HT29, VACO4S and SW837). Western blot for Mcl-1 shows the dominant band at approximately 40kDa (Appendix Fig. 3), which correlates to the molecular weight of anti-apoptotic Mcl-1L. A fainter band at around 31kDa for Mcl-1S could also be seen. Mcl-1ES has a molecular weight of 24kDa [500] and was not detected. These results suggest that the increased protein expression quantified using this antibody following transfection with miR-29b presents both the Mcl-1L and Mcl-1S isoforms. However, the fact that this antibody does not detect the shortest Mcl-1ES isoform in CRC cell lines does not necessarily mean that this would be the case in intestinal fibroblasts. Therefore, additional western blots should

be performed on protein extracted from intestinal fibroblasts transfected with NTC and pre-miR-29b to identify which isoform is modulated by miR-29b.

Nonetheless, studies that show Mcl-1 attenuates liver fibrosis in mice are a consequence of the knockdown of entire Mcl-1 gene which potentially involves all three isoforms. Therefore, future work to elucidate the role of Mcl-1 in intestinal fibrosis could include:

1. The investigation of the expression of Mcl-1 at both protein and mRNA following TGF-β treatments in intestinal fibroblasts. If the hypothesis were that Mcl-1 is anti-fibrotic, I would predict TGF-β to down-regulate its expression; and
2. If Mcl-1 is modulated by TGF-β, ectopic over-expression of Mcl-1 with the use of an expression vector in combination with TGF-β treatments may determine if the pro-fibrotic abilities of TGF-β could be abrogated by the presence of Mcl-1.

4.6.5 miR-29b up-regulates Mcl-1 potentially through IL-6 and IL-8

MiRNAs down-regulate their targets through binding predominantly within the 3'-UTR region of the mRNA resulting in mRNA degradation or inhibited protein translation. Although the direct up-regulation of genes by miRNAs has been reported, mechanistic evidence is currently lacking (reviewed in [508]). I, therefore, hypothesised that the up-regulation of Mcl-1 by miR-29b is indirect in nature in this context. Literature reports suggests that Mcl-1 expression is induced by IL-6 [509] and IL-8 [514]. In Section 4.5, I demonstrated that intestinal fibroblasts treated with 10 ng/ml of IL-8 for 4 hr significantly up-regulated the protein expression of Mcl-1 (4 hr treatment with 10 ng/ml IL-6 approached significance, $p=0.06$). Interestingly, transfection with pre-miR-29b increased the levels of both cytokines at the mRNA and protein level, indicating a potential link between miR-29b, IL-6/IL-8 and Mcl-1. Evidence from the literature on the effect of miR-29b on the expression of IL-6 or IL-8 in other cell types seems conflicting and contradictory to my findings. For example, Amodio and colleagues demonstrate a reduction of *IL8* mRNA but no change in *IL6* mRNA in endothelial cells following pre-

miR-29b transfection [520], and Xing and colleagues showed that transfection with anti-miR-29b resulted in an increase in *IL8* mRNA in HEK293T cells [521]. On the contrary, Salama and colleagues demonstrated an induction of IL-6 cytokine production by macrophages following pre-miR-29b transfection [522], which supports my observations. The different contexts and cell types used in these studies may account for these apparently conflicting results. Nonetheless, the up-regulation of IL-6 and IL-8 by miR-29b and the subsequent up-regulation of Mcl-1 by both cytokines still support the anti-fibrotic miR-29b/IL-6/IL-8/Mcl-1 axis in intestinal fibrosis. A hypothetical model of how TGF-β may exert its pro-fibrotic action through miR-29b is shown in Fig. 4.9.

Further experiments are warranted to confirm this anti-fibrotic pathway. For example, to test whether the increase in Mcl-1 by miR-29b is a result of the increased expression of IL-6 and/or IL-8, knockdown of IL-6 and IL-8 via siRNA in combination with miR-29b transfection could be performed.

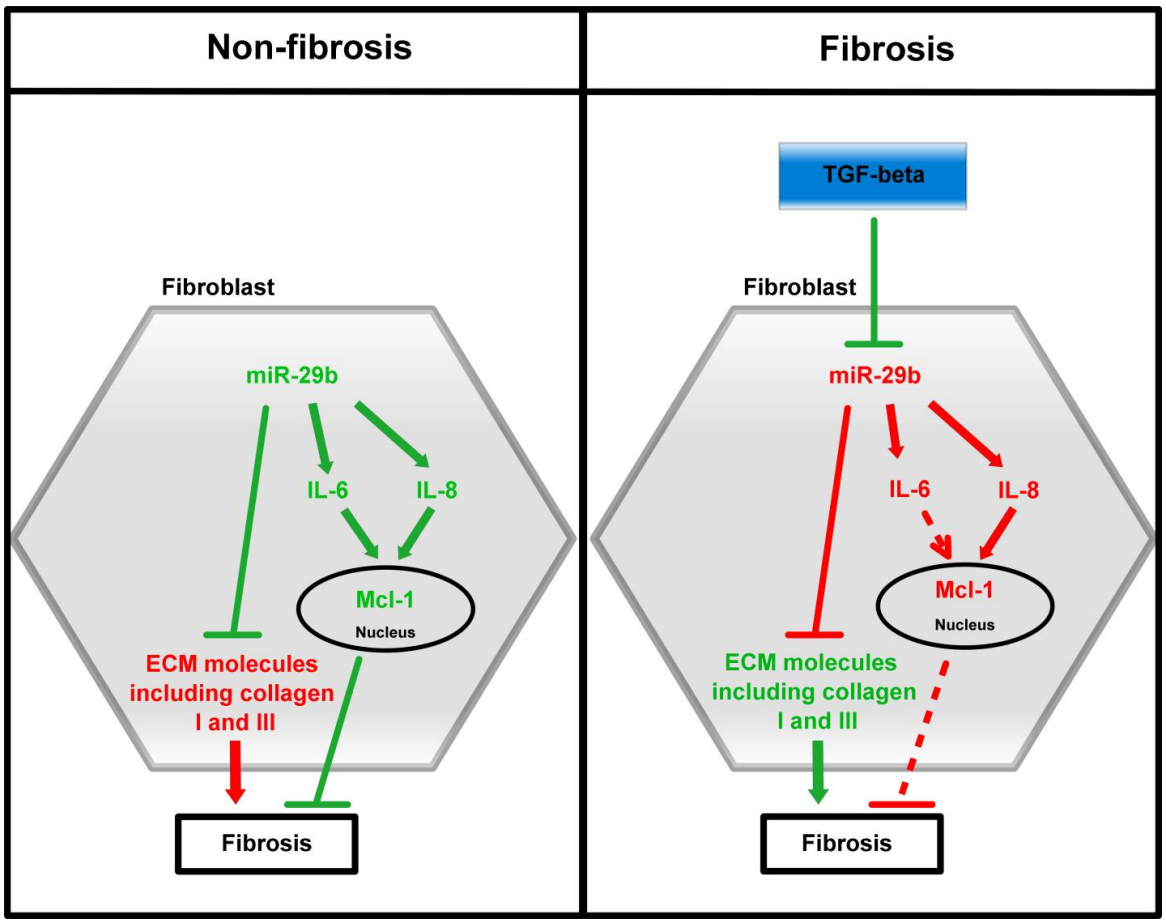

Figure 4.9 Hypothetical model of the role of miR-29b in CD fibrosis. TGF-β is a potent pro-inflammatory cytokine. TGF-β modulates fibrosis through down-regulation of miR-29b, resulting in increased deposition of collagen and therefore fibrosis. In CD fibrosis, additional down-stream pathways of miR-29b are unknown. Up-regulation of anti-fibrotic mediator Mcl-1 by miR-29b may potentially be mediated through IL-6 and IL-8. Up-regulated genes in green, down-regulated genes in red.

Chapter 5: Hypoxia-responsive miRNAs in colorectal cancer

5.1 Introduction and aims

One of the biggest challenges in the management of CRC patients remains the wide spectrum of response to preoperative or neo-adjuvant treatments. This can range from tumours that do not respond to those that shrink completely following treatment (pathological complete response, pCR). Knowledge as to why there is such a great range of response to therapy is limited. However, it has been generally accepted that the effectiveness of therapy is dependent on a number of factors, including the tumour microenvironment. For example, the lack of oxygen (hypoxia) within the tumour is known to be detrimental for tumour response to CRT. Hypoxia within the tumour is a consequence of the rapid acceleration in growth of the tumour cells combined with a lack of adequately formed blood vessels. Radiotherapy relies on the transformation of oxygen molecules into radical oxygen which in turn aids killing of cancer cells; efficacy is, therefore, hindered under low oxygen tensions. In addition, some chemotherapy drugs require oxygen molecules to generate free radicals that contribute to cytotoxicity. Moreover, hypoxia induces cellular adaptation that may result in chemoresistance.

Over recent decades, miRNAs have been identified as key post-transcriptional regulators and are dysregulated in many cancers, including CRC (Section 1.3.2). Literature reports have previously demonstrated altered miRNA profiles under hypoxic conditions *in vitro*. However, these are often dependent on cellular context and oxygen concentration and generally limited to just one or two cell lines. Therefore, I aimed to analyse the change in miRNA expression in six colorectal cancer cell lines (DLD-1, HCT116, HT29, HT55, SW837 and VACO4s) under three oxygen conditions (20.9%, 1% or 0.2%), thereby allowing a more comprehensive insight in miRNA changes under hypoxia in CRC *in vitro*.

Aims for this chapter:

1. Identify differentially expressed miRNAs in six CRC cell lines under hypoxic conditions;
2. Validate selected candidate miRNAs identified by the array using qRT-PCR;
3. Further validate candidate miRNAs in CRC tissue and search for correlation to hypoxia marker CAIX;
4. Determine the role of candidate miRNAs in the resistance to the chemotherapy drug 5-FU in CRC cell line under hypoxic conditions;
5. Identify altered cellular metabolism under hypoxia in six CRC cell lines using CE-TOFMS; and
6. Establish a cell line stably expressing the Target ID Library system to identify genome-wide mRNA targets for selected candidate miRNAs.

5.2 Differential expression of miRNAs under hypoxia

To identify differentially expressed miRNAs under hypoxic conditions *in vitro*, three colon cancer cell lines (DLD-1, HCT116 and HT29) and three rectal cancer cell lines (HT55, SW837 and VACO4s) were cultured under three different oxygen tensions (20.9%, 1% or 0.2%) for 48 hr. Global miRNA expression profiling was performed using the Exiqon 7th generation miRCURY LNA miRNA Array (Capture probes for 3,100 miRNAs, miRBase v 19.0). Raw data was initially analysed by Exiqon and data normalisation was performed using the mean plate intensity.

Often, it is difficult to interpret large miRNA data sets easily, preventing the scientist from getting the most out of the data obtained. Multivariate analysis allows the investigation of many variables at once and helps to understand the relationship that may exist between each variable. For the analysis of the miRNA data, a PLS-DA was used. A PLS-DA is a supervised extension of the principle component analysis (PCA) and aims to project data into a 2D plot with axes that explain the majority of the variance in the data. In addition, this regression model intends to maximise the separation between groups of observations and identify the variables (in this case, miRNAs) that contribute to this separation.

Log-transformed miRNA expression data of all six cancer cell lines under the three oxygen conditions was subject to PLS-DA modelling. Generally, axis 1 and 2 explain the majority of the variance in the data (Fig. 5.1A), which show that the biggest variance in the miRNA expression data is between the six different cell lines and not between the three oxygen conditions within each cell line. This is illustrated by the clustering of the three data points for each oxygen tensions for each cell line (Fig. 5.1A). Interestingly, PLS-DA axis 1 can slightly differentiate between the origin of the cell line, as rectal cancer cell lines are predominantly clustered on the left half of the graph, and colon cancer cell lines on the right half (Fig. 5.1A). Smaller changes in the miRNA expression data can be observed in subsequent axes of the PLS-DA model. Indeed, an unsupervised

separation of oxygen tensions within each cell line (apart from SW837) could be identified along PLS axis 6 (Fig. 5.1B), demonstrating the existence of altered miRNAs between the three different oxygen tensions within each cell line. Finally, the magnitude of change for each miRNA contributing to this separation under hypoxic conditions was extracted from the PLS-DA analysis (Appendix Fig. 4).

Because the PLS-DA is merely an exploratory tool and cannot uncover significant changes in the variables between different samples, an alternative multivariate analysis (linear regression) was used to model the relationship between miRNA expression profiles between the three different oxygen tensions for each cell line. In this model, oxygen tensions were assigned a numerical variable meaning that the oxygen tensions are linked (i.e. 20.9% is higher than 1% and 1% is higher than 0.2%). This enabled the identification of miRNAs whose expression was significantly different between the three oxygen conditions. A single p-value was then determined for each miRNA across all six cell lines, and revealed 41 miRNAs with a p-value less than 0.05 (Table 5.1).

Fold change in expression in both hypoxic tensions (1% and 0.2%) were normalised to the normoxic (20.9%) counterpart. Log transformed fold changes for the 41 altered miRNAs are illustrated in a heatmap and ranked according to their PLS-DA axis 6 loadings (Fig. 5.1C). Not surprisingly, one of the most significantly altered miRNA across the six cell lines was miR-210. Previous literature reports indicate that miR-210 is the most consistently up-regulated miRNA following hypoxia (reviewed in [523]). In fact, sequencing data analysis from literature reports show that the promoter region of miR-210 contains hypoxia-responsive-elements (HREs) [329, 523], which are strongly conserved among species. In conclusion, the up-regulation of miR-210 in all six cell lines confirms the importance of this miRNA in the cellular response to lack of oxygen in CRC *in vitro*.

miRNAs are often found to be clustered within the genome and can be produced from the same primary transcript (Section 1.3.1.1) which generally contain members of the same

miRNA family (reviewed in [431]). In addition, miRNA families are often co-expressed (especially those that are clustered together) and have close similarity in their seed sequences thereby increasing the synergistic effect they have on a common target. Interestingly, more than one member of five different miRNA families were shown to be dysregulated under hypoxia (colour coded miRNAs; Table 5.1). For instance, two members of the miR-320 family, miR-320b and miR-320c, were shown to be up-regulated under hypoxic conditions. Also, the PLS-DA loadings of PLS axis 6 (Appendix Fig. 4) of miR-320b and miR-320c demonstrated high loading scores, highlighting the fact that these miRNAs have a large impact on the separation of the miRNA data between the three oxygen conditions.

In conclusion, the microarray and subsequent analysis discovered a number of significantly altered miRNAs under hypoxic conditions in CRC *in vivo*. To confirm these changes, validation of the candidate miRNAs using a second experimental method is critical. In total, 12 miRNAs (miR-19b, -106b, -141, -147, -1180, -21, -29a*, -210, -30d, -320a, -320b and -320c) were selected for further validation by qRT-PCR. The selection of these miRNAs was non-random and based on previous reports linking these miRNAs to hypoxia or therapy resistance and/or based on their significance value (p-value).

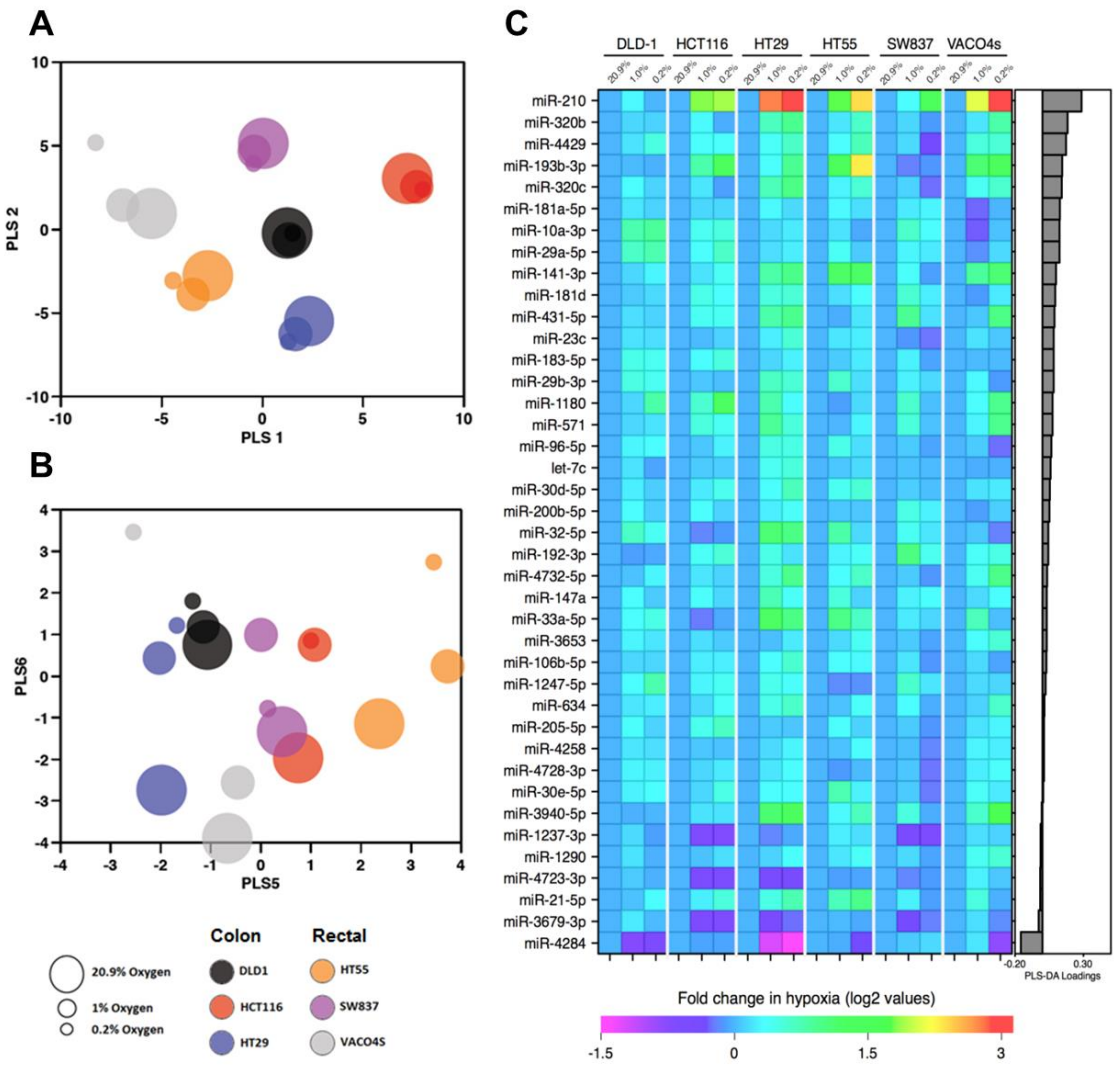

Figure 5.1. Altered miRNA expression profile under hypoxic conditions. Fold change (log2) in expression of significant altered miRNAs between normoxia (20.9%) and both low oxygen conditions (1% and 0.2%) in six CRC cell lines. (A) Data was subjected to PLS-DA, which was supervised according to cell line and unsupervised to oxygen tension. PLS Axis 1 vs Axis 2 is shown. (B) Subsequent PLS-DA Axis 5 vs Axis 6 are illustrated. (C) Significantly altered miRNAs under hypoxia were subsequently identified by linear regression multivariate analysis. A heatmap of log transformed fold changes between the different oxygen tensions normalised to 20.9% is shown. The miRNAs are ranked according to PLS-DA loadings on the right-hand side of the heatmap.

Table 5.1. Differentially expressed miRNAs under hypoxic conditions. Significant differentially expressed miRNAs under hypoxia determined by multivariate analysis, ranked by p-value. A $p<0.05$ was considered significant. miRNA family and cluster information is noted for each miRNA. Families with more than one miRNA altered under hypoxia are indicated with a different colour. Candidate miRNAs selected for further validated are in bold and underlined.

miRNA	Chr Location/cluster/family	p-value	miRNA	Chr Location/cluster/family	p-value
hsa-miR-210	Chr 11	0.0002	hsa-miR-1247-5p	Chr 14	0.0199
hsa-miR-141-3p	Chr 12/miR-200 family (miR-200a/b/c, -141, -429)	0.0003	hsa-miR-1290	Chr 1	0.0223
hsa-miR-193b-3p	Chr 16/clustered with miR-365a/miR-193 family (a/b)	0.0019	hsa-miR-3940-5p	Chr 19	0.0225
hsa-miR-30d-5p	Chr 8/miR-30 family (a/b/c/d/e)	0.0024	hsa-miR-32-5p	Chr 9	0.0245
hsa-miR-4723-3p	Chr 17	0.0041	***hsa-miR-106b-5p***	Chr 7/miR-17 family (miR-20a/b, -93, -106a/b)	0.0264
hsa-miR-10a-3p	Chr 17	0.0065	hsa-miR-200b-5p	Chr 1/miR-200 family (miR-200a/b/c, -141, -429)	0.0275
hsa-miR-29a-5p	Chr 7/miR-29 family (a/b/c)	0.0076	hsa-miR-571	Chr 4	0.0286
hsa-miR-3614-3p	Chr 17	0.0079	hsa-miR-30e-5p	Chr 1/miR-30 family (a/b/c/d)	0.0319
hsa-miR-181d	Chr 19/miR-181 family (a/b/c/d/)	0.0085	hsa-let-7c	Chr 21/clustered with miR-99 and miR-125b/Let 7 family (a/b/c/d/e/f/i)	0.0321
hsa-miR-4429	Chr 2	0.0091	hsa-miR-181a-5p	Chr 1/miR-181 family (a/b/c/d/)	0.0325
hsa-miR-192-3p	Chr 11/miR-192 family (miR-192 and -215)	0.0093	hsa-miR-634	Chr 17	0.034
hsa-miR-183-5p	Chr 7/miR-182 family (miR-182, -183, -96)	0.0119	hsa-miR-4728-3p	Chr 17	0.0354
hsa-miR-33a-5p	Chr 22/miR-33 family (a/b)	0.012	***hsa-miR-320b***	Chr 1/miR-320 family (a/b/cd)	0.0356
hsa-miR-320c	Chr 18/miR-320 family (a/b/c/d)	0.0134	hsa-miR-4284	Chr 7	0.0357
hsa-miR-3653	Chr 22	0.0163	hsa-miR-3679-3p	Chr 2	0.0362
hsa-miR-21-5p	Chr 17	0.0164	hsa-miR-23c	Chr X/miR-23 family (a/b/c)	0.038
hsa-miR-205-5p	Chr 1	0.0173	***hsa-miR-1180***	Chr 17	0.0415
hsa-miR-4732-5p	Chr 17/Clustered with miR-144, -451	0.0176	hsa-miR-4258	Chr 1	0.0421
hsa-miR-1237-3p	Chr 11	0.0181	hsa-miR-96-5p	Chr 7/miR-182 family (miR-182, -183, -96)	0.0428
hsa-miR-29b-3p	Chr 7/miR-29 family (a/b/c)	0.0192	hsa-miR-431-5p	Chr 14/C14MC	0.0482
hsa-miR-147	Chr 9	0.0195			

5.3 MiRNA array validation

In the hunt for a potential miRNA biomarker for hypoxia in CRC tissue, the validation of the miRNA array was focused on up-regulated miRNAs as these would be more easily detected than miRNAs that were to be down-regulated. Validation of 12 up-regulated candidate miRNAs in hypoxia (miR-19b, -106b, -141, -147, -1180, -21, -29a*, -210, -30d, -320a, -320b and -320c) was performed via qRT-PCR on an independent set of experiments in all six cell lines (n=3). One of the main challenges faced when validating miRNAs via a different platform (i.e. qRT-PCR) is the way in which the data is normalised. Microarrays are often normalised to the overall plate mean intensity which takes into account the intensity of all probes, producing robust and reliable signatures of differentially expressed miRNAs. By contrast, qRT-PCR relies on the selection of one or more stable miRNAs for normalisation. To identify a stable miRNA for normalisation of the qRT-PCR, expression values from the original array were investigated. Two miRNAs displayed stable expression across all three oxygen tensions and all six cell lines (miR-16 and let-7a). In addition, a third small non-coding RNA (RNU19) was also tested. The expression of miR-16, let-7a and RNU19 was assayed via qRT-PCR in the six cell lines under three oxygen conditions (n=3). One way ANOVA analysis indicated that the expression of let-7a was significantly altered between the three different oxygen tensions in two of the six cell lines (HCT116, $p=0.0053$; HT29, $p=0.0326$; Fig. 5.2A). The expression of miR-16 and RNU19 was not significantly altered between the three different oxygen tensions in any of the six cell lines. RNU19 expression was slightly up-regulated in VACO4s but this was not significant ($p=0.08$; Fig. 5.2A). Closer inspection of the variation (standard deviation) between the expression in 20.9% oxygen vs hypoxia (both 1% and 0.2%) of miR-16 and RNU19 showed that this was much smaller for RNU19 than for miR-16. In particular, when 20.9% was compared to 0.2%, the standard deviation was significantly lower (20.9% vs 0.2%, $p=0.0135$; Fig. 5.2B). In addition, RNU19 has been used for normalisation purposes in previously published *in vitro* hypoxic experiments [524, 525]. For these reasons, RNU19 was selected to normalise the miRNA expression data.

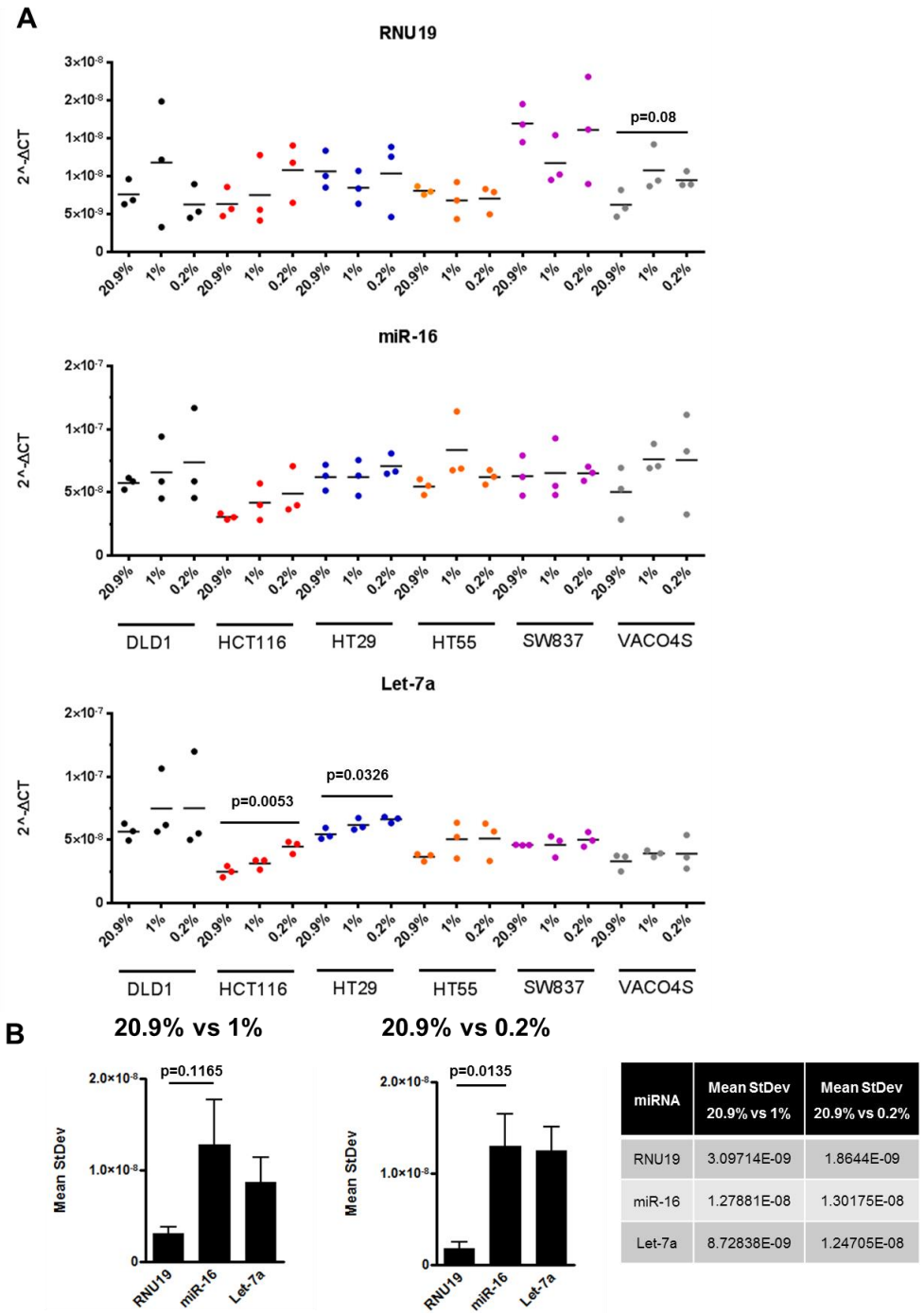

miRNA	Mean StDev 20.9% vs 1%	Mean StDev 20.9% vs 0.2%
RNU19	3.09714E-09	1.8644E-09
miR-16	1.27881E-08	1.30175E-08
Let-7a	8.72838E-09	1.24705E-08

Figure 5.2. RNU19 is an appropriate normaliser for miRNA expression. Three miRNAs (RNU19, miR-16 and let-7a) were tested for miRNA normalisation. (A) The expression ($2^{-\Delta CT}$) for each miRNA was determined by qRT-PCR (n=3). (B) The graphs represent the standard deviation (StDev) for each of the miRNAs in six cell lines between 20.9% oxygen and 1% or 0.2% oxygen tensions, respectively. Bars represent mean values with SEM.

Next, normalised qRT-PCR data of the 12 candidate miRNAs was subjected to multivariate analysis to uncover the relationship between the expression of each miRNA and the three oxygen conditions within each cell line. In collaboration with Dr. Jake Bundy (Imperial College, UK), a linear regression model was used to determine a p-value for each miRNA. Expression values for the 12 miRNAs are displayed in a heatmap and ranked according to their p-value (Fig. 5.3A).

In summary, validation by qRT-PCR confirmed the up-regulation of six (miR-21, -210, -30d, -320a, -320b and -320c) of the 12 candidate hypoxia-responsive miRNAs. To explore the relevance of two of these miRNAs in CRC tissue samples, miR-21 and miR-210 were selected for further investigation in *ex vivo* human CRC tumour samples.

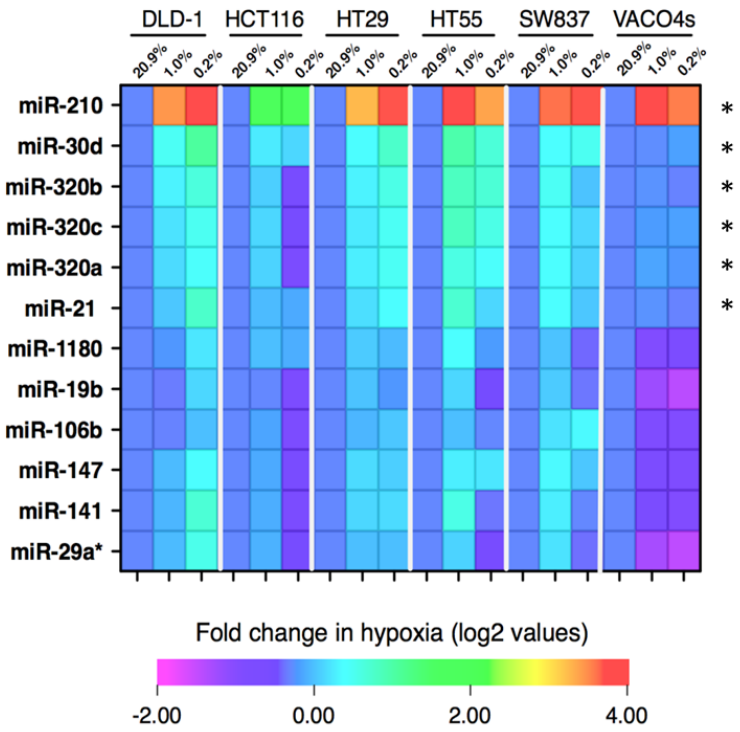

miRNA ID	p-value
miR-210	0.0002
miR-30d	0.0067
miR-320b	0.0133
miR-320c	0.0137
miR-320a	0.0184
miR-21	0.0405
miR-1180	0.1482
miR-19b	0.2853
miR-106b	0.3303
miR-147	0.3724
miR-141	0.3724
miR-29a-3p	0.4423

Figure 5.3. Candidate miRNA validation by qRT-PCR. Twelve candidate miRNAs were selected for validation by qRT-PCR in an independent set of experiments (n=3) in three colon (DLD-1, HCT116 and HT29) and three rectal (HT55, SW837 and VACO4s) cell lines. A heatmap of fold change (log2) in miRNA expression between the three oxygen conditions normalised to 20.9% oxygen (n=3). The heatmap is ranked according to the p-values obtained from the multivariate analysis. Asterisks indicate significantly altered ($p<0.05$) miRNAs.

5.4 MiR-210 is up-regulated in rectal cancer tissue and positively correlates with the expression of hypoxia marker CAIX

In vitro validation by qRT-PCR confirmed the up-regulation of six candidate miRNAs in hypoxic conditions (Section 5.3). However, assessing their expression in CRC tissue is essential to evaluate their potential as biomarkers for hypoxia *ex vivo*. Therefore, small RNAs (including miRNAs) were extracted from 13 FFPE blocks with CRC tumour tissue by a previous PhD student without our lab (Dr. Alexandra Parker). Hematoxylin & eosin staining on a serial section was used to outline tumour tissue. A second serial section was stained for the hypoxia marker CAIX (Section 2.17) via IHC and percentage CAIX expression within the CRC tumour was determined according to protocols used by others [430]. I, then determined the expression of miR-210 and miR-21 by qRT-PCR and normalised to let-7a and miR-16. The correlation between the expression of both miRNAs and CAIX staining within the tumour was determined (Spearman's Rank correlation). Correlation analysis demonstrated that the expression of miR-210 positively corresponded to the expression of the hypoxia marker CAIX in the 13 CRC tumours analysed (Rho=0.679, p=0.012, Fig. 5.4A). By contrast, miR-21 expression did not show a correlation to CAIX expression (Rho=-0.019, p=0.938, Fig. 5.4A). Furthermore, three other miRNAs (miR-30d, -141 and -147) were also tested for correlation between CIAX and miRNA expression. Neither of these miRNAs demonstrated a correlation to CAIX expression in CRC tumour tissue (Appendix Fig. 5).

To further explore the localisation of the miRNAs in CRC tumour tissue, I performed *in situ* hybridisation for miR-210 and miR-21 on eight FFPE blocks containing CRC tumour tissue. A serial section was stained for CAIX for comparative analysis. MiR-21 was selected despite the lack of correlation with CAIX shown by qRT-PCR. miR-21 is increased under hypoxic conditions *in vitro* and *in situ* hybridisation will reveal which cell types express this miRNA in comparison with CAIX. Images of CAIX, miR-210 and miR-21 are shown in Fig 5.4C-E, respectively. In all tumours, both CAIX and miR-210

expression was found in the epithelial cells of the gut crypts and their expression coincided in the majority of the tumours (Fig. 5.4C-D). Conversely, miR-21 expression was predominantly present in stromal cells underneath the epithelial cells, regardless of the presence of CAIX in the overlying epithelial cells (Fig. 5.4C, E). These observations explain the positive correlation between miR-210 and CAIX as well as the lack of correlation between miR-21 and CAIX. The positive expression of miR-21 in the stroma surrounding the cancer cells may suggest that miR-21 plays a role in tumour progression and invasion via modulation of the tumour microenvironment.

In conclusion, expression analysis of miR-210 demonstrated a positive correlation to the tumour hypoxia marker CAIX in CRC tissue, emphasising the importance of miR-210 in CRC tumour hypoxia. To further elucidate the potential of miR-210 as a biomarker of treatment response, evaluation of miR-210 expression in additional CRC tumour samples with treatment response data is required.

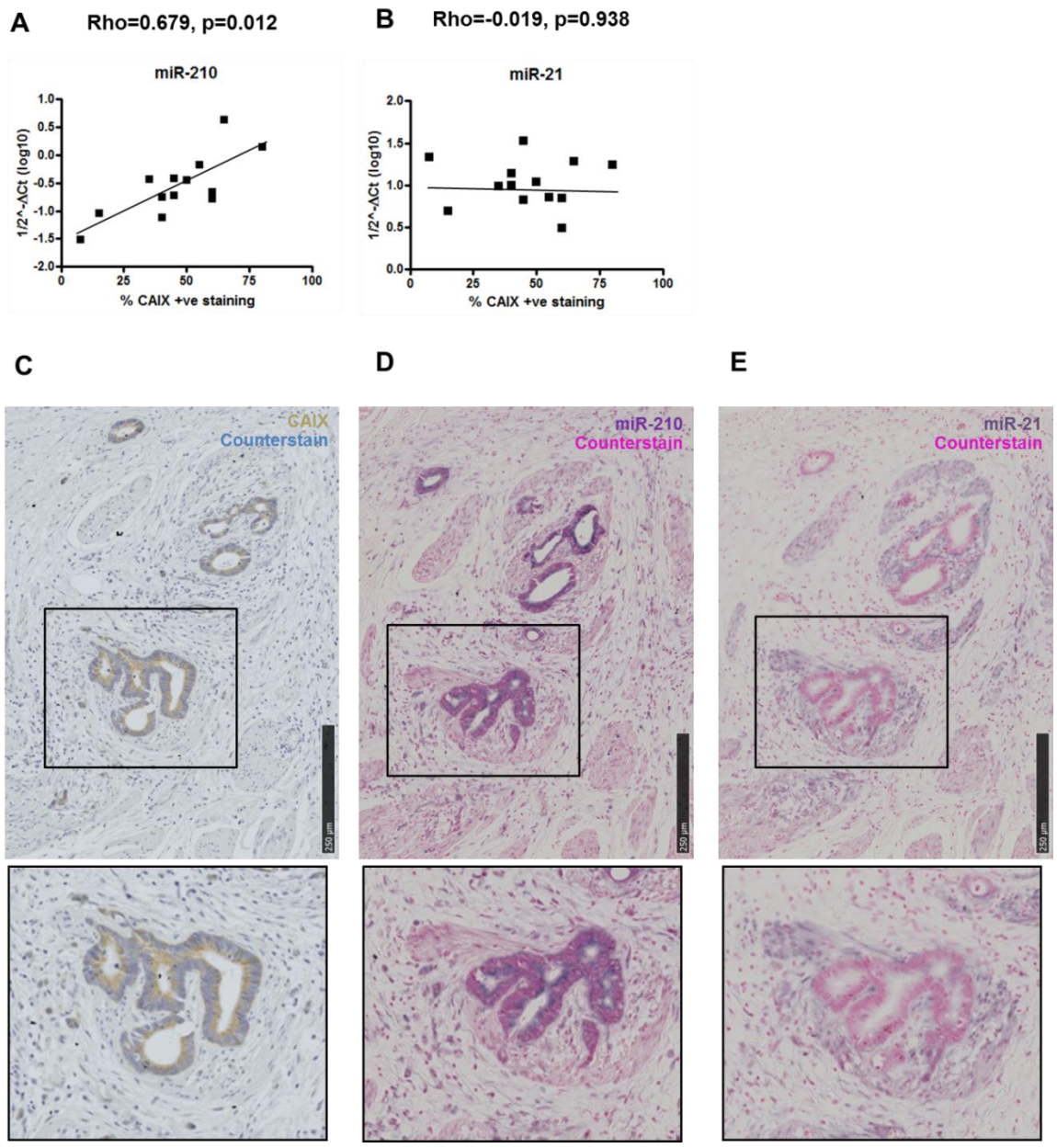

Figure 5.4. *In situ* expression of miR-210 positively correlates with the hypoxia marker CAIX in CRC tissue. (A-B) Scatter plots of miR-210 and miR-21 expression ($1/2^{-\Delta CT}$) assessed by qRT-PCR and percentage of CAIX-positive staining within the tumour (n=13). Correlation efficiency calculated with Spearman's Rank. Rho values and p-value are shown above. (C-E) IHC of CAIX and *in situ* hybridisation of miR-210 and miR-21 performed on serial sections of FFPE blocks of CRC tumours (n=8). Black rectangles outline the position of the zoomed images shown below.

5.5 HCT116 cells are resistant to 5-FU under hypoxia

The chemotherapeutic agent 5-FU has been the standard first-line treatment for many cancers, including CRC, for the past 40 years [95]. In recent years, the availability of other compounds used in combination with 5-FU has broadened treatment options. For example, adjuvant treatment with 5-FU/Leucovorin in CRC has been shown to increase overall survival in a number of studies [96-98]. This combined treatment now forms the basis of treatment for patients with CRC stage III, although, the benefit of the use in stage II CRC tumours is less obvious [99]. Despite increased response rates with combined therapy, tumour resistance is still a major concern in the treatment management of advanced CRC [526]. Solid tumours are a very complex and heterogeneous tissue, comprising of cancer, stromal and immune cells. Nearly all solid tumours contain regions of hypoxia and early evidence indicated that a decrease in oxygen tension could contribute to this drug resistance in solid tumours (reviewed in [121-123]). Indeed, tumour expression of HIF-1α has been correlated to 5-FU resistance in gastric cancer [527], and the colon cancer cell line HCT116 is more resistant to 5-FU under hypoxic conditions, which may be reversed by knockdown of HIF-1α [528].

To verify hypoxia-induced resistance to 5-FU under hypoxia in my CRC cell line model, HCT116 cells were treated with various concentrations of 5-FU (1 µM, 5 µM, 10 µM, 100 µM and 1 mM) or the same concentration of vehicle (Dimethyl sulfoxide, DMSO) under three oxygen conditions (20.9%, 1% or 0.2%) for 48 hr. Cells were fixed with 3.7% PFA and nuclei were stained with Hoechst 33342. Nuclei were imaged using the IN Cell Analyzer microscope 1000 and were then counted. Cell counts for each drug concentration was normalised to the vehicle control treated cells. One-way ANOVA statistical analysis was performed and demonstrated that HCT116 grown under hypoxic conditions are more resistant to 5-FU compared to their normoxic counterpart. This was the case for all 5-FU concentrations measured (all 5-FU concentrations $p<0.05$, Fig. 5.5A). Post-hoc tests (Tukey's) were performed to determine which groups differed and

demonstrated that HCT116 cells maintained under 0.2% oxygen were significantly different compared to 20.9% (Fig. 5.5A).

Having previously validated hypoxia-responsive miRNAs (Section 5.3), including miR-21, miR-210 and miR-30d, I hypothesised that a) these hypoxic-responsive miRNAs may play a role in the resistance to 5-FU in HCT116 cells under hypoxic conditions and b) that the inhibition of the expression of these miRNAs under hypoxia could sensitise the cells to 5-FU. To test the hypotheses, HCT116 cells were transfected with NTC, pre- or anti-miR for all three miRNAs (miR-21, -210 and -30d) for 48 hr and then treated with 10 μM 5-FU or DMSO for a further 48 hr under 20.9% or 0.2% oxygen (Fig. 5.5B). This timeline was selected to allow for sufficient functional knockdown of targets by the miRNAs. Following treatment with 5-FU, an increase in survival was observed when cells were cultured under 0.2% oxygen and transfected with NTC (20.9%, NTC, mean=48.6%; 0.2%, NTC, mean=83.2%; p=0.0390, Fig. 5.5C). This resistance was similar to that previously obtained with 10 μM 5-FU (20.9%, mean 45.5%; 0.2%, mean=80.3%; Fig. 5.5A). Also, when cells were cultured under 20.9% oxygen, the combination of miRNAs and 5-FU treatment did not significantly alter the cell survival compared to NTC transfected cells, indicating that the transfection of NTC did not the response to 5-FU. By contrast, when the expression of miR-21 and miR-30d was inhibited with transfection of the anti-miR, cells were slightly more sensitive to the 5-FU treatment. (NTC, mean=83.2%; anti-miR-21, mean=69.4%; anti-miR-30d, mean=71.1%; Fig. 5.5C). Statistical analysis, however, demonstrated this decrease was not significant when compared to NTC transfected cells (anti-miR-21, p=0.2027; anti-miR-30d, p=0.1297; Fig. 5.5C).

In addition, further over-expression of miR-210 under 0.2% oxygen reduced cell survival compared to NTC transfected cells (pre-miR-210, p=0.0838, Fig. 5.5C). Literature reports have shown that miR-210 targets key modulators of cell cycle progression resulting in a decrease of cell proliferation (reviewed in [529]). Indeed, cells transfected with pre-miR-210 (DMSO treated only) demonstrated a decrease in cell survival under both oxygen

tensions (Appendix Fig. 6), indicating that in HCT116 cells an overexpression of miR-210 results in a decrease in cell survival. In summary, this data demonstrated that HCT116 cells are more resistant to 5-FU under 0.2% oxygen conditions compared to normoxic conditions. The inhibition of hypoxia-responsive miRNAs miR-21 and miR-30d may be a potential method to increase sensitivity to 5-FU but requires further investigation.

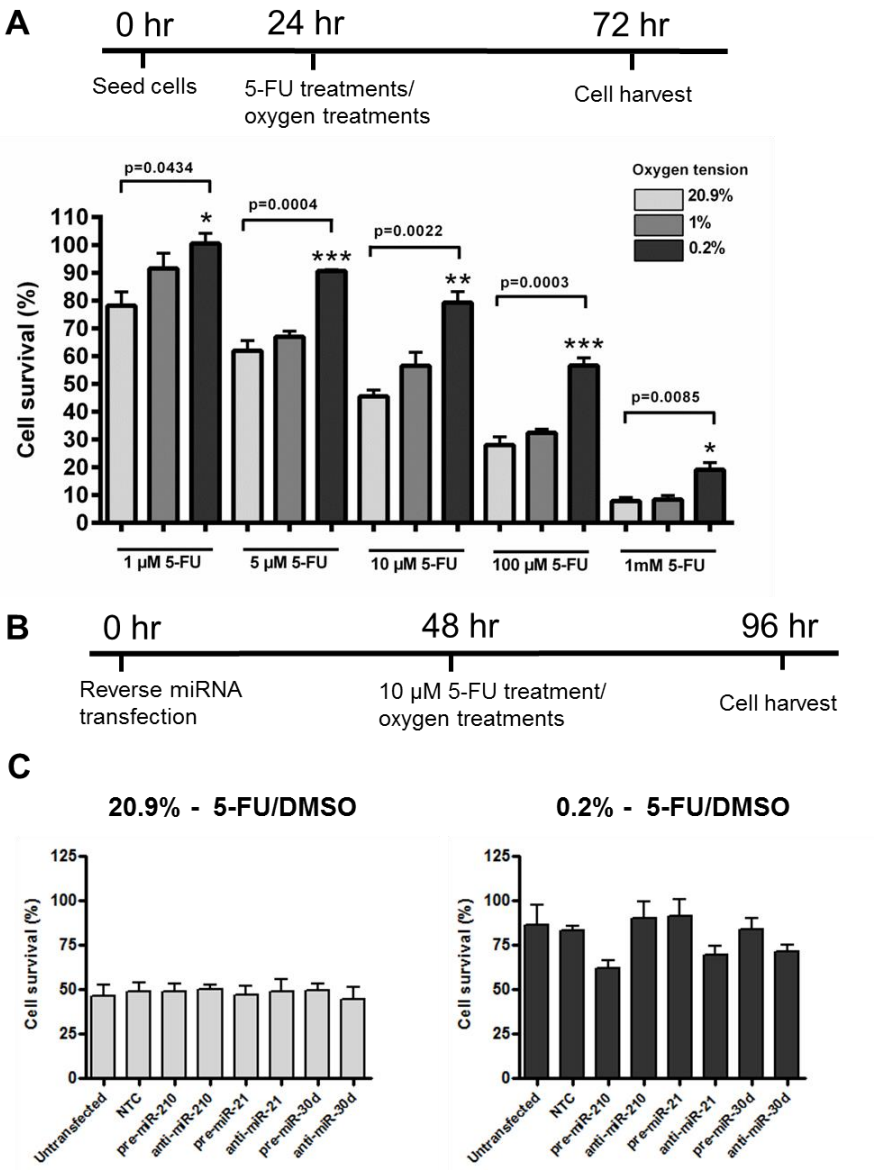

Figure 5.5. HCT116 cells are resistant to 5-FU under low oxygen conditions. (A) HCT116 cells were treated with various concentrations of 5-FU (1 µM, 10 µM, 100 µM or 1 mM) or the appropriate vehicle control (DMSO) for 48 hr under three oxygen conditions (20.9%, 1% or 0.2%). The graph represents the percentage of cell survival normalised to each vehicle control. Significance was calculated with one-way ANOVA tests. Asterisks indicate significant changes between 20.9% and 0.2% identified by post-hoc tests (Tukey's). (B) The experimental time-line of transient transfections of miRNAs in combination with 5-FU treatment under two oxygen conditions (20.9% or 0.2%). (C) The graph represents the percentage of cell survival normalised to vehicle controls following transfection with NTC and pre- or anti-miR of miR-210, -21 or 30d. Bars represent mean values with SEM. *p<0.05, **p<0.01 and ***p<0.001.

5.6 In vitro cell metabolism is altered under hypoxic conditions

Cells have evolved mechanisms to adapt to low oxygen conditions which include decreasing their mitochondrial respiratory rate by decreasing the cellular ATP levels [530-532]. Additionally, HIF-1α may be activated by low cellular ATP levels indirectly; ATP deficit increases glycolysis and HIF-1α activity [533]. Also, AMP-activated protein, induced following ATP-deprived cellular conditions, activates HIF-1 [534]. These observations link the hypoxia induced-HIF-1 signalling pathway to altered metabolic activity. Recent research is focussed on exploiting these cellular metabolomic changes under hypoxia to identify new strategies for anticancer drug development and/or identifying prognostic biomarkers for treatment response.

To identify changes in cellular metabolites under hypoxia, the six CRC cell lines used previously (DLD-1, HCT116, HT29, HT55, SW837 and VACO4s) were maintained under three differential oxygen conditions (20.9%, 1% or 0.2%) for 48 hr. In collaboration with Dr. Adam (Oxford University), the six cell lines were prepared for CE-TOF/MS (Section 2.20) and shipped to the Institute for Advanced Biosciences at Keio University, Japan, where cellular metabolites were assessed. The resulting metabolite profile was subsequently modelled using multivariate analysis, in collaboration with Dr. J. Bundy (Imperial College, UK) (Section 2.21). Similar to the multivariate analysis performed on the miRNA data, metabolite profile in the six cell lines was modelled against the three oxygen conditions. This analysis demonstrated a significant ($p<0.05$) relationship between 92 metabolites under hypoxia.

Various computational tools are available to group the metabolites into metabolic networks or pathways. Two examples are MetaboAnalyst (www.metaboanalyst.ca) and ImPaLa (http://impala.molgen.mpg.de), which offer a range of functions including metabolic pathway analysis. Both tools use the KEGG database [535]. An overview of the online computational tools is reviewed in [536]. The 92 significantly ($p<0.05$) altered metabolites were subject to an over-representation analysis to identify altered pathways

under hypoxia using these two different platforms. An over-representation analysis evaluates whether a particular group of metabolites is represented more than expected by chance within a metabolite list. In the context of pathway analysis, this illustrates if metabolites involved in a particular pathway are enriched. To further enhance the over-representation analysis, the user may upload a list of all metabolites that were detected by the platform to acts as a "background" for the analysis. The analysis in MetaboAnalyst was performed both with (Fig. 5.6A) and without (Fig. 5.6B) the background. Ten pathways were significantly ($p<0.05$) enriched in hypoxia of which the top five are shown (Fig. 5.6A). However, once background metabolites were taken into account, this was reduced to only a single enriched pathway in hypoxia, which was the aminoacyl-tRNA biosynthesis (Fig. 5.6B). Next, a second analysis with ImPaLa was performed on the same metabolite profile (with background) which identified six metabolite pathways that were enriched in hypoxic conditions (Fig. 5.6C). Interestingly, the aminoacyl-tRNA biosynthesis pathway was also enriched using this different analysis software (highlighted in red; Fig. 5.6A-C).

Among the 92 significantly altered metabolites in hypoxia, 13 are involved in the amino-acyl-tRNA biosynthesis pathway. To illustrate their expression profile, fold change (log2) in concentration (fmol/cell) was calculated for each of the six cell lines and is shown in Fig. 5.7. Strikingly, the metabolite profile in hypoxia is very different amongst the six cell lines. For instance, in two cell lines (SW837 and HT55) all 13 metabolites were altered consistently in both 1% and 0.2% oxygen compared to 20.9%. By contrast, the change in metabolite concentration in hypoxia in the other cell lines is mixed, with some of these metabolites increased whilst others were decreased (Fig. 5.7).

In conclusion, *in silico* analysis of altered metabolites under hypoxia in six CRC cell lines demonstrated an enrichment of the aminoacyl-tRNA biosynthesis pathway. This preliminary data will need to be validated and could form a platform for future experiments which will be discussed in the discussion in Section 5.8.4.

A

Metabolite pathway	Total	Expected	Hits	p-value
Beta-Alanine metabolism	28	1.05	10	0.00000195
Aminoacyl-tRNA biosynthesis	75	2.80	13	0.000175
Glutathione metabolism	38	1.42	9	0.000498
Nitrogen metabolism	39	1.46	9	0.000620
Alanine, aspartate and glutamate metabolism	24	0.90	7	0.00127

B

Metabolite pathway	Detected/Total	Expected	Hits	p-value
Aminoacyl-tRNA biosynthesis	21/75	5.71	13	0.0477

C

Metabolite pathway	Detected/Total	Hits	p-value
Central carbon metabolism in cancer	32/37	21	0.000204
ABC transporters	34/123	18	0.00343
Aminoacyl-tRNA biosynthesis	21/75	13	0.00463
Mineral absorption	13/29	9	0.0173
Protein digestion and absorption	29/47	15	0.0179
Cyanomino acid metabolism	11/45	8	0.0218

Figure 5.6. Altered metabolite pathways under hypoxia. (A) The top five metabolite pathways altered in hypoxia determined by an over-representation analysis performed with MetaboAnalyst software. Metabolites with a $p<0.05$ were used for the analysis. Total = the total number of metabolites in a given pathway, Expected = the number of hits expected by chance, Hits = number of metabolites significantly altered in hypoxia, and p-value = Bonferoni correct p-value. (B) The same analysis as in A, but with background metabolite profile taken into account. Detected/total = the number of metabolites detected using CE-TOF/MS / the total number of metabolites in a given pathway. (C) The six metabolite pathways significantly ($p<0.05$) altered in hypoxia determined by an over-representation analysis performed with ImPaLa software. Metabolites with a $p<0.05$ were used and background metabolite profile has been taken into account. The common pathway, aminoacyl-tRNA biosynthesis, is highlighted in red.

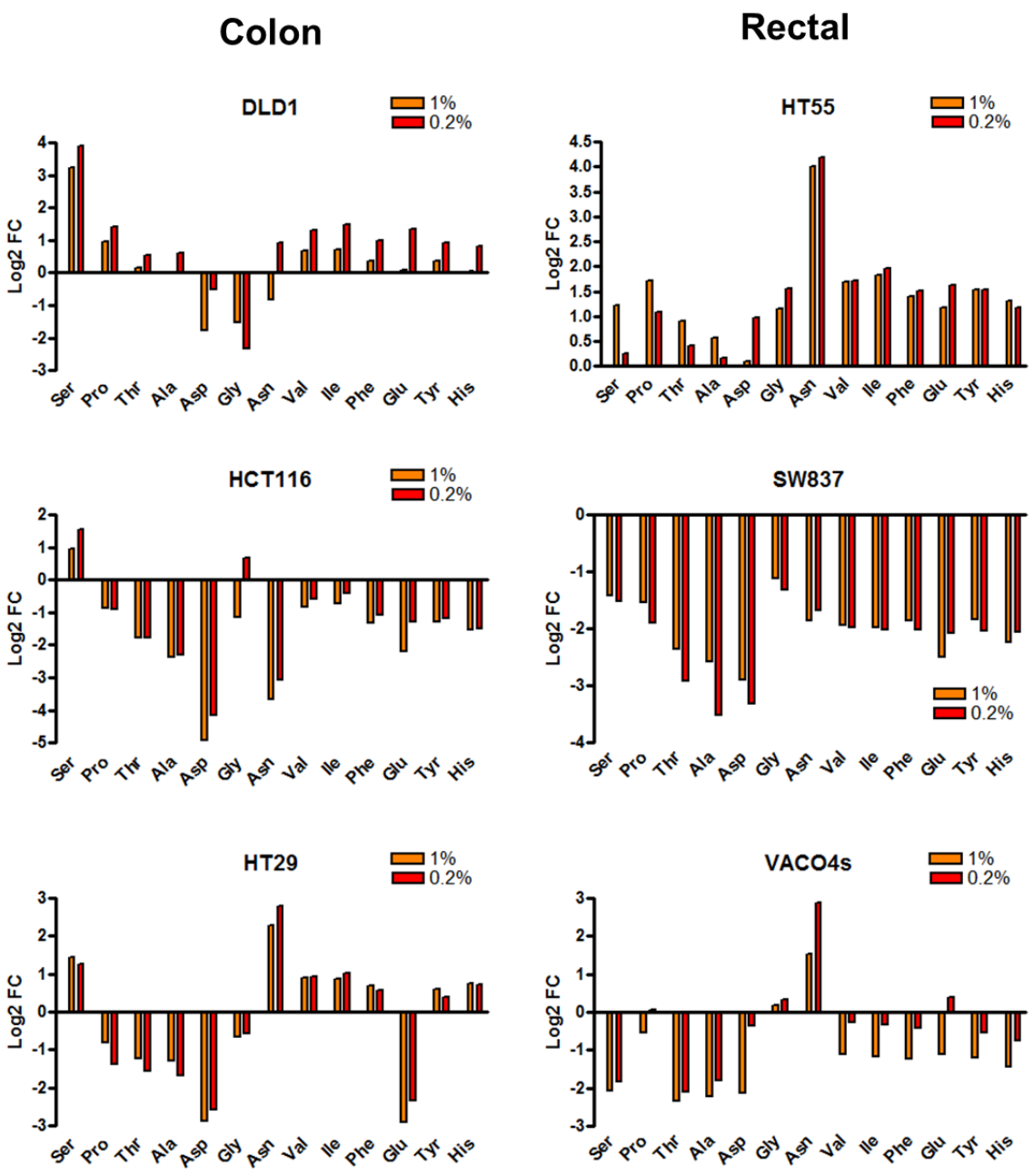

Figure 5.7. Altered metabolites under hypoxia involved in the aminoacyl-tRNA biosynthesis pathway. Fold changes (log2) in metabolite concentration compared to 20.9% oxygen are shown for each of the six CRC cell lines.

5.8 Discussion and future work

5.8.1 Altered miRNA profiles under hypoxia in six CRC cell lines

Using three colon (DLD-1, HCT116 and HT29) and three rectal (HT55, SW837 and VACO4s) cancer cell lines as a model, differential expression of miRNAs were determined using a miRNA microarray (Section 5.2). MiRNA profiling under hypoxia in CRC has been previously studied, however, often the cell lines used, oxygen tension, and the time under hypoxia are variable. For example, many publications reports altered miRNA profiles in a single cell line such as Caco-2 [537] or HeLa cells [538]. Oxygen concentration and the time under hypoxic conditions also vary; Caco-2 cells were cultured under 1% oxygen for 48 hr, whilst HeLa cells were maintained at 0.01% oxygen for a 24 hr period. The closest comparison to the microarray performed in this thesis is a miRNA analysis by Kulshreshtha and colleagues in 2009 [323]. In this study, two colon (HT29 and HCT116) and two breast cancer (MCF7 and MDA-MB231) cell lines were maintained at 0.02% oxygen for 24 and 48 hr [323]. Statistical analysis of all four cell lines combined across both time lines identified a number of miRNAs significantly altered, and four were common between their results and mine (miR-181a, -192, -21 and -210). This suggests that some miRNAs are commonly up-regulated under hypoxia in both colon and breast cancer cell lines.

The miRNA analysis performed in this thesis represents the change in expression under three different oxygen conditions in six cell lines combined. This was done to uncover miRNAs that were hypoxia-responsive despite differences between the cell lines. Undeniably, the PLS-DA analysis demonstrated the presence of inherent differences in miRNA expression between the six different cell lines (Section 5.2). Further analysis of each of the six cell lines independently, or grouped into rectal and colon cancer cell lines, might uncover additional hypoxia-responsive miRNAs regulated in an origin-specific manner.

Data validation by a second method is crucial to confirm the changes observed by microarrays are genuine. The expression of 12 candidate miRNAs was determined by qRT-PCR in an independent set of experiments for all six cell lines (Section 5.3). In contrast to the array, data normalisation of qRT-PCR data relies on one or two genes that are stable under the various conditions. The small non-coding RNA RNU19 was shown to be most stable under hypoxia of the miRNAs that were tested (miR-16, let-7a and RNU19), and has been previously shown in the literature to be a stable housekeeping control under hypoxia [524, 525], and was therefore used for normalisation. Of the twelve candidate miRNAs tested, six were successfully validated by qRT-PCR (miR-21, -210, -30d, -320a, -320b and -320c). One of the most significantly up-regulated miRNA in the array was miR-210 ($p=0.002$). In addition, the loadings from the PLS-DA analysis showed that miR-210 had the largest loading score (Appendix Fig. 4), indicating that miR-210 contributed highly to the separation of the groups along PLS-DA axis 6. These results echo literature reports demonstrating that miR-210 is up-regulated under various oxygen conditions in a range of cell lines from different tumours (reviewed in [523]).

miRNAs tend to be up-regulated in clusters, many of which contain members of the same miRNA family (introduced in Section 1.3.1.1). Interestingly, five miRNA families of which more than one family member was altered under hypoxia, were identified. Apart from the miR-320 family which was subsequently validated, two members of the miR-182 family (miR-182, -183 and -96) were significantly up-regulated (miR-182 and miR-96). Also, miR-183 was up-regulated but just missed the significance cut off of $p<0.05$ ($p=0.067$). The expression of miR-182 has been previously shown to be up-regulated in CRC [539-541], and correlated to poor prognosis and overall survival [540, 541]. Furthermore, overexpression of miR-182 promoted cell survival and proliferation of colon cancer cell lines [542]. The second member of the family altered under hypoxia, miR-96, was shown to be induced in CRC tissue and correlated to liver metastasis [283].

Further experiments could include:

1. The validation of the three members of the miR-182 family (miR-96, -182, and -183) by qRT-PCR;
2. If these validate, *in situ* hybridisation of these miRNAs in CRC tissue could be performed to test a) the localisation in CRC tissue and b) whether the expression correlates with the hypoxia inducible factor CAIX;
3. The knockdown of this family via transfection of anti-miRs in CRC cell lines could be performed to assess whether they are able to modulate the response to 5-FU under hypoxia; and
4. The Target ID Library system could be used to elucidate of genome-wide targets of this miRNA family.

5.8.2 miR-210 is up-regulated in rectal cancer tissue and positively correlates to hypoxia marker CAIX

To benchmark the *in vitro* findings, miRNA expression of miR-21, -210 and -30d was determined in rectal cancer *ex vivo* and correlated to the expression of hypoxia-inducible protein CAIX. Correlation efficiency analysis demonstrated a positive correlation between miR-210 and CAIX expression in rectal cancer tissue (Section 5.4). A recent report by Qu and colleagues indicates that miR-210 expression is up-regulated in human CRC tissue compared to normal tissue [543]. This work demonstrated a positive correlation between miR-210 and HIF-1α mRNA expression, which supports a common conclusion between their data and mine. In this report, miR-21 was shown to be up-regulated in CRC tissue compared to normal tissue, however, it was not apparent whether this correlated with HIF-1α mRNA expression [543]. This might be because Qu and colleagues did not observe any correlation but did not report this. This might provide an explanation as to why I did not observe a correlation between miR-21 and CAIX.

In situ hybridisation experiments demonstrated co-localisation between miR-210 and CAIX expression in the epithelial cells in rectal cancer tissue (Fig 5.4C, D). A study in 2012 also showed a correlation between miR-210 and CAIX in cancer tissue samples of

non-small cell lung carcinoma [544], which lends support to the hypothesis that miR-210 is up-regulated in hypoxic regions of solid tumours. Furthermore, *in situ* expression of miR-210 expression was co-localised to VEGF expression in idiopathic osteonecrosis, an area prone to being hypoxic [545]. VEGF is involved in angiogenesis and its expression is driven by HIF-1α, further indicating a link between miR-210 and hypoxic tissues.

In addition to miR-210, miR-21 was also investigated by *in situ* in rectal cancer tissue sections. miR-21 was found to be expressed in the stromal-like cells in rectal cancer tissue, but this did not correlate with the expression of CAIX (Fig. 5.3C-E). However, the lack of direct correlation between miR-21 and CAIX expression does not mean that miR-21 is not expressed in hypoxic regions. In other tissue types there might be a link with expression of this miRNA and hypoxia. For example, *in situ* analysis of miR-21 expression found up-regulation in hypoxic cells in the lungs of mice [546] and human hypoxic arteries [547]. Furthermore, the observation that miR-21 is predominantly expressed in fibroblast-like cells within tumour has been confirmed by others who have used the same probe: miR-21 is up-regulated in stromal-like cells in colon cancer [548, 549] and breast cancer [550]. By contrast, groups that performed *in situ* hybridisation with other commercial probes for miR-21 observed expression mainly in the tumour cells [286, 551]. The differences in probe might explain some of the differences in localisation of miR-21 expression.

Assessing miRNA as potential biomarker is a rapidly developing area of research. To predict whether a patient's tumour will respond to CRT by using miRNA expression profiles as a guide is the ultimate goal. For instance, the prognostic value of miR-210 expression in tissue samples has been studied in many cancers (reviewed in [343]). A single paper has recently identified that high miR-210 expression in CRC tissue is a prognostic factor for overall survival [543]. However, further investigation of the prognostic value of miRNAs, including miR-210, is required. For example, to determine if miRNAs could be used for predicting response to neo-adjuvant treatment of CRCs, a retrospective study should be performed using at least two large independent cohorts of

patients; miRNA expression would be determined in a routinely-taken tumour biopsy before treatment, scored, and then be used to classify patients and determine if differentially expressed miRNA profiles can predict treatment outcome.

Circulating miRNAs could be exploited as biomarkers in clinical use as they have several advantages: readily detectable, stable in serum, and profiling is relatively cheap and quantitative [552]. Circulating miRNAs, including miR-21 and miR-210, have been intensively studied in various cancers [343, 553]. Interestingly, circulating expression levels of miR-21 were dysregulated in prostate [554, 555], ovarian [556, 557], pancreatic [352, 558], liver [559, 560] and oesophageal cancers [561], but has not yet been investigated in CRC. Similarly, miR-210, was dysregulated in blood samples (serum or plasma) in pancreatic [352], lung [562], non-small lung [563] and renal cancers [564, 565], but again has not yet been looked at in CRC. Therefore, there is a real need to investigate the potential for circulating miRNAs as a diagnostic/prognostic biomarker for CRC and to predict treatment response. Future work to investigate this could include:

1) The collection of blood samples at time of diagnosis or pre-treatment. Circulating miRNA profiles should be determined, preferably by array or RNA sequencing. This data could then be used to determine if certain miRNA signatures may predict treatment outcome;
2) Candidate miRNAs could then be further investigated *ex vivo*. For example, *in situ* hybridisation of candidate miRNA could be performed in CRCs that did not respond to neo-adjuvant therapy; and
3) The investigation of candidate miRNAs could be performed *in vivo*. The response to chemotherapeutic drugs, such as 5-FU, following transfection with pre-miR and anti-miR of candidate miRNAs in CRC cell lines. These experiments could elucidate their role in the sensitivity of chemotherapy drugs *in vivo*.

5.8.3. Hypoxia induces resistance to chemotherapy drug 5-FU in HCT116 cell line.

The chemotherapeutic agent 5-FU forms the basis of the standard treatment of many cancers, although resistance to this drug is a major concern in treatment of CRC patients. Interestingly, hypoxia in solid tumours is linked to 5-FU therapy resistance [121-123]. In Section 5.5, I demonstrated that HCT116 colon cancer cells maintained under hypoxia demonstrated a significant resistance to the chemotherapy drug 5-FU at various dosages, which confirms existing literature reports in the same cell line [528]. However, Ravizza and colleagues showed that HCT116 maintained under 1% oxygen for 24 hr demonstrated an increased resistance to 100 μM and 250 μM 5-FU, but they did not observe increased resistance using 10 μM 5-FU. This is in contrast to my observations where HCT116 cells maintained under lower oxygen tensions (0.2% oxygen) were significantly more resistant to a range of 5-FU dosages, but not significantly different under 1% oxygen (Fig. 5.5A). These contradicting results might be due to the differences in treatment time: Ravizza and colleagues treated HCT116 cells with 5-FU for 24 hr, whereas I cultured mine for 48 hr. Nevertheless, resistance to 5-FU under hypoxic conditions has been demonstrated in other cell lines, including gastric cancer cell lines [566], oral squamous cell carcinoma cell lines [567] and oesophageal squamous cell cancer cell lines [568], indicating that resistance to 5-FU under hypoxic conditions is a feature of cell lines originating from multiple tumour types.

I hypothesised that the hypoxia-responsive miRNAs might play a role in the 5-FU resistance observed in the HCT116 colon cancer cell line. The suppression of miR-21 or miR-30d by transfection with an anti-sense miRNA induced a slight, but not significant, sensitivity to 5-FU under 0.2% oxygen (Fig. 5.4C). Interestingly, no change in 5-FU sensitivity was observed under normoxic conditions, suggesting that the miRNA regulatory effect may be oxygen tension dependent and that some of their targets are only present under these hypoxic conditions. Other groups have shown that miRNAs are able to modulate the sensitivity to 5-FU under normoxic conditions of a number of CRC cell lines. These including miR-31 (HCT116; [569]), miR-129 (HCT116; [570]), miR-192

(RKO; LoVo; [571]), miR-21 (HT29; [572]), miR-23a (HCT116; HT29; [573]) and miR-143 (HCT116; [574]). These literature reports show that the experimental time lines, including the duration of 5-FU treatment and the transfection time-frame are crucial. For example, Wang and colleagues demonstrated that HCT116 were more sensitive to 5-FU following 24 hr of suppression of miR-31 but not after 48, 72 or 96 hr [569]. Further experiments to optimise experimental conditions will need to be performed to assess if the suppression of miR-21 and miR-30d could modulate 5-FU sensitivity in HCT116 cells under hypoxic conditions. For future experiments I would propose to conduct the following experiments:

1) The treatment of 10 μM 5-FU in HCT116 cells (and potentially other cell lines) for various lengths of time. Firstly, cell survival should be assayed following 5-FU treatment under 0.2% oxygen to determine drug resistance across a variety of time point;
2) Next, cell lines could be created with lenti-viral vectors producing anti-sense miRNA of the candidate miRNA in order to assure sustained suppression of these miRNAs over a longer period of time; and
3) Cell survival would be assayed following 5-FU treatment under 0.2% oxygen in these cells to elucidate the role of miRNAs in 5-FU resistance.

miR-210 is one of the most studied miRNAs under hypoxia and is greatly induced under these conditions. It was, therefore, surprising that the suppression of miR-210 with an anti-sense miRNAs under hypoxia did not modulate 5-FU sensitivity (Fig. 5.5C), particularly as miR-210 is a direct target of HIF-1α which has been previously shown to be involved in the resistance to 5-FU under hypoxic conditions in HCT116 cells [528]. It may be that the up-regulation of miR-210 under hypoxia is too strong to be counteracted with the transient transfection of the anti-sense miRNA strands. As mentioned above, in order to assure stable knockdown of miR-210, a stably expressing cell line could be produced with the use of lenti-viral vectors producing anti-sense miR-210. Future experiments using this cell line could include:

1) The maintenance under hypoxic conditions for various lengths of time. To confirm the knockdown of miR-210, qRT-PCR should be performed at various time points to assure sufficient knockdown to counteract the strong up-regulation of miR-210 under hypoxia;
2) A number of tumourigenicity assays could be performed to elucidate the role of miR-210 in tumourigenesis under hypoxia: cell survival/proliferation, cell migration and colony formation. These experiments could highlight the importance of miR-210 under hypoxic conditions; and
3) Sensitivity to 5-FU could be assayed in these cells under hypoxic conditions, especially under 0.2% oxygen.

5.8.4. Altered metabolite profile in six CRC cell lines under hypoxia

Metabolomics is a powerful tool developed to systematically analyse the metabolic fingerprint of a cell. In Section 5.6, I demonstrated an altered metabolite profile under hypoxic conditions (1% and 0.2%) and pathway analysis revealed an enrichment in the aminoacyl-tRNA biosynthesis pathway by two independent pathway analysis tools (MetaboAnalyst and ImPaLa). However, the metabolic profile of the 13 metabolites altered in this pathway for each of the six cell lines is very different. For instance, in two cell lines, the majority (DLD-1) or all (HT55) of the 13 metabolites are increased. In three cell lines, the majority (HCT116 and VACO4s) or all (SW837) of the 13 metabolites are decreased and in one cell line (HT29) approximately half of the 13 metabolites are either increased or decreased response under hypoxia (Fig 5.8). Due to the intrinsic differences between the cell lines, the mixed changes observed here is perhaps unsurprising. In fact, the PLS-DA analysis already demonstrated that these cells are very different based on their miRNA expression. (Fig. 5.1A, Section 5.2).

A similar study by Frezza and colleagues was conducted on a single cell line [575]. They investigated the metabolite profiles of HCT116 when maintained at 1% oxygen for 36 hr,

and detected 241 metabolites, 32 of which were significantly altered under hypoxia. Interestingly, of the 32, 18 were amino acids and were increased in concentration (apart from L-kynurenine which was decreased). Seven of these amino acids were commonly dysregulated under hypoxia in HCT116 cells between the two studies: Threonine, Proline, Phenylalanine, Histidine, Methionine, Asparagine and Serine. In contrast to their findings, these seven amino acids were down-regulated in HCT116 cells under both 1% and 0.2% oxygen in my analysis.

There are several important differences between the study conducted by Frezza and colleagues vs the one conducted in this thesis. These are outlines below.

1. Timepoint: 36hr vs 48hr.
2. Oxygen concentration: 1% oxygen vs 1% and 0.2% oxygen combined.
3. Mass-spec platform: LC-MS vs CE-TOFMS.

These differences, especially the different mass-spec technique, may have contributed to the differences in the concentration of the amino acids. For instance, LC-MS uses high-powered liquid chromatography (LC) to separate the particles before its mass-to-charge ratio is analysed. By contrast, CE-TOFMS is a relatively new technique in which the mass-to-charge ratios are determined by the time that it takes for the particles to reach a detector (time of flight (TOF)).

Future experiments to further this research could include:

1) The validation of the altered metabolites under hypoxia *in vitro*. A targeted metabolomics experiment could be performed to validate the change in metabolite expression of the 92 significantly altered metabolites and/or metabolites; and
2) To determine whether there is a link between the changes in miRNA expression and the altered metabolite profile, the expression of both miRNAs and metabolites should be determined for each individual cell line. Target prediction tools could

then be used to identify potential mRNA targets that involved in regulating the production of the altered metabolites.

One interesting additional finding by Frezza and colleagues was that autophagy increases under hypoxia [575]. Autophagy is a catabolic pathway in which proteins and organelles are sequestered into autophagosomes and fused with lysomes for digestion. The autophagy pathway is part of a normal cell homeostasis process to replace damaged cell membranes and organelles, however, autophagy is up-regulated under physiological stress conditions, including cell starvation (reviewed in [576]). Recently, reports indicate that hypoxia-induced autophagy is HIF-1α dependent [577, 578] and inhibition of autophagy under hypoxic conditions reduces tumour cell viability [578].

Furthermore, miRNAs have been implicated to regulate various steps in the autophagy pathway (reviewed in [579]). For instance, miR-30d targets multiple genes involved in the autophagy pathway including many of the ATG core proteins [580], and miR-30d regulates cisplatin-resistance by promoting autophagic survival in thyroid carcinoma cells [581]. Additionally, miR-210 enhances autophagy by down-regulating Bcl-2 expression in colon cancer cells [582]. Interestingly, the inhibition of hypoxia-induced autophagy resulted in an increased sensitivity to the chemotherapy drug 5-FU in DLD-1 cells [583]. Therefore, work to further this line of investigation would include:

1) To determine the expression of putative targets in the autophagy pathway for miR-30d and miR-210 under both normoxia and hypoxia. CRC cell lines would be transfected with pre- or anti- miRs and cells cultured under normoxia and hypoxia. qRT-PCR and western blotting techniques would be used to confirm the regulation of key autophagy players by these miRNAs at the mRNA and protein level, respectively; and
2) To determine the involvement of autophagy in 5-FU resistance under hypoxic conditions in HCT116 cells. Similar experiments to those conducted in Section 5.5 could be performed. In addition to 10 μM 5-FU treatment, cells could be

transfected with siRNA against *ATG5* (siRNA against this gene is most often used to disturb the autophagy pathway) under both 20.9% and 0.2% oxygen. Nuclei counts would be calculated using the IN Cell Developer v1.8 to determine cell viability.

The pathway analysis that was performed with two independent tools highlighted a common pathway dysregulated under hypoxia; the aminoacyl-tRNA biosynthesis. This pathway plays an important role in decoding the genetic message by facilitating the transfer of the amino acids onto the growing peptide chain to create proteins. The enzymes that catalyse the ligation of amino acids to their tRNA are aminoacyl tRNA synthesases (AARs). Besides their role in protein synthesis, their non-canonical function has been linked to metabolic conditions, neural pathologies and several cancers (reviewed in [584]). Very early reports already reported an increase in methionine-acyl tRNA synthesase in colon cancer [585], and, more recently, trypophanyl-tRNA synthesase was associated with disease recurrence of colon cancer [586].

During cellular stress, such as hypoxia, tRNAs can be cleaved to produce transfer RNA-derived fragments (tRFs), which can inhibit protein synthesis [587] and modulate cell proliferation [588]. A recent report demonstrated that tRFs contain anti-tumour and anti-metastatic properties in breast cancer in vitro and in vivo, and that this is mediated through Y-box binding protein-1 (YB-1) [589]. Interestingly, YB-1 promotes EMT [590] and is linked to the response to therapy in various cancers [591], including rectal cancer [592]. To further this line of research I would:

1. Perform a targeted mass-spectrometry of all amino acids to validate the CE-TOF/MS findings under hypoxic conditions *in vitro*.
2. Evaluate the expression of the AARs enzymes under hypoxic conditions *in vitro*. Their expression could be measured at the RNA and protein level by qRT-PCR and western blotting, respectively.

3. Assess the expression of YB-1 at the RNA and protein level under hypoxic conditions *in vitro*. Further evaluation of YB-1 could be performed in FFPE sections in CRC *in vivo,* and correlated with hypoxia markers miR-210 and CAIX.

5.8.5. Target ID Library preparation (Appendix)

Target identification of miRNAs is crucial to provide information on which cellular processes a given miRNA influences. To date, 3'-UTR luciferase reporter assays are considered the gold standard to confirm whether a miRNA targets a particular mRNA sequence. However, this is a highly laborious exercise and requires preliminary knowledge guided by *in silico* target prediction identification. In our laboratory, we have recently obtained a novel system (Target ID Library, Sigma, UK) which will allow us to discover genome-wide direct mRNA targets of any miRNA of choice and provide insight into the regulatory function of miRNAs in key cellular pathways.

HeLa cells were chosen as a suitable cell type for creating a cell line stably expressing the Target ID Library constructs as expression analysis demonstrated a low endogenous level of our three key candidate miRNAs (miR-21, -210 and -30d) relative to the six CRC cell lines. Transfected cells were treated with Zeocin (500 μg/ml) to positively select cells that had stably integrated cDNA constructs containing a TKzeo fusion gene and PCR analysis on DNA from selected cells indicate the presence of the library of constructs (Appendix Fig. 9). Although the Target ID Library claims to contain constructs for 16,922 unique genes, next generation sequencing (NGS) performed by Gaken and colleagues demonstrated the presence of only 5,626 genes in their MCF7 clones [593]. Therefore, the next step is to sequence the library cDNA inserts to confirm satisfactory genomic coverage within the HeLa cell population.

Once we are satisfied with the genomic coverage of the cDNA inserts, transfection with lenti-viral vectors producing our candidate miRNAs (miR-21, -210 or -30d) will be performed. Additionally, a fourth miRNA, miR-34a, will be screened for targets, too.

NGS analysis to uncover genes that are directly targeted by these miRNAs within their 3'-UTR region will be performed. More importantly, to benchmark the results, NGS data will be compared directly to the publically available combined pulsed SILAC and microarray analysis data sets for miR-34a [475, 476]. The data generated will provide a comprehensive cross-platform analysis, which will demonstrate the similarities but also, importantly, highlight the difference between these different technologies. Next, identified targets from the Mission ID/NGS analysis will be analysed with Ingenuity Pathways Analysis (IPA) software in collaboration with QMUL Bioinformatic service in order to elucidate relevant pathways modified by the candidate miRNAs. Identified targets in potentially dysregulated pathways will then be validated at the protein level via transfection of the candidate miRNAs in isolated fibroblasts (miR-34a) and CRC cell lines (miR-21, -210 and -30d). The validation of important pathways regulated by these miRNAs may provide valuable insights into cellular mechanisms that are fundamental to the development of fibrosis (miR-34a) and the cellular responses to hypoxia and/or 5-FU resistance mechanisms in CRC (miR-21, -210 and -30d). Finally, once validated *in vitro*, key targets will be validated *in vivo* in CD fibrosis and CRC tissue and their potential as biomarker will be investigated.

Chapter 6: General conclusions

6.1 Summary of main findings

- Identification of a subset of miRNAs that play a significant role in the development and progression of two intestinal diseases, CD and CRC.
- Changes in miRNA expression in the epithelial mucosa often reflect changes in other parts of the intestine and/or tumour. For example:
    - The expression of miRNAs is different between mucosa overlying strictured compared to non-strictured mucosa,
    - The miR-29 family is down-regulated in SCD vs NSCD.
- Experimental studies using both primary cultures and cell lines can be used to model disease processes and identify mechanisms involving miRNAs notably:
    - TGF-β-mediated down-regulation of miR-29b results in the up-regulation of ECM molecule production, such as collagen 1 and 3,
    - The anti-apoptotic protein Mcl-1 is indirectly up-regulated by miR-29b via IL-6 and IL-8.
- That hypoxia has a significant impact of miRNA expression, which in turn influences cellular metabolism profiles and drug response in CRC cell lines. For example:
    - Hypoxia alters the miRNAs signature in CRC cells *in vitro*;
    - miR-210 is overexpressed in hypoxic regions of CRC and correlated with the hypoxia marker CAIX;
    - CRC cell line HCT116 is more resistant to the chemotherapy drug 5-FU under 0.2% oxygen compared to 20.9%;
    - The inhibition of miR-21 or miR-30d under 0.2% slightly increases the sensitivity of HCT116 cells to 5-FU; and
    - Hypoxia alters cellular metabolism in CRC cell lines *in vitro*.

6.2 The clinical relevance of these findings

6.2.1 How are miRNAs altered during disease processes and what role does the intestinal microenvironment play in this?

The absence of appropriate animal models that mimic intestinal fibrosis in CD have historically hindered the functional analysis and discovery of genes and pathways involved in the progression of fibrosis. The majority of mouse models are used primarily to study inflammation, and do not reproduce the fibrogenic changes that occur in CD patients. Additionally, a fundamental problem with studying the pathogenesis of intestinal fibrosis in humans is that by the time fibrosis is detected, early pathogenic events have already occurred and the fibrogenic process is fully established. Consequently, the key initiating events in the pathogenesis of fibrosis can no longer be investigated. If the early events could be modelled *in vivo* (e.g. mouse models) then this would represent a significant step forward and offer the opportunity to test new drugs that target fibrosis rather than just interfere with the inflammatory process. However, recently, a number of mouse models have been established that mimic in part the initial events of fibrosis [594]. The evaluation of miRNA-based therapeutic, such as the miR-29 family, will determine their potential in modulating the various stages of intestinal fibrosis.

Molecular changes in the human gut mucosa reflect the changes that happen in the deeper layers [201]. Therefore, the down-regulation of the miR-29 family in the mucosa in SCD areas may provide information regarding the cellular processes that happen deeper in the tissue. Functionally, this family of miRNAs is important in the pathogenesis of fibrosis in various organs [372-378]. Therefore, assessing the expression miRNAs, such as miR-29 family, in biopsies taken routinely during CD disease monitoring could be used to detect early changes in the mucosa that may reflect the initial stages of intestinal fibrosis in the deeper layers. Evaluating the utility of the miR-29 family as biomarkers would require a significant prospective clinical trial focussed on newly diagnosed CD patients and following their progress over time by collecting samples during routine surveillance

endoscopy. The expression of miRNAs in these samples (biopsies/serum) should be correlated to clinical parameters such as disease activity and progression into the various disease subtypes (inflammatory, stricturing or penetrating CD).

Environmental factors play a key role in the development of many human diseases, including IBD and cancer. An excessive immune-response to antigens and microbiota in the gut is one of the contributing factors leading to IBD (both CD and UC). The modulatory effects of the gut microbiota on miRNA expression have broadened our view of the regulatory functions of miRNAs in disease. Interestingly, two members of the miR-200 family (miR-200b and miR-200c) were decreased in conventional mice upon infection with microbiota [595]. These miRNAs are known to regulate EMT, an important process that is often dysregulated in both cancer and inflammation/fibrosis. In fact, work in our laboratory has demonstrated that three members of the miR-200 family (miR-141, -200a and -200c) are down-regulated in inflamed strictured areas of CD patients where there is evidence of EMT (Mehta et al., unpublished data). The impact of the microbiota on miRNA profiles and the cellular inflammatory responses in the mucosa is an undeveloped area of research. Further work should evaluate whether the use of faecal transplants could be a beneficial therapeutic strategy to modulate the inflammatory/fibrogenic events through altering the miRNA profiles in the mucosa of IBD patients.

6.2.2 Can miRNAs be used as diagnostic or prognostic tools in CD or CRC?

Clinical features in CD have some prognostic value, although, they are often heterogeneous and their use remains problematic. Inflammatory biomarkers, such as C-reactive protein and fecal calprotectin, may be used to distinguish active from inactive IBD, but hold no true predictive value for the development of fibrosis [596]. Bodily fluids provide an excellent source of circulating miRNAs and have non-invasive biomarker potential as their expression is stable and can be readily detected. Work in our laboratory has demonstrated the potential use of serum-based miRNAs as biomarkers to distinguish

the stricturing CD phenotype (Lewis et al., 2015, in print). This has opened up opportunities to investigate further the expression of circulating miRNAs, such as miR-29b, as potential prognostic biomarkers for intestinal fibrosis.

Particular miRNAs are able to discriminate tumour subtype, origin and identify important cellular mechanisms in tumourigenesis. Also, circulating miRNAs can be used to distinguish cancer patients from healthy individuals and diagnose early stage cancer [399, 597]. Additionally, miRNAs can be used to predict response to treatment, which is of significant clinical value and has been investigated intensively over the past decades. For example, increased miR-21 expression is an indicator of poor outcome in various cancers [286, 415]. However, these studies were performed in tumour tissue, retrospectively. Giving the importance of hypoxia-responsive miR-21 in tumourigenesis, and its potential role in 5-FU resistance under hypoxic conditions *in vitro*, the use of miR-21 to predict treatment response in CRC needs to be evaluated in prospective cohort studies with validation across independent centres.

Recently, the expression of miR-210 in CRC tissue was significantly correlated to large tumour size, lymph node metastasis, advanced clinical stage and poor prognosis [543]. To confirm these findings the expression of miR-210 should be further investigated retrospectively in a large number of CRC tissues and a correlation between miR-210 expression and clinical parameters including treatment response should be determined. Additionally, miR-210 expression should be evaluated in the serum of early diagnosed CRC patients. These patients should be followed up and miR-210 expression correlated to various clinical parameters to assess the utility of miR-210 as a non-invasive biomarker to predict treatment in CRC.

While the use of miRNAs as biomarkers clearly has significant potential advantages when compared to protein-based serum biomarkers, systematic high-throughput miRNA measurement for clinical samples is still in its infancy. The results obtained from different platforms (qPCR or NGS based) from different vendors are likely to contribute to

inconsistent measurements. Also, miRNA data normalisation remains a fundamental challenge. Currently, there is no standardised method and steps to generalise this method are urgently needed to obtain more consistent, comprehensive and accurate miRNA signatures that may be adopted for clinical use.

6.2.3 Do miRNAs represent suitable anti-fibrotic or anti-cancer therapeutic targets?

An ideal drug target should have disease-modifying properties, a proven function in the pathophysiology of the disease and predictable potential side effects. miRNAs are an attractive therapeutic target as they regulate many cellular processes. The majority of current therapeutic agents are aimed towards a single molecular target which induces a modest response. Hence, the ability to repress many targets at once across various oncogenic pathways provides a strong rationale for developing miRNA-based therapeutics, although this does have the potential to increase off-target effects and consequent side-effects. A number of miRNAs have already shown potential in pre-clinical models and a few have entered the initial phases of clinical trials (http://mirnarx.com/pipeline/mirna-pipeline.html). Biopharmaceutical company miRNA Therapeutics Inc is leading the way by having developed a broad pipeline of miRNA-based therapeutics. Their main compound, MRX34, is a miR-34a mimic drug which entered phase I clinical trials in 2013. MRX34 is piloted as an anti-cancer drug in patients with un-resectable liver cancer (www.clinicaltrials.gov) and the phase I results are encouraging. In the context of fibrosis, an antagonist for miR-21, RG-012, is a potential anti-fibrotic agent in renal fibrosis in mice. Phase I clinical trials for the use of RG-012 in Alport syndrome patients (a hereditary nephritis disorder disease characterised by end-stage kidney disease) are to begin in 2015. Important for future anti-miR drugs, this trial will determine the pharmacokinetics, cellular uptake, miRNA inhibition and off-target effects of the therapeutic drug. The knowledge this will determine whether anti-miR-21 may present a suitable anti-fibrotic therapy and in the longer-term could be piloted in other fibrotic diseases, including intestinal fibrosis.

The role of miR-210 has been investigated intensively over the past decade and miR-210 is now considered a master sensor of reduced oxygen tension. Its impact on a large number of cellular pathways has presented miR-210-based therapeutics with exciting prospects. Many studies have demonstrated the anti-tumourigenesis properties of miR-210 *in vitro*. However, more importantly, miR-210 is able to repress tumour growth of *in vivo* xenografts of laryngal [598] and liver cancer [599]. Further evaluation of the anti-tumour properties of miR-210 in additional tumour xenografts models, including CRC, will provide additional evidence for miR-210-based therapeutic in cancer.

MiRNAs have emerged recently as key regulators of cellular metabolism, including the metabolism of glucose, lipids and amino acids [600]. A shift in glucose metabolism from oxidative phosphorylation to aerobic glycolysis is a classic hallmark of tumour cells, called the "Warburg effect". Under hypoxia, this adaptive metabolic shift has been proposed to be advantageous to the tumour cell through the promotion of survival, proliferation and even resistance to cancer treatment. The altered miRNA and metabolite profiles obtained under hypoxia *in vitro* in this thesis provide valuable insights into the way that miRNAs regulate the cellular metabolism under these conditions. The development of miRNA-based therapeutic to suppress this metabolic shift could lead to novel therapeutic strategies to inhibit tumour growth or drug-resistance in CRC. For instance, miR-210 is known to target a variety of key players in important metabolic pathways to reduce mitochondrial metabolism and increase glycolysis. Particularly under hypoxia, the development of anti-miR-210 therapeutics is one that holds much promise.

While the use for miRNA-based therapeutics is encouraging, some of the limitations for miRNAs as therapeutic entities should be considered. For instance, the safe delivery of the miRNA mimic or antagonist to the target cell is crucial for the treatment to be functionally successful. The complex intestinal human defence includes the innate and adaptive immune system and drug degradation by gastric enzymes, which may prevent drugs reaching their target site. Also, the variability of these factors between CD patients is high, which may further impact the successful delivery of miRNAs in these patients.

However, several promising strategies to enhance colon-specific delivery, such as microcapsules, might facilitate the transport of therapeutic agent to the site of disease. Results from initial clinical trials are awaited and will address some of the challenges that miRNA-based therapeutics is faced with.

6.2.4 Limitations of this thesis

The functional *in vitro* studies performed in this thesis have highlighted potential candidate miRNAs as therapeutic entities in intestinal fibrosis in CD, as well as anti-cancer agents in CRC. In order to unravel the downstream mechanism of miRNAs, the most fundamental step is the identification of mRNA targets. Much of the current knowledge on the cellular function of miRNAs and their targets is predominantly built around online prediction tools. The incorporation of pathway analysis into these prediction models have allowed identification of putative targets for miRNAs and the pathways they might impact on. However, despite the significant increased knowledge on miRNA biogenesis and function, gaps in the precise mechanism by which they modulate protein expression remain. For instance, novel targets that are not identified by the prediction algorithms have been elucidated, highlighting the existence of alternative ways in which miRNAs modulate their targets. The Target ID Library is a recent development which enables high-throughput analysis of genome-wide targets of candidate miRNAs (Target ID Library appendix). Follow-up studies using this system will include the identification of novel targets of selected candidate miRNAs. Secondly, mRNA targets will be validated subsequently at the protein level *in vitro* and *in vivo*. The modulation of 5-FU resistance by inhibition of miR-21 and miR-30d was only observed under hypoxic conditions, suggesting that perhaps the targets involved in 5-FU resistance are only present under these circumstances. Therefore it will be more importantly to confirm novel miRNA targets in the correct cellular and disease contexts.

Chapter 7: References

1. Ferlay, J., et al., *Cancer incidence and mortality worldwide: Sources, methods and major patterns in GLOBOCAN 2012.* Int J Cancer, 2015. **136**(5): p. E359-86.
2. Www.cancerresearchuk.org.
3. www.cancerresearchuk.org, *Statistics on the risk of developing cancer, by cancer type and age. Calculated using 2008 data for the UK using the 'Adjusted for Multiple Primaries (AMP)' method).*
4. Ferguson, L.R., *Meat and cancer.* Meat Sci, 2010. **84**(2): p. 308-13.
5. Zisman, A.L., et al., *Associations between the age at diagnosis and location of colorectal cancer and the use of alcohol and tobacco: implications for screening.* Arch Intern Med, 2006. **166**(6): p. 629-34.
6. Tsong, W.H., et al., *Cigarettes and alcohol in relation to colorectal cancer: the Singapore Chinese Health Study.* Br J Cancer, 2007. **96**(5): p. 821-7.
7. Lee, K.J., et al., *Physical activity and risk of colorectal cancer in Japanese men and women: the Japan Public Health Center-based prospective study.* Cancer Causes Control, 2007. **18**(2): p. 199-209.
8. de Jong, A.E., et al., *Prevalence of adenomas among young individuals at average risk for colorectal cancer.* Am J Gastroenterol, 2005. **100**(1): p. 139-43.
9. Donohoe, C.L., et al., *Obesity and gastrointestinal cancer.* Br J Surg, 2010. **97**(5): p. 628-42.
10. Platz, E.A., et al., *Proportion of colon cancer risk that might be preventable in a cohort of middle-aged US men.* Cancer Causes Control, 2000. **11**(7): p. 579-88.
11. Johns, L.E. and R.S. Houlston, *A systematic review and meta-analysis of familial colorectal cancer risk.* Am J Gastroenterol, 2001. **96**(10): p. 2992-3003.
12. BB, C., *The sigmoidoscopic picture of chronic ulcerative colitis (non-specific).* Amer J Med Sci, 1925(170).
13. Munkholm, P., *Review article: the incidence and prevalence of colorectal cancer in inflammatory bowel disease.* Aliment Pharmacol Ther, 2003. **18 Suppl 2**: p. 1-5.
14. *www.cancer.gov*.
15. Fearon, E.R. and B. Vogelstein, *A genetic model for colorectal tumorigenesis.* Cell, 1990. **61**(5): p. 759-67.
16. Knudson, A.G., Jr., *Mutation and cancer: statistical study of retinoblastoma.* Proc Natl Acad Sci U S A, 1971. **68**(4): p. 820-3.
17. Iacopetta, B., et al., *Functional categories of TP53 mutation in colorectal cancer: results of an International Collaborative Study.* Ann Oncol, 2006. **17**(5): p. 842-7.
18. Garraway, L.A. and E.S. Lander, *Lessons from the cancer genome.* Cell, 2013. **153**(1): p. 17-37.
19. Vogelstein, B., et al., *Cancer genome landscapes.* Science, 2013. **339**(6127): p. 1546-58.
20. Stratton, M.R., P.J. Campbell, and P.A. Futreal, *The cancer genome.* Nature, 2009. **458**(7239): p. 719-24.
21. Gonzalez-Perez, A., et al., *Computational approaches to identify functional genetic variants in cancer genomes.* Nat Methods, 2013. **10**(8): p. 723-9.
22. Walther, A., R. Houlston, and I. Tomlinson, *Association between chromosomal instability and prognosis in colorectal cancer: a meta-analysis.* Gut, 2008. **57**(7): p. 941-50.

23. Fodde, R., R. Smits, and H. Clevers, *APC, signal transduction and genetic instability in colorectal cancer.* Nat Rev Cancer, 2001. **1**(1): p. 55-67.
24. Burrell, R.A., et al., *Replication stress links structural and numerical cancer chromosomal instability.* Nature, 2013. **494**(7438): p. 492-6.
25. Groden, J., et al., *Identification and characterization of the familial adenomatous polyposis coli gene.* Cell, 1991. **66**(3): p. 589-600.
26. Kinzler, K.W., et al., *Identification of FAP locus genes from chromosome 5q21.* Science, 1991. **253**(5020): p. 661-5.
27. Nagase, H. and Y. Nakamura, *Mutations of the APC (adenomatous polyposis coli) gene.* Hum Mutat, 1993. **2**(6): p. 425-34.
28. Korinek, V., et al., *Constitutive transcriptional activation by a beta-catenin-Tcf complex in APC-/- colon carcinoma.* Science, 1997. **275**(5307): p. 1784-7.
29. Albuquerque, C., et al., *The 'just-right' signaling model: APC somatic mutations are selected based on a specific level of activation of the beta-catenin signaling cascade.* Hum Mol Genet, 2002. **11**(13): p. 1549-60.
30. Liu, W., et al., *Mutations in AXIN2 cause colorectal cancer with defective mismatch repair by activating beta-catenin/TCF signalling.* Nat Genet, 2000. **26**(2): p. 146-7.
31. Morin, P.J., et al., *Activation of beta-catenin-Tcf signaling in colon cancer by mutations in beta-catenin or APC.* Science, 1997. **275**(5307): p. 1787-90.
32. Najdi, R., R.F. Holcombe, and M.L. Waterman, *Wnt signaling and colon carcinogenesis: beyond APC.* J Carcinog, 2011. **10**: p. 5.
33. Santini, D., et al., *High concordance of KRAS status between primary colorectal tumors and related metastatic sites: implications for clinical practice.* Oncologist, 2008. **13**(12): p. 1270-5.
34. Karapetis, C.S., et al., *K-ras mutations and benefit from cetuximab in advanced colorectal cancer.* N Engl J Med, 2008. **359**(17): p. 1757-65.
35. Amado, R.G., et al., *Wild-type KRAS is required for panitumumab efficacy in patients with metastatic colorectal cancer.* J Clin Oncol, 2008. **26**(10): p. 1626-34.
36. Lane, D.P., *Cancer. p53, guardian of the genome.* Nature, 1992. **358**(6381): p. 15-6.
37. Meek, D.W., *The p53 response to DNA damage.* DNA Repair (Amst), 2004. **3**(8-9): p. 1049-56.
38. Tominaga, T., et al., *Combination of p53 codon 72 polymorphism and inactive p53 mutation predicts chemosensitivity to 5-fluorouracil in colorectal cancer.* Int J Cancer, 2010. **126**(7): p. 1691-701.
39. Soussi, T., *TP53 mutations in human cancer: database reassessment and prospects for the next decade.* Adv Cancer Res, 2011. **110**: p. 107-39.
40. Baker, S.J., et al., *p53 gene mutations occur in combination with 17p allelic deletions as late events in colorectal tumorigenesis.* Cancer Res, 1990. **50**(23): p. 7717-22.
41. Vogelstein, B., et al., *Genetic alterations during colorectal-tumor development.* N Engl J Med, 1988. **319**(9): p. 525-32.
42. Fearon, E.R., et al., *Identification of a chromosome 18q gene that is altered in colorectal cancers.* Science, 1990. **247**(4938): p. 49-56.
43. Riggins, G.J., et al., *Mad-related genes in the human.* Nat Genet, 1996. **13**(3): p. 347-9.
44. Howe, J.R., et al., *Mutations in the SMAD4/DPC4 gene in juvenile polyposis.* Science, 1998. **280**(5366): p. 1086-8.
45. Aaltonen, L.A., et al., *Incidence of hereditary nonpolyposis colorectal cancer and the feasibility of molecular screening for the disease.* N Engl J Med, 1998. **338**(21): p. 1481-7.

46. Hampel, H., et al., *Screening for the Lynch syndrome (hereditary nonpolyposis colorectal cancer).* N Engl J Med, 2005. **352**(18): p. 1851-60.
47. Kunkel, T.A., *Nucleotide repeats. Slippery DNA and diseases.* Nature, 1993. **365**(6443): p. 207-8.
48. Ionov, Y., et al., *Ubiquitous somatic mutations in simple repeated sequences reveal a new mechanism for colonic carcinogenesis.* Nature, 1993. **363**(6429): p. 558-61.
49. Thibodeau, S.N., G. Bren, and D. Schaid, *Microsatellite instability in cancer of the proximal colon.* Science, 1993. **260**(5109): p. 816-9.
50. Toyota, M., et al., *CpG island methylator phenotype in colorectal cancer.* Proc Natl Acad Sci U S A, 1999. **96**(15): p. 8681-6.
51. Weisenberger, D.J., et al., *CpG island methylator phenotype underlies sporadic microsatellite instability and is tightly associated with BRAF mutation in colorectal cancer.* Nat Genet, 2006. **38**(7): p. 787-93.
52. McGivern, A., et al., *Promoter hypermethylation frequency and BRAF mutations distinguish hereditary non-polyposis colon cancer from sporadic MSI-H colon cancer.* Fam Cancer, 2004. **3**(2): p. 101-7.
53. Nosho, K., et al., *Comprehensive biostatistical analysis of CpG island methylator phenotype in colorectal cancer using a large population-based sample.* PLoS One, 2008. **3**(11): p. e3698.
54. Samowitz, W.S., et al., *Evaluation of a large, population-based sample supports a CpG island methylator phenotype in colon cancer.* Gastroenterology, 2005. **129**(3): p. 837-45.
55. Slattery, M.L., et al., *A comparison of colon and rectal somatic DNA alterations.* Dis Colon Rectum, 2009. **52**(7): p. 1304-11.
56. Hawkins, N., et al., *CpG island methylation in sporadic colorectal cancers and its relationship to microsatellite instability.* Gastroenterology, 2002. **122**(5): p. 1376-87.
57. van Rijnsoever, M., et al., *Characterisation of colorectal cancers showing hypermethylation at multiple CpG islands.* Gut, 2002. **51**(6): p. 797-802.
58. Barault, L., et al., *Hypermethylator phenotype in sporadic colon cancer: study on a population-based series of 582 cases.* Cancer Res, 2008. **68**(20): p. 8541-6.
59. Gryfe, R., et al., *Tumor microsatellite instability and clinical outcome in young patients with colorectal cancer.* N Engl J Med, 2000. **342**(2): p. 69-77.
60. Popat, S., R. Hubner, and R.S. Houlston, *Systematic review of microsatellite instability and colorectal cancer prognosis.* J Clin Oncol, 2005. **23**(3): p. 609-18.
61. Lanza, G., et al., *Immunohistochemical test for MLH1 and MSH2 expression predicts clinical outcome in stage II and III colorectal cancer patients.* J Clin Oncol, 2006. **24**(15): p. 2359-67.
62. Carethers, J.M., et al., *Use of 5-fluorouracil and survival in patients with microsatellite-unstable colorectal cancer.* Gastroenterology, 2004. **126**(2): p. 394-401.
63. Arnold, C.N., A. Goel, and C.R. Boland, *Role of hMLH1 promoter hypermethylation in drug resistance to 5-fluorouracil in colorectal cancer cell lines.* Int J Cancer, 2003. **106**(1): p. 66-73.
64. Ribic, C.M., et al., *Tumor microsatellite-instability status as a predictor of benefit from fluorouracil-based adjuvant chemotherapy for colon cancer.* N Engl J Med, 2003. **349**(3): p. 247-57.
65. Georgiades, I.B., et al., *Heterogeneity studies identify a subset of sporadic colorectal cancers without evidence for chromosomal or microsatellite instability.* Oncogene, 1999. **18**(56): p. 7933-40.

66. Chan, T.L., et al., *Early-onset colorectal cancer with stable microsatellite DNA and near-diploid chromosomes.* Oncogene, 2001. **20**(35): p. 4871-6.
67. Silver, A., et al., *A distinct DNA methylation profile associated with microsatellite and chromosomal stable sporadic colorectal cancers.* Int J Cancer, 2012. **130**(5): p. 1082-92.
68. Tang, R., et al., *Colorectal cancer without high microsatellite instability and chromosomal instability--an alternative genetic pathway to human colorectal cancer.* Carcinogenesis, 2004. **25**(5): p. 841-6.
69. Jones, A.M., et al., *Array-CGH analysis of microsatellite-stable, near-diploid bowel cancers and comparison with other types of colorectal carcinoma.* Oncogene, 2005. **24**(1): p. 118-29.
70. Cai, G., et al., *Clinicopathologic and molecular features of sporadic microsatellite- and chromosomal-stable colorectal cancers.* Int J Colorectal Dis, 2008. **23**(4): p. 365-73.
71. Gulati, S., S. Gustafson, and H.A. Daw, *Lynch Syndrome Associated With PMS2 Mutation: Understanding Current Concepts.* Gastrointest Cancer Res, 2011. **4**(5-6): p. 188-90.
72. Kohlmann, W. and S.B. Gruber, *Hereditary Non-Polyposis Colon Cancer*. 1993.
73. Papadopoulos, N., et al., *Mutation of a mutL homolog in hereditary colon cancer.* Science, 1994. **263**(5153): p. 1625-9.
74. Al-Tassan, N., et al., *Inherited variants of MYH associated with somatic G:C-->T:A mutations in colorectal tumors.* Nat Genet, 2002. **30**(2): p. 227-32.
75. Hemminki, A., et al., *A serine/threonine kinase gene defective in Peutz-Jeghers syndrome.* Nature, 1998. **391**(6663): p. 184-7.
76. Jenne, D.E., et al., *Peutz-Jeghers syndrome is caused by mutations in a novel serine threonine kinase.* Nat Genet, 1998. **18**(1): p. 38-43.
77. Sayed, M.G., et al., *Germline SMAD4 or BMPR1A mutations and phenotype of juvenile polyposis.* Ann Surg Oncol, 2002. **9**(9): p. 901-6.
78. Burger, B., et al., *Novel de novo mutation of MADH4/SMAD4 in a patient with juvenile polyposis.* Am J Med Genet, 2002. **110**(3): p. 289-91.
79. Palles, C., et al., *Germline mutations affecting the proofreading domains of POLE and POLD1 predispose to colorectal adenomas and carcinomas.* Nat Genet, 2013. **45**(2): p. 136-44.
80. Valle, L., et al., *New insights into POLE and POLD1 germline mutations in familial colorectal cancer and polyposis.* Hum Mol Genet, 2014. **23**(13): p. 3506-12.
81. Chen, S., et al., *Prediction of germline mutations and cancer risk in the Lynch syndrome.* JAMA, 2006. **296**(12): p. 1479-87.
82. Chung, L., et al., *Unexpected endometrial cancer at prophylactic hysterectomy in a woman with hereditary nonpolyposis colon cancer.* Obstet Gynecol, 2003. **102**(5 Pt 2): p. 1152-5.
83. Furlan, D., et al., *Genetic progression in sporadic endometrial and gastrointestinal cancers with high microsatellite instability.* J Pathol, 2002. **197**(5): p. 603-9.
84. Galiatsatos, P. and W.D. Foulkes, *Familial adenomatous polyposis.* Am J Gastroenterol, 2006. **101**(2): p. 385-98.
85. Lynch, P.M., *Standards of care in diagnosis and testing for hereditary colon cancer.* Fam Cancer, 2008. **7**(1): p. 65-72.
86. Iqbal, C.W., et al., *Surgical management and outcomes of 165 colonoscopic perforations from a single institution.* Arch Surg, 2008. **143**(7): p. 701-6; discussion 706-7.
87. Rabeneck, L., et al., *Bleeding and perforation after outpatient colonoscopy and their risk factors in usual clinical practice.* Gastroenterology, 2008. **135**(6): p. 1899-1906, 1906 e1.

88. Winawer, S.J., et al., *Colorectal cancer screening: clinical guidelines and rationale.* Gastroenterology, 1997. **112**(2): p. 594-642.
89. Atkin, W.S., et al., *Once-only flexible sigmoidoscopy screening in prevention of colorectal cancer: a multicentre randomised controlled trial.* Lancet, 2010. **375**(9726): p. 1624-33.
90. Edge, S.B. and C.C. Compton, *The American Joint Committee on Cancer: the 7th edition of the AJCC cancer staging manual and the future of TNM.* Ann Surg Oncol, 2010. **17**(6): p. 1471-4.
91. Dukes, C., *Histological Grading of Rectal Cancer: (Section of Pathology).* Proc R Soc Med, 1937. **30**(4): p. 371-6.
92. Dukes, C.E. and H.J. Bussey, *The spread of rectal cancer and its effect on prognosis.* Br J Cancer, 1958. **12**(3): p. 309-20.
93. Dukes, C., *The classification of cancer of the rectum.* The Journal of Pathology, 1932. **35**(3): p. 323-332.
94. seer.cancer.goc/statfacts/html/colorect/html.
95. Moertel, C.G., *Chemotherapy for colorectal cancer.* N Engl J Med, 1994. **330**(16): p. 1136-42.
96. Porschen, R., et al., *Fluorouracil plus leucovorin as effective adjuvant chemotherapy in curatively resected stage III colon cancer: results of the trial adjCCA-01.* J Clin Oncol, 2001. **19**(6): p. 1787-94.
97. Taal, B.G., et al., *Adjuvant 5FU plus levamisole in colonic or rectal cancer: improved survival in stage II and III.* Br J Cancer, 2001. **85**(10): p. 1437-43.
98. Staib, L., et al., *Toxicity and effects of adjuvant therapy in colon cancer: results of the German prospective, controlled randomized multicenter trial FOGT-1.* J Gastrointest Surg, 2001. **5**(3): p. 275-81.
99. *Efficacy of adjuvant fluorouracil and folinic acid in B2 colon cancer. International Multicentre Pooled Analysis of B2 Colon Cancer Trials (IMPACT B2) Investigators.* J Clin Oncol, 1999. **17**(5): p. 1356-63.
100. Rothenberg, M.L., et al., *Mortality associated with irinotecan plus bolus fluorouracil/leucovorin: summary findings of an independent panel.* J Clin Oncol, 2001. **19**(18): p. 3801-7.
101. de Gramont, A., et al., *Leucovorin and fluorouracil with or without oxaliplatin as first-line treatment in advanced colorectal cancer.* J Clin Oncol, 2000. **18**(16): p. 2938-47.
102. Giacchetti, S., et al., *Phase III multicenter randomized trial of oxaliplatin added to chronomodulated fluorouracil-leucovorin as first-line treatment of metastatic colorectal cancer.* J Clin Oncol, 2000. **18**(1): p. 136-47.
103. Cunningham, D., et al., *Randomised trial of irinotecan plus supportive care versus supportive care alone after fluorouracil failure for patients with metastatic colorectal cancer.* Lancet, 1998. **352**(9138): p. 1413-8.
104. Douillard, J.Y., et al., *Irinotecan combined with fluorouracil compared with fluorouracil alone as first-line treatment for metastatic colorectal cancer: a multicentre randomised trial.* Lancet, 2000. **355**(9209): p. 1041-7.
105. Rougier, P., et al., *Randomised trial of irinotecan versus fluorouracil by continuous infusion after fluorouracil failure in patients with metastatic colorectal cancer.* Lancet, 1998. **352**(9138): p. 1407-12.
106. Saltz, L.B., et al., *Irinotecan plus fluorouracil and leucovorin for metastatic colorectal cancer. Irinotecan Study Group.* N Engl J Med, 2000. **343**(13): p. 905-14.

107. Van Cutsem, E., et al., *Cetuximab plus irinotecan, fluorouracil, and leucovorin as first-line treatment for metastatic colorectal cancer: updated analysis of overall survival according to tumor KRAS and BRAF mutation status.* J Clin Oncol, 2011. **29**(15): p. 2011-9.
108. Douillard, J.Y., et al., *Randomized, phase III trial of panitumumab with infusional fluorouracil, leucovorin, and oxaliplatin (FOLFOX4) versus FOLFOX4 alone as first-line treatment in patients with previously untreated metastatic colorectal cancer: the PRIME study.* J Clin Oncol, 2010. **28**(31): p. 4697-705.
109. Peeters, M., et al., *Randomized phase III study of panitumumab with fluorouracil, leucovorin, and irinotecan (FOLFIRI) compared with FOLFIRI alone as second-line treatment in patients with metastatic colorectal cancer.* J Clin Oncol, 2010. **28**(31): p. 4706-13.
110. Bokemeyer, C., et al., *Fluorouracil, leucovorin, and oxaliplatin with and without cetuximab in the first-line treatment of metastatic colorectal cancer.* J Clin Oncol, 2009. **27**(5): p. 663-71.
111. van Cutsem, E., *Cetuximab and Chemotherapy as Initial Treatment for Metastatic Colorectal Cancer.* N Engl J Med, 2009. **360**.
112. Brown, G., et al., *Preoperative assessment of prognostic factors in rectal cancer using high-resolution magnetic resonance imaging.* Br J Surg, 2003. **90**(3): p. 355-64.
113. Heald, R.J. and R.D. Ryall, *Recurrence and survival after total mesorectal excision for rectal cancer.* Lancet, 1986. **1**(8496): p. 1479-82.
114. Sauer, R., et al., *Preoperative versus postoperative chemoradiotherapy for locally advanced rectal cancer: results of the German CAO/ARO/AIO-94 randomized phase III trial after a median follow-up of 11 years.* J Clin Oncol, 2004. **30**(16): p. 1926-33.
115. Bosset, J.F., et al., *Chemotherapy with preoperative radiotherapy in rectal cancer.* N Engl J Med, 2006. **355**(11): p. 1114-23.
116. *Prolongation of the disease-free interval in surgically treated rectal carcinoma. Gastrointestinal Tumor Study Group.* N Engl J Med, 1985. **312**(23): p. 1465-72.
117. Fisher, B., et al., *Postoperative adjuvant chemotherapy or radiation therapy for rectal cancer: results from NSABP protocol R-01.* J Natl Cancer Inst, 1988. **80**(1): p. 21-9.
118. *Clinico-pathological features of prognostic significance in operable rectal cancer in 17 centres in the U.K. (Third report of the M.R.C. Trial, on behalf of the Working Party).* Br J Cancer, 1984. **50**(4): p. 435-42.
119. *Improved survival with preoperative radiotherapy in resectable rectal cancer. Swedish Rectal Cancer Trial.* N Engl J Med, 1997. **336**(14): p. 980-7.
120. Sprangers, M.A., et al., *Quality of life in colorectal cancer. Stoma vs. nonstoma patients.* Dis Colon Rectum, 1995. **38**(4): p. 361-9.
121. Brown, J.M. and A.J. Giaccia, *The unique physiology of solid tumors: opportunities (and problems) for cancer therapy.* Cancer Res, 1998. **58**(7): p. 1408-16.
122. Sutherland, R.M., *Cell and environment interactions in tumor microregions: the multicell spheroid model.* Science, 1988. **240**(4849): p. 177-84.
123. Moulder, J.E. and S. Rockwell, *Tumor hypoxia: its impact on cancer therapy.* Cancer Metastasis Rev, 1987. **5**(4): p. 313-41.
124. Guedj, N., et al., *Predictors of tumor response after preoperative chemoradiotherapy for rectal adenocarcinomas.* Hum Pathol. **42**(11): p. 1702-9.
125. Hockel, M., et al., *Tumor oxygenation: a new predictive parameter in locally advanced cancer of the uterine cervix.* Gynecol Oncol, 1993. **51**(2): p. 141-9.

126. Wang, G.L. and G.L. Semenza, *Purification and characterization of hypoxia-inducible factor 1.* J Biol Chem, 1995. **270**(3): p. 1230-7.
127. Dachs, G.U. and I.J. Stratford, *The molecular response of mammalian cells to hypoxia and the potential for exploitation in cancer therapy.* Br J Cancer Suppl, 1996. **27**: p. S126-32.
128. Bruick, R.K. and S.L. McKnight, *A conserved family of prolyl-4-hydroxylases that modify HIF.* Science, 2001. **294**(5545): p. 1337-40.
129. Epstein, A.C., et al., *C. elegans EGL-9 and mammalian homologs define a family of dioxygenases that regulate HIF by prolyl hydroxylation.* Cell, 2001. **107**(1): p. 43-54.
130. Huang, L.E., et al., *Regulation of hypoxia-inducible factor 1alpha is mediated by an O2-dependent degradation domain via the ubiquitin-proteasome pathway.* Proc Natl Acad Sci U S A, 1998. **95**(14): p. 7987-92.
131. Kallio, P.J., et al., *Regulation of the hypoxia-inducible transcription factor 1alpha by the ubiquitin-proteasome pathway.* J Biol Chem, 1999. **274**(10): p. 6519-25.
132. Benita, Y., et al., *An integrative genomics approach identifies Hypoxia Inducible Factor-1 (HIF-1)-target genes that form the core response to hypoxia.* Nucleic Acids Res, 2009. **37**(14): p. 4587-602.
133. Mole, D.R., et al., *Genome-wide association of hypoxia-inducible factor (HIF)-1alpha and HIF-2alpha DNA binding with expression profiling of hypoxia-inducible transcripts.* J Biol Chem, 2009. **284**(25): p. 16767-75.
134. Xia, X., et al., *Integrative analysis of HIF binding and transactivation reveals its role in maintaining histone methylation homeostasis.* Proc Natl Acad Sci U S A, 2009. **106**(11): p. 4260-5.
135. Xia, X. and A.L. Kung, *Preferential binding of HIF-1 to transcriptionally active loci determines cell-type specific response to hypoxia.* Genome Biol, 2009. **10**(10): p. R113.
136. Tanimoto, K., et al., *Genome-wide identification and annotation of HIF-1alpha binding sites in two cell lines using massively parallel sequencing.* Hugo J, 2010. **4**(1-4): p. 35-48.
137. Wiesener, M.S., et al., *Widespread hypoxia-inducible expression of HIF-2alpha in distinct cell populations of different organs.* FASEB J, 2003. **17**(2): p. 271-3.
138. Maynard, M.A., et al., *Multiple splice variants of the human HIF-3 alpha locus are targets of the von Hippel-Lindau E3 ubiquitin ligase complex.* J Biol Chem, 2003. **278**(13): p. 11032-40.
139. Manalo, D.J., et al., *Transcriptional regulation of vascular endothelial cell responses to hypoxia by HIF-1.* Blood, 2005. **105**(2): p. 659-69.
140. Carroll, A.A., M., *HIF-1a regulation by proline hydroxylation.* Exp reviews in molecular science, 2005. **7**(6).
141. Grote, J., R. Susskind, and P. Vaupel, *Oxygen diffusion constants D and K of tumor tissue (DS-carcinosarcoma) and their temperature dependence.* Adv Exp Med Biol, 1977. **94**: p. 361-5.
142. Forsythe, J.A., et al., *Activation of vascular endothelial growth factor gene transcription by hypoxia-inducible factor 1.* Mol Cell Biol, 1996. **16**(9): p. 4604-13.
143. Levy, A.P., et al., *Transcriptional regulation of the rat vascular endothelial growth factor gene by hypoxia.* J Biol Chem, 1995. **270**(22): p. 13333-40.
144. Ishigami, S.I., et al., *Predictive value of vascular endothelial growth factor (VEGF) in metastasis and prognosis of human colorectal cancer.* Br J Cancer, 1998. **78**(10): p. 1379-84.
145. Kim, K.J., et al., *Inhibition of vascular endothelial growth factor-induced angiogenesis suppresses tumour growth in vivo.* Nature, 1993. **362**(6423): p. 841-4.

146. Hurwitz, H., et al., *Bevacizumab plus irinotecan, fluorouracil, and leucovorin for metastatic colorectal cancer.* N Engl J Med, 2004. **350**(23): p. 2335-42.
147. Saltz, L.B., et al., *Bevacizumab in combination with oxaliplatin-based chemotherapy as first-line therapy in metastatic colorectal cancer: a randomized phase III study.* J Clin Oncol, 2008. **26**(12): p. 2013-9.
148. Giantonio, B.J., et al., *Bevacizumab in combination with oxaliplatin, fluorouracil, and leucovorin (FOLFOX4) for previously treated metastatic colorectal cancer: results from the Eastern Cooperative Oncology Group Study E3200.* J Clin Oncol, 2007. **25**(12): p. 1539-44.
149. Lu, X. and Y. Kang, *Hypoxia and hypoxia-inducible factors: master regulators of metastasis.* Clin Cancer Res, 2010. **16**(24): p. 5928-35.
150. Yang, M.H., et al., *Direct regulation of TWIST by HIF-1alpha promotes metastasis.* Nat Cell Biol, 2008. **10**(3): p. 295-305.
151. Evans, A.J., et al., *VHL promotes E2 box-dependent E-cadherin transcription by HIF-mediated regulation of SIP1 and snail.* Mol Cell Biol, 2007. **27**(1): p. 157-69.
152. Krishnamachary, B., et al., *Hypoxia-inducible factor-1-dependent repression of E-cadherin in von Hippel-Lindau tumor suppressor-null renal cell carcinoma mediated by TCF3, ZFHX1A, and ZFHX1B.* Cancer Res, 2006. **66**(5): p. 2725-31.
153. Shyu, K.G., et al., *Hypoxia-inducible factor 1alpha regulates lung adenocarcinoma cell invasion.* Exp Cell Res, 2007. **313**(6): p. 1181-91.
154. Semenza, G.L., *Regulation of cancer cell metabolism by hypoxia-inducible factor 1.* Semin Cancer Biol, 2009. **19**(1): p. 12-6.
155. Kim, J.W., et al., *HIF-1-mediated expression of pyruvate dehydrogenase kinase: a metabolic switch required for cellular adaptation to hypoxia.* Cell Metab, 2006. **3**(3): p. 177-85.
156. Papandreou, I., et al., *HIF-1 mediates adaptation to hypoxia by actively downregulating mitochondrial oxygen consumption.* Cell Metab, 2006. **3**(3): p. 187-97.
157. Firth, J.D., B.L. Ebert, and P.J. Ratcliffe, *Hypoxic regulation of lactate dehydrogenase A. Interaction between hypoxia-inducible factor 1 and cAMP response elements.* J Biol Chem, 1995. **270**(36): p. 21021-7.
158. Chen, C., et al., *Regulation of glut1 mRNA by hypoxia-inducible factor-1. Interaction between H-ras and hypoxia.* J Biol Chem, 2001. **276**(12): p. 9519-25.
159. Esterman, A., et al., *The effect of hypoxia on human trophoblast in culture: morphology, glucose transport and metabolism.* Placenta, 1997. **18**(2-3): p. 129-36.
160. Hayashi, M., et al., *Induction of glucose transporter 1 expression through hypoxia-inducible factor 1alpha under hypoxic conditions in trophoblast-derived cells.* J Endocrinol, 2004. **183**(1): p. 145-54.
161. Baumann, M.U., S. Zamudio, and N.P. Illsley, *Hypoxic upregulation of glucose transporters in BeWo choriocarcinoma cells is mediated by hypoxia-inducible factor-1.* Am J Physiol Cell Physiol, 2007. **293**(1): p. C477-85.
162. Warburg, O., *On respiratory impairment in cancer cells.* Science, 1956. **124**(3215): p. 269-70.
163. Semenza, G.L., et al., *'The metabolism of tumours': 70 years later.* Novartis Found Symp, 2001. **240**: p. 251-60; discussion 260-4.
164. Rohren, E.M., T.G. Turkington, and R.E. Coleman, *Clinical applications of PET in oncology.* Radiology, 2004. **231**(2): p. 305-32.
165. Graeber, T.G., et al., *Hypoxia-mediated selection of cells with diminished apoptotic potential in solid tumours.* Nature, 1996. **379**(6560): p. 88-91.

166. Gatenby, R.A. and E.T. Gawlinski, *A reaction-diffusion model of cancer invasion.* Cancer Res, 1996. **56**(24): p. 5745-53.
167. Brown, J.M. and W.R. Wilson, *Exploiting tumour hypoxia in cancer treatment.* Nat Rev Cancer, 2004. **4**(6): p. 437-47.
168. Dikmen, Z.G., et al., *In vivo and in vitro effects of a HIF-1alpha inhibitor, RX-0047.* J Cell Biochem, 2008. **104**(3): p. 985-94.
169. Gillespie, D.L., et al., *Silencing of hypoxia inducible factor-1alpha by RNA interference attenuates human glioma cell growth in vivo.* Clin Cancer Res, 2007. **13**(8): p. 2441-8.
170. Welsh, S., et al., *Antitumor activity and pharmacodynamic properties of PX-478, an inhibitor of hypoxia-inducible factor-1alpha.* Mol Cancer Ther, 2004. **3**(3): p. 233-44.
171. Koh, M.Y., et al., *Molecular mechanisms for the activity of PX-478, an antitumor inhibitor of the hypoxia-inducible factor-1alpha.* Mol Cancer Ther, 2008. **7**(1): p. 90-100.
172. Sapra, P., et al., *Novel delivery of SN38 markedly inhibits tumor growth in xenografts, including a camptothecin-11-refractory model.* Clin Cancer Res, 2008. **14**(6): p. 1888-96.
173. Sapra, P., et al., *Potent and sustained inhibition of HIF-1alpha and downstream genes by a polyethyleneglycol-SN38 conjugate, EZN-2208, results in anti-angiogenic effects.* Angiogenesis, 2011. **14**(3): p. 245-53.
174. Baumgart, D.C. and S.R. Carding, *Inflammatory bowel disease: cause and immunobiology.* Lancet, 2007. **369**(9573): p. 1627-40.
175. Farmer, R.G., W.M. Michener, and E.A. Mortimer, *Studies of family history among patients with inflammatory bowel disease.* Clin Gastroenterol, 1980. **9**(2): p. 271-7.
176. Monsen, U., et al., *Prevalence of inflammatory bowel disease among relatives of patients with Crohn's disease.* Scand J Gastroenterol, 1991. **26**(3): p. 302-6.
177. Orholm, M., et al., *Familial occurrence of inflammatory bowel disease.* N Engl J Med, 1991. **324**(2): p. 84-8.
178. Peeters, M., et al., *Familial aggregation in Crohn's disease: increased age-adjusted risk and concordance in clinical characteristics.* Gastroenterology, 1996. **111**(3): p. 597-603.
179. Satsangi, J., et al., *Genetics of inflammatory bowel disease.* Gut, 1994. **35**(5): p. 696-700.
180. Orholm, M., et al., *Concordance of inflammatory bowel disease among Danish twins. Results of a nationwide study.* Scand J Gastroenterol, 2000. **35**(10): p. 1075-81.
181. Halfvarson, J., et al., *Inflammatory bowel disease in a Swedish twin cohort: a long-term follow-up of concordance and clinical characteristics.* Gastroenterology, 2003. **124**(7): p. 1767-73.
182. Thompson, N.P., et al., *Genetics versus environment in inflammatory bowel disease: results of a British twin study.* BMJ, 1996. **312**(7023): p. 95-6.
183. Hugot, J.P., et al., *Mapping of a susceptibility locus for Crohn's disease on chromosome 16.* Nature, 1996. **379**(6568): p. 821-3.
184. McGovern, D.P., et al., *NOD2 (CARD15), the first susceptibility gene for Crohn's disease.* Gut, 2001. **49**(6): p. 752-4.
185. Hugot, J.P., et al., *Association of NOD2 leucine-rich repeat variants with susceptibility to Crohn's disease.* Nature, 2001. **411**(6837): p. 599-603.
186. Ogura, Y., et al., *A frameshift mutation in NOD2 associated with susceptibility to Crohn's disease.* Nature, 2001. **411**(6837): p. 603-6.
187. Tanabe, T., et al., *Association analysis of the NOD2 gene with susceptibility to graft-versus-host disease in a Japanese population.* Int J Hematol, 2011. **93**(6): p. 771-8.
188. Pauleau, A.L. and P.J. Murray, *Role of nod2 in the response of macrophages to toll-like receptor agonists.* Mol Cell Biol, 2003. **23**(21): p. 7531-9.

189. Kobayashi, K.S., et al., *Nod2-dependent regulation of innate and adaptive immunity in the intestinal tract.* Science, 2005. **307**(5710): p. 731-4.
190. Yamazaki, K., et al., *Single nucleotide polymorphisms in TNFSF15 confer susceptibility to Crohn's disease.* Hum Mol Genet, 2005. **14**(22): p. 3499-506.
191. Hampe, J., et al., *A genome-wide association scan of nonsynonymous SNPs identifies a susceptibility variant for Crohn disease in ATG16L1.* Nat Genet, 2007. **39**(2): p. 207-11.
192. Parkes, M., et al., *Sequence variants in the autophagy gene IRGM and multiple other replicating loci contribute to Crohn's disease susceptibility.* Nat Genet, 2007. **39**(7): p. 830-2.
193. Kuballa, P., et al., *Impaired autophagy of an intracellular pathogen induced by a Crohn's disease associated ATG16L1 variant.* PLoS One, 2008. **3**(10): p. e3391.
194. McCarroll, S.A., et al., *Deletion polymorphism upstream of IRGM associated with altered IRGM expression and Crohn's disease.* Nat Genet, 2008. **40**(9): p. 1107-12.
195. Louis, E., et al., *Behaviour of Crohn's disease according to the Vienna classification: changing pattern over the course of the disease.* Gut, 2001. **49**(6): p. 777-82.
196. Munkholm, P., et al., *Disease activity courses in a regional cohort of Crohn's disease patients.* Scand J Gastroenterol, 1995. **30**(7): p. 699-706.
197. Rieder, F., et al., *Predictors of fibrostenotic Crohn's disease.* Inflamm Bowel Dis, 2011. **17**(9): p. 2000-7.
198. van der Valk, M.E., et al., *Crohn's disease patients treated with adalimumab benefit from co-treatment with immunomodulators.* Gut, 2012. **61**(2): p. 324-5.
199. Lewis, A., et al., *Intestinal Fibrosis in Crohn's Disease: Role of microRNAs as Fibrogenic Modulators, Serum Biomarkers, and Therapeutic Targets.* Inflamm Bowel Dis, 2015. **21**(5): p. 1141-50.
200. Regan, M.C., et al., *Stricture formation in Crohn's disease: the role of intestinal fibroblasts.* Ann Surg, 2000. **231**(1): p. 46-50.
201. Di Sabatino, A., et al., *Transforming growth factor beta signalling and matrix metalloproteinases in the mucosa overlying Crohn's disease strictures.* Gut, 2009. **58**(6): p. 777-89.
202. Beck, P.L. and D.K. Podolsky, *Growth factors in inflammatory bowel disease.* Inflamm Bowel Dis, 1999. **5**(1): p. 44-60.
203. Fiocchi, C., *TGF-beta/Smad signaling defects in inflammatory bowel disease: mechanisms and possible novel therapies for chronic inflammation.* J Clin Invest, 2001. **108**(4): p. 523-6.
204. Hahm, K.B., et al., *Loss of transforming growth factor beta signalling in the intestine contributes to tissue injury in inflammatory bowel disease.* Gut, 2001. **49**(2): p. 190-8.
205. Derynck, R. and Y.E. Zhang, *Smad-dependent and Smad-independent pathways in TGF-beta family signalling.* Nature, 2003. **425**(6958): p. 577-84.
206. Wotton, D. and J. Massague, *Smad transcriptional corepressors in TGF beta family signaling.* Curr Top Microbiol Immunol, 2001. **254**: p. 145-64.
207. Lutz, M. and P. Knaus, *Integration of the TGF-beta pathway into the cellular signalling network.* Cell Signal, 2002. **14**(12): p. 977-88.
208. Pinzani, M. and F. Marra, *Cytokine receptors and signaling in hepatic stellate cells.* Semin Liver Dis, 2001. **21**(3): p. 397-416.
209. Galera, P., et al., *Transforming growth factor-beta 1 (TGF-beta 1) up-regulation of collagen type II in primary cultures of rabbit articular chondrocytes (RAC) involves increased mRNA levels without affecting mRNA stability and procollagen processing.* J Cell Physiol, 1992. **153**(3): p. 596-606.

210. Kanzler, S., et al., *TGF-beta1 in liver fibrosis: an inducible transgenic mouse model to study liver fibrogenesis.* Am J Physiol, 1999. **276**(4 Pt 1): p. G1059-68.
211. Qi, W.N. and S.P. Scully, *Effect of type II collagen in chondrocyte response to TGF-beta 1 regulation.* Exp Cell Res, 1998. **241**(1): p. 142-50.
212. Dounchis, J.S., et al., *Chondrogenic phenotype of perichondrium-derived chondroprogenitor cells is influenced by transforming growth factor-beta 1.* J Orthop Res, 1997. **15**(6): p. 803-7.
213. Bertelli, R., et al., *Cell-specific regulation of alpha1(III) and alpha2(V) collagen by TGF-beta1 in tubulointerstitial cell models.* Nephrol Dial Transplant, 1998. **13**(3): p. 573-9.
214. Poncelet, A.C. and H.W. Schnaper, *Regulation of human mesangial cell collagen expression by transforming growth factor-beta1.* Am J Physiol, 1998. **275**(3 Pt 2): p. F458-66.
215. Silbiger, S., et al., *Estradiol reverses TGF-beta1-stimulated type IV collagen gene transcription in murine mesangial cells.* Am J Physiol, 1998. **274**(6 Pt 2): p. F1113-8.
216. Park, I.S., et al., *Expression of transforming growth factor-beta and type IV collagen in early streptozotocin-induced diabetes.* Diabetes, 1997. **46**(3): p. 473-80.
217. Jakowlew, S.B., et al., *Differential regulation of protease and extracellular matrix protein expression by transforming growth factor-beta 1 in non-small cell lung cancer cells and normal human bronchial epithelial cells.* Biochim Biophys Acta, 1997. **1353**(2): p. 157-70.
218. Rajagopal, S., et al., *Efficacy and specificity of antisense laminin chain-specific expression vectors in blocking laminin induction by TGFbeta1: effect of laminin blockade on TGFbeta1-mediated cellular responses.* J Cell Physiol, 1999. **178**(3): p. 296-303.
219. Virolle, T., et al., *Three activator protein-1-binding sites bound by the Fra-2.JunD complex cooperate for the regulation of murine laminin alpha3A (lama3A) promoter activity by transforming growth factor-beta.* J Biol Chem, 1998. **273**(28): p. 17318-25.
220. Kagami, S., et al., *Transforming growth factor-beta (TGF-beta) stimulates the expression of beta1 integrins and adhesion by rat mesangial cells.* Exp Cell Res, 1996. **229**(1): p. 1-6.
221. Kreisberg, J.I., et al., *High glucose and TGF beta 1 stimulate fibronectin gene expression through a cAMP response element.* Kidney Int, 1994. **46**(4): p. 1019-24.
222. Shlopov, B.V., et al., *Differential patterns of response to doxycycline and transforming growth factor beta1 in the down-regulation of collagenases in osteoarthritic and normal human chondrocytes.* Arthritis Rheum, 1999. **42**(4): p. 719-27.
223. Eickelberg, O., et al., *Extracellular matrix deposition by primary human lung fibroblasts in response to TGF-beta1 and TGF-beta3.* Am J Physiol, 1999. **276**(5 Pt 1): p. L814-24.
224. Uria, J.A., et al., *Differential effects of transforming growth factor-beta on the expression of collagenase-1 and collagenase-3 in human fibroblasts.* J Biol Chem, 1998. **273**(16): p. 9769-77.
225. Johansson, N., et al., *Collagenase 3 (matrix metalloproteinase 13) gene expression by HaCaT keratinocytes is enhanced by tumor necrosis factor alpha and transforming growth factor beta.* Cell Growth Differ, 1997. **8**(2): p. 243-50.
226. Rydziel, S., S. Varghese, and E. Canalis, *Transforming growth factor beta1 inhibits collagenase 3 expression by transcriptional and post-transcriptional mechanisms in osteoblast cultures.* J Cell Physiol, 1997. **170**(2): p. 145-52.
227. Edwards, D.R., et al., *Differential effects of transforming growth factor-beta 1 on the expression of matrix metalloproteinases and tissue inhibitors of metalloproteinases in young and old human fibroblasts.* Exp Gerontol, 1996. **31**(1-2): p. 207-23.

228. Basile, D.P., D.R. Martin, and M.R. Hammerman, *Extracellular matrix-related genes in kidney after ischemic injury: potential role for TGF-beta in repair.* Am J Physiol, 1998. **275**(6 Pt 2): p. F894-903.
229. Mozes, M.M., et al., *Renal expression of fibrotic matrix proteins and of transforming growth factor-beta (TGF-beta) isoforms in TGF-beta transgenic mice.* J Am Soc Nephrol, 1999. **10**(2): p. 271-80.
230. Su, S., et al., *Up-regulation of tissue inhibitor of metalloproteinases-3 gene expression by TGF-beta in articular chondrocytes is mediated by serine/threonine and tyrosine kinases.* J Cell Biochem, 1998. **70**(4): p. 517-27.
231. Mattila, L., et al., *Activation of tissue inhibitor of metalloproteinases-3 (TIMP-3) mRNA expression in scleroderma skin fibroblasts.* J Invest Dermatol, 1998. **110**(4): p. 416-21.
232. Su, S., F. Dehnade, and M. Zafarullah, *Regulation of tissue inhibitor of metalloproteinases-3 gene expression by transforming growth factor-beta and dexamethasone in bovine and human articular chondrocytes.* DNA Cell Biol, 1996. **15**(12): p. 1039-48.
233. Lee, R.C., R.L. Feinbaum, and V. Ambros, *The C. elegans heterochronic gene lin-4 encodes small RNAs with antisense complementarity to lin-14.* Cell, 1993. **75**(5): p. 843-54.
234. Wightman, B., et al., *Negative regulatory sequences in the lin-14 3'-untranslated region are necessary to generate a temporal switch during Caenorhabditis elegans development.* Genes Dev, 1991. **5**(10): p. 1813-24.
235. Lu, C., et al., *Elucidation of the small RNA component of the transcriptome.* Science, 2005. **309**(5740): p. 1567-9.
236. Mineno, J., et al., *The expression profile of microRNAs in mouse embryos.* Nucleic Acids Res, 2006. **34**(6): p. 1765-71.
237. Berezikov, E., et al., *Diversity of microRNAs in human and chimpanzee brain.* Nat Genet, 2006. **38**(12): p. 1375-7.
238. Calabrese, J.M., et al., *RNA sequence analysis defines Dicer's role in mouse embryonic stem cells.* Proc Natl Acad Sci U S A, 2007. **104**(46): p. 18097-102.
239. Babiarz, J.E., et al., *Mouse ES cells express endogenous shRNAs, siRNAs, and other Microprocessor-independent, Dicer-dependent small RNAs.* Genes Dev, 2008. **22**(20): p. 2773-85.
240. Kuchenbauer, F., et al., *In-depth characterization of the microRNA transcriptome in a leukemia progression model.* Genome Res, 2008. **18**(11): p. 1787-97.
241. Bushati, N. and S.M. Cohen, *microRNA functions.* Annu Rev Cell Dev Biol, 2007. **23**: p. 175-205.
242. Lee, Y., et al., *MicroRNA genes are transcribed by RNA polymerase II.* EMBO J, 2004. **23**(20): p. 4051-60.
243. Cai, X., C.H. Hagedorn, and B.R. Cullen, *Human microRNAs are processed from capped, polyadenylated transcripts that can also function as mRNAs.* RNA, 2004. **10**(12): p. 1957-66.
244. Tanzer, A. and P.F. Stadler, *Molecular evolution of a microRNA cluster.* J Mol Biol, 2004. **339**(2): p. 327-35.
245. Lagos-Quintana, M., et al., *Identification of novel genes coding for small expressed RNAs.* Science, 2001. **294**(5543): p. 853-8.
246. Bentwich, I., et al., *Identification of hundreds of conserved and nonconserved human microRNAs.* Nat Genet, 2005. **37**(7): p. 766-70.

247. Bortolin-Cavaille, M.L., et al., *C19MC microRNAs are processed from introns of large Pol-II, non-protein-coding transcripts.* Nucleic Acids Res, 2009. **37**(10): p. 3464-73.
248. Seitz, H., et al., *A large imprinted microRNA gene cluster at the mouse Dlk1-Gtl2 domain.* Genome Res, 2004. **14**(9): p. 1741-8.
249. Han, J., et al., *Molecular basis for the recognition of primary microRNAs by the Drosha-DGCR8 complex.* Cell, 2006. **125**(5): p. 887-901.
250. Han, J., et al., *The Drosha-DGCR8 complex in primary microRNA processing.* Genes Dev, 2004. **18**(24): p. 3016-27.
251. Yi, R., et al., *Exportin-5 mediates the nuclear export of pre-microRNAs and short hairpin RNAs.* Genes Dev, 2003. **17**(24): p. 3011-6.
252. Stark, A., et al., *Systematic discovery and characterization of fly microRNAs using 12 Drosophila genomes.* Genome Res, 2007. **17**(12): p. 1865-79.
253. Kuchenbauer, F., et al., *Comprehensive analysis of mammalian miRNA* species and their role in myeloid cells.* Blood, 2011. **118**(12): p. 3350-8.
254. Yang, J.S., et al., *Widespread regulatory activity of vertebrate microRNA* species.* RNA, 2011. **17**(2): p. 312-26.
255. Di Leva, G., M. Garofalo, and C.M. Croce, *MicroRNAs in cancer.* Annu Rev Pathol, 2014. **9**: p. 287-314.
256. Bartel, D.P., *MicroRNAs: target recognition and regulatory functions.* Cell, 2009. **136**(2): p. 215-33.
257. Lai, E.C., *Micro RNAs are complementary to 3' UTR sequence motifs that mediate negative post-transcriptional regulation.* Nat Genet, 2002. **30**(4): p. 363-4.
258. Lewis, B.P., et al., *Prediction of mammalian microRNA targets.* Cell, 2003. **115**(7): p. 787-98.
259. Jones-Rhoades, M.W., D.P. Bartel, and B. Bartel, *MicroRNAS and their regulatory roles in plants.* Annu Rev Plant Biol, 2006. **57**: p. 19-53.
260. Baumberger, N. and D.C. Baulcombe, *Arabidopsis ARGONAUTE1 is an RNA Slicer that selectively recruits microRNAs and short interfering RNAs.* Proc Natl Acad Sci U S A, 2005. **102**(33): p. 11928-33.
261. Llave, C., et al., *Cleavage of Scarecrow-like mRNA targets directed by a class of Arabidopsis miRNA.* Science, 2002. **297**(5589): p. 2053-6.
262. Fabian, M.R., N. Sonenberg, and W. Filipowicz, *Regulation of mRNA translation and stability by microRNAs.* Annu Rev Biochem, 2010. **79**: p. 351-79.
263. Guo, H., et al., *Mammalian microRNAs predominantly act to decrease target mRNA levels.* Nature, 2010. **466**(7308): p. 835-40.
264. Larsson O, N.R., *Re-analysis of genome wide data on mammalian microRNA-mediated suppression of gene expression.* Translation, 2013. **1**(e24557).
265. Mathonnet, G., et al., *MicroRNA inhibition of translation initiation in vitro by targeting the cap-binding complex eIF4F.* Science, 2007. **317**(5845): p. 1764-7.
266. Djuranovic, S., A. Nahvi, and R. Green, *miRNA-mediated gene silencing by translational repression followed by mRNA deadenylation and decay.* Science, 2012. **336**(6078): p. 237-40.
267. Bazzini, A.A., M.T. Lee, and A.J. Giraldez, *Ribosome profiling shows that miR-430 reduces translation before causing mRNA decay in zebrafish.* Science, 2012. **336**(6078): p. 233-7.
268. Meijer, H.A., et al., *Translational repression and eIF4A2 activity are critical for microRNA-mediated gene regulation.* Science, 2013. **340**(6128): p. 82-5.

269. Pillai, R.S., et al., *Inhibition of translational initiation by Let-7 MicroRNA in human cells.* Science, 2005. **309**(5740): p. 1573-6.
270. Thermann, R. and M.W. Hentze, *Drosophila miR2 induces pseudo-polysomes and inhibits translation initiation.* Nature, 2007. **447**(7146): p. 875-8.
271. Iwasaki, S., T. Kawamata, and Y. Tomari, *Drosophila argonaute1 and argonaute2 employ distinct mechanisms for translational repression.* Mol Cell, 2009. **34**(1): p. 58-67.
272. Humphreys, D.T., et al., *MicroRNAs control translation initiation by inhibiting eukaryotic initiation factor 4E/cap and poly(A) tail function.* Proc Natl Acad Sci U S A, 2005. **102**(47): p. 16961-6.
273. Wakiyama, M., et al., *Let-7 microRNA-mediated mRNA deadenylation and translational repression in a mammalian cell-free system.* Genes Dev, 2007. **21**(15): p. 1857-62.
274. Li, L.C., et al., *Small dsRNAs induce transcriptional activation in human cells.* Proc Natl Acad Sci U S A, 2006. **103**(46): p. 17337-42.
275. Vasudevan, S., Y. Tong, and J.A. Steitz, *Switching from repression to activation: microRNAs can up-regulate translation.* Science, 2007. **318**(5858): p. 1931-4.
276. Calin, G.A., et al., *Frequent deletions and down-regulation of micro- RNA genes miR15 and miR16 at 13q14 in chronic lymphocytic leukemia.* Proc Natl Acad Sci U S A, 2002. **99**(24): p. 15524-9.
277. Luo, X., et al., *MicroRNA signatures: novel biomarker for colorectal cancer?* Cancer Epidemiol Biomarkers Prev, 2011. **20**(7): p. 1272-86.
278. Cheng, C.J. and F.J. Slack, *The duality of oncomiR addiction in the maintenance and treatment of cancer.* Cancer J, 2012. **18**(3): p. 232-7.
279. Lu, J., et al., *MicroRNA expression profiles classify human cancers.* Nature, 2005. **435**(7043): p. 834-8.
280. Necela, B.M., et al., *Differential expression of microRNAs in tumors from chronically inflamed or genetic (APC(Min/+)) models of colon cancer.* PLoS One, 2011. **6**(4): p. e18501.
281. Nagel, R., et al., *Regulation of the adenomatous polyposis coli gene by the miR-135 family in colorectal cancer.* Cancer Res, 2008. **68**(14): p. 5795-802.
282. Gaedcke, J., et al., *The rectal cancer microRNAome--microRNA expression in rectal cancer and matched normal mucosa.* Clin Cancer Res, 2012. **18**(18): p. 4919-30.
283. Xu, X.M., et al., *Expression of miR-21, miR-31, miR-96 and miR-135b is correlated with the clinical parameters of colorectal cancer.* Oncol Lett, 2012. **4**(2): p. 339-345.
284. Faltejskova, P., et al., *Identification and functional screening of microRNAs highly deregulated in colorectal cancer.* J Cell Mol Med, 2012. **16**(11): p. 2655-66.
285. Valeri, N., et al., *MicroRNA-135b promotes cancer progression by acting as a downstream effector of oncogenic pathways in colon cancer.* Cancer Cell, 2014. **25**(4): p. 469-83.
286. Schetter, A.J., et al., *MicroRNA expression profiles associated with prognosis and therapeutic outcome in colon adenocarcinoma.* JAMA, 2008. **299**(4): p. 425-36.
287. Slaby, O., et al., *Altered expression of miR-21, miR-31, miR-143 and miR-145 is related to clinicopathologic features of colorectal cancer.* Oncology, 2007. **72**(5-6): p. 397-402.
288. Medina, P.P., M. Nolde, and F.J. Slack, *OncomiR addiction in an in vivo model of microRNA-21-induced pre-B-cell lymphoma.* Nature, 2010. **467**(7311): p. 86-90.
289. Hatley, M.E., et al., *Modulation of K-Ras-dependent lung tumorigenesis by MicroRNA-21.* Cancer Cell, 2010. **18**(3): p. 282-93.
290. Lu, Z., et al., *MicroRNA-21 promotes cell transformation by targeting the programmed cell death 4 gene.* Oncogene, 2008. **27**(31): p. 4373-9.

291. Wickramasinghe, N.S., et al., *Estradiol downregulates miR-21 expression and increases miR-21 target gene expression in MCF-7 breast cancer cells.* Nucleic Acids Res, 2009. **37**(8): p. 2584-95.
292. Shi, L., et al., *MiR-21 protected human glioblastoma U87MG cells from chemotherapeutic drug temozolomide induced apoptosis by decreasing Bax/Bcl-2 ratio and caspase-3 activity.* Brain Res, 2010. **1352**: p. 255-64.
293. Sayed, D., et al., *MicroRNA-21 is a downstream effector of AKT that mediates its antiapoptotic effects via suppression of Fas ligand.* J Biol Chem, 2010. **285**(26): p. 20281-90.
294. Wang, P., et al., *microRNA-21 negatively regulates Cdc25A and cell cycle progression in colon cancer cells.* Cancer Res, 2009. **69**(20): p. 8157-65.
295. Roush, S. and F.J. Slack, *The let-7 family of microRNAs.* Trends Cell Biol, 2008. **18**(10): p. 505-16.
296. Johnson, S.M., et al., *RAS is regulated by the let-7 microRNA family.* Cell, 2005. **120**(5): p. 635-47.
297. Motoyama, K., et al., *Clinical significance of high mobility group A2 in human gastric cancer and its relationship to let-7 microRNA family.* Clin Cancer Res, 2008. **14**(8): p. 2334-40.
298. Nam, E.J., et al., *MicroRNA expression profiles in serous ovarian carcinoma.* Clin Cancer Res, 2008. **14**(9): p. 2690-5.
299. Akao, Y., Y. Nakagawa, and T. Naoe, *let-7 microRNA functions as a potential growth suppressor in human colon cancer cells.* Biol Pharm Bull, 2006. **29**(5): p. 903-6.
300. Sampson, V.B., et al., *MicroRNA let-7a down-regulates MYC and reverts MYC-induced growth in Burkitt lymphoma cells.* Cancer Res, 2007. **67**(20): p. 9762-70.
301. Vickers, M.M., et al., *Stage-dependent differential expression of microRNAs in colorectal cancer: potential role as markers of metastatic disease.* Clin Exp Metastasis, 2012. **29**(2): p. 123-32.
302. Ruzzo, A., et al., *High let-7a microRNA levels in KRAS-mutated colorectal carcinomas may rescue anti-EGFR therapy effects in patients with chemotherapy-refractory metastatic disease.* Oncologist, 2012. **17**(6): p. 823-9.
303. Michael, M.Z., et al., *Reduced accumulation of specific microRNAs in colorectal neoplasia.* Mol Cancer Res, 2003. **1**(12): p. 882-91.
304. Akao, Y., et al., *Role of anti-oncomirs miR-143 and -145 in human colorectal tumors.* Cancer Gene Ther, 2010. **17**(6): p. 398-408.
305. Suzuki, H.I., et al., *Modulation of microRNA processing by p53.* Nature, 2009. **460**(7254): p. 529-33.
306. Sachdeva, M., et al., *p53 represses c-Myc through induction of the tumor suppressor miR-145.* Proc Natl Acad Sci U S A, 2009. **106**(9): p. 3207-12.
307. Chen, X., et al., *Role of miR-143 targeting KRAS in colorectal tumorigenesis.* Oncogene, 2009. **28**(10): p. 1385-92.
308. Ng, E.K., et al., *MicroRNA-143 targets DNA methyltransferases 3A in colorectal cancer.* Br J Cancer, 2009. **101**(4): p. 699-706.
309. Akao, Y., Y. Nakagawa, and T. Naoe, *MicroRNA-143 and -145 in colon cancer.* DNA Cell Biol, 2007. **26**(5): p. 311-20.
310. Shi, B., et al., *Micro RNA 145 targets the insulin receptor substrate-1 and inhibits the growth of colon cancer cells.* J Biol Chem, 2007. **282**(45): p. 32582-90.
311. Raver-Shapira, N., et al., *Transcriptional activation of miR-34a contributes to p53-mediated apoptosis.* Mol Cell, 2007. **26**(5): p. 731-43.

312. Okada, N., et al., *A positive feedback between p53 and miR-34 miRNAs mediates tumor suppression.* Genes Dev, 2014. **28**(5): p. 438-50.
313. Corney, D.C., et al., *MicroRNA-34b and MicroRNA-34c are targets of p53 and cooperate in control of cell proliferation and adhesion-independent growth.* Cancer Res, 2007. **67**(18): p. 8433-8.
314. Christoffersen, N.R., et al., *p53-independent upregulation of miR-34a during oncogene-induced senescence represses MYC.* Cell Death Differ, 2010. **17**(2): p. 236-45.
315. Chang, T.C., et al., *Transactivation of miR-34a by p53 broadly influences gene expression and promotes apoptosis.* Mol Cell, 2007. **26**(5): p. 745-52.
316. Bommer, G.T., et al., *p53-mediated activation of miRNA34 candidate tumor-suppressor genes.* Curr Biol, 2007. **17**(15): p. 1298-307.
317. Tazawa, H., et al., *Tumor-suppressive miR-34a induces senescence-like growth arrest through modulation of the E2F pathway in human colon cancer cells.* Proc Natl Acad Sci U S A, 2007. **104**(39): p. 15472-7.
318. Roy, S., et al., *Expression of miR-34 is lost in colon cancer which can be re-expressed by a novel agent CDF.* J Hematol Oncol, 2012. **5**: p. 58.
319. Vogt, M., et al., *Frequent concomitant inactivation of miR-34a and miR-34b/c by CpG methylation in colorectal, pancreatic, mammary, ovarian, urothelial, and renal cell carcinomas and soft tissue sarcomas.* Virchows Arch, 2011. **458**(3): p. 313-22.
320. Migliore, C., et al., *MicroRNAs impair MET-mediated invasive growth.* Cancer Res, 2008. **68**(24): p. 10128-36.
321. Yamakuchi, M. and C.J. Lowenstein, *MiR-34, SIRT1 and p53: the feedback loop.* Cell Cycle, 2009. **8**(5): p. 712-5.
322. Rokavec, M., et al., *IL-6R/STAT3/miR-34a feedback loop promotes EMT-mediated colorectal cancer invasion and metastasis.* J Clin Invest, 2014. **124**(4): p. 1853-67.
323. Kulshreshtha, R., et al., *A microRNA signature of hypoxia.* Mol Cell Biol, 2007. **27**(5): p. 1859-67.
324. Hua, Z., et al., *MiRNA-directed regulation of VEGF and other angiogenic factors under hypoxia.* PLoS One, 2006. **1**: p. e116.
325. Camps, C., et al., *hsa-miR-210 Is induced by hypoxia and is an independent prognostic factor in breast cancer.* Clin Cancer Res, 2008. **14**(5): p. 1340-8.
326. Giannakakis, A., et al., *miR-210 links hypoxia with cell cycle regulation and is deleted in human epithelial ovarian cancer.* Cancer Biol Ther, 2008. **7**(2): p. 255-64.
327. Fasanaro, P., et al., *MicroRNA-210 modulates endothelial cell response to hypoxia and inhibits the receptor tyrosine kinase ligand Ephrin-A3.* J Biol Chem, 2008. **283**(23): p. 15878-83.
328. Pulkkinen, K., et al., *Hypoxia induces microRNA miR-210 in vitro and in vivo ephrin-A3 and neuronal pentraxin 1 are potentially regulated by miR-210.* FEBS Lett, 2008. **582**(16): p. 2397-401.
329. Huang, X., et al., *Hypoxia-inducible mir-210 regulates normoxic gene expression involved in tumor initiation.* Mol Cell, 2009. **35**(6): p. 856-67.
330. Kelly, T.J., et al., *A hypoxia-induced positive feedback loop promotes hypoxia-inducible factor 1alpha stability through miR-210 suppression of glycerol-3-phosphate dehydrogenase 1-like.* Mol Cell Biol, 2011. **31**(13): p. 2696-706.
331. Nakada, C., et al., *Overexpression of miR-210, a downstream target of HIF1alpha, causes centrosome amplification in renal carcinoma cells.* J Pathol, 2011. **224**(2): p. 280-8.
332. Zhang, Z., et al., *MicroRNA miR-210 modulates cellular response to hypoxia through the MYC antagonist MNT.* Cell Cycle, 2009. **8**(17): p. 2756-68.

333. Kim, J.H., et al., *Reactive oxygen species-responsive miR-210 regulates proliferation and migration of adipose-derived stem cells via PTPN2.* Cell Death Dis, 2013. **4**: p. e588.
334. Alaiti, M.A., et al., *Up-regulation of miR-210 by vascular endothelial growth factor in ex vivo expanded CD34+ cells enhances cell-mediated angiogenesis.* J Cell Mol Med, 2012. **16**(10): p. 2413-21.
335. Liu, F., et al., *Upregulation of microRNA-210 regulates renal angiogenesis mediated by activation of VEGF signaling pathway under ischemia/perfusion injury in vivo and in vitro.* Kidney Blood Press Res, 2012. **35**(3): p. 182-91.
336. Lou, Y.L., et al., *miR-210 activates notch signaling pathway in angiogenesis induced by cerebral ischemia.* Mol Cell Biochem, 2012. **370**(1-2): p. 45-51.
337. Zeng, L., et al., *MicroRNA-210 overexpression induces angiogenesis and neurogenesis in the normal adult mouse brain.* Gene Ther, 2014. **21**(1): p. 37-43.
338. Colleoni, F., et al., *Suppression of mitochondrial electron transport chain function in the hypoxic human placenta: a role for miRNA-210 and protein synthesis inhibition.* PLoS One, 2013. **8**(1): p. e55194.
339. Chan, S.Y., et al., *MicroRNA-210 controls mitochondrial metabolism during hypoxia by repressing the iron-sulfur cluster assembly proteins ISCU1/2.* Cell Metab, 2009. **10**(4): p. 273-84.
340. Chen, Z., et al., *Hypoxia-regulated microRNA-210 modulates mitochondrial function and decreases ISCU and COX10 expression.* Oncogene, 2010. **29**(30): p. 4362-8.
341. Favaro, E., et al., *MicroRNA-210 regulates mitochondrial free radical response to hypoxia and krebs cycle in cancer cells by targeting iron sulfur cluster protein ISCU.* PLoS One, 2010. **5**(4): p. e10345.
342. McCormick, R.I., et al., *miR-210 is a target of hypoxia-inducible factors 1 and 2 in renal cancer, regulates ISCU and correlates with good prognosis.* Br J Cancer, 2013. **108**(5): p. 1133-42.
343. Qin, Q., W. Furong, and L. Baosheng, *Multiple functions of hypoxia-regulated miR-210 in cancer.* J Exp Clin Cancer Res, 2014. **33**: p. 50.
344. Gou, D., et al., *miR-210 has an antiapoptotic effect in pulmonary artery smooth muscle cells during hypoxia.* Am J Physiol Lung Cell Mol Physiol, 2012. **303**(8): p. L682-91.
345. Tsuchiya, S., et al., *MicroRNA-210 regulates cancer cell proliferation through targeting fibroblast growth factor receptor-like 1 (FGFRL1).* J Biol Chem, 2011. **286**(1): p. 420-8.
346. Schmaltz, C., et al., *Regulation of proliferation-survival decisions during tumor cell hypoxia.* Mol Cell Biol, 1998. **18**(5): p. 2845-54.
347. Radojicic, J., et al., *MicroRNA expression analysis in triple-negative (ER, PR and Her2/neu) breast cancer.* Cell Cycle, 2011. **10**(3): p. 507-17.
348. Toyama, T., et al., *High expression of microRNA-210 is an independent factor indicating a poor prognosis in Japanese triple-negative breast cancer patients.* Jpn J Clin Oncol, 2012. **42**(4): p. 256-63.
349. Rothe, F., et al., *Global microRNA expression profiling identifies MiR-210 associated with tumor proliferation, invasion and poor clinical outcome in breast cancer.* PLoS One, 2011. **6**(6): p. e20980.
350. Gee, H.E., et al., *hsa-mir-210 is a marker of tumor hypoxia and a prognostic factor in head and neck cancer.* Cancer, 2010. **116**(9): p. 2148-58.
351. Scapoli, L., et al., *MicroRNA expression profiling of oral carcinoma identifies new markers of tumor progression.* Int J Immunopathol Pharmacol, 2010. **23**(4): p. 1229-34.
352. Wang, J., et al., *MicroRNAs in plasma of pancreatic ductal adenocarcinoma patients as novel blood-based biomarkers of disease.* Cancer Prev Res (Phila), 2009. **2**(9): p. 807-13.

353. Greither, T., et al., *Elevated expression of microRNAs 155, 203, 210 and 222 in pancreatic tumors is associated with poorer survival.* Int J Cancer, 2010. **126**(1): p. 73-80.
354. Papaconstantinou, I.G., et al., *Expression of microRNAs in patients with pancreatic cancer and its prognostic significance.* Pancreas, 2013. **42**(1): p. 67-71.
355. Miko, E., et al., *Differentially expressed microRNAs in small cell lung cancer.* Exp Lung Res, 2009. **35**(8): p. 646-64.
356. Puissegur, M.P., et al., *miR-210 is overexpressed in late stages of lung cancer and mediates mitochondrial alterations associated with modulation of HIF-1 activity.* Cell Death Differ, 2011. **18**(3): p. 465-78.
357. Eilertsen, M., et al., *Positive prognostic impact of miR-210 in non-small cell lung cancer.* Lung Cancer, 2014. **83**(2): p. 272-8.
358. Neal, C.S., et al., *The VHL-dependent regulation of microRNAs in renal cancer.* BMC Med, 2010. **8**: p. 64.
359. Redova, M., et al., *MiR-210 expression in tumor tissue and in vitro effects of its silencing in renal cell carcinoma.* Tumour Biol, 2013. **34**(1): p. 481-91.
360. Vaksman, O., et al., *miRNA profiling along tumour progression in ovarian carcinoma.* J Cell Mol Med, 2011. **15**(7): p. 1593-602.
361. Wu, F., et al., *Identification of microRNAs associated with ileal and colonic Crohn's disease.* Inflamm Bowel Dis, 2010. **16**(10): p. 1729-38.
362. Fasseu, M., et al., *Identification of restricted subsets of mature microRNA abnormally expressed in inactive colonic mucosa of patients with inflammatory bowel disease.* PLoS One, 2010. **5**(10).
363. Rastaldi, M.P., *Epithelial-mesenchymal transition and its implications for the development of renal tubulointerstitial fibrosis.* J Nephrol, 2006. **19**(4): p. 407-12.
364. Zeisberg, M. and J.S. Duffield, *Resolved: EMT produces fibroblasts in the kidney.* J Am Soc Nephrol, 2010. **21**(8): p. 1247-53.
365. Carew, R.M., B. Wang, and P. Kantharidis, *The role of EMT in renal fibrosis.* Cell Tissue Res, 2012. **347**(1): p. 103-16.
366. Zeisberg, E.M., et al., *Endothelial-to-mesenchymal transition contributes to cardiac fibrosis.* Nat Med, 2007. **13**(8): p. 952-61.
367. Kim, T., et al., *p53 regulates epithelial-mesenchymal transition through microRNAs targeting ZEB1 and ZEB2.* J Exp Med, 2011. **208**(5): p. 875-83.
368. Zeisberg, M., et al., *Fibroblasts derive from hepatocytes in liver fibrosis via epithelial to mesenchymal transition.* J Biol Chem, 2007. **282**(32): p. 23337-47.
369. Flier, S.N., et al., *Identification of epithelial to mesenchymal transition as a novel source of fibroblasts in intestinal fibrosis.* J Biol Chem, 2010. **285**(26): p. 20202-12.
370. Park, S.M., et al., *The miR-200 family determines the epithelial phenotype of cancer cells by targeting the E-cadherin repressors ZEB1 and ZEB2.* Genes Dev, 2008. **22**(7): p. 894-907.
371. Gregory, P.A., et al., *The miR-200 family and miR-205 regulate epithelial to mesenchymal transition by targeting ZEB1 and SIP1.* Nat Cell Biol, 2008. **10**(5): p. 593-601.
372. Qin, W., et al., *TGF-beta/Smad3 signaling promotes renal fibrosis by inhibiting miR-29.* J Am Soc Nephrol, 2011. **22**(8): p. 1462-74.
373. Chung, A.C., et al., *Smad7 suppresses renal fibrosis via altering expression of TGF-beta/Smad3-regulated microRNAs.* Mol Ther, 2013. **21**(2): p. 388-98.

374. Roderburg, C., et al., *Micro-RNA profiling reveals a role for miR-29 in human and murine liver fibrosis.* Hepatology, 2011. **53**(1): p. 209-18.
375. van Rooij, E., et al., *Dysregulation of microRNAs after myocardial infarction reveals a role of miR-29 in cardiac fibrosis.* Proc Natl Acad Sci U S A, 2008. **105**(35): p. 13027-32.
376. Pandit, K.V., J. Milosevic, and N. Kaminski, *MicroRNAs in idiopathic pulmonary fibrosis.* Transl Res, 2011. **157**(4): p. 191-9.
377. Cushing, L., et al., *miR-29 is a major regulator of genes associated with pulmonary fibrosis.* Am J Respir Cell Mol Biol, 2011. **45**(2): p. 287-94.
378. Maurer, B., et al., *MicroRNA-29, a key regulator of collagen expression in systemic sclerosis.* Arthritis Rheum, 2010. **62**(6): p. 1733-43.
379. Luna, C., et al., *Role of miR-29b on the regulation of the extracellular matrix in human trabecular meshwork cells under chronic oxidative stress.* Mol Vis, 2009. **15**: p. 2488-97.
380. Cacchiarelli, D., et al., *MicroRNAs involved in molecular circuitries relevant for the Duchenne muscular dystrophy pathogenesis are controlled by the dystrophin/nNOS pathway.* Cell Metab, 2010. **12**(4): p. 341-51.
381. Nguyen-Tran, D.H., et al., *Molecular mechanism of sphingosine-1-phosphate action in Duchenne muscular dystrophy.* Dis Model Mech, 2014. **7**(1): p. 41-54.
382. Mannaerts, I., et al., *Class II HDAC inhibition hampers hepatic stellate cell activation by induction of microRNA-29.* PLoS One, 2013. **8**(1): p. e55786.
383. Katare, R., et al., *Transplantation of human pericyte progenitor cells improves the repair of infarcted heart through activation of an angiogenic program involving micro-RNA-132.* Circ Res, 2011. **109**(8): p. 894-906.
384. Mann, J., et al., *MeCP2 controls an epigenetic pathway that promotes myofibroblast transdifferentiation and fibrosis.* Gastroenterology, 2010. **138**(2): p. 705-14, 714 e1-4.
385. Guo, C.J., et al., *miR-15b and miR-16 are implicated in activation of the rat hepatic stellate cell: An essential role for apoptosis.* J Hepatol, 2009. **50**(4): p. 766-78.
386. Ezzie, M.E., et al., *Gene expression networks in COPD: microRNA and mRNA regulation.* Thorax, 2012. **67**(2): p. 122-31.
387. Pogribny, I.P., et al., *Difference in expression of hepatic microRNAs miR-29c, miR-34a, miR-155, and miR-200b is associated with strain-specific susceptibility to dietary nonalcoholic steatohepatitis in mice.* Lab Invest, 2010. **90**(10): p. 1437-46.
388. Pottier, N., et al., *Identification of keratinocyte growth factor as a target of microRNA-155 in lung fibroblasts: implication in epithelial-mesenchymal interactions.* PLoS One, 2009. **4**(8): p. e6718.
389. Kodama, T., et al., *Increases in p53 expression induce CTGF synthesis by mouse and human hepatocytes and result in liver fibrosis in mice.* J Clin Invest, 2011. **121**(8): p. 3343-56.
390. Pandit, K.V., et al., *Inhibition and role of let-7d in idiopathic pulmonary fibrosis.* Am J Respir Crit Care Med, 2010. **182**(2): p. 220-9.
391. van Almen, G.C., et al., *MicroRNA-18 and microRNA-19 regulate CTGF and TSP-1 expression in age-related heart failure.* Aging Cell, 2011. **10**(5): p. 769-79.
392. da Costa Martins, P.A., et al., *MicroRNA-199b targets the nuclear kinase Dyrk1a in an auto-amplification loop promoting calcineurin/NFAT signalling.* Nat Cell Biol, 2010. **12**(12): p. 1220-7.
393. Murakami, Y., et al., *The progression of liver fibrosis is related with overexpression of the miR-199 and 200 families.* PLoS One, 2011. **6**(1): p. e16081.

394. Oba, S., et al., *miR-200b precursor can ameliorate renal tubulointerstitial fibrosis.* PLoS One, 2010. **5**(10): p. e13614.
395. Wang, B., et al., *miR-200a Prevents renal fibrogenesis through repression of TGF-beta2 expression.* Diabetes, 2011. **60**(1): p. 280-7.
396. Liu, G., et al., *miR-21 mediates fibrogenic activation of pulmonary fibroblasts and lung fibrosis.* J Exp Med, 2010. **207**(8): p. 1589-97.
397. Thum, T., et al., *MicroRNA-21 contributes to myocardial disease by stimulating MAP kinase signalling in fibroblasts.* Nature, 2008. **456**(7224): p. 980-4.
398. Zhong, X., et al., *Smad3-mediated upregulation of miR-21 promotes renal fibrosis.* J Am Soc Nephrol, 2011. **22**(9): p. 1668-81.
399. Mitchell, P.S., et al., *Circulating microRNAs as stable blood-based markers for cancer detection.* Proc Natl Acad Sci U S A, 2008. **105**(30): p. 10513-8.
400. Schwarzenbach, H., D.S. Hoon, and K. Pantel, *Cell-free nucleic acids as biomarkers in cancer patients.* Nat Rev Cancer, 2011. **11**(6): p. 426-37.
401. Hanke, M., et al., *A robust methodology to study urine microRNA as tumor marker: microRNA-126 and microRNA-182 are related to urinary bladder cancer.* Urol Oncol, 2010. **28**(6): p. 655-61.
402. Ahmed, F.E., et al., *Diagnostic microRNA markers for screening sporadic human colon cancer and active ulcerative colitis in stool and tissue.* Cancer Genomics Proteomics, 2009. **6**(5): p. 281-95.
403. Volinia, S., et al., *A microRNA expression signature of human solid tumors defines cancer gene targets.* Proc Natl Acad Sci U S A, 2006. **103**(7): p. 2257-61.
404. Imperiale, T.F., et al., *Fecal DNA versus fecal occult blood for colorectal-cancer screening in an average-risk population.* N Engl J Med, 2004. **351**(26): p. 2704-14.
405. Lieberman, D.A., D.G. Weiss, and G. Veterans Affairs Cooperative Study, *One-time screening for colorectal cancer with combined fecal occult-blood testing and examination of the distal colon.* N Engl J Med, 2001. **345**(8): p. 555-60.
406. Kanaoka, S., et al., *Potential usefulness of detecting cyclooxygenase 2 messenger RNA in feces for colorectal cancer screening.* Gastroenterology, 2004. **127**(2): p. 422-7.
407. Takai, T., et al., *Fecal cyclooxygenase 2 plus matrix metalloproteinase 7 mRNA assays as a marker for colorectal cancer screening.* Cancer Epidemiol Biomarkers Prev, 2009. **18**(6): p. 1888-93.
408. Li, J.M., et al., *Down-regulation of fecal miR-143 and miR-145 as potential markers for colorectal cancer.* Saudi Med J, 2012. **33**(1): p. 24-9.
409. Aslam, M.I., et al., *MicroRNAs are novel biomarkers of colorectal cancer.* Br J Surg, 2009. **96**(7): p. 702-10.
410. Wu, C.W., et al., *Detection of miR-92a and miR-21 in stool samples as potential screening biomarkers for colorectal cancer and polyps.* Gut, 2012. **61**(5): p. 739-45.
411. Link, A., et al., *Fecal MicroRNAs as novel biomarkers for colon cancer screening.* Cancer Epidemiol Biomarkers Prev, 2010. **19**(7): p. 1766-74.
412. Wu, C.W., et al., *Identification of microRNA-135b in stool as a potential noninvasive biomarker for colorectal cancer and adenoma.* Clin Cancer Res, 2014. **20**(11): p. 2994-3002.
413. Ng, E.K., et al., *Differential expression of microRNAs in plasma of patients with colorectal cancer: a potential marker for colorectal cancer screening.* Gut, 2009. **58**(10): p. 1375-81.
414. Huang, Z., et al., *Plasma microRNAs are promising novel biomarkers for early detection of colorectal cancer.* Int J Cancer, 2010. **127**(1): p. 118-26.

415. Dillhoff, M., et al., *MicroRNA-21 is overexpressed in pancreatic cancer and a potential predictor of survival.* J Gastrointest Surg, 2008. **12**(12): p. 2171-6.
416. Kulda, V., et al., *Relevance of miR-21 and miR-143 expression in tissue samples of colorectal carcinoma and its liver metastases.* Cancer Genet Cytogenet, 2010. **200**(2): p. 154-60.
417. Nakajima, G., et al., *Non-coding MicroRNAs hsa-let-7g and hsa-miR-181b are Associated with Chemoresponse to S-1 in Colon Cancer.* Cancer Genomics Proteomics, 2006. **3**(5): p. 317-324.
418. Svoboda, M., et al., *Micro-RNAs miR125b and miR137 are frequently upregulated in response to capecitabine chemoradiotherapy of rectal cancer.* Int J Oncol, 2008. **33**(3): p. 541-7.
419. Della Vittoria Scarpati, G., et al., *A specific miRNA signature correlates with complete pathological response to neoadjuvant chemoradiotherapy in locally advanced rectal cancer.* Int J Radiat Oncol Biol Phys, 2012. **83**(4): p. 1113-9.
420. Kheirelseid, E.A., et al., *miRNA expressions in rectal cancer as predictors of response to neoadjuvant chemoradiation therapy.* Int J Colorectal Dis, 2013. **28**(2): p. 247-60.
421. Xu, J.Z. and C.W. Wong, *Hunting for robust gene signature from cancer profiling data: sources of variability, different interpretations, and recent methodological developments.* Cancer Lett, 2010. **296**(1): p. 9-16.
422. Ji, F., et al., *Circulating microRNAs in hepatitis B virus-infected patients.* J Viral Hepat, 2011. **18**(7): p. e242-51.
423. Vandesompele, J., et al., *Accurate normalization of real-time quantitative RT-PCR data by geometric averaging of multiple internal control genes.* Genome Biol, 2002. **3**(7): p. RESEARCH0034.
424. Brase, J.C., et al., *Circulating miRNAs are correlated with tumor progression in prostate cancer.* Int J Cancer, 2011. **128**(3): p. 608-16.
425. Zahm, A.M., et al., *Circulating microRNA is a biomarker of pediatric Crohn disease.* J Pediatr Gastroenterol Nutr, 2011. **53**(1): p. 26-33.
426. Van Assche, G., et al., *The second European evidence-based Consensus on the diagnosis and management of Crohn's disease: Definitions and diagnosis.* J Crohns Colitis, 2010. **4**(1): p. 7-27.
427. Griffiths-Jones, S., *miRBase: the microRNA sequence database.* Methods Mol Biol, 2006. **342**: p. 129-38.
428. Liu, D., O. Davydenko, and M.A. Lampson, *Polo-like kinase-1 regulates kinetochore-microtubule dynamics and spindle checkpoint silencing.* J Cell Biol, 2012. **198**(4): p. 491-9.
429. Livak, K.J. and T.D. Schmittgen, *Analysis of relative gene expression data using real-time quantitative PCR and the 2(-Delta Delta C(T)) Method.* Methods, 2001. **25**(4): p. 402-8.
430. Korkeila, E.A., et al., *Carbonic anhydrase IX, hypoxia-inducible factor-1alpha, ezrin and glucose transporter-1 as predictors of disease outcome in rectal cancer: multivariate Cox survival models following data reduction by principal component analysis of the clinicopathological predictors.* Anticancer Res, 2011. **31**(12): p. 4529-35.
431. Bartel, D.P., *MicroRNAs: genomics, biogenesis, mechanism, and function.* Cell, 2004. **116**(2): p. 281-97.
432. Filipowicz, W., S.N. Bhattacharyya, and N. Sonenberg, *Mechanisms of post-transcriptional regulation by microRNAs: are the answers in sight?* Nat Rev Genet, 2008. **9**(2): p. 102-14.

433. Lindsay, M.A., *microRNAs and the immune response.* Trends Immunol, 2008. **29**(7): p. 343-51.
434. O'Connell, R.M., et al., *Physiological and pathological roles for microRNAs in the immune system.* Nat Rev Immunol, 2010. **10**(2): p. 111-22.
435. Vettori, S., S. Gay, and O. Distler, *Role of MicroRNAs in Fibrosis.* Open Rheumatol J, 2012. **6**: p. 130-9.
436. Bolstad, B.M., et al., *A comparison of normalization methods for high density oligonucleotide array data based on variance and bias.* Bioinformatics, 2003. **19**(2): p. 185-93.
437. Nymark, P., et al., *Integrative analysis of microRNA, mRNA and aCGH data reveals asbestos- and histology-related changes in lung cancer.* Genes Chromosomes Cancer, 2011. **50**(8): p. 585-97.
438. Boon, R.A., et al., *MicroRNA-34a regulates cardiac ageing and function.* Nature, 2013. **495**(7439): p. 107-10.
439. Meng, F., et al., *Epigenetic regulation of miR-34a expression in alcoholic liver injury.* Am J Pathol, 2012. **181**(3): p. 804-17.
440. Li, W.Q., et al., *The rno-miR-34 family is upregulated and targets ACSL1 in dimethylnitrosamine-induced hepatic fibrosis in rats.* FEBS J, 2011. **278**(9): p. 1522-32.
441. Zhou, Y., et al., *Secreted fibroblast miR-34a induces tubular cell apoptosis in fibrotic kidney.* J Cell Sci, 2014.
442. Milosevic, J., et al., *Profibrotic role of miR-154 in pulmonary fibrosis.* Am J Respir Cell Mol Biol, 2012. **47**(6): p. 879-87.
443. Zhu, H., et al., *MicroRNA expression abnormalities in limited cutaneous scleroderma and diffuse cutaneous scleroderma.* J Clin Immunol, 2012. **32**(3): p. 514-22.
444. Huebert, R.C., et al., *Aquaporin-1 promotes angiogenesis, fibrosis, and portal hypertension through mechanisms dependent on osmotically sensitive microRNAs.* Am J Pathol, 2011. **179**(4): p. 1851-60.
445. Applied-Biosystems, *Endogenous Controls for Real-Time Quantitation of miRNA using Taqman MicroRNa assays. Application Note.*
446. Di Sabatino, A., et al., *Functional modulation of Crohn's disease myofibroblasts by anti-tumor necrosis factor antibodies.* Gastroenterology, 2007. **133**(1): p. 137-49.
447. Tseng, Y.C., S. Mozumdar, and L. Huang, *Lipid-based systemic delivery of siRNA.* Adv Drug Deliv Rev, 2009. **61**(9): p. 721-31.
448. Genovese, G., et al., *microRNA regulatory network inference identifies miR-34a as a novel regulator of TGF-beta signaling in glioblastoma.* Cancer Discov, 2012. **2**(8): p. 736-49.
449. Cao, W., et al., *Expression and regulatory function of miRNA-34a in targeting survivin in gastric cancer cells.* Tumour Biol, 2013. **34**(2): p. 963-71.
450. Kadera, B.E., et al., *MicroRNA-21 in pancreatic ductal adenocarcinoma tumor-associated fibroblasts promotes metastasis.* PLoS One, 2013. **8**(8): p. e71978.
451. Verghese, E.T., et al., *MiR-26b is down-regulated in carcinoma-associated fibroblasts from ER-positive breast cancers leading to enhanced cell migration and invasion.* J Pathol, 2013. **231**(3): p. 388-99.
452. Fridman, J.S. and S.W. Lowe, *Control of apoptosis by p53.* Oncogene, 2003. **22**(56): p. 9030-40.
453. Lodygin, D., et al., *Inactivation of miR-34a by aberrant CpG methylation in multiple types of cancer.* Cell Cycle, 2008. **7**(16): p. 2591-600.

454. Cui, X., et al., *Inactivation of miR-34a by aberrant CpG methylation in Kazakh patients with esophageal carcinoma.* J Exp Clin Cancer Res, 2014. **33**: p. 20.
455. Wang, L.Q., et al., *Epigenetic inactivation of mir-34b/c in addition to mir-34a and DAPK1 in chronic lymphocytic leukemia.* J Transl Med, 2014. **12**: p. 52.
456. Chim, C.S., et al., *Methylation of miR-34a, miR-34b/c, miR-124-1 and miR-203 in Ph-negative myeloproliferative neoplasms.* J Transl Med, 2011. **9**: p. 197.
457. Hussain, S.P. and C.C. Harris, *Molecular epidemiology of human cancer: contribution of mutation spectra studies of tumor suppressor genes.* Cancer Res, 1998. **58**(18): p. 4023-37.
458. Beroud, C. and T. Soussi, *The UMD-p53 database: new mutations and analysis tools.* Hum Mutat, 2003. **21**(3): p. 176-81.
459. Tarasov, V., et al., *Differential regulation of microRNAs by p53 revealed by massively parallel sequencing: miR-34a is a p53 target that induces apoptosis and G1-arrest.* Cell Cycle, 2007. **6**(13): p. 1586-93.
460. Kuwano, K., et al., *P21Waf1/Cip1/Sdi1 and p53 expression in association with DNA strand breaks in idiopathic pulmonary fibrosis.* Am J Respir Crit Care Med, 1996. **154**(2 Pt 1): p. 477-83.
461. Nakashima, N., et al., *The p53-Mdm2 association in epithelial cells in idiopathic pulmonary fibrosis and non-specific interstitial pneumonia.* J Clin Pathol, 2005. **58**(6): p. 583-9.
462. Samarakoon, R., J.M. Overstreet, and P.J. Higgins, *TGF-beta signaling in tissue fibrosis: redox controls, target genes and therapeutic opportunities.* Cell Signal, 2013. **25**(1): p. 264-8.
463. Dagher, P.C., et al., *The p53 inhibitor pifithrin-alpha can stimulate fibrosis in a rat model of ischemic acute kidney injury.* Am J Physiol Renal Physiol, 2012. **302**(2): p. F284-91.
464. Lujambio, A., et al., *Non-cell-autonomous tumor suppression by p53.* Cell, 2013. **153**(2): p. 449-60.
465. Valoczi, A., et al., *Sensitive and specific detection of microRNAs by northern blot analysis using LNA-modified oligonucleotide probes.* Nucleic Acids Res, 2004. **32**(22): p. e175.
466. Wienholds, E., et al., *MicroRNA expression in zebrafish embryonic development.* Science, 2005. **309**(5732): p. 310-1.
467. Saini, S., et al., *miRNA-708 control of CD44(+) prostate cancer-initiating cells.* Cancer Res, 2012. **72**(14): p. 3618-30.
468. Akhmetshina, A., et al., *Activation of canonical Wnt signalling is required for TGF-beta-mediated fibrosis.* Nat Commun, 2012. **3**: p. 735.
469. Monteleone, G., et al., *A failure of transforming growth factor-beta1 negative regulation maintains sustained NF-kappaB activation in gut inflammation.* J Biol Chem, 2004. **279**(6): p. 3925-32.
470. Shen, Z., et al., *MicroRNA-34a affects the occurrence of laryngeal squamous cell carcinoma by targeting the antiapoptotic gene survivin.* Med Oncol, 2012. **29**(4): p. 2473-80.
471. Yamakuchi, M., M. Ferlito, and C.J. Lowenstein, *miR-34a repression of SIRT1 regulates apoptosis.* Proc Natl Acad Sci U S A, 2008. **105**(36): p. 13421-6.
472. Yang, F., et al., *MicroRNA-34a targets Bcl-2 and sensitizes human hepatocellular carcinoma cells to sorafenib treatment.* Technol Cancer Res Treat, 2014. **13**(1): p. 77-86.
473. Hermeking, H., *The miR-34 family in cancer and apoptosis.* Cell Death Differ, 2010. **17**(2): p. 193-9.

474. Selbach, M., et al., *Widespread changes in protein synthesis induced by microRNAs.* Nature, 2008. **455**(7209): p. 58-63.
475. Kaller, M., et al., *Genome-wide characterization of miR-34a induced changes in protein and mRNA expression by a combined pulsed SILAC and microarray analysis.* Mol Cell Proteomics, 2011. **10**(8): p. M111 010462.
476. Ebner, O.A. and M. Selbach, *Quantitative proteomic analysis of gene regulation by miR-34a and miR-34c.* PLoS One, 2014. **9**(3): p. e92166.
477. Selman, M. and A. Pardo, *Role of epithelial cells in idiopathic pulmonary fibrosis: from innocent targets to serial killers.* Proc Am Thorac Soc, 2006. **3**(4): p. 364-72.
478. Muir, A.B., et al., *Esophageal epithelial and mesenchymal cross-talk leads to features of epithelial to mesenchymal transition in vitro.* Exp Cell Res, 2013. **319**(6): p. 850-9.
479. Andrew, A.S., et al., *Expression of tumor suppressive microRNA-34a is associated with a reduced risk of bladder cancer recurrence.* Int J Cancer, 2014.
480. Peurala, H., et al., *MiR-34a expression has an effect for lower risk of metastasis and associates with expression patterns predicting clinical outcome in breast cancer.* PLoS One, 2011. **6**(11): p. e26122.
481. Agarwal, S., et al., *Quantitative assessment of miR34a as an independent prognostic marker in breast cancer.* Br J Cancer, 2015. **112**(1): p. 61-8.
482. Wang, Y., et al., *The role of miRNA-29 family in cancer.* Eur J Cell Biol, 2013. **92**(3): p. 123-8.
483. Nijhuis, A., et al., *In Crohn's disease fibrosis-reduced expression of the miR-29 family enhances collagen expression in intestinal fibroblasts.* Clin Sci (Lond), 2014. **127**(5): p. 341-50.
484. Xiao, J., et al., *miR-29 inhibits bleomycin-induced pulmonary fibrosis in mice.* Mol Ther, 2012. **20**(6): p. 1251-60.
485. Stallmach, A., et al., *Increased collagen type III synthesis by fibroblasts isolated from strictures of patients with Crohn's disease.* Gastroenterology, 1992. **102**(6): p. 1920-9.
486. Lang, M., et al., *Gene expression profiles of mucosal fibroblasts from strictured and nonstrictured areas of patients with Crohn's disease.* Inflamm Bowel Dis, 2009. **15**(2): p. 212-23.
487. Pohlers, D., et al., *TGF-beta and fibrosis in different organs - molecular pathway imprints.* Biochim Biophys Acta, 2009. **1792**(8): p. 746-56.
488. Butz, H., et al., *Crosstalk between TGF-beta signaling and the microRNA machinery.* Trends Pharmacol Sci, 2012. **33**(7): p. 382-93.
489. Lewis, B.P., C.B. Burge, and D.P. Bartel, *Conserved seed pairing, often flanked by adenosines, indicates that thousands of human genes are microRNA targets.* Cell, 2005. **120**(1): p. 15-20.
490. Huang, S.K., et al., *Histone modifications are responsible for decreased Fas expression and apoptosis resistance in fibrotic lung fibroblasts.* Cell Death Dis, 2013. **4**: p. e621.
491. Mott, J.L., et al., *mir-29 regulates Mcl-1 protein expression and apoptosis.* Oncogene, 2007. **26**(42): p. 6133-40.
492. Zhang, Y.K., et al., *Overexpression of microRNA-29b induces apoptosis of multiple myeloma cells through down regulating Mcl-1.* Biochem Biophys Res Commun, 2011. **414**(1): p. 233-9.
493. Xiong, Y., et al., *Effects of microRNA-29 on apoptosis, tumorigenicity, and prognosis of hepatocellular carcinoma.* Hepatology, 2010. **51**(3): p. 836-45.

494. Steele, R., J.L. Mott, and R.B. Ray, *MBP-1 upregulates miR-29b that represses Mcl-1, collagens, and matrix-metalloproteinase-2 in prostate cancer cells.* Genes Cancer, 2010. **1**(4): p. 381-387.
495. Garzon, R., et al., *MicroRNA 29b functions in acute myeloid leukemia.* Blood, 2009. **114**(26): p. 5331-41.
496. Roggli, E., et al., *Changes in microRNA expression contribute to pancreatic beta-cell dysfunction in prediabetic NOD mice.* Diabetes, 2012. **61**(7): p. 1742-51.
497. Kozopas, K.M., et al., *MCL1, a gene expressed in programmed myeloid cell differentiation, has sequence similarity to BCL2.* Proc Natl Acad Sci U S A, 1993. **90**(8): p. 3516-20.
498. Bae, J., et al., *MCL-1S, a splicing variant of the antiapoptotic BCL-2 family member MCL-1, encodes a proapoptotic protein possessing only the BH3 domain.* J Biol Chem, 2000. **275**(33): p. 25255-61.
499. Bingle, C.D., et al., *Exon skipping in Mcl-1 results in a bcl-2 homology domain 3 only gene product that promotes cell death.* J Biol Chem, 2000. **275**(29): p. 22136-46.
500. Kim, J.H., et al., *MCL-1ES, a novel variant of MCL-1, associates with MCL-1L and induces mitochondrial cell death.* FEBS Lett, 2009. **583**(17): p. 2758-64.
501. Kim, J.H. and J. Bae, *MCL-1ES induces MCL-1L-dependent BAX- and BAK-independent mitochondrial apoptosis.* PLoS One, 2013. **8**(11): p. e79626.
502. Weng, S.Y., et al., *Synergism between p53 and Mcl-1 in protecting from hepatic injury, fibrosis and cancer.* J Hepatol, 2011. **54**(4): p. 685-94.
503. Kahraman, A., et al., *Overexpression of mcl-1 attenuates liver injury and fibrosis in the bile duct-ligated mouse.* Dig Dis Sci, 2009. **54**(9): p. 1908-17.
504. Vick, B., et al., *Knockout of myeloid cell leukemia-1 induces liver damage and increases apoptosis susceptibility of murine hepatocytes.* Hepatology, 2009. **49**(2): p. 627-36.
505. Wightman, B., I. Ha, and G. Ruvkun, *Posttranscriptional regulation of the heterochronic gene lin-14 by lin-4 mediates temporal pattern formation in C. elegans.* Cell, 1993. **75**(5): p. 855-62.
506. Reinhart, B.J., et al., *The 21-nucleotide let-7 RNA regulates developmental timing in Caenorhabditis elegans.* Nature, 2000. **403**(6772): p. 901-6.
507. Brennecke, J., et al., *bantam encodes a developmentally regulated microRNA that controls cell proliferation and regulates the proapoptotic gene hid in Drosophila.* Cell, 2003. **113**(1): p. 25-36.
508. Vasudevan, S., *Posttranscriptional upregulation by microRNAs.* Wiley Interdiscip Rev RNA, 2012. **3**(3): p. 311-30.
509. Puthier, D., R. Bataille, and M. Amiot, *IL-6 up-regulates mcl-1 in human myeloma cells through JAK / STAT rather than ras / MAP kinase pathway.* Eur J Immunol, 1999. **29**(12): p. 3945-50.
510. Eberhard, A., et al., *Heterogeneity of angiogenesis and blood vessel maturation in human tumors: implications for antiangiogenic tumor therapies.* Cancer Res, 2000. **60**(5): p. 1388-93.
511. O'Reilly, S., M. Chiechomska, and J.M. van Laar, *A3.22 IL-6 trans signalling drives collagen via an epigenetic mechanism mediated through SMAD3.* Ann Rheum Dis, 2014. **73 Suppl 1**: p. A50-1.
512. Fielding, C.A., et al., *Interleukin-6 signaling drives fibrosis in unresolved inflammation.* Immunity, 2014. **40**(1): p. 40-50.
513. O'Reilly, S., et al., *Interleukin-6, its role in fibrosing conditions.* Cytokine Growth Factor Rev, 2012. **23**(3): p. 99-107.

514. Sarkar, A., et al., *Infection with Anaplasma phagocytophilum activates the phosphatidylinositol 3-Kinase/Akt and NF-kappaB survival pathways in neutrophil granulocytes.* Infect Immun, 2012. **80**(4): p. 1615-23.
515. Nobili, V., et al., *Association of serum interleukin-8 levels with the degree of fibrosis in infants with chronic liver disease.* J Pediatr Gastroenterol Nutr, 2004. **39**(5): p. 540-4.
516. Rucklidge, G.J., et al., *Turnover rates of different collagen types measured by isotope ratio mass spectrometry.* Biochim Biophys Acta, 1992. **1156**(1): p. 57-61.
517. Yuan, C., et al., *IL-10 treatment is associated with prohibitin expression in the Crohn's disease intestinal fibrosis mouse model.* Mediators Inflamm, 2013. **2013**: p. 617145.
518. Kogure, T., et al., *Hepatic miR-29ab1 expression modulates chronic hepatic injury.* J Cell Mol Med, 2012. **16**(11): p. 2647-54.
519. Wang, L., et al., *Loss of miR-29 in myoblasts contributes to dystrophic muscle pathogenesis.* Mol Ther, 2012. **20**(6): p. 1222-33.
520. Amodio, N., et al., *miR-29b induces SOCS-1 expression by promoter demethylation and negatively regulates migration of multiple myeloma and endothelial cells.* Cell Cycle, 2013. **12**(23): p. 3650-62.
521. Xing, L.N., et al., *Reduced mir-29b-3p expression up-regulate CDK6 and contributes to IgA nephropathy.* Int J Clin Exp Med, 2014. **7**(12): p. 5275-81.
522. Salama, A., et al., *MicroRNA-29b modulates innate and antigen-specific immune responses in mouse models of autoimmunity.* PLoS One, 2014. **9**(9): p. e106153.
523. Huang, X., Q.T. Le, and A.J. Giaccia, *MiR-210--micromanager of the hypoxia pathway.* Trends Mol Med, 2010. **16**(5): p. 230-7.
524. Crosby, M.E., et al., *MicroRNA regulation of DNA repair gene expression in hypoxic stress.* Cancer Res, 2009. **69**(3): p. 1221-9.
525. Chang, W., et al., *Survival of hypoxic human mesenchymal stem cells is enhanced by a positive feedback loop involving miR-210 and hypoxia-inducible factor 1.* J Vet Sci, 2013. **14**(1): p. 69-76.
526. Chau, I. and D. Cunningham, *Chemotherapy in colorectal cancer: new options and new challenges.* Br Med Bull, 2002. **64**: p. 159-80.
527. Nakamura, J., et al., *Hypoxia-inducible factor-1alpha expression predicts the response to 5-fluorouracil-based adjuvant chemotherapy in advanced gastric cancer.* Oncol Rep, 2009. **22**(4): p. 693-9.
528. Ravizza, R., et al., *Effect of HIF-1 modulation on the response of two- and three-dimensional cultures of human colon cancer cells to 5-fluorouracil.* Eur J Cancer, 2009. **45**(5): p. 890-8.
529. Chan, Y.C., et al., *miR-210: the master hypoxamir.* Microcirculation, 2012. **19**(3): p. 215-23.
530. Budinger, G.R., et al., *Cellular energy utilization and supply during hypoxia in embryonic cardiac myocytes.* Am J Physiol, 1996. **270**(1 Pt 1): p. L44-53.
531. Budinger, G.R., et al., *Hibernation during hypoxia in cardiomyocytes. Role of mitochondria as the O2 sensor.* J Biol Chem, 1998. **273**(6): p. 3320-6.
532. Chandel, N.S., et al., *Cellular respiration during hypoxia. Role of cytochrome oxidase as the oxygen sensor in hepatocytes.* J Biol Chem, 1997. **272**(30): p. 18808-16.
533. Lu, H., R.A. Forbes, and A. Verma, *Hypoxia-inducible factor 1 activation by aerobic glycolysis implicates the Warburg effect in carcinogenesis.* J Biol Chem, 2002. **277**(26): p. 23111-5.

534. Lee, M., et al., *AMP-activated protein kinase activity is critical for hypoxia-inducible factor-1 transcriptional activity and its target gene expression under hypoxic conditions in DU145 cells.* J Biol Chem, 2003. **278**(41): p. 39653-61.
535. Ogata, H., et al., *KEGG: Kyoto Encyclopedia of Genes and Genomes.* Nucleic Acids Res, 1999. **27**(1): p. 29-34.
536. Booth, S.C., A.M. Weljie, and R.J. Turner, *Computational tools for the secondary analysis of metabolomics experiments.* Comput Struct Biotechnol J, 2013. **4**: p. e201301003.
537. Bruning, U., et al., *MicroRNA-155 promotes resolution of hypoxia-inducible factor 1alpha activity during prolonged hypoxia.* Mol Cell Biol, 2011. **31**(19): p. 4087-96.
538. Crosby, M.E., et al., *Emerging roles of microRNAs in the molecular responses to hypoxia.* Curr Pharm Des, 2009. **15**(33): p. 3861-6.
539. Li, E., et al., *Differential expression of miRNAs in colon cancer between African and Caucasian Americans: implications for cancer racial health disparities.* Int J Oncol, 2014. **45**(2): p. 587-94.
540. Rapti, S.M., et al., *Enhanced miR-182 transcription is a predictor of poor overall survival in colorectal adenocarcinoma patients.* Clin Chem Lab Med, 2014. **52**(8): p. 1217-27.
541. Liu, H., et al., *Up-regulation of miR-182 expression in colorectal cancer tissues and its prognostic value.* Int J Colorectal Dis, 2013. **28**(5): p. 697-703.
542. Cekaite, L., et al., *MiR-9, -31, and -182 deregulation promote proliferation and tumor cell survival in colon cancer.* Neoplasia, 2012. **14**(9): p. 868-79.
543. Qu, A., et al., *Hypoxia-inducible MiR-210 is an independent prognostic factor and contributes to metastasis in colorectal cancer.* PLoS One, 2014. **9**(3): p. e90952.
544. Noman, M.Z., et al., *Hypoxia-inducible miR-210 regulates the susceptibility of tumor cells to lysis by cytotoxic T cells.* Cancer Res, 2012. **72**(18): p. 4629-41.
545. Yamasaki, K., et al., *Angiogenic microRNA-210 is present in cells surrounding osteonecrosis.* J Orthop Res, 2012. **30**(8): p. 1263-70.
546. Yang, S., et al., *miR-21 regulates chronic hypoxia-induced pulmonary vascular remodeling.* Am J Physiol Lung Cell Mol Physiol, 2012. **302**(6): p. L521-9.
547. Wang, M., et al., *MicroRNA-21 regulates vascular smooth muscle cell function via targeting tropomyosin 1 in arteriosclerosis obliterans of lower extremities.* Arterioscler Thromb Vasc Biol, 2011. **31**(9): p. 2044-53.
548. Nielsen, B.S., et al., *High levels of microRNA-21 in the stroma of colorectal cancers predict short disease-free survival in stage II colon cancer patients.* Clin Exp Metastasis, 2011. **28**(1): p. 27-38.
549. Kjaer-Frifeldt, S., et al., *The prognostic importance of miR-21 in stage II colon cancer: a population-based study.* Br J Cancer, 2012. **107**(7): p. 1169-74.
550. Rask, L., et al., *High expression of miR-21 in tumor stroma correlates with increased cancer cell proliferation in human breast cancer.* APMIS, 2011. **119**(10): p. 663-73.
551. Yamamichi, N., et al., *Locked nucleic acid in situ hybridization analysis of miR-21 expression during colorectal cancer development.* Clin Cancer Res, 2009. **15**(12): p. 4009-16.
552. Etheridge, A., et al., *Extracellular microRNA: a new source of biomarkers.* Mutat Res, 2011. **717**(1-2): p. 85-90.
553. Wang, J., et al., *Tumor-associated circulating microRNAs as biomarkers of cancer.* Molecules, 2014. **19**(2): p. 1912-38.

554. Zhang, H.L., et al., *Serum miRNA-21: elevated levels in patients with metastatic hormone-refractory prostate cancer and potential predictive factor for the efficacy of docetaxel-based chemotherapy.* Prostate, 2011. **71**(3): p. 326-31.
555. Shen, J., et al., *Dysregulation of circulating microRNAs and prediction of aggressive prostate cancer.* Prostate, 2012. **72**(13): p. 1469-77.
556. Resnick, K.E., et al., *The detection of differentially expressed microRNAs from the serum of ovarian cancer patients using a novel real-time PCR platform.* Gynecol Oncol, 2009. **112**(1): p. 55-9.
557. Taylor, D.D. and C. Gercel-Taylor, *MicroRNA signatures of tumor-derived exosomes as diagnostic biomarkers of ovarian cancer.* Gynecol Oncol, 2008. **110**(1): p. 13-21.
558. Sadakari, Y., et al., *MicroRNA expression analyses in preoperative pancreatic juice samples of pancreatic ductal adenocarcinoma.* JOP, 2010. **11**(6): p. 587-92.
559. Zhou, J., et al., *Plasma microRNA panel to diagnose hepatitis B virus-related hepatocellular carcinoma.* J Clin Oncol, 2011. **29**(36): p. 4781-8.
560. Xu, J., et al., *Circulating microRNAs, miR-21, miR-122, and miR-223, in patients with hepatocellular carcinoma or chronic hepatitis.* ngMol Carcinog, 2011. **50**(2): p. 136-42.
561. Komatsu, S., et al., *Circulating microRNAs in plasma of patients with oesophageal squamous cell carcinoma.* Br J Cancer, 2011. **105**(1): p. 104-11.
562. Shen, J., et al., *Diagnosis of lung cancer in individuals with solitary pulmonary nodules by plasma microRNA biomarkers.* BMC Cancer, 2011. **11**: p. 374.
563. Li, Z.H., et al., *Prognostic significance of serum microRNA-210 levels in nonsmall-cell lung cancer.* J Int Med Res, 2013. **41**(5): p. 1437-44.
564. Zhao, A., et al., *Serum miR-210 as a novel biomarker for molecular diagnosis of clear cell renal cell carcinoma.* Exp Mol Pathol, 2013. **94**(1): p. 115-20.
565. Iwamoto, H., et al., *Serum miR-210 as a potential biomarker of early clear cell renal cell carcinoma.* Int J Oncol, 2014. **44**(1): p. 53-8.
566. Xuan, Y., et al., *Dichloroacetate attenuates hypoxia-induced resistance to 5-fluorouracil in gastric cancer through the regulation of glucose metabolism.* Exp Cell Res, 2014. **321**(2): p. 219-30.
567. Yoshiba, S., et al., *Hypoxia induces resistance to 5-fluorouracil in oral cancer cells via G(1) phase cell cycle arrest.* Oral Oncol, 2009. **45**(2): p. 109-15.
568. Liu, J., et al., *Notch1 is a 5-fluorouracil resistant and poor survival marker in human esophagus squamous cell carcinomas.* PLoS One, 2013. **8**(2): p. e56141.
569. Wang, C.J., et al., *Suppression of microRNA-31 increases sensitivity to 5-FU at an early stage, and affects cell migration and invasion in HCT-116 colon cancer cells.* BMC Cancer, 2010. **10**: p. 616.
570. Karaayvaz, M., H. Zhai, and J. Ju, *miR-129 promotes apoptosis and enhances chemosensitivity to 5-fluorouracil in colorectal cancer.* Cell Death Dis, 2013. **4**: p. e659.
571. Boni, V., et al., *miR-192/miR-215 influence 5-fluorouracil resistance through cell cycle-mediated mechanisms complementary to its post-transcriptional thymidilate synthase regulation.* Mol Cancer Ther, 2010. **9**(8): p. 2265-75.
572. Deng, J., et al., *Targeting miR-21 enhances the sensitivity of human colon cancer HT-29 cells to chemoradiotherapy in vitro.* Biochem Biophys Res Commun, 2014. **443**(3): p. 789-95.
573. Shang, J., et al., *MicroRNA-23a antisense enhances 5-fluorouracil chemosensitivity through APAF-1/caspase-9 apoptotic pathway in colorectal cancer cells.* J Cell Biochem, 2014. **115**(4): p. 772-84.

574. Borralho, P.M., et al., *MicroRNA-143 reduces viability and increases sensitivity to 5-fluorouracil in HCT116 human colorectal cancer cells.* FEBS J, 2009. **276**(22): p. 6689-700.
575. Frezza, C., et al., *Metabolic profiling of hypoxic cells revealed a catabolic signature required for cell survival.* PLoS One, 2011. **6**(9): p. e24411.
576. Mehrpour, M., et al., *Overview of macroautophagy regulation in mammalian cells.* Cell Res, 2010. **20**(7): p. 748-62.
577. Zhang, H., et al., *Mitochondrial autophagy is an HIF-1-dependent adaptive metabolic response to hypoxia.* J Biol Chem, 2008. **283**(16): p. 10892-903.
578. Wilkinson, S., et al., *Hypoxia-selective macroautophagy and cell survival signaled by autocrine PDGFR activity.* Genes Dev, 2009. **23**(11): p. 1283-8.
579. Frankel, L.B. and A.H. Lund, *MicroRNA regulation of autophagy.* Carcinogenesis, 2012. **33**(11): p. 2018-25.
580. Yang, X., et al., *mir-30d Regulates multiple genes in the autophagy pathway and impairs autophagy process in human cancer cells.* Biochem Biophys Res Commun, 2013. **431**(3): p. 617-22.
581. Zhang, Y., et al., *Regulation of autophagy by miR-30d impacts sensitivity of anaplastic thyroid carcinoma to cisplatin.* Biochem Pharmacol, 2014. **87**(4): p. 562-70.
582. Sun, Y., et al., *Hypoxia-induced autophagy reduces radiosensitivity by the HIF-1alpha/miR-210/Bcl-2 pathway in colon cancer cells.* Int J Oncol, 2015. **46**(2): p. 750-6.
583. Li, J., et al., *Inhibition of autophagy augments 5-fluorouracil chemotherapy in human colon cancer in vitro and in vivo model.* Eur J Cancer, 2010. **46**(10): p. 1900-9.
584. Park, S.G., P. Schimmel, and S. Kim, *Aminoacyl tRNA synthetases and their connections to disease.* Proc Natl Acad Sci U S A, 2008. **105**(32): p. 11043-9.
585. Kushner, J.P., et al., *Elevated methionine-tRNA synthetase activity in human colon cancer.* Proc Soc Exp Biol Med, 1976. **153**(2): p. 273-6.
586. Ghanipour, A., et al., *The prognostic significance of tryptophanyl-tRNA synthetase in colorectal cancer.* Cancer Epidemiol Biomarkers Prev, 2009. **18**(11): p. 2949-56.
587. Emara, M.M., et al., *Angiogenin-induced tRNA-derived stress-induced RNAs promote stress-induced stress granule assembly.* J Biol Chem, 2010. **285**(14): p. 10959-68.
588. Gebetsberger, J. and N. Polacek, *Slicing tRNAs to boost functional ncRNA diversity.* RNA Biol, 2013. **10**(12): p. 1798-806.
589. Goodarzi, H., et al., *Endogenous tRNA-Derived Fragments Suppress Breast Cancer Progression via YBX1 Displacement.* Cell, 2015. **161**(4): p. 790-802.
590. Khan, M.I., et al., *YB-1 expression promotes epithelial-to-mesenchymal transition in prostate cancer that is inhibited by a small molecule fisetin.* Oncotarget, 2014. **5**(9): p. 2462-74.
591. Kosnopfel, C., T. Sinnberg, and B. Schittek, *Y-box binding protein 1--a prognostic marker and target in tumour therapy.* Eur J Cell Biol, 2014. **93**(1-2): p. 61-70.
592. Zhang, Y., et al., *The expression level and prognostic value of Y-box binding protein-1 in rectal cancer.* PLoS One, 2015. **10**(3): p. e0119385.
593. Gaken, J., et al., *A functional assay for microRNA target identification and validation.* Nucleic Acids Res, 2012. **40**(10): p. e75.
594. Rieder, F., et al., *Animal models of intestinal fibrosis: new tools for the understanding of pathogenesis and therapy of human disease.* Am J Physiol Gastrointest Liver Physiol, 2012. **303**(7): p. G786-801.
595. Archambaud, C., et al., *The intestinal microbiota interferes with the microRNA response upon oral Listeria infection.* MBio, 2013. **4**(6): p. e00707-13.

596. Vermeire, S., G. Van Assche, and P. Rutgeerts, *Laboratory markers in IBD: useful, magic, or unnecessary toys?* Gut, 2006. **55**(3): p. 426-31.
597. Chen, X., et al., *Characterization of microRNAs in serum: a novel class of biomarkers for diagnosis of cancer and other diseases.* Cell Res, 2008. **18**(10): p. 997-1006.
598. Zuo, J., et al., *MiR-210 Links Hypoxia With Cell Proliferation Regulation in Human Laryngocarcinoma Cancer.* J Cell Biochem, 2015. **116**(6): p. 1039-49.
599. Yang, W., et al., *Effects of knockdown of miR-210 in combination with ionizing radiation on human hepatoma xenograft in nude mice.* Radiat Oncol, 2013. **8**: p. 102.
600. Rottiers, V. and A.M. Naar, *MicroRNAs in metabolism and metabolic disorders.* Nat Rev Mol Cell Biol, 2012. **13**(4): p. 239-50.
601. Flicek, P., et al., *Ensembl 2008.* Nucleic Acids Res, 2008. **36**(Database issue): p. D707-14.
602. Bina, M., *The genome browser at UCSC for locating genes, and much more!* Mol Biotechnol, 2008. **38**(3): p. 269-75.
603. Bentwich, I., *Prediction and validation of microRNAs and their targets.* FEBS Lett, 2005. **579**(26): p. 5904-10.
604. Sethupathy, P., M. Megraw, and A.G. Hatzigeorgiou, *A guide through present computational approaches for the identification of mammalian microRNA targets.* Nat Methods, 2006. **3**(11): p. 881-6.
605. Easow, G., A.A. Teleman, and S.M. Cohen, *Isolation of microRNA targets by miRNP immunopurification.* RNA, 2007. **13**(8): p. 1198-204.
606. Coussens, M.J., et al., *Genome-wide screen for miRNA targets using the MISSION target ID library.* J Vis Exp, 2012(62): p. e3303.

Chapter 8: Appendix Tables and Figures

Appendix Table 1. MiRNAs outside the microarray detection limit. miRNAs with fluorescent values over 60000 in either group were considered outside the detection range Mean fluorescent intensity and standard deviation values of miRNAs are shown for each group (n=6). The miRNAs are ranked in numerical order.

miRNA	NSCD mean	NSCD Stdev	SCD mean	SCD Stdev
hsa-let-7a	65231	90.72854	64719.42	713.5631
hsa-let-7c	53165.05	10852.14	61298.38	4353.523
hsa-let-7f	64550.27	1048.211	64728.45	581.9631
hsa-let-7g	65259.99	42.7569	64516.42	1300.471
hsa-miR-1246	63777.89	3194.615	61946.67	3149.818
hsa-miR-125a-5p	62567.12	2103.862	62010.74	3076.071
hsa-miR-125b	62040.64	2897.026	64645.71	1565.292
hsa-miR-1274b	62649.88	3852.055	64467.1	1080.001
hsa-miR-143	64573.46	910.919	64720.56	505.6736
hsa-miR-145	61774.85	1862.461	59771.46	4054.616
hsa-miR-146a	58928.45	5332.376	63229.99	2859.887
hsa-miR-148a	61695.38	3502.753	63722.82	1234.12
hsa-miR-150	64782.89	491.8828	64545.14	1120.818
hsa-miR-191	63458	1803.962	64728.41	1009.837
hsa-miR-192	64700.54	791.1251	52806.59	22664.21
hsa-miR-194	64970.88	464.6906	54832.75	21872.47
hsa-miR-200b	64682.57	1003.68	53010.34	21983.21
hsa-miR-200c	64776.06	912.2013	58880.99	14979.28
hsa-miR-21	64975.96	582.5917	64614.2	948.4555
hsa-miR-214	57484.82	6560.773	62260.69	4286.634
hsa-miR-215	63966.94	1817.542	52483.16	24551.44
hsa-miR-223	63357.81	2285.193	63123.24	3768.269
hsa-miR-23a	64298.17	1304.531	64714.14	717.0644
hsa-miR-23b	64594.38	935.3724	64106.89	788.4298

hsa-miR-24	59316.12	3257.537	61121.67	3381.464
hsa-miR-25	61741.95	4026.395	64263.52	1635.017
hsa-miR-26a	64929.19	551.2634	64849.67	782.2091
hsa-miR-26b	64472.19	603.2704	64441.05	1880.022
hsa-miR-27a	58097.38	5052.814	63581.89	1805.699
hsa-miR-27b	55278.55	5277.181	60173.87	4441.18
hsa-miR-29b	62140.1	3882.261	62976.71	3538.593
hsa-miR-30c	57763.14	5669.622	60297.95	4990.575
hsa-miR-30d	64204.91	1421.48	63907.17	2073.305
miR-320a,b,c,d	63925.98	1917.901	63372.55	1820.957
hsa-miR-375	65051.37	282.7126	55421.88	19594.96
hsa-miR-544	60152.79	12570.68	54914.52	15177.2
hsa-miR-720	64319.63	2034.63	64149	1039.136
hsa-miR-768-3p	63424.84	3896.227	64523.2	1125.593
hsa-miR-92a	62243.82	2337.274	62269	2723.357

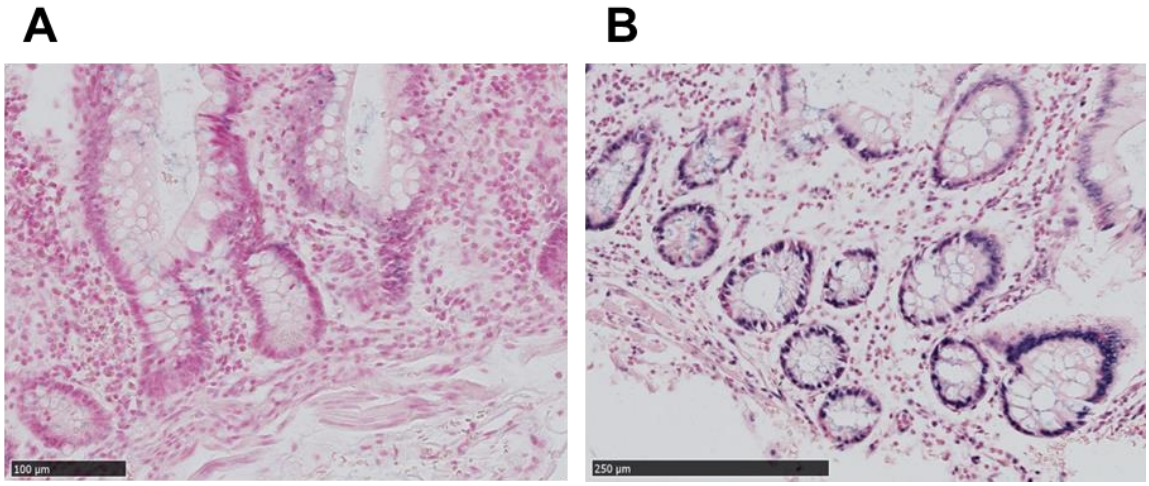

Appendix Figure 1. ***In situ*** **hybridisation of U6 in intestinal mucosa.** FFPE section of intestinal mucosa probed with in situ hybridisation probe for small RNA U6. (A) Negative and (B) positive staining for U6 within the same section.

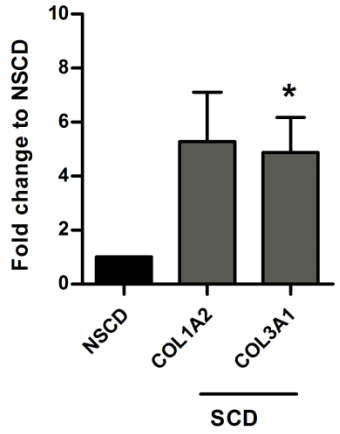

Appendix Figure 2. Collagen transcripts are up-regulated in SCD vs NSCD tissues. Paired NSCD and SCD tissue samples (n=5) were assayed for the expression of *COL1A2* and *COL3A1* via qRT-PCR. Bars represent mean values with SEM. *p<0.05.

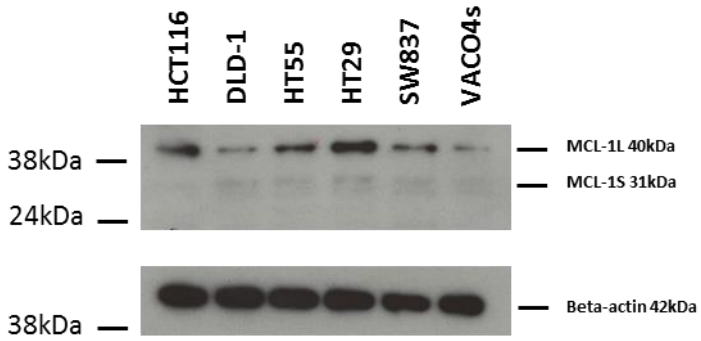

Appendix Figure 3. **Mcl-1 antibody validation**. Cell lysates from six CRC cell lines were subjected to western blotting. Antibodies against Mcl-1 and Beta-actin were used at 1:250 and 1:50,000, respectively. Molecular weight for Mcl-1L, Mcl-1S and Mcl-1ES are 40kDa, 31kDa and 24kDa, respectively

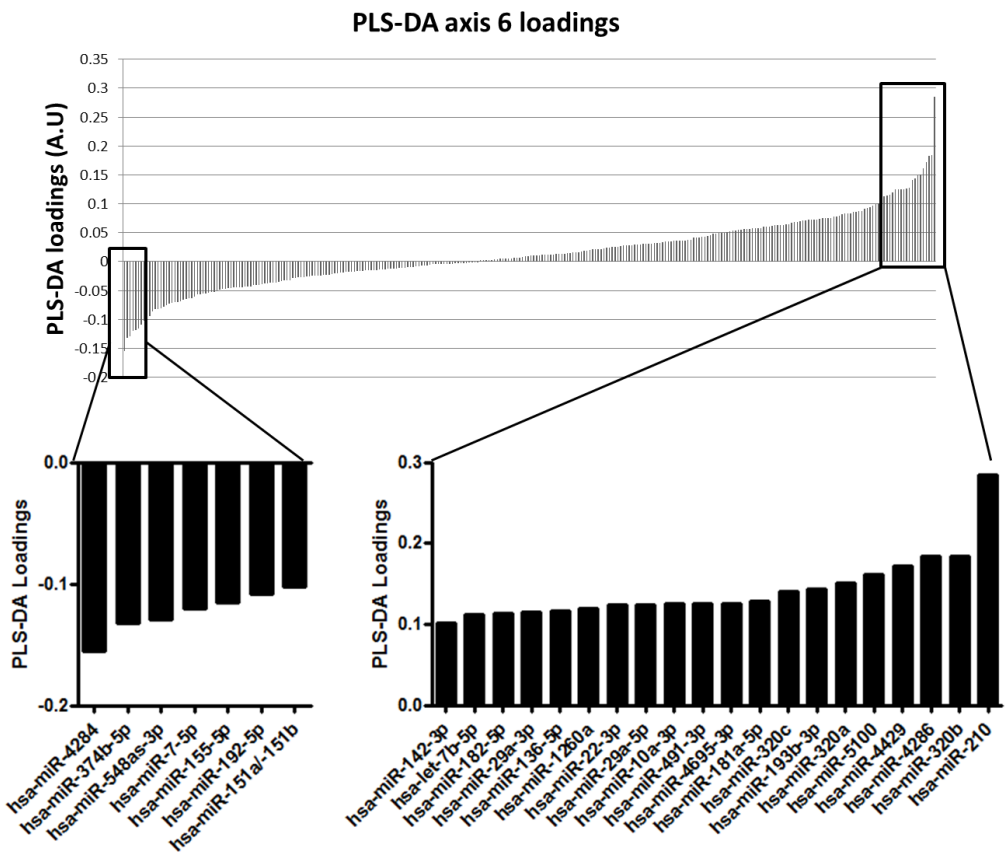

Appendix Figure 4. PLS-DA axis 6 loadings. Log transformed miRNA data was subjected to unsupervised PLS-DA analysis. Loadings from PLS-DA axis 6 for each of the miRNAs are shown. Rectangle boxes outline the location of the bar graphs below.

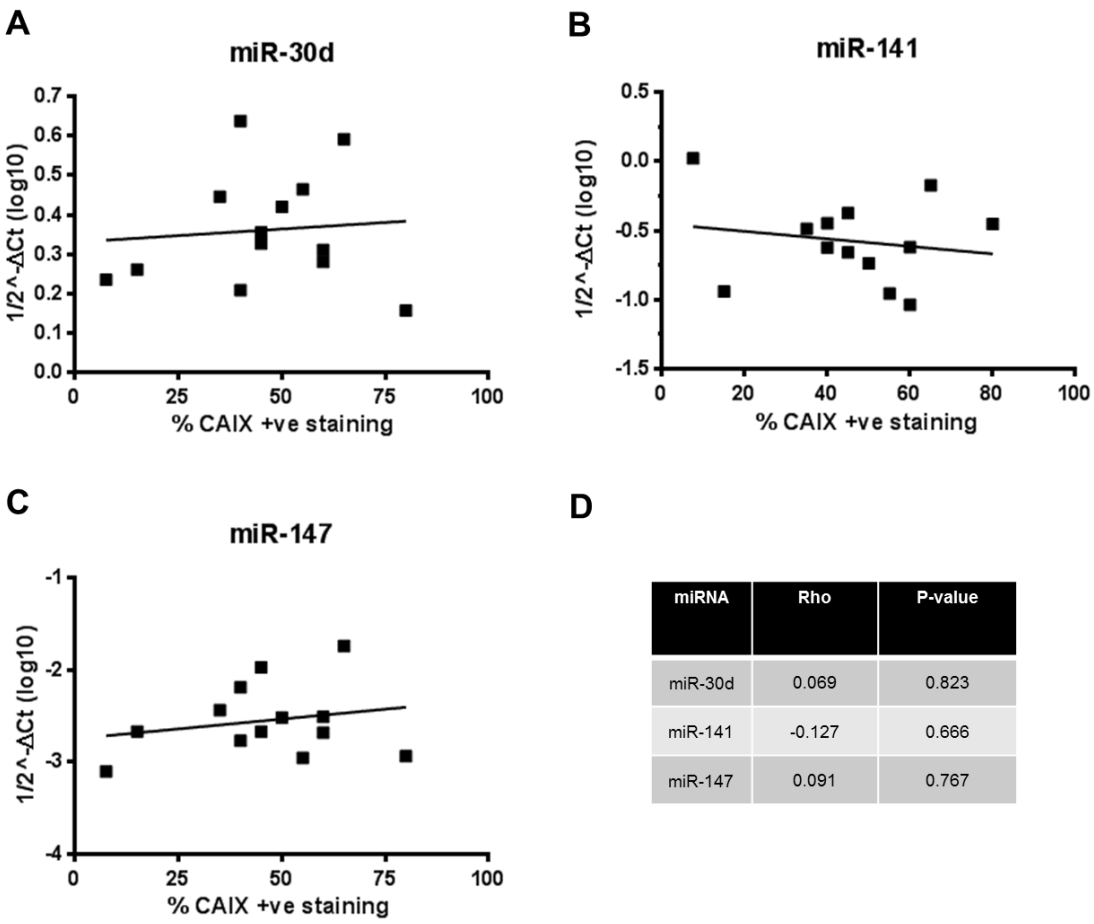

D

miRNA	Rho	P-value
miR-30d	0.069	0.823
miR-141	-0.127	0.666
miR-147	0.091	0.767

Appendix Figure 5. Expression of miR-30d, -141 and -147 did not correlate to the expression of hypoxia marker CAIX. (A-C) Scatter plots of miR-30, -141 and -147 expression ($1/2^{-\Delta CT}$) assessed by qRT-PCR and percentage of CAIX-positive staining within the tumour (n=13). (D) Correlation efficiency are calculated with Spearman's Rank. Rho values and p-value are shown.

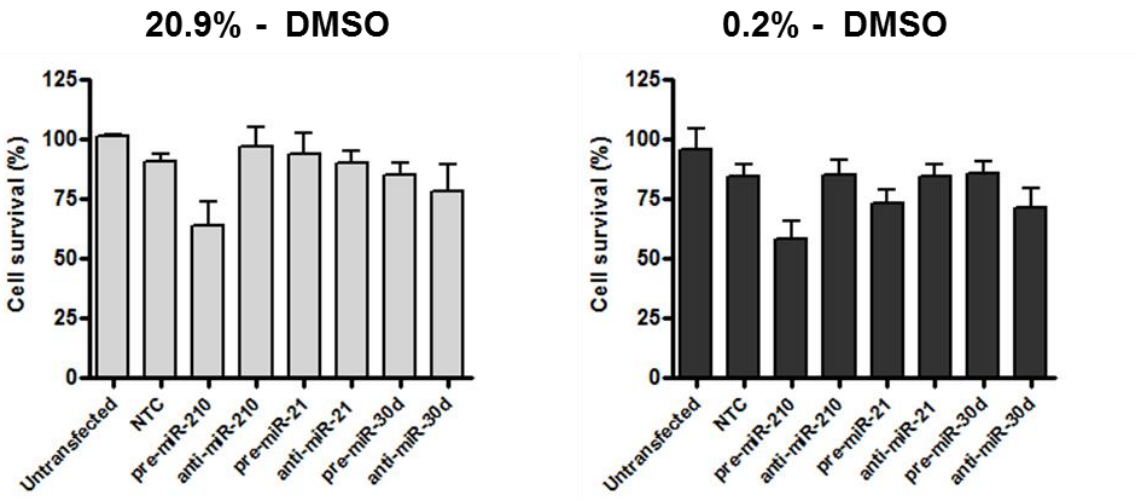

Appendix Figure 6. Cell survival following transfection of pre- and anti-miR candidate miRNAs. HCT116 cells were transfected with pre- and anti-miRs and treated with DMSO (vehicle control) for a further 48hr under two oxygen conditions (20.9% or 0.2%). Graph represents percentage of cell survival normalised to untransfected cells. Bars represent mean values with SEM.

Target ID Library

Due to their short seed sequence, miRNAs have the capability to modulate the expression a large number of genes. Identifying these targets would provide an important insight in the cellular pathways that a miRNA is involved in. Since miRNAs were discovered, many prediction tools are now available to identify targets based on the complementarity between the miRNA and mRNA sequences. However, these various tools utilise different algorithms to predict miRNA targets. Alternative 3'-UTR sequence databases are used between the various programmes [601, 602], resulting in major differences between prediction results. Additionally, the false positive rate of these identification tools has been shown to be up to 70% [603-605], emphasising the importance of experimental validation of mRNA targets for each specific miRNA. Luciferase reporter assays containing the 3'-UTR sequence of the mRNA, combined with mutagenesis of the predicted miRNA binding site, still remain the gold standard practise to validate novel targets. This, however, is a highly laborious exercise and a limited number of targets are selected based on preliminary knowledge guided by the online prediction tools. Recently, a novel system, the MISSION® Target ID Library (Sigma, UK), has been designed which essentially removes this target discovery bottleneck and allows novel mRNA targets to be identified on a genome-wide scale. The library contains ~17,000 unique human cDNAs cloned downstream of the 3'UTR of a thymidine kinase-zeocin fusion protein (Appendix Fig. 7). This library is then stably transfected into a cell model of choice. Subsequently, cells stably expressing the library are transfected with a miRNA of choice and genome-wide mRNA targets can then be identified.

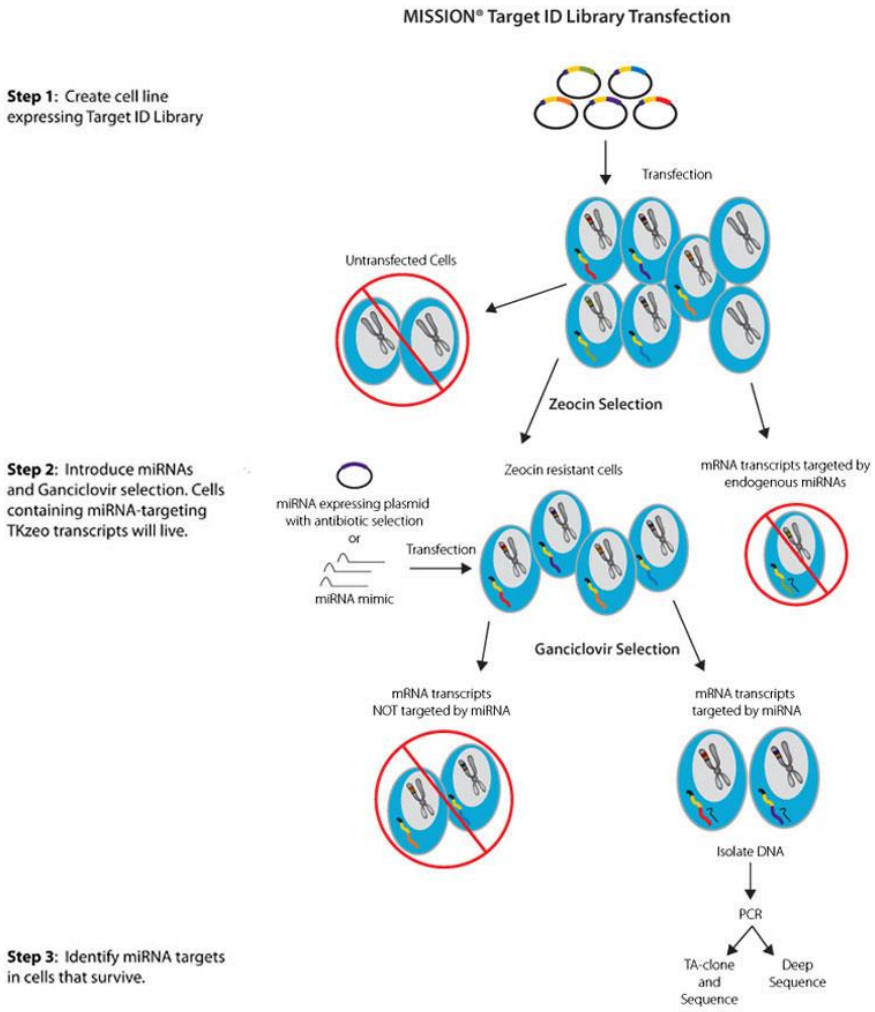

Appendix Figure 7. MISSION® Target ID Library. The Target ID Library is a pool of plasmids, each with a human cDNA inserted into the 3'-UTR after a thymidine kinase-Zeocin fusion protein (TKzeo). Cells are transfected with the Target ID Library and allowed to recover for 3–5 days. Constructs can integrate into the genome during this recovery period and express the encoded transcript. After recovery, cells are exposed to Zeocin. Cells expressing the TK/Zeo fusion protein from stably integrated Target ID constructs survive Zeocin selection, whilst untransfected cells die. Following the transfection of these Target ID cells with a miRNA expression construct of interest, cells are selected with gancliclovir. Cells producing thymidine kinase (TK) in the presence of ganciclovir (i.e., cells expressing TK/Zeo constructs not targeted by the miRNA) will die. On the other hand, cells containing Library constructs with miRNA target sites will not produce TK, and therefore, will survive ganciclovir selection. Surviving cells can be grown, gDNA isolated, and the cDNA containing miRNA target sites PCR-amplified using the Target ID Amplification primers. PCR products will be sequenced by Next Generation Sequencing (NGS) and aligned with the human genome to identify miRNA targets.

Cells that express a cDNA construct (or constructs) that is targeted by the candidate miRNA will survive and the cDNA will be picked up by sequencing as a target. Therefore, to keep experimental background to a minimum, a cell line with low endogenous expression of the candidate miRNA is required. Based on the work presented previously (Section 5.2-Section 5.5), miR-21, -210 and -30d were selected for further investigation. Three colon cancer cell lines (DLD-1, HCT116 and HT29), three rectal cancer cell lines (HT55, SW837 and VACO4s), a cervical cancer cell line (HeLa) and a breast cancer cell line (MCF7) were tested for endogenous expression of miR-21, -210 and -30d by qRT-PCR. Analysis demonstrated that HeLa cells presented a consistent low expression of all three miRNAs (Appendix Fig. 8A-C) and was, therefore, selected as the cell line model for the transfection of the Target ID Library. The Library cDNA constructs contain a Zeocin resistance element enabling transfected cells to be positively selected using this antibiotic. A kill curve for Zeocin was performed on untransfected HeLa cells to determine the minimal lethal dose. Cells were treated with a range of concentrations of Zeocin (0, 300, 400, 500, 600 or 700 μg/ml) and cell survival measured at day 3, 6 and 9. A concentration of 500 μg/ml Zeocin killed 95% of cells after 9 days (Appendix Fig. 8D), and this reached 100% by day 14. This same concentration (500 μg/ml) was used previously by others when the system was optimised [606]. Subsequently, HeLa cells were transfected with 2 μg cDNA construct (Target ID Library, Sigma, UK) for 5 days before transfected cells were selected with 500 μg/ml. HeLa cells were expanded with Zeocin-containing media for two weeks and stocks frozen down for future use.

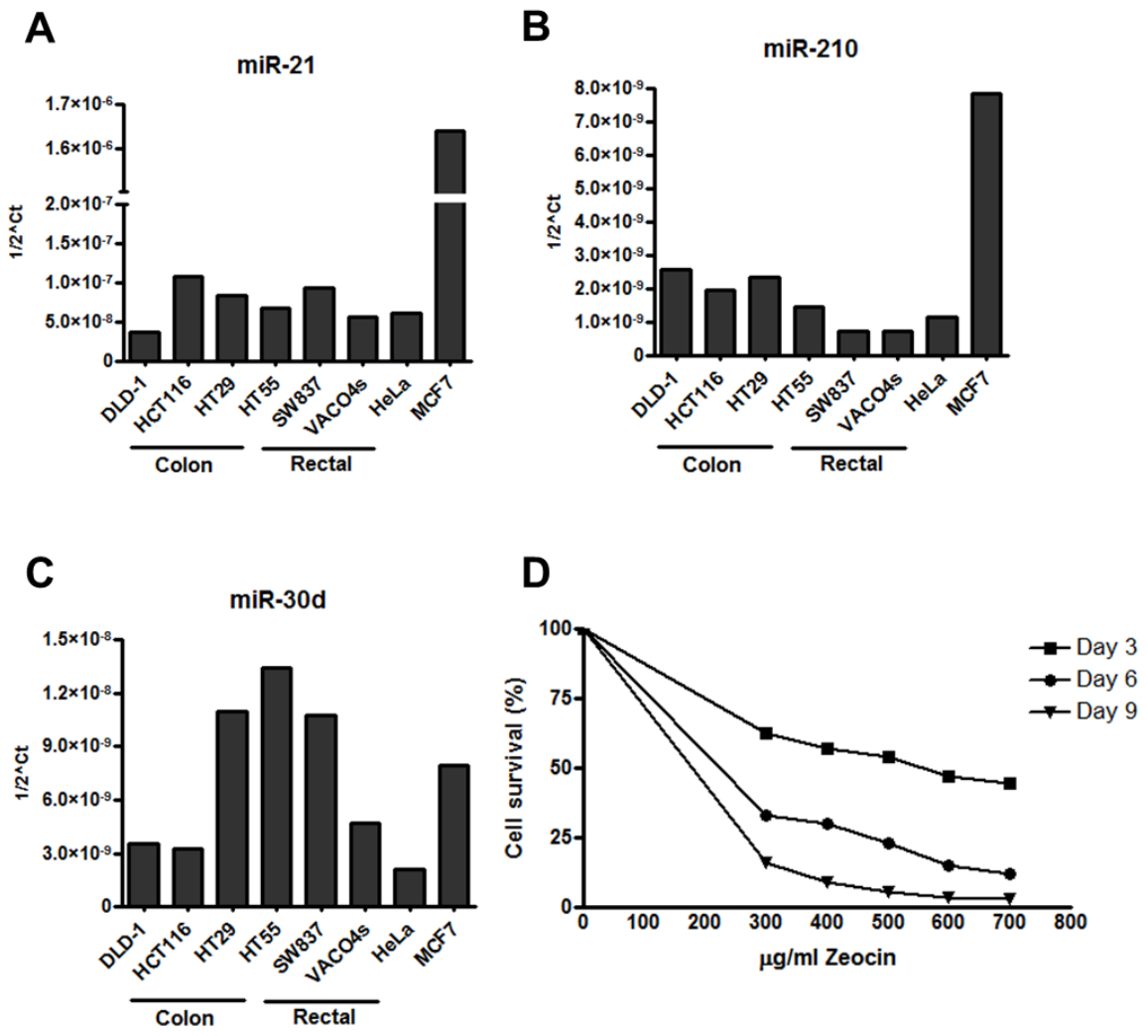

Appendix Figure 8. Target ID Library preparation (n=1). (A-C) Endogenous levels of miR-21, miR-210 and miR-30d in three colon (DLD-1, HCT116 and HT29), three rectal (HT55, SW837 and VACO4s), a cervical cell line (HeLa) and a breast cancer cell line (MCF7). The graphs represent the un-normalised Ct values determined via qRT-PCR. (D) Untransfected HeLa cells were exposed to a range of concentrations of Zeocin to determine the minimum concentration to achieve maximum cell death. Cell survival was measured at three time points (3, 6 and 9 days). 500 µg/ml Zeocin was sufficient for maximum death after 9 days.

Next, DNA was extracted from three individual flasks of cells stably expressing the Target ID Library constructs and one flask of untransfected HeLa cells. PCR amplification was performed using the amplification primers which specifically amplified the cDNA constructs (provided by Sigma, UK). PCR products were then were run on a 2% agarose gel for visualisation (Appendix Fig. 9A). The DNA samples from cells transfected with the Target ID Library (HeLa + ID Library) demonstrated clear bands, while the untransfected cells (HeLa – ID Library) and the water control was negative, suggesting that the transfection of the cDNA constructs was successful (Appendix Fig. 9A). The cDNA constructs vary in length between 0.5kb and 4kb (Target ID Library Technical Bulletin, http://www.sigma-aldrich.com), and a smear of DNA was observed with a few distinct bands between 700bp and 2000bp. Sigma provided a similar PCR from cells (unknown) transfected with the Target ID Library. A similar DNA smear with a few distinct bands can be seen (Appendix Fig. 9B).

These results demonstrate that HeLa cells were successfully transfected with the Target ID Library constructs. In the future, these cells will be used for the screening of genome wide targets of candidate miRNAs.

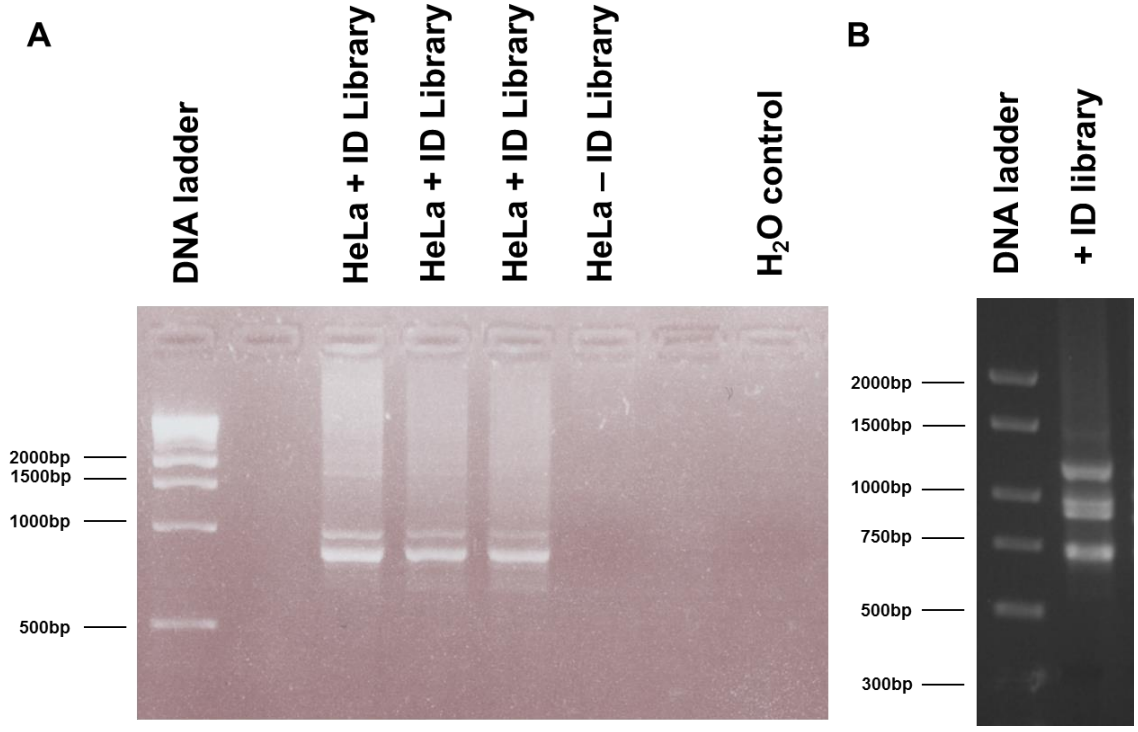

Appendix Figure 9. Target ID Library cDNA contructs in HeLa cells. (A) PCR performed with primers that amplify cDNA insert specifically. Four DNA samples were used: HeLa transfected with the Target ID Library x3 and one of untransfected HeLa cells. PCR products were run on a 2% gel. (B) PCR image supplied by Sigma demonstrating the presence of the target ID library (cell line unknown).